A FEASIBILITY STUDY OF HEAD-END STEERING FOR A SIMPLIFIED MANNED SPACE VEHICLE

DOUGLAS MISSILE & SPACE SYSTEMS DIVISION

A FEASIBILITY STUDY OF HEAD END STEERING FOR A
SIMPLIFIED MANNED SPACE VEHICLE

ABSTRACT

/6017

The primary objective of this study was to determine the feasibility of a manned space vehicle concept which would have a wide flexibility of operation, quick response, and launch vehicle simplicity. These goals were achieved by use of an HL-10, high L/D, reusable, spacecraft; fixed nozzle, large solid propellant booster stages; and steering of the launch vehicle from the head end by use of engines mounted within the spacecraft. The concept concentrates the complexity in the manned spacecraft which is reusable over a large number of flights with only minor refurbishment.

The results of the study show that such a concept is feasible and would have the following characteristics and capabilities:

The space vehicle would consist of a three-stage solid propellant booster, a steering propellant tank - cargo module - adapter section, and a 44 ft. length HL-10 spacecraft. The gross vehicle lift-off weight would be 6.65 m pounds, the adapter section weight 102,000 pounds, and HL-10 spacecraft weight 91,000 pounds. The vehicle could provide a ferry-resupply capability to an orbiting laboratory in a 300 n.m., 31° inclination orbit, of up to 23,750 pounds of cargo, 11 passengers plus two crewmen, and have an in-orbit maneuvering capability of up to 6,312 ft./sec. Maximum cargo, crew, and velocity capability do not occur simultaneously, but must be determined according to mission requirements. A continuous launch window for space station rendezvous is provided. Other types of missions such as a polar orbit resupply, reconnaissance, intercept, inspection, and repair could also be accomplished. The returning spacecraft could land on any 10,000 ft. runway in the United States.

The study was accomplished by the Douglas Aircraft Co. under Langley Research Center Contract NAS1-4149 and the complete results are reported in Douglas Report SM-48152.

Author

CONTENTS

FIGURES

TABLES

The HES-2G Spacecraft (HL-10 and Cargo Module) Showing Outboard Fins
and Steering Engines in Position for Boosted Flight.

Section 1
INTRODUCTION AND SUMMARY

A feasibility study of head-end steering for a manned space vehicle was conducted by the Douglas Aircraft Company, Inc. , for the National Aeronautics and Space Administration, Langley Research Center, under Contract NAS 1-4149. The study period was from June 1964 to December 1964. The study resulted from a NASA interest in cost reduction and increased simplicity for large launch vehicles.

In the area of cost reduction, the reuse of space boosters and spacecraft hardware provides definite savings. Reusability of the manned module would be especially advantageous for manned systems because this module must be recovered in any event. When many launches are planned, reusability of almost all hardware provides decided savings; however, when a program involves only a few launches, reusability does not afford as decided an economic advantage because of the higher development costs associated with a recoverable and reusable system. The purpose of this study effort was to evaluate a concept which offered significant cost reductions and increased simplicity in development and operations. This concept is based on (1) the use of relatively inexpensive solid-propellant motors for the booster and (2) the recovery of relatively high-cost hardware in a reusable manned module. This concept implies a mode of booster control in which all system hardware is contained in a single module located at the front end or head-end of the vehicle. This location of the steering function permits consideration to be given to recovery of the steering system components and suggests simplified checkout and handling operations.

The initial investigation, therefore, has a two-fold purpose: (1) to perform a first-order design definition of a reusable manned spacecraft launched by a large multistage solid fueled booster for the logistics support of an Earth-orbiting space station and (2) to evaluate the technical and economical

feasibility of the resulting system and components.

To permit a reasonable depth to the technical and economical analysis within the limits of the resources allotted to the study, a system optimization was not performed limiting the conclusions from the study to those pertaining to feasibility. The characteristics of the spacecraft and booster are based on the use of existing hardware and technology, therefore no evaluations or forecasts were made on contemplated advancements in the state-of-the-art.

This study has resulted in a first-order definition of a manned space vehicle system whose principal mission is the logistics support of an Earth-orbiting space station at an altitude of 300 n. mi. The spacecraft configuration selected for final evaluation is composed of an HL-10 spacecraft with the capability of transporting up to eleven passengers and two crew; a booster steering and spacecraft maneuvering propulsion system (located on the HL-10); cargo provisions for up to 5,000 lb. (in the HL-10), and up to 18,750 lb. of cargo in a cargo-module adapter; and an all solid-propellant booster propulsion system. The booster consists of three stages: (1) a 260-in.-dia. solid propellant first stage motor with a propellant loading of 4,000,000 lb.; (2) a 260-in.-dia. second stage motor with a propellant loading of 1,350,000 lb.; and (3) a 156-in.-dia. third stage motor with a propellant loading of 526,100 lb.

While results of the study have not demonstrated that the head-end steering concept is a preferred approach, a first-order cost analysis indicates there would probably be significant cost benefits in this approach. This results not only from the use of large solid boosters, but from the concentration of the steering function at the head-end. The use of the head-end steering concept may also show cost advantages when used with liquid propellant upper stage boosters.

A brief summary of the study results are:

1. Steering the vehicle during boost with two engines located on the HL-10 spacecraft is feasible with a thrust-level of 50,000 lb./engine, a gimbaling range of $\pm 30^\circ$, and using a storable liquid propellant.

2

2. The steering thrust requirement is more sensitive to changes in booster thrust misalignment than to any other design parameter considered. An increase in misalignment of 50% from 0.1° to 0.15° results in a 30% increase in steering thrust.

3. The incorporation of steering propellant in the HL-10 was not found to be feasible. However, the HL-10 lifting body vehicle was shown to be an extremely flexible configuration for transporting personnel, cargo, for in-orbit maneuvering propellants, and for the installation of rocket engine components.

4. Because the study has shown the technical feasibility of concentrating the steering function in the HL-10 spacecraft, the booster stage interfaces need to accommodate only range safety, ignition, and thrust termination functions.

5. The total vehicle shows performance sensitivities to design parameter variations typical of three-stage vehicles designed for a near optimum ratio of gross weight to payload weight.

6. Recovery of all major vehicle components except the fixed-nozzle solid motor boosters and the steering propellant tankage has been shown to be feasible.

7. A first-order evaluation of the prelaunch preparation time for the head-end steering solid motor vehicle resulted in a requirement of only 38 days of which 20 days are required for pad occupancy. This compares to 56 days for the Saturn I of which 47 days are used for pad occupancy.

8. A first-order cost evaluation of the vehicle concept shows a launch cost of $15.1 million based on cost of operations only; total program cost of $1.4 billion, and a cost/lb. of delivered cargo of $793/lb. based on the cost of operations only. These costs are based on a 5-year span of operation with ten flights/year.

Section 2
OBJECTIVES

The fundamental premise at the beginning of this study, was that a manned space vehicle design concept incorporating steering at the head-end, with solid-propellant motor boosters, and a lifting body logistics spacecraft could be developed to maximize the technical and economic advantages of expendable boosters and a recoverable spacecraft.

The study objectives were to:

1. Select and define a simplified, manned space vehicle system concept stressing partial reusability of the vehicle system to comply with a flight frequency requirement of 10 flights/year.

2. Establish, if possible, the technical and economic feasibility of the selected design concept.

Section 3
GUIDELINES

The baseline mission selected for this study is the logistic supply of both cargo and personnel to a manned space station in low Earth orbit. The space station orbit is at an altidude of 300-n. mi. and in a circular orbit inclined 31° from the equatorial plane. The base for the logistic operations is Cape Kennedy.

The nominal resupply requirement of the space station is 4,000 lb. of cargo (unpackaged weight) and four space-station personnel every 90 days. A crew of two will be required for the logistics spacecraft operations. The space-craft will have provisions for maneuvering at the space station's altitude and orbital inclination. The maneuvering capability will be equivalent to 4,000 fps impulsive velocity at the space station altitude and orbit inclination. Mission duration is assumed to be 7 days.

The external configuration of the recoverable part of the spacecraft consists of an HL-10 lifting body with a lift-to-drag ratio of approximately 1.2 in the hypersonic flight regime. The HL-10 lifting body will be the crew and pas-senger module and will perform whatever other functions the study may show to be desirable. The HL-10 vehicle must maintain a center of gravity no further aft than 53% of its body centerline length and no further forward than is consistent with existing control capability as defined by NASA-LRC exper-imental data.

The principal booster energy requirements will be provided by large solid-propellant motors. The longitudinal acceleration will not exceed 322 fpsps. Provisions for abort from incipient booster motor failure will be based on a 2% TNT equivalence for the solid propellants and 10 psi overpressure limit on the HL-10 vehicle. The steering system energy requirements will be provided by a single propulsion system utilizing storable liquid propellants and located at the head-end of the vehicle.

In addition to these guidelines a number of goals were established as a basis for the final selection of a conceptual design:

1. Maintain simple stage interfaces.

2. Incorporate as much of the steering system as possible aboard the recoverable HL-10.

3. Provide recovery for a significant fraction of the cargo.

4. Provide for a simple exchange of cargo and passengers.

5. Provide for a short turn-around time at the space station.

6. Preserve the external aerodynamic contours of the HL-10 in accordance with the NASA-LRC loft-line definition.

7. Incorporate as much modularization of the cargo as possible.

8. Provide continuous opportunity to return passengers from the space station.

9. Use the steering system for as many additional functions as possible.

It was recognized early in the study that feasibility might be demonstrated for a system concept too limited in mission capability. And, if design were to proceed on such a limited basis, it might not be possible for the concept to be broadened to accommodate even small changes in future mission requirements. Hence, to preclude establishment of a limited system concept, the extended nine-man, MORL requirements were examined, and the ability of HL-10 to satisfy them became a major criterion in the feasibility study.

Section 4

MISSION CONSIDERATIONS

This section begins with a discussion of the baseline-mission elements: the mission profile, launch window characteristics, launch azimuth characteristics, ascent, rendezvous, docking, separation, deorbit, re-entry, and landing. The latter portion of this section is concerned with energy and payload requirements for various alternate missions.

4.1 BASELINE MISSION

In the baseline mission, a space station resupply, ferry vehicle is launched from Cape Kennedy into a 300-n.mi. orbit, inclined at 31°. Its dry unpackaged cargo capacity is 4,000 lb.; it can carry four passengers plus its crew of two. It will have an impulsive velocity capability of 4,000 fps at the space station. The maximum mission duration will be 7 days.

Figure 4-1 is a schematic of the baseline mission profile. Launch occurs instantaneously at planned time zero, and the booster ascends through the atmosphere and injects the spacecraft into a 100-n.mi. transfer orbit. The spacecraft's propulsion will provide vernier injection control. Approximately 21 min. after third-stage burnout, the spacecraft makes a plane-change maneuver to achieve coplanarity with the space station. Rendezvous is completed some 25 min. after the plane-change maneuver; the docking maneuver then follows. After separation of the spacecraft from the space station, the deorbit impulse is applied to the spacecraft, which thereupon follows a coasting descent orbit to the re-entry point. At the re-entry point the attitude-control system has oriented the spacecraft attitude to that required for the re-entry pullout maneuver. At the bottom of the pullout, the re-entry vehicle rolls about the velocity vector to the position which allows it to hold a constant altitude. The re-entry vehicle remains in a rolled-out position during a constant-altitude deceleration phase, slowly rolling back to an upright

EVENT	TIME
1. LIFT-OFF	0
2. FIRST-STAGE BURNOUT & SECOND-STAGE IGNITION	2.1 MIN.
3. SECOND-STAGE BURNOUT & THIRD-STAGE IGNITION	4.2 MIN.
4. THIRD-STAGE BURNOUT & INJECTION	6.1 MIN.
5. PLANE CHANGE	27.0 MIN.
6. RENDEZVOUS	52.0 MIN.
7. DEORBIT	0
8. RE-ENTRY	35 MIN.
9. TOUCHDOWN	90 MIN.
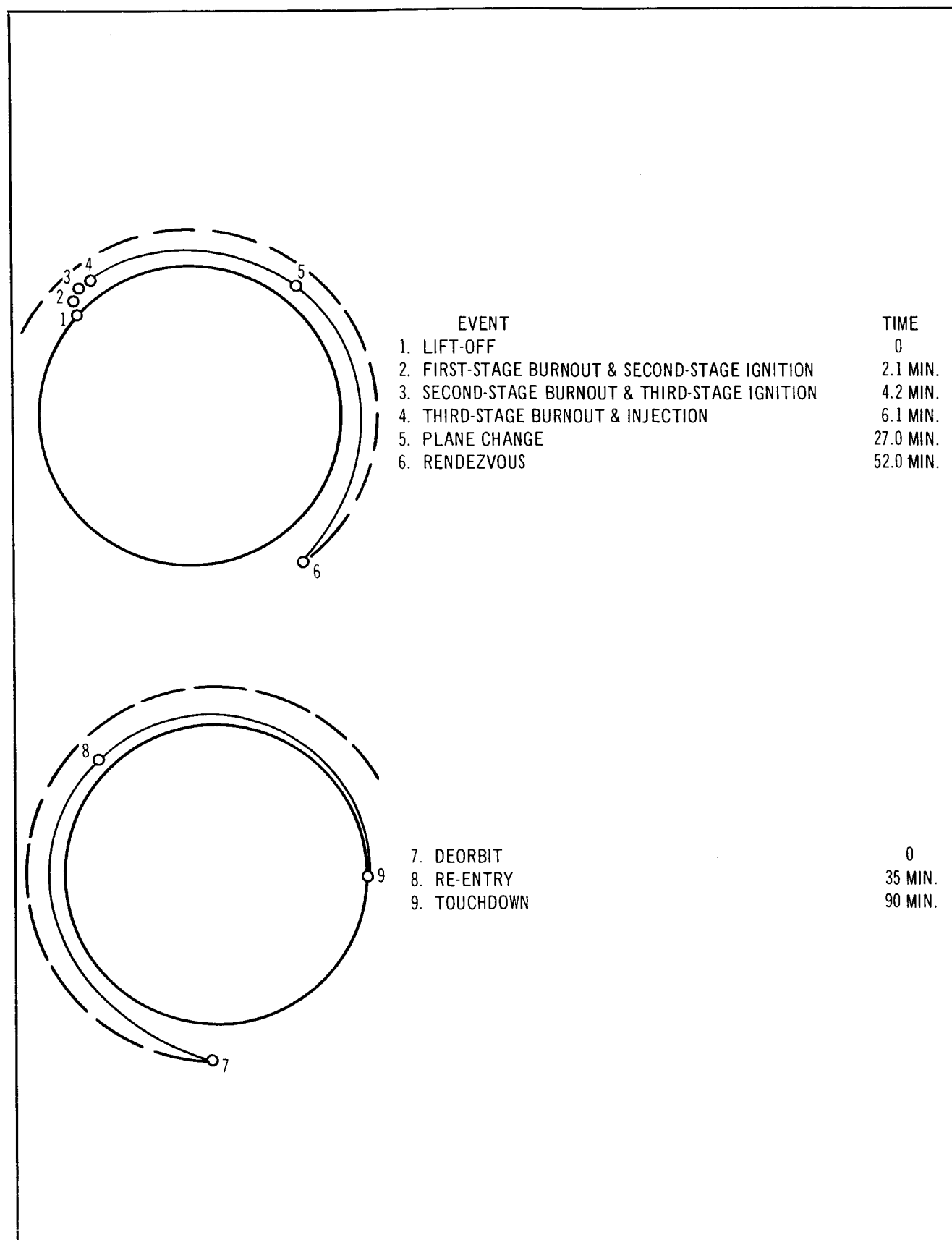
Figure 4-1   Baseline Mission Profile

position. An upright position is achieved at the desired equilibrium glide condition. This glide is followed down to the point where an equilibrium descent path is maintained to high key, where maneuvering is initiated to achieve proper approach conditions, at which point the final landing maneuver is initiated. Note that the in-space plane-change maneuver used to eliminate the parking orbit technique results in a very short total time to rendezvous -- about 1 hour. The maximum time from space station departure to Earth touchdown is about 1.5 hours. Thus, for the nominal mission, the total time spent in transit is only about 2.5 hours.

To eliminate the need for a parking orbit, the parallel-launch technique was adopted. This technique permits a launch when there is no relative movement between the target and the launch craft. In general, this technique requires that a launch be made when the launch point is not in the plane of the target; and therefore, a plane-change maneuver is required at the spacecraft-target node line. The magnitude of the out-of-plane maneuver is a function of the time span over which a synchronized launch is desired, and this time span in turn must be equal to, or greater than, successive in-phase conditions for the launch vehicle and the target. Figure 4-2 presents this relationship in terms of impulsive velocity and presents relative inclination as a function of time for a launch latitude of 28.5° and an orbit inclination of 31°. Figure 4-3 is a plot of the total time available for a given amount of impulsive velocity capability. It is seen that this launch window increases sharply in the vicinity of 1,100 fps. This increase occurs because, as the impulsive-velocity capability increases, the two separate launch windows on either side of time zero merge into a single window.

Three separate launch windows can be chosen in order to perform the required mission properly. The first is when a launch is guaranteed in either one of the windows about time zero. This means that if a launch opportunity does not occur in one window, it will occur in the other. A second possibility is to have a guaranteed launch in each of the two windows. The third possibility is the single continuous window achieved for the lowest possible impulsive velocity. As can be seen from the figure, the additional impulsive velocity required to achieve the large single continuous window is only about 300 fps

EARTH TRACE OF SPACE STATION ORBIT

LATITUDE OF LAUNCH SITE

POSITION OF LAUNCH SITE

POSITION OF SPACE STATION
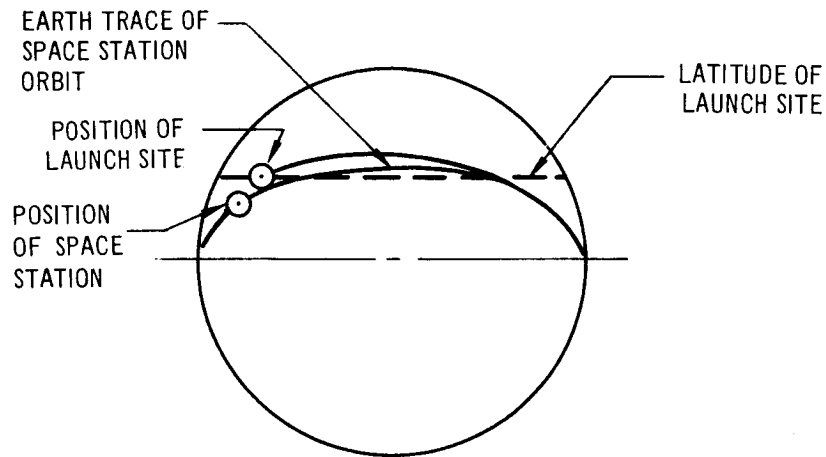
$\Delta i_{RELATIVE}$ = RELATIVE INCLINATION OF THE INITIAL LOGISTICS VEHICLE ORBIT AND THE SPACE STATION ORBIT.

NOTE: $\Delta i_{RELATIVE}$ APPROACHES ZERO AS THE LAUNCH SITE APPROACHES AN IN-PLANE LAUNCH CONDITION.

LAUNCH LATITUDE = 28.5°
ORBIT INCLINATION = 31°
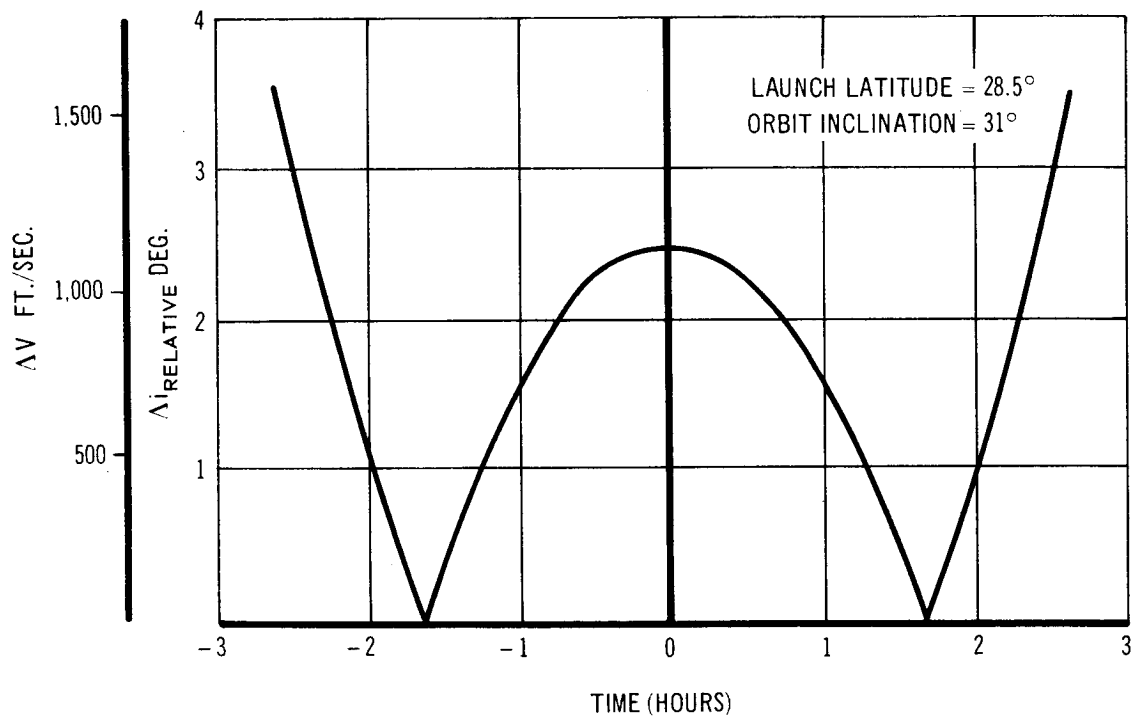
Figure 4-2   Launch Window Characteristics, Parallel Launch Technique
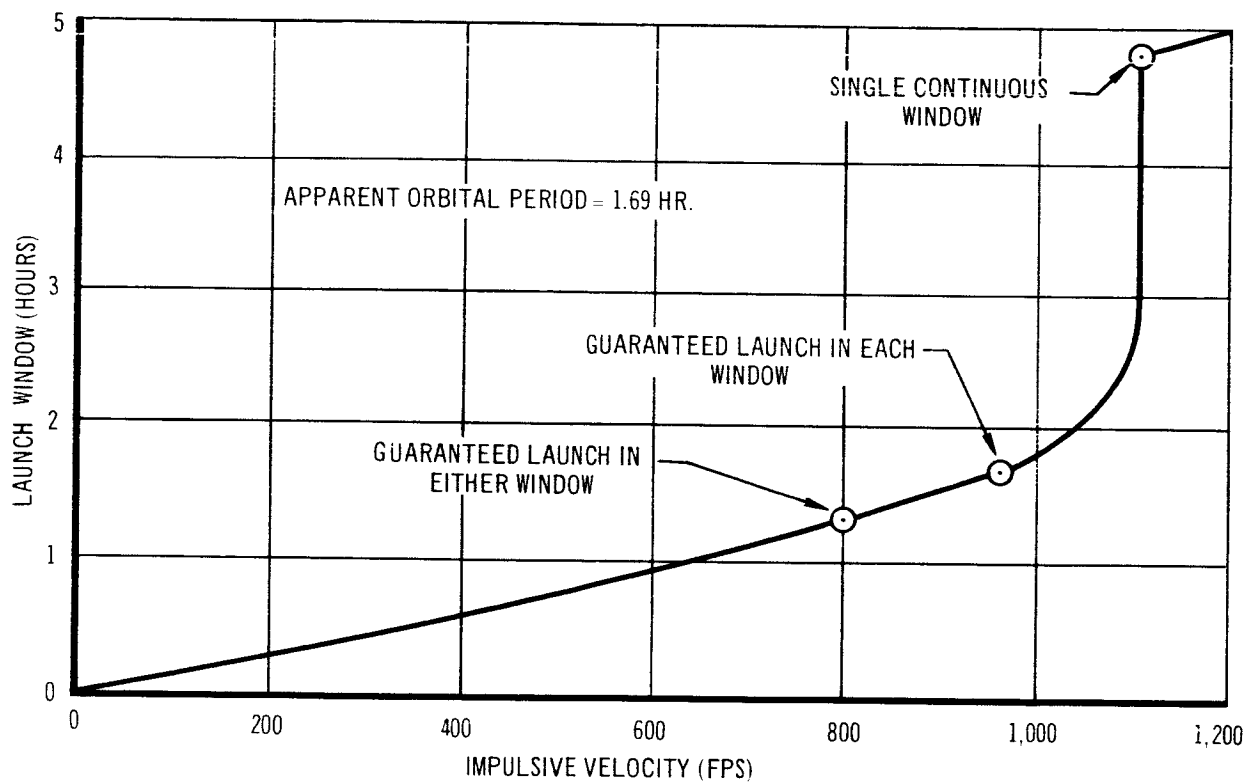
Figure 4-3   Launch Window Energy Requirements

over that required to achieve guaranteed launch in either separate window. Thus, for this study, the conservative case of the single continuous window was chosen.

The required launch azimuth range is shown in Figure 4-4 as a function of launch window size. Clearly, the single continuous window as chosen is quite oversized for the requirements, since it allows two to three launch opportunities per day. Thus, it was considered advantageous to launch in a narrower azimuth band so that no down range tracking ships would be required. If this band is translated into an equivalent launch window, a guaranteed launch can be made each day within the no-tracking-ship band.

The 300-n.mi.-apogee transfer orbit is equivalent to the Hohmann transfer orbit between a circular orbit at 100 n.mi. and a circular orbit at 300 n.mi. Thus, the rendezvous impulsive velocity requirement was based on the Hohmann transfer case including a terminal maneuver penalty of 70% of the circularization impulse. An equivalent 250 ft./sec. for docking, separation, and attitude control throughout the flight profile was accounted for separately and therefore was not included on the impulsive velocity budget.

Finally, to complete the velocity budget, the deorbit impulse was determined on the basis of the considerations shown in Figure 4-5. This figure gives the re-entry flight path angle as a function of the deorbit firing angle and the deorbit impulse. The design point was selected to be approximately 0.2° above the HL-10 skip limit on the contour defining zero range sensitivity with respect to firing angle error. This results in a deorbit impulsive requirement of 460 fps.

A summary of the spacecraft maneuvering requirements is given in Table 4-1. To those requirements must be added the 4,000 fps of in-orbit maneuvering capability, bringing the desired total impulsive velocity aboard the spacecraft to 6,250 fps.

APPARENT ORBITAL PERIOD - 1.69 HR.
ORBITAL INCLINATION = 31°
LAUNCH LATITUDE = 28.5°
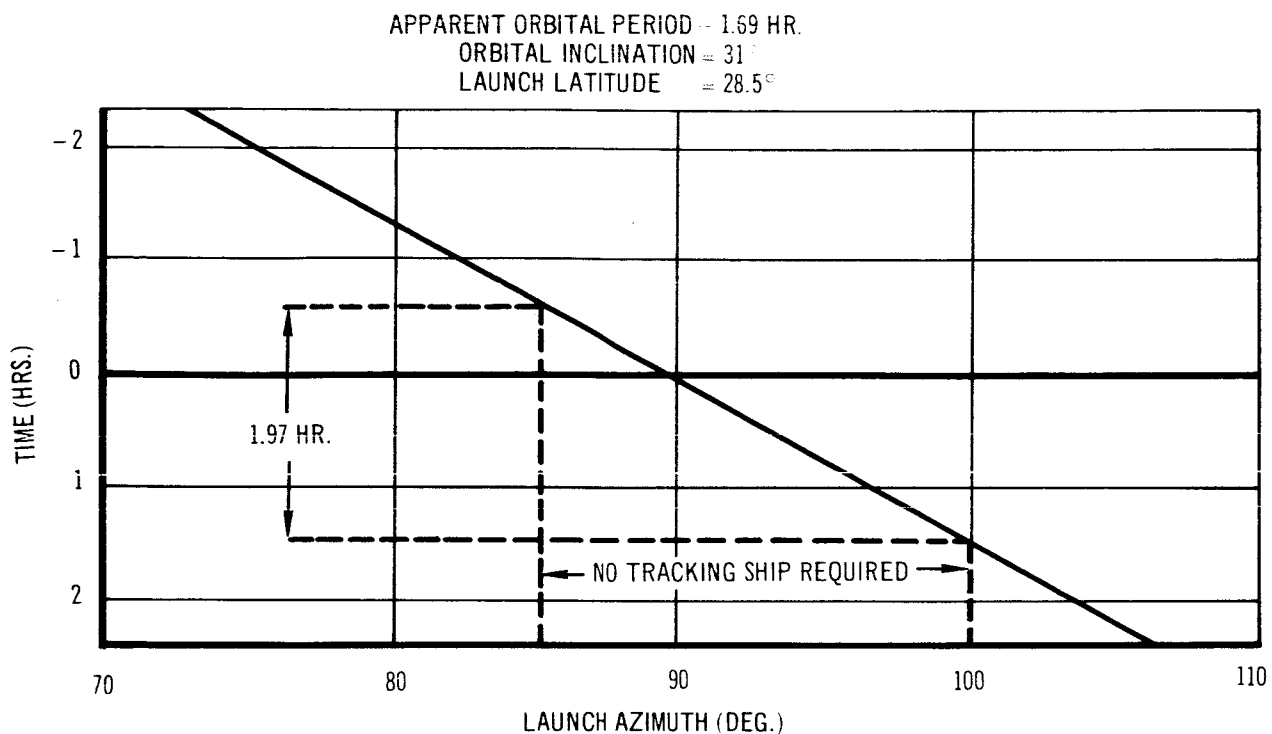
Figure 4-4 Azimuth Range for Parallel Launch Technique
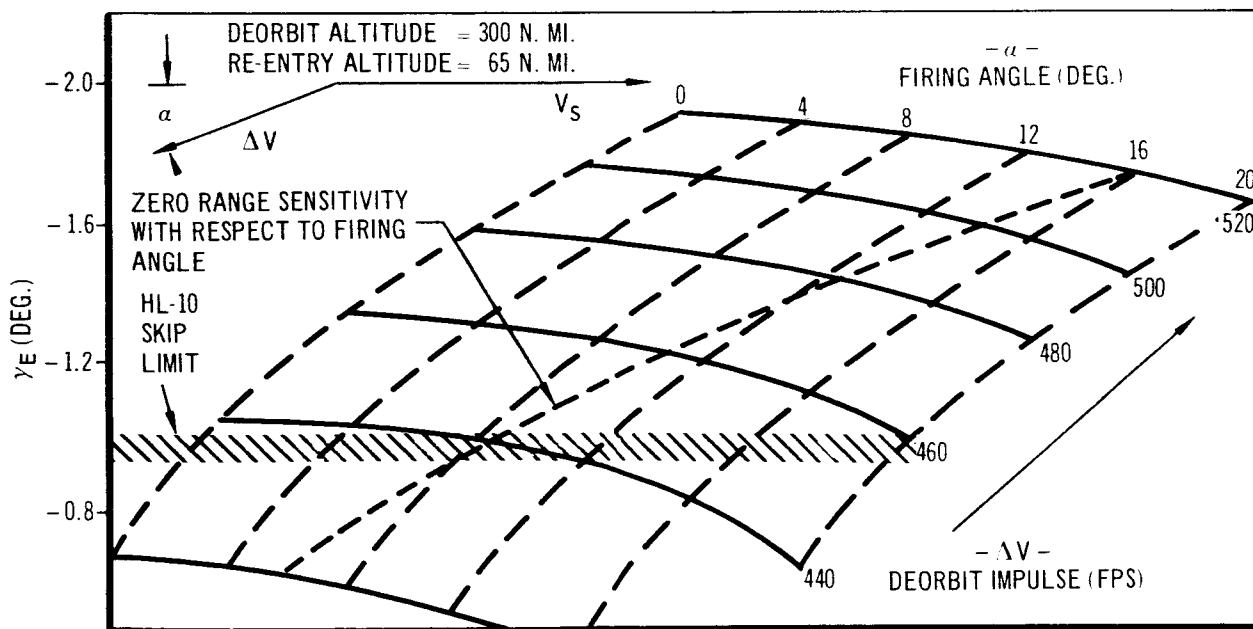
Figure 4-5 Effect of Deorbit Conditions on Re-entry Angle

Table 4-1

BASELINE MISSION MANEUVERING
REQUIREMENTS

Maneuver	Impulsive Velocity Requirement, ΔV Ft./Sec.
Vernier Injection Control*	80
Plane Change During Coast	1110
Coast To 300-n.mi. Apogee	0
Rendezvous (including injection)	600
Dock	0**
Separate	0**
Deorbit and Coast	460
Re-enter and Descend	0**
Approach and Land	0
	2,250
Discretionary Maneuvers Capability	4,000
TOTAL REQUIRED	6,250

*Injection conditions will result in a 300-n.mi. apogee.
**Provided by attitude control system (ΔV equivalent of 250 fps)

4.2 ALTERNATE MISSION REQUIREMENTS

Energy requirements for alternate missions were investigated for the following reasons:

1. To evaluate the alternate mission capability of a spacecraft using the baseline impulsive velocity budget for a mission other than spacecraft ferry and resupply.

2. To evaluate the discrepancy between current impulsive velocity capability and that which will be required in more extensive missions.

Figure 4-6 shows the excursion and return capability in terms of circular-orbit altitude and plane-change angle for various amounts of available impulsive velocity. For the baseline case with 4,000 ft./sec. of discretionary maneuvering capability, an excursion to and circularization at 1,000 n. mi. and a return to and recircularization at 300 n. mi. is seen to be feasible. This may also be translated into about 4.5° plane change and return.

In the event a launch is desired to an orbit inclination other than 31°, the impulsive velocity requirement for the out-of-plane maneuver, consistent with a daily launch opportunity, will increase for higher inclinations and also for inclinations below about 27°. Figure 4-7 shows the velocity requirement as a function of orbit inclination angle. Here it is seen that if the 4,000 ft./sec. second capability is added to the 1,110 ft./sec. capability already budgeted for plane-change, a daily direct ascent launch can be made to orbits inclined anywhere between 18° and 90°.

Another possible mission is a surveillance type. This mission can be flown when the spacecraft is parked in orbit and can precisely overfly a given point on the Earth's surface the first time the target approaches the orbital plane. Figure 4-8 shows the impulsive velocity requirements in order to ensure an overfly of a target within a band defined by a minimum and a maximum latitude. It is seen that if world-wide coverage is desired, the optimum parking orbit inclination is 78.54° and the impulsive velocity requirement is 5,040 ft./sec. This is also consistent with the baseline configuration when the 4,000 ft./sec. maneuvering capability is added to the 1,110 ft./sec. already budgeted for a plane-change maneuver. For this particular case the launch would
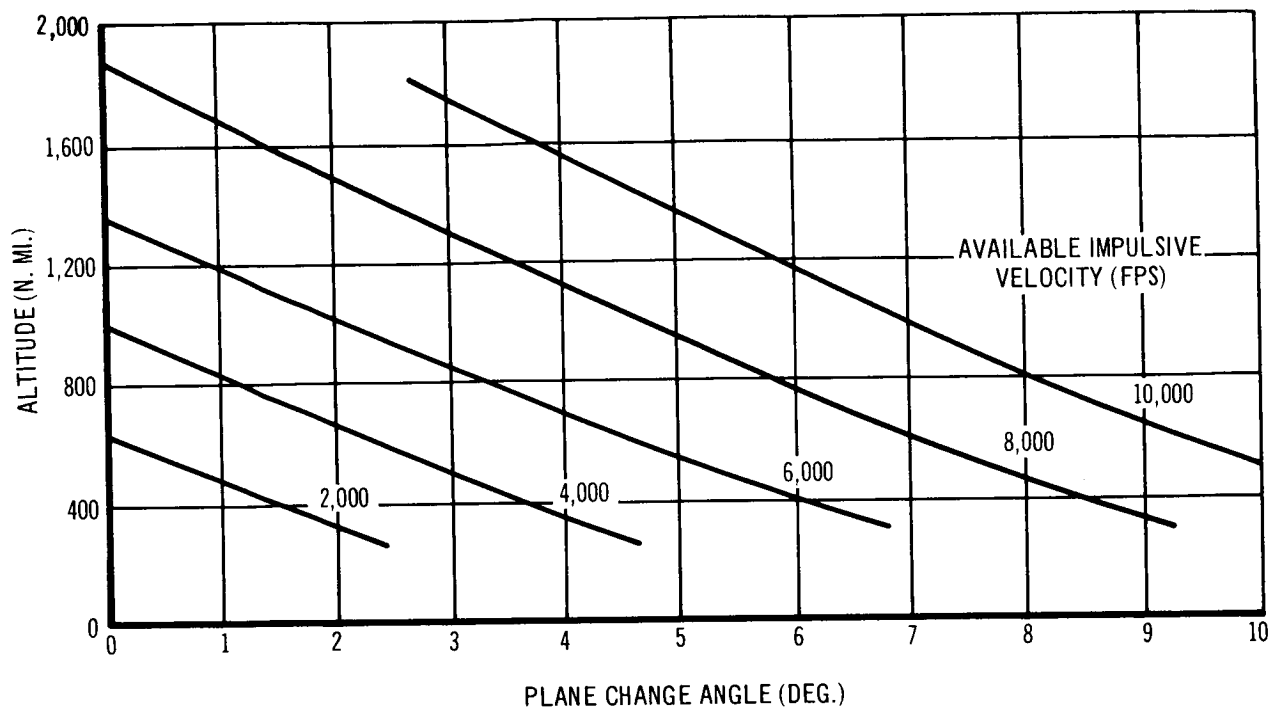
Figure 4-6 Excursion and Return Requirements
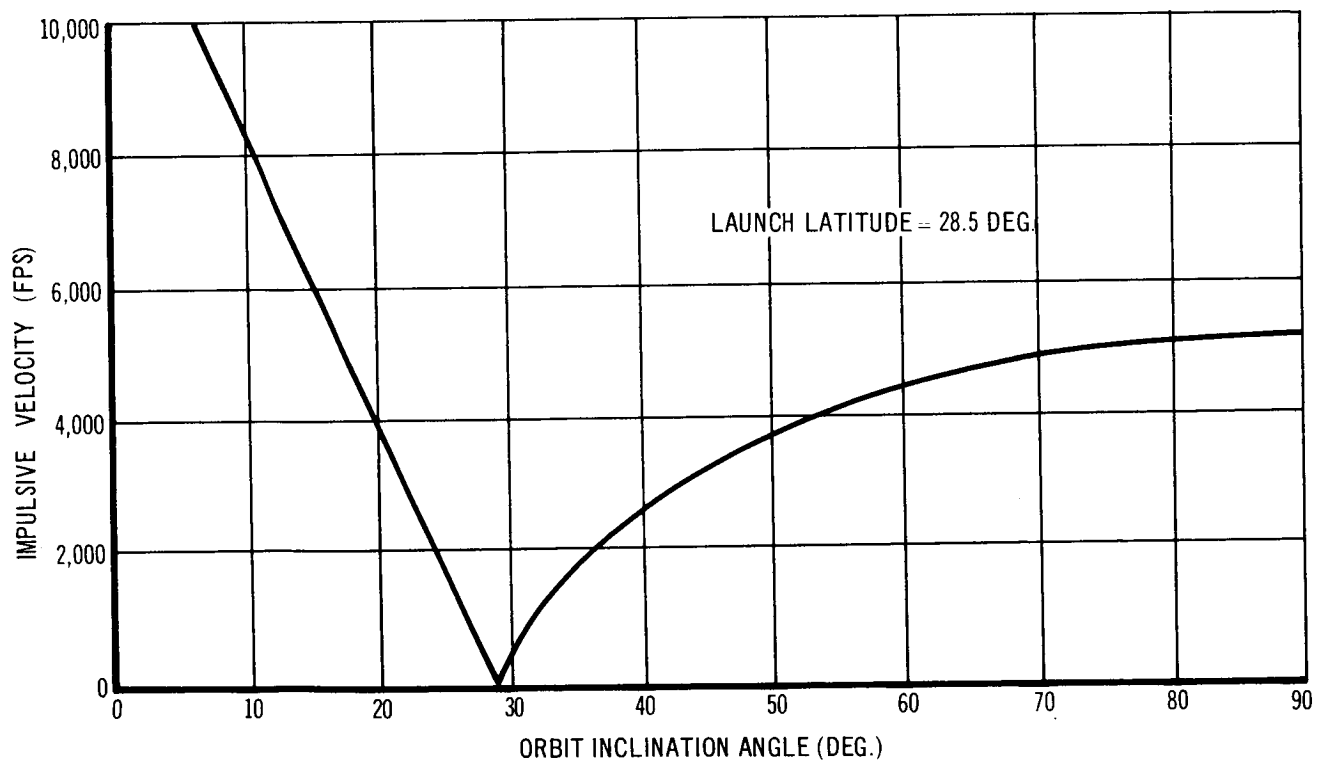
Figure 4-7 Minimum Impulsive Velocity Requirement for Daily
Launch Opportunity and Direct Ascent
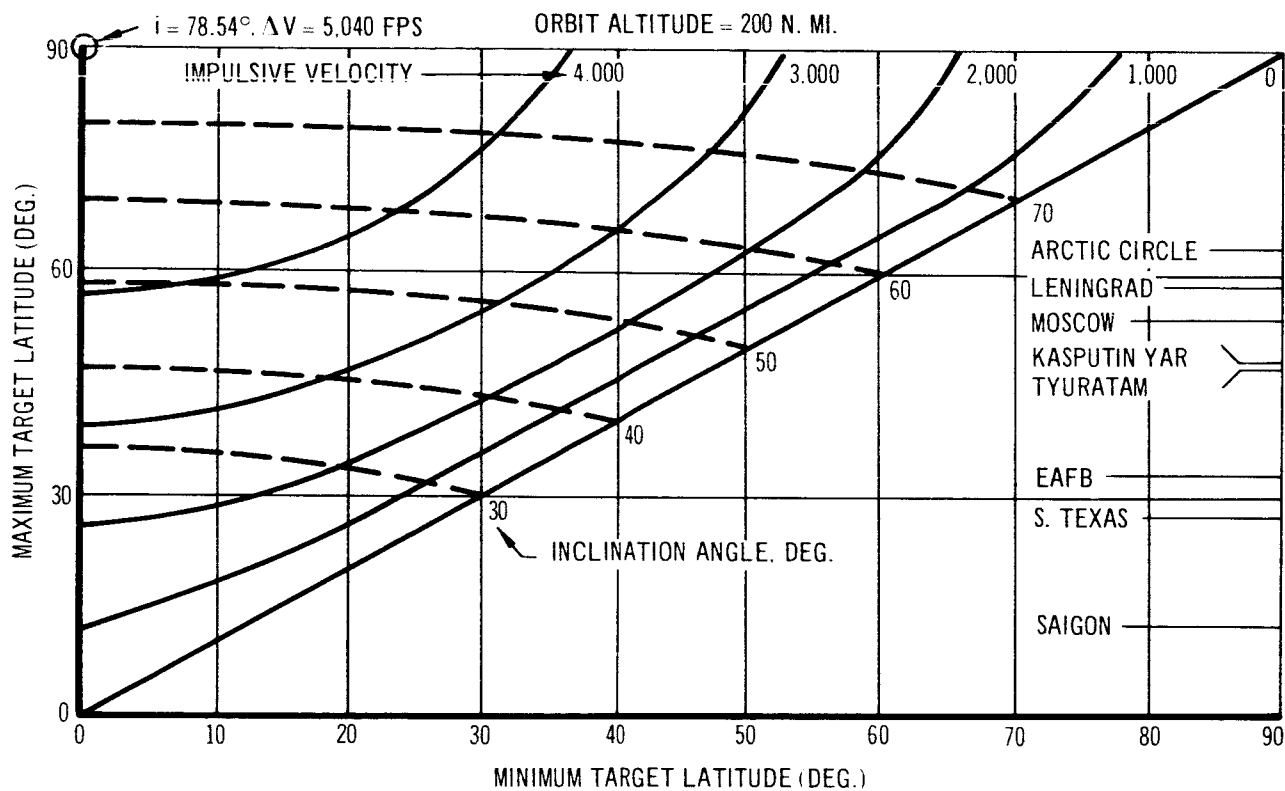
Figure 4-8 Impulsive Velocity and Orbit Inclination Requirements
for Over-Fly Assurance

be made directly into a 78.54° orbit without a plane change during the ascent. However, because of this high inclination some payload degradation from the nominal 4,000 lb. would have to be expected.

Still another alternate mission would be rendezvous with a number of equally spaced co-orbital satellites. Figure 4-9 shows the impulsive velocity requirements for such a mission as a function of the satellite altitude and the number of co-orbital satellites. Initial conditions are taken to be at a 100-n.mi. circular orbit and the final re-entry condition is taken to be also at 100 n.mi. These data do not reflect velocity losses caused by terminal maneuvering at rendezvous, but only include Hohmann transfer requirements plus the energy requirements for transferring from one satellite to the other. Transfer is accomplished using an elliptical parking orbit with an apogee in excess of the target orbit altitude, assuming three parking orbit revolutions for each satellite-to-satellite transfer. It is immediately seen that 4,000 or even 5,000 ft./sec. impulsive velocity does not represent a large capability. The end of the curve at approximately an altitude of 19,000 n.mi. represents the condition of a 24-hour synchronous orbit. The velocity requirements for this condition are on the order of 18,000 to 20,000 ft./sec. This is clearly not achievable if it is assumed that the spacecraft alone must supply this much energy.

In addition to the velocity requirements for alternate missions, an alternate payload requirement was also investigated. This requirement was derived from projected MORL logistics requirements. Table 4-2 summarizes these logistics requirements for the various alternative conditions considered in the MORL study. The various possible alternatives are (1) a spinning and a nonspinning laboratory, (2) a 60-or 90-day crew-rotation cycle, and (3) a baseline or extended MORL system.

The choice of these alternatives is affected by the following factors:

1. The MORL system spin capability is to be utilized only if proven necessary.

2. The 90-day crew-rotation cycle is optimum from a cost effectiveness standpoint. In order to achieve maximum experiment flexibility, however, a 60-day crew-rotation cycle is best.
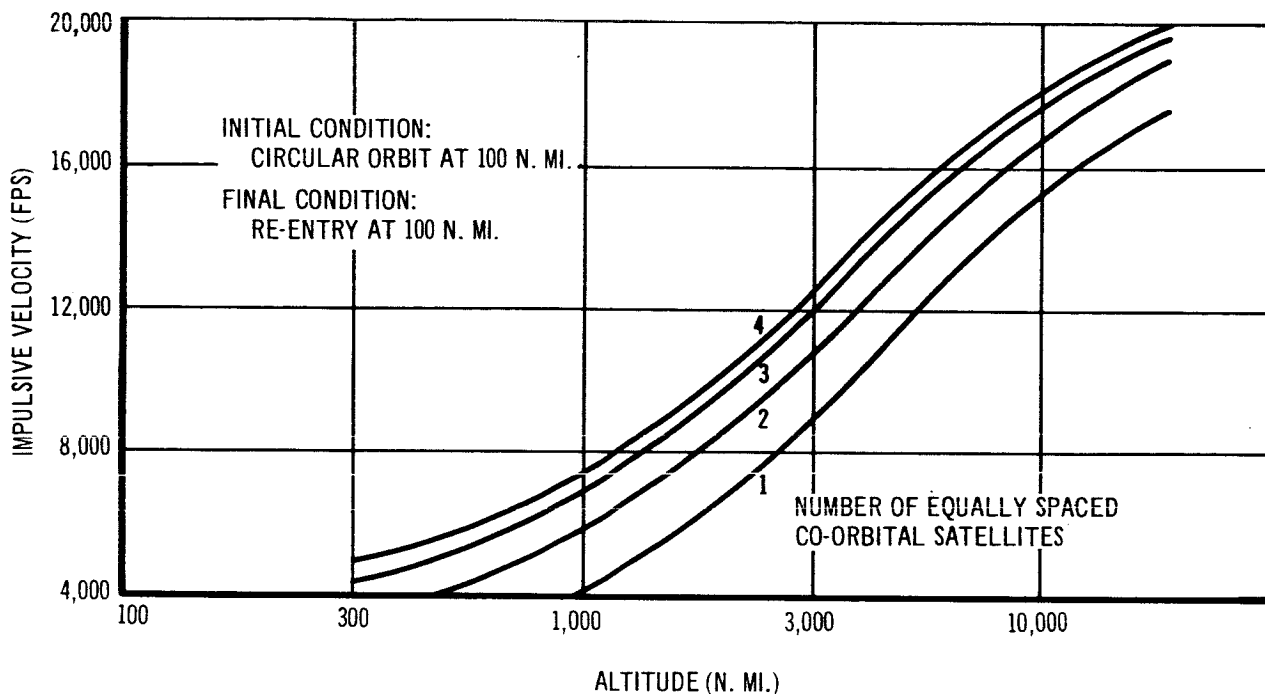
Figure 4-9 Energy Requirements for Multiple Co-Orbital Rendezvous

3.   The extended MORL system has a complement of three more men
     than the baseline system and thus offers a more flexible and
     effective experimentation system.

Inspection of Table 4-2 shows a minimum cargo/crew requirement of 6,500 lb.
and four men, and a maximum cargo/crew requirement of 19,000 lb. and six
men. These are the extremes, but one other critical case can be identified;
this is the possible evacuation of an extended nine-man system. These three
extreme cases are summarized in Table 4-3.

Hence, for the alternate mission which would resupply the nine-man MORL,
it is found that the maximum cargo/crew requirement is 19,000 lb. of payload
and six men, with a capability of carrying nine men when the cargo is removed.
Subsequent to the definition of the original guidelines, the extended MORL
mission was added as a design requirement for the head-end steering study.
Hence, having once established the baseline configuration, it is necessary to
have the capability of (1) off-loading the maneuvering propellant established
by the 4,000 ft./sec. maneuvering capability, and of (2) achieving, in this off-
loaded condition, the extended MORL requirements.

21

Table 4-2

PROJECTED MORL LOGISTICS REQUIREMENTS
COMBINED CARGO/CREW PAYLOAD REQUIREMENTS

NONSPINNING		SPINNING	
90-Day Crew Rotation	60-Day Crew Rotation	90-Day Crew Rotation	60-Day Crew Rotation
BASELINE SYSTEM MORL (6 MAN)			
10,000 lb. + 4 men	6,500 lb. + 4 men	15,000 lb. + 4 men	10,000 lb. + 4 men
EXTENDED SYSTEM MORL (9 MEN)			
13,500 lb. + 6 men	9,000 lb. + 6 men	19,000 lb. + 6 men	12,500 lb. + 6 men

Table 4-3

MORL LOGISTICS REQUIREMENTS
PAYLOAD RANGE SUMMARY

	CREW	CARGO
Minimum		
Baseline		
Nonspin		
60-day		
Rotation	4	6,500 lb.
Maximum		
Extended		
Spinning		
90-day		
Rotation	6	19,000 lb.
Emergency		
Evacuation	9	---

Section 5
DESCRIPTION OF VEHICLE DESIGN CONCEPT

5.1 SUMMARY OF CHARACTERISTICS

The spacecraft configuration selected as that which best meets the study objectives is the HL-10 and the adapter, designated HES-2G. The boost vehicle required by this configuration consists of three solid-propellant stages. The characteristics of HES-2G are summarized in Table 5-1. The vehicle, as it would appear at launch, is shown in Figure 5-1.

The HES-2G lifting body configuration is shown in profile, plan, and rear views in Figure 5-2. The inboard profile of the HL-10 is shown in Figure 5-3. This spacecraft is capable of carrying two crewmen and six passengers in the forward crew compartment. An optional arrangement places an additional three to five passengers in the empty cargo compartment. The crew and arrangements for several different loading conditions are shown in Figure 5-4. The pressurized cargo compartment is volume balanced around the HL-10 CG, which is 53% of the length aft of the nose. The volume of the cargo section is 400 cu. ft. which allows for a packaged cargo-carrying capability of 5,000 lb., with unobstructed crew access through the compartment. Sufficient propellant is carried aboard to provide an impulsive velocity capability of 6,300 fps to the loaded HL-10. The propellant used to provide this capability is the storable liquid propellant combination of Nitrogen Tetroxide (N_2O_4) and Monomethyl Hydrazine (MMH). Propulsion requirements for steering and for providing impulsive velocity capability are satisfied by two liquid-propellant turbopump rocket engines rated at 50,000 lb. of vacuum thrust and mounted in the outboard sections of the aft end of the HL-10. These engines require a gimbal capability of ±30° for steering during the boost phase. As a consequence of this requirement, a unique design feature of this configuration is the outboard fin configuration, which rotates forward during boost to provide engine gimbaling clearance. A docking cone is located at the aft end of the HL-10 to provide

Table 5-1

SUMMARY OF CHARACTERISTICS (Page 1 of 2)

Configuration Designation	HES-2G
General Characteristics:	
Number of crew	2 men
Number of passengers:	
in crew compartment	6 men
in cargo compartment	3-5 men
Cargo carrying capability:	
on-board HL-10 (packaged)	5,000 lb.
in adapter cargo module (packaged)	18,750 lb.
Location of maneuver propellant	HL-10
Location of steering propellant	Adapter
Vacuum thrust per HL-10 engine	50,000 lb.
Engine gimbal capability	±30°
Dimensional characteristics:	
HL-10 length	44 ft.
Adapter length:	
cargo module	14.7 ft.
steering propellant module	13.6 ft.
Total adapter length	28.3 ft.
Adapter diameter	156 in.
Booster Length:	
third stage length	56.1 ft.
third stage dia.	156 in.
second stage length	67.7 ft.
second stage dia.	260 in.
first stage length	158.1 ft.
first stage dia.	260 in.
Overall booster length	283 ft.
Total vehicle length	355.3 ft.
HL-10 span	28.3 ft.
HL-10 plan area	690 sq. ft.
Weight Characteristics:	
HL-10 weights:	
empty weight including crew	36,500 lb.
cargo weight including packaging	5,000 lb.
Reaction control propellant:	
usable	1,900 lb.
residual	100 lb.
Maneuver propellant:	
usable	43,000 lb.
residual	900 lb.
Abort motors (4)	3,600 lb.
Gross weight at liftoff	91,000 lb.

0.0 ── HL-10 SPACECRAFT
── CREW COMPARTMENT
── FUEL TANK - ORBITAL MANEUVERING PROPELLANT
── CARGO COMPARTMENT
── OXIDIZER - ORBITAL MANEUVERING PROPELLANT
── ABORT ROCKETS
528.0 SEPARATION PLANE ── STEERING ENGINES
676.0 SEPARATION PLANE ── CARGO COMPARTMENT ADAPTER
── OXIDIZER - STEERING PROPELLANT
── FUEL - STEERING PROPELLANT

── 3RD. STAGE (156 INCH DIA.)

1544.0 SEPARATION PLANE

── 2 ND. STAGE (260 INCH DIA.)

2361.0 SEPARATION PLANE

── 1ST. STAGE (260 INCH DIA.)

4263.0 ── 355.25 FEET

SCALE 1 INCH = 200 INCHES

Figure 5-1 General Arrangement

Table 5-1 (Page 2 of 2)

Configuration Designation	HES-2G

Weight Characteristics (continued)

Adapter weights:
    empty cargo module — 3,900 lb.
    empty steering propellant module — 10,300 lb.
    steering propellant:
        usable — 85,800 lb.
        contingency for booster burn time
          variation — 1,700 lb.
        residual — 900 lb.
    gross adapter weight at liftoff — 102,600 lb.
Booster Weights:
    third stage weight:
        empty — 58,900 lb.
        propellant — 526,100 lb.
    total third stage weight — 585,000 lb.
    second stage weight:
        empty — 158,500 lb.
        propellant — 1,350,000 lb.
    total second stage weight — 1,508,500 lb.
    first stage weight:
        empty — 364,500 lb.
        propellant — 4,000,000 lb.
    total first stage weight — 4,364,500 lb.
Gross vehicle weight at liftoff — 6,651,600 lb.
Payload weight to 100 n. mi. — 106,000 lb.
HL-10 wing loading at normal landing
(with 5,000 lb. cargo) — 54.4
HL-10 wing loading at first stage
abort landing — 62.3

Performance Characteristics:
    Design point cargo carrying
    capability (packaged) — 5,000 lb.
    Total cargo carrying capability
    (packaged) — 23,750 lb.
    ΔV capability with 5,000 lb. cargo — 6,312 ft./sec.
    ΔV capability with 23,750 lb. cargo — 2,864 ft./sec.

SPAN
28.325
FEET

LENGTH
44 FEET

C.G.
STA.
279.84

17.75 FEET

GROUND

30°

GROUND LINE
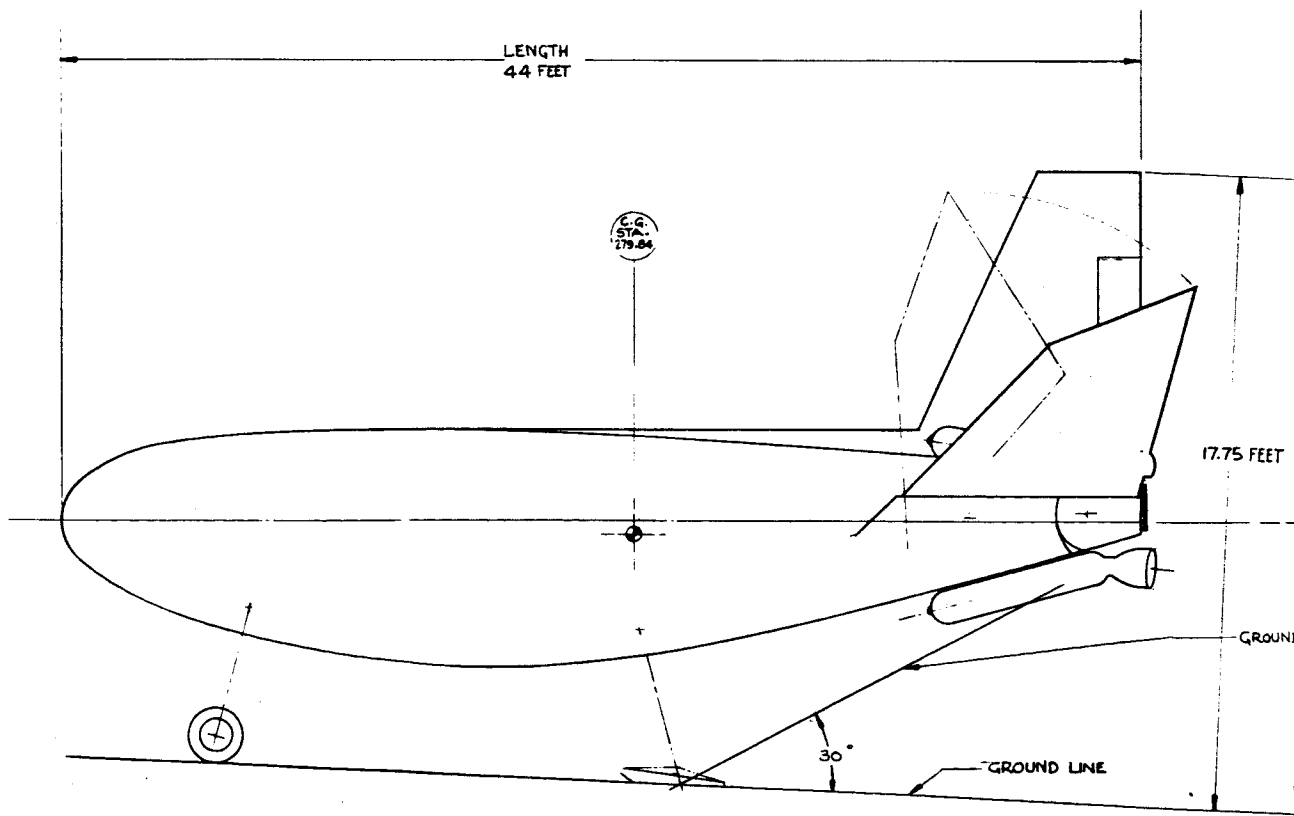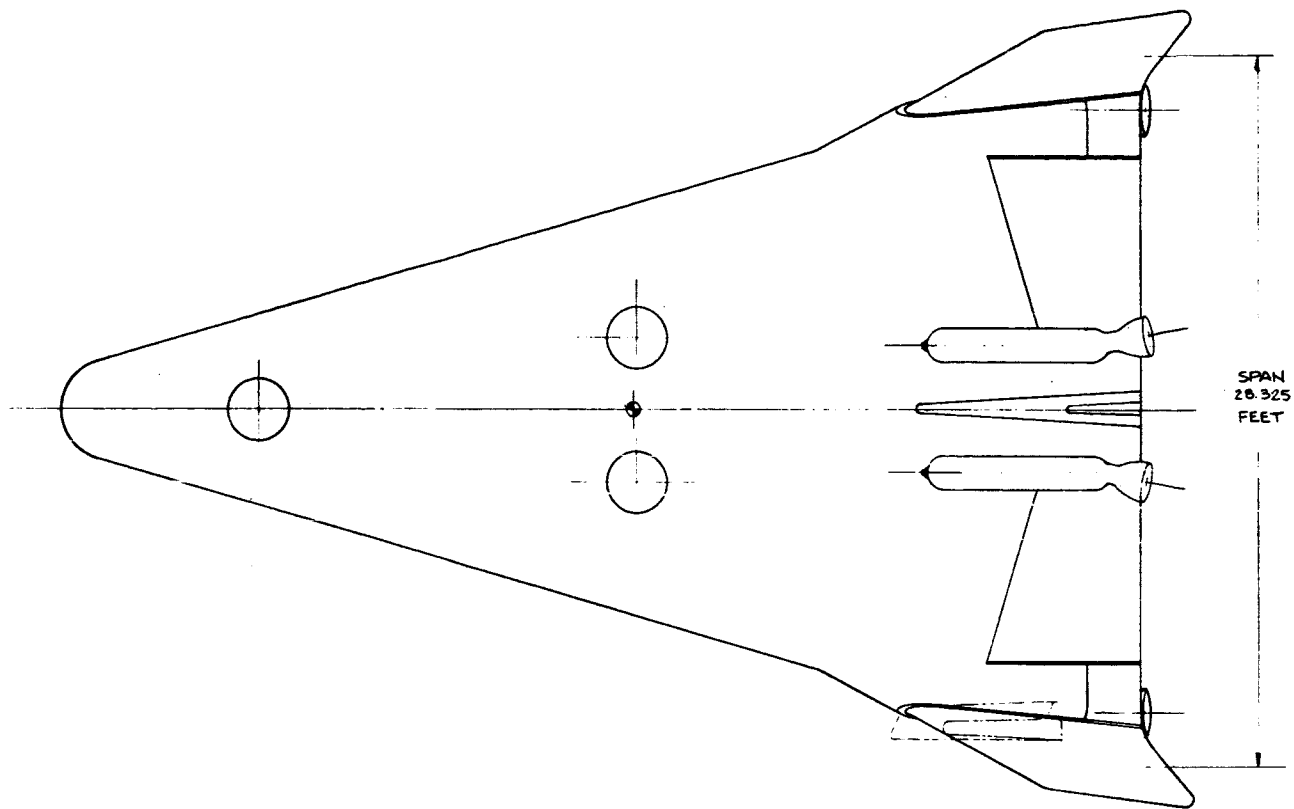
1#

29

DESIGN DATA

$S_{REF.}$	PLANFORM (NO FINS)	=	691. FT^2
$S_{REF.}$	FIN TOTAL (2)	=	101. FT^2
$S_{REF.}$	VERTICAL TAIL	=	68.5 FT^2
$S_{REF.}$	ELEVON TOTAL (2)	=	74.3 FT^2
TOTAL INTERNAL VOLUME (BODY)		=	4,200. FT^3
WETTED AREA		=	1,742. FT^2
GROSS WT. (INCLUDING ABORT ROCKETS)		=	91,000. LBS.
NORMAL LANDING WT.		=	37,200. LBS.
W/S NORMAL LANDING		=	54.4 P.S.F.

WL 100

LINE LIMIT

GROUND LINE
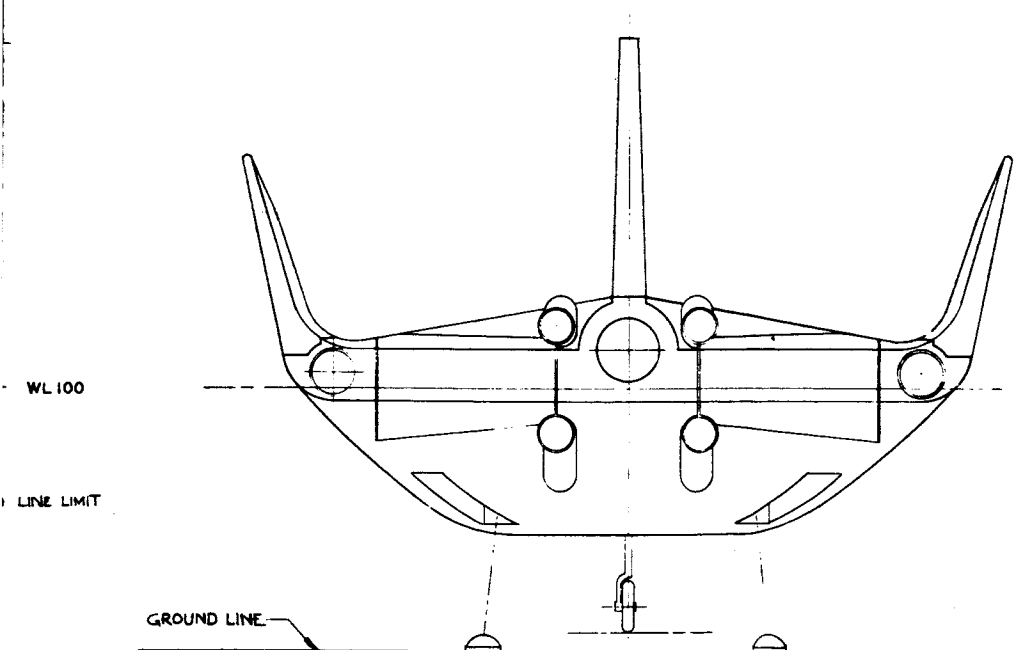
Figure 5-2 3 View Drawing HES-2G

2 #

BLOW-OFF WINDSHIELD FAIRING
WINDSHIELD
PILOT AND CO-PILOT
COMPARTMENT FLOOR
INSIDE SKIN AT STA. 66
PRESSURE BULKHEAD
CREW ACCESS HATCH

WL-100

VIEW LOOKING AFT - STA 66

WINDSHIELD
INSTRUMENT PANEL
CREW COMPARTMENT - 8 SEATS
COMPARTMENT FLOOR
INSIDE SKIN AT STA. 132
SUB-SYSTEMS EQUIPMENT
NOSE WHEEL WELL

WL 100

VIEW LOOKING AFT - STA 132

SAFETY HATCH - CREW COMPARTMENT
PRESSURIZED FUEL TANKS
CARGO COMPARTMENT AND CARGO
SUB-SYSTEMS
CRAWL TUBE
FUEL TANKS
INSIDE SKIN AT STA. 198

WL 100

VIEW LOOKING AFT - STA 198

INSIDE SKIN AT STA. 264
PRESSURIZED SHELL
CRAWL TUBE
CARGO
TUNNEL THROUGH CARGO COMPARTMENT
SUB-SYSTEMS EQUIPMENT
₵ CRAWL TUBE
₵ CREW ACCESS HATCH
INSTRUMENT PANEL
FWD EQUIPMENT STOWAGE
BLOW-OFF WINDSHIELD FAIRING
WINDSHIELD
STOWAGE UNDER SEATS
COMPARTMENT FLOOR

WL 100

VIEW LOOKING AFT - STA 264

STA 0

CRAWL TUBE
OXIDIZER TANKS
INSIDE SKIN AT STA. 330
NOSE WHEEL
STATIC GROUND LINE

WL 100

VIEW LOOKING AFT - STA 330

30

Figure 5-3 Inboard Profile – HES-2G

1 H

30

GIMB[...]
STEE[...]
ELEVO[...]
LAND[...]
FUEL[...]
OXID[...]
RCS[...]
ABOR[...]
AFT[...]
DOCK[...]
DOCK[...]

SPAN
28.325 FEET

RCS FUE[...]
CARGO [...]
OXIDIZE[...]
ELEVON[...]
GIMBAL[...]
STEERIN[...]

LENGTH
44 FEET

TIP FIN [...]
TIP FIN [...]
TIP FIN [...]
RUDDER

STA 66   STA 132   STA 198   STA 264   STA 330   STA 396   STA 462   STA 528

C.G.
STA
219.84

C OF CRA[...]
DOCKING[...]

STEERIN[...]
STEERIN[...]
FAIRED [...]

ABORT [...]

TIP FIN [...]

ALTERNA[...]
CARGO [...]
GROUND[...]

30°

2#   30
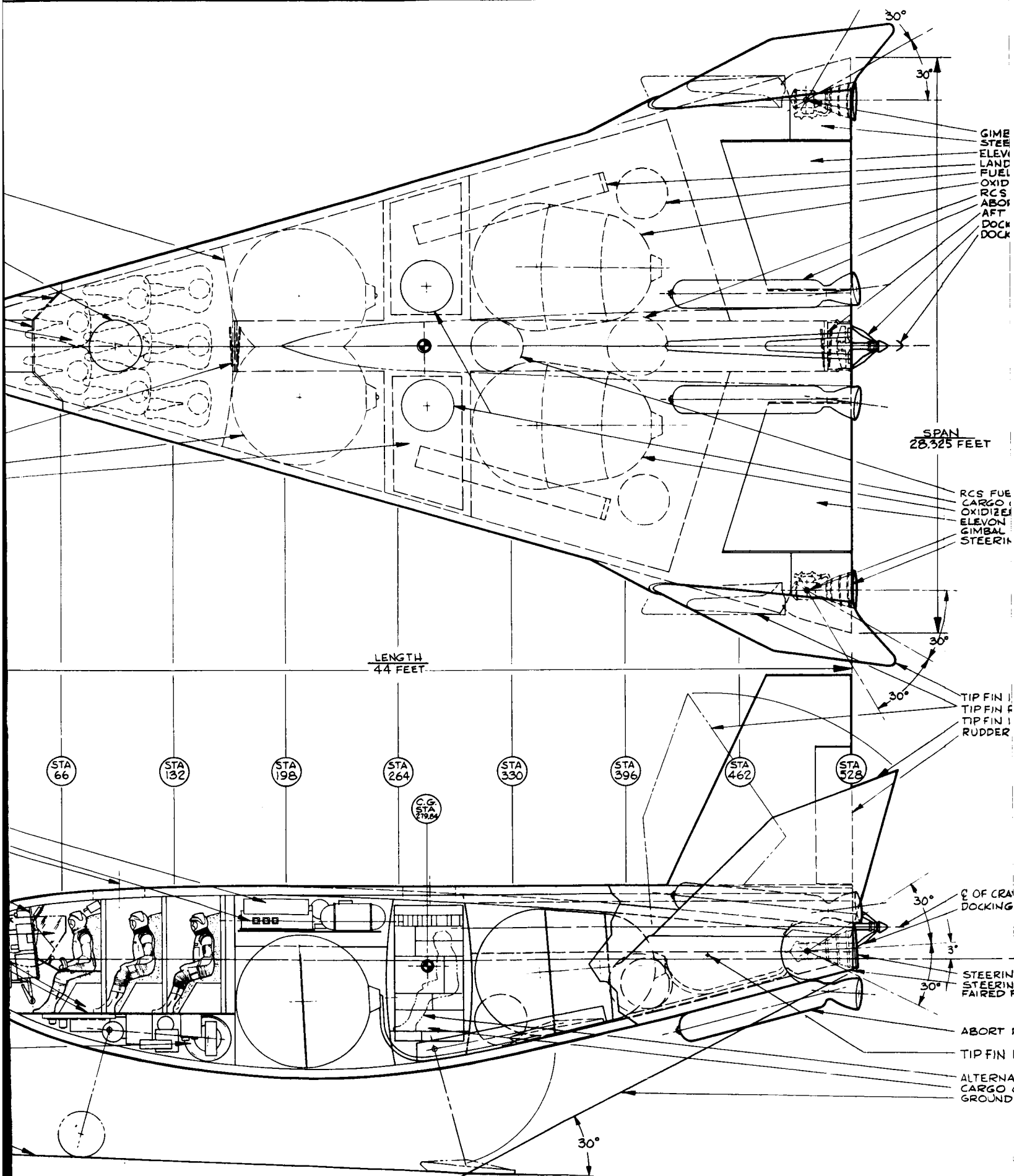
AL POINT FOR STEERING ENGINE
RING ENGINE AND SHROUD
ON
ING GEAR WELL
- PRESSURIZATION BOTTLE
IZER TANK-IN-ORBIT MANUEVERING PROPELLANT
OXIDIZER TANK
RT ROCKETS -TOP AND BOTTOM
HATCH IN CRAWL TUBE
ING MECHANISM
ING PROBE EXTENDED

L TANK
COMPARTMENT LOADING HATCH
R TANK-IN-ORBIT MANUEVERING PROPELLANT

POINT
IG ENGINE SHROUD

N RE-ENTRY POSITION
ROTATED FORWARD DURING BOOST
N RE-ENTRY POSITION
SURFACE

VL TUBE
MECHANISM

-- WL 100 --
ENGINE
ENGINE SHROUD
OR RE-ENTRY

ROCKETS

PIVOT

TE SEATING -3 TO 5 PASSENGERS
COMPARTMENT
LIMIT LINE

VIEW LOOKING FWD

2 CREW

4 PASSENGERS

4000 LBS. CARGO
(UNPACKAGED)

DOCKING

NORMAL LOADING-BASELINE MISSION

2 CREW

6 PASSENGERS

ADAPTER

4000 LBS. CARGO
(UNPACKAGED)

DOCKING

15000 LBS CARGO
(UNPACKAGED)

NORMAL LOADING-EXTENDED MORL MISSION

2 CREW

6 PASSENGERS

DOCKING

ADDITIONAL 3 TO 5 PASSENGERS
IN CARGO COMPARTMENT

ALTERNATE LOADING - EXTENDED MORL RESCUE MISSION
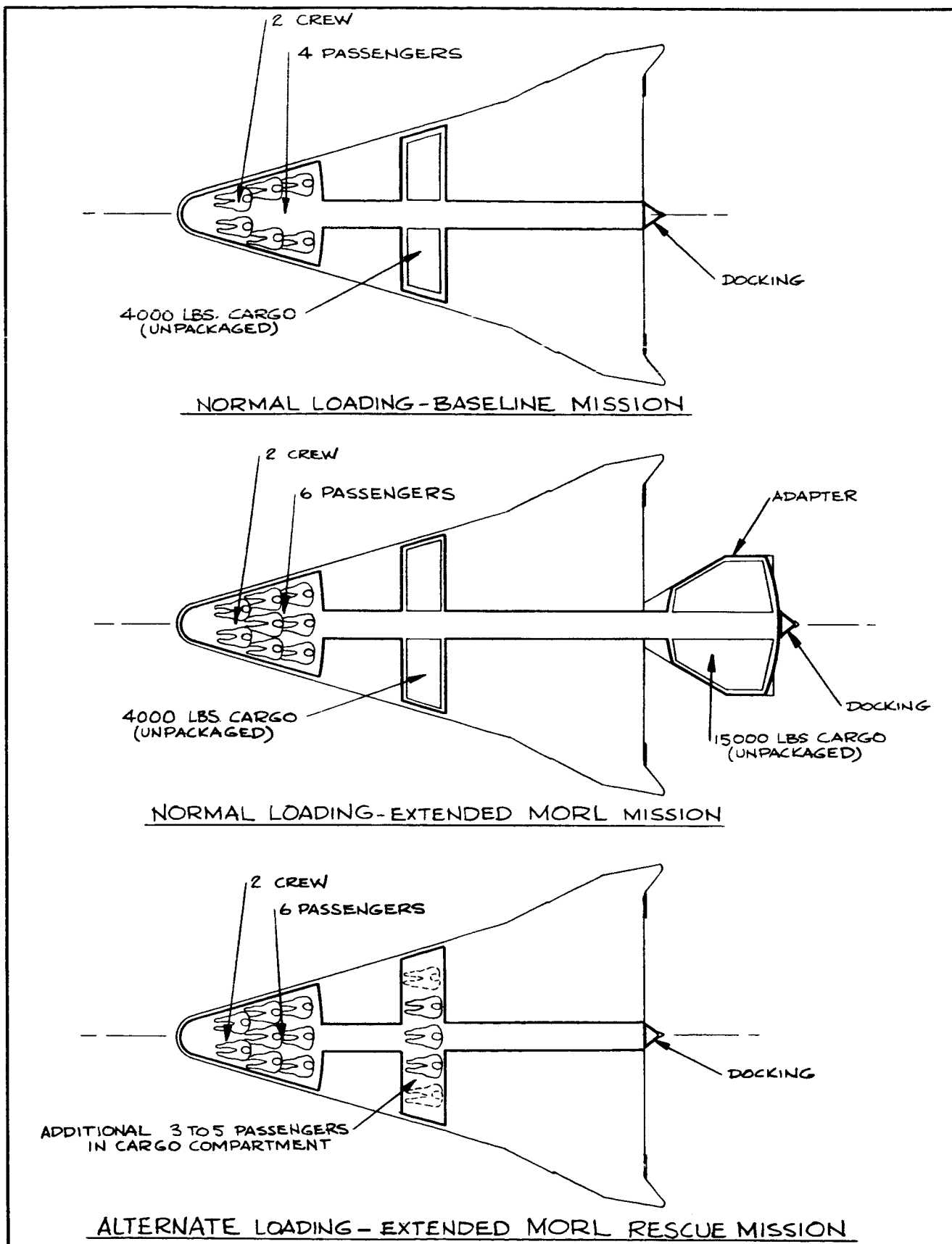
Figure 5-4 Crew-Cargo Arrangement – HES-2G

docking capability when the HL-10 is operated independently of the cargo adapter.

The adapter consists of two modules; a cargo module and a steering propellant module. This arrangement is shown in Figure 5-5. The cargo module has storage capability of 18,750 lb. of packaged cargo. The volume of the pressurized cargo compartment is 1,000 cu. ft. which allows for storage of the cargo, access through the compartment, and a one-man control station for the rendezvous and docking maneuver. This section of the adapter would be carried through rendezvous when the package cargo weight requirement is in excess of 5,000 lb. A docking cone is located on the aft end of the cargo module for this requirement, and the docking cone at the aft end of the HL-10 would be in a stowed position. Inflight separation planes are located at the aft end of the HL-10 and at the aft end of the cargo module.

The steering propellant module is located aft of the cargo module and is attached to the third stage booster motor by an assembly separation plane. This module consists of a common bulkhead propellant tank containing N_2O_4 and MMH. The propellants are forced up to the HL-10 mounted steering engines by means of a nitrogen pressurization system. The tanks are of sufficient volume to carry 88,400 lb. of steering propellant. The module is dropped at the end of the third stage burning as part of the expended third stage booster stage.

The third stage booster is a 156-in.-dia. monolithic, solid-propellant motor. This motor contains 526,100 lb. of an HC-type composite, solid propellant and develops 1,429,000 lb. of vacuum thrust. It provides an impulsive velocity increment of 13,550 fps to the vehicle.

The second stage booster is a 260-in.-dia. monolithic, solid-propellant motor containing 1,350,000 lb. of HC-type propellant. It develops 3,240,000 lb. of vacuum thrust and provides an impulsive velocity increment of 8,534 fps to the vehicle.

The first stage booster is also a 260-in.-dia. monolithic solid-propellant motor containing 4,000,000 lb. of propellant and developing 8,263,000 lb. of
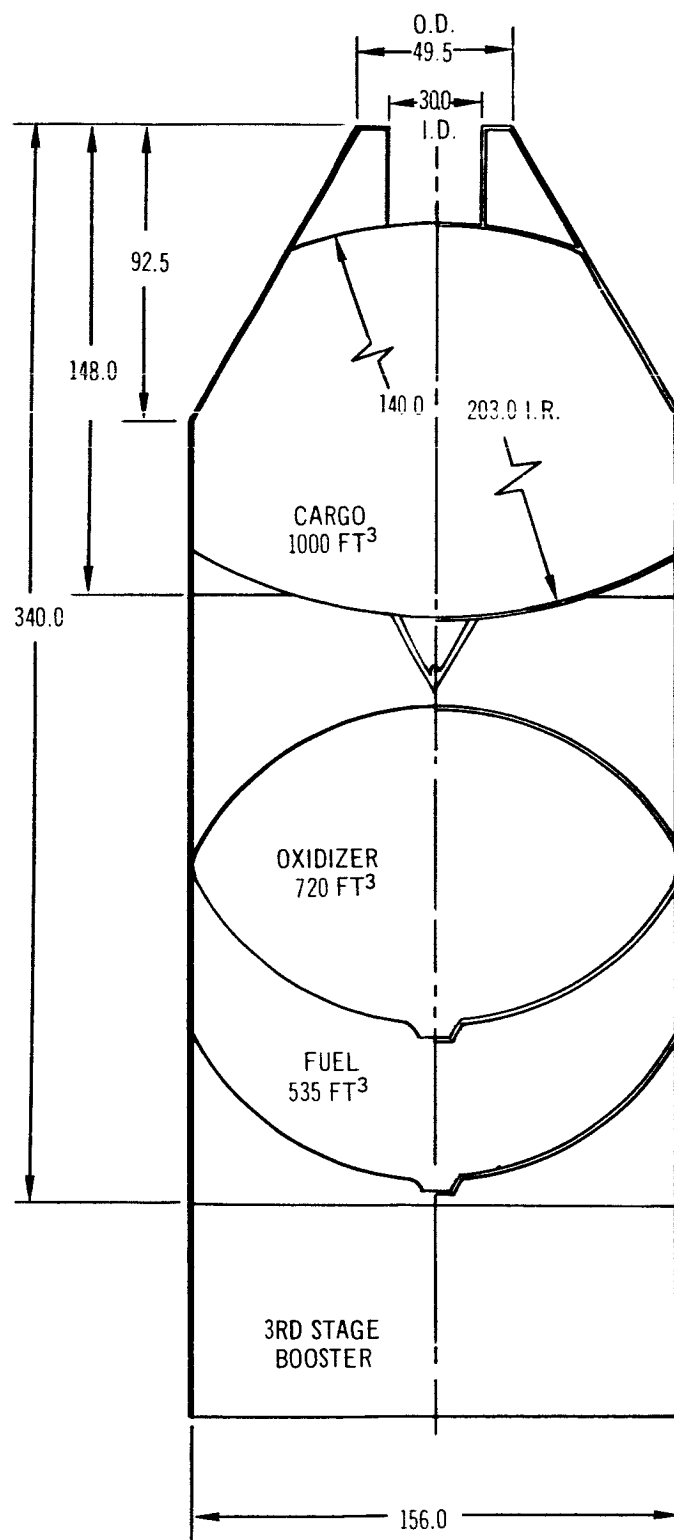
Figure 5-5   Adapter Arrangement Drawing

sea level thrust. It provides an impulsive velocity increment of 7,799 fps to the vehicle.

The actual payload carried to 100 n.mi. by the boosters is 106,000 lb. The payload placed in a 300 n.mi. circular orbit at an inclination of 31° is 71,900 lb. (5,000 lb. of packaged cargo). The 6,300 fps impulsive velocity capability on board the HL-10 provides for approximately 2,250 fps of required maneuvers and 4,050 fps for optional missions with 5,000 lb. of cargo on board the HL-10.

5.2 SPACECRAFT SUBSYSTEM

The scope of the study, as defined in Sections 1, 2, and 3, is to develop a concept for a simplified, partially reusable manned space vehicle using head-end steering and solid-propellant booster motors, and then to evaluate the feasibility of this concept. The HL-10, as defined in Reference 1, was selected as the spacecraft to be used in the study. This spacecraft was to be defined only to the depth required to fulfill study objectives. Therefore, only those spacecraft subsystems which affected the concept feasibility were investigated in detail. This includes those subsystems which are affected by the unique guidelines and mission requirements associated with this study, and which, in turn, affect the operation, size, or weight of the spacecraft. The subsystems which were found to fit into this category included:

1. Structure and thermal protection
2. Propulsion
3. Stability and control
4. Onboard checkout

These systems are discussed in the following subsections.

Model subsystems, based on the previous work with the HL-10 outlined in Section 5.8, Reference 1, were established for those spacecraft subsystems which had a minor effect on vehicle weight and operation as related to the head-end steering concept. These systems were investigated only with respect to their capability to meet the functional requirements established by the study variables, and with respect to the resultant effect on spacecraft size and weight. Subsystems in this category include:

34

1. Environmental control
2. Crew systems
3. Landing systems
4. Electrical power
5. Guidance and navigation
6. Communications, telemetry, and tracking
7. Rendezvous and docking
8. Displays
9. Abort system

The weights resulting from the limited investigation performed on these subsystems are shown in Section 5.5. The abort, rendezvous and docking systems are described in some detail in Sections 6.3 and 6.4.

Previous preliminary design experience with lifting body spacecraft, such as that documented in Section 5.8, Reference 2, was used both to guide the design of subsystems investigated in detail and to determine the capability of existing HL-10 subsystems to meet the demands placed on them.

5.2.1 HL-10 Structure and Thermal Protection

The HL-10 structure was assumed to consist of aluminum sheet and stringer construction with an ablative coating providing thermal protection for the entire vehicle. An average ablative coating weight of 3.5 lb./sq. ft. of HL-10 surface was assumed to provide adequate protection. The average weight of the corrugated aluminum skin was estimated at 1.0 lb./sq. ft. of HL-10 surface. Frame and stringer weights were based on data provided in Reference 1 and modified to account for HL-10 size. The pressurized crew and cargo compartments were designed to ultimate pressures of 20 psia based on a safety factor of 4.0 times operating pressure. Pressurized bulkheads were considered to be of aluminum monocoque construction.

5.2.2 Propulsion Subsystem

The propulsion subsystem is designed to fulfill two primary functions. One of these functions is to provide pitch, yaw, and roll control, or steering, during the launch trajectory boost phase. The other function is to provide translational control for various spacecraft maneuvers. These spacecraft maneuvers include vernier injection immediately following third stage booster burnout,

plane change during coast to 300 n. mi., terminal rendezvous, deorbit and alternate mission translational maneuvers. The impulsive velocity requirements for all of these maneuvers are shown in Section 5.6 under Mission and Performance Capability. The microrendezvous, docking, separation, and other attitude control functions throughout the flight profile will be provided by the low-thrust positive-expulsion reaction control system. The propulsion system is described under functional headings in the following subsections. A schematic illustrating the more important features of the entire propulsion system is shown in Figure 5-6. Characteristics of the propulsion system are listed in Table 5-2.

Table 5-2
PROPULSION SUBSYSTEM CHARACTERISTICS

Rocket engine (2):

Type -	Storable liquid, turbopump-fed
Thrust -	50,000 lb. vacuum
	44,600 lb. sea level
Propellants	Nitrogen tetroxide
	Mono methyl hydrazine
Oxidizer/fuel ratio	2.2:1
Expansion ratio	10:1
Chamber pressure	800 psia
Delivered specific impulse	284.5 sec. (vacuum)
Overall length	40.0 in.
Throttle ratio	32% full thrust
Gimbal capability	±30° pitch and yaw

Weights:
Engines and actuation	1550 lb.
In-orbit maneuver subsystem:	
Usable propellant	43,000 lb.
residual propellant	900 lb.
Pressurization system	680 lb.
Tankage, supports and distribution	1,560 lb.
Total wet weight on board HL-10	47,690 lb.

Steering Subsystem:
Usable propellant	85,800 lb.
Allowance for booster burn-time variation	1,700 lb.
Residual propellant	900 lb.
Pressurization system	2,030 lb.
Tankage, supports and distribution	8,270 lb.
Total wet weight in adapter	98,700 lb.

FUEL

OXIDIZER

OXIDIZER

GAS

GAS

HL-10

CARGO
MODULE

INFLIGHT
SEPARATION PLANE

STEERING
PROPELLANT
MODULE

OXIDIZER

FUEL

GAS

GAS
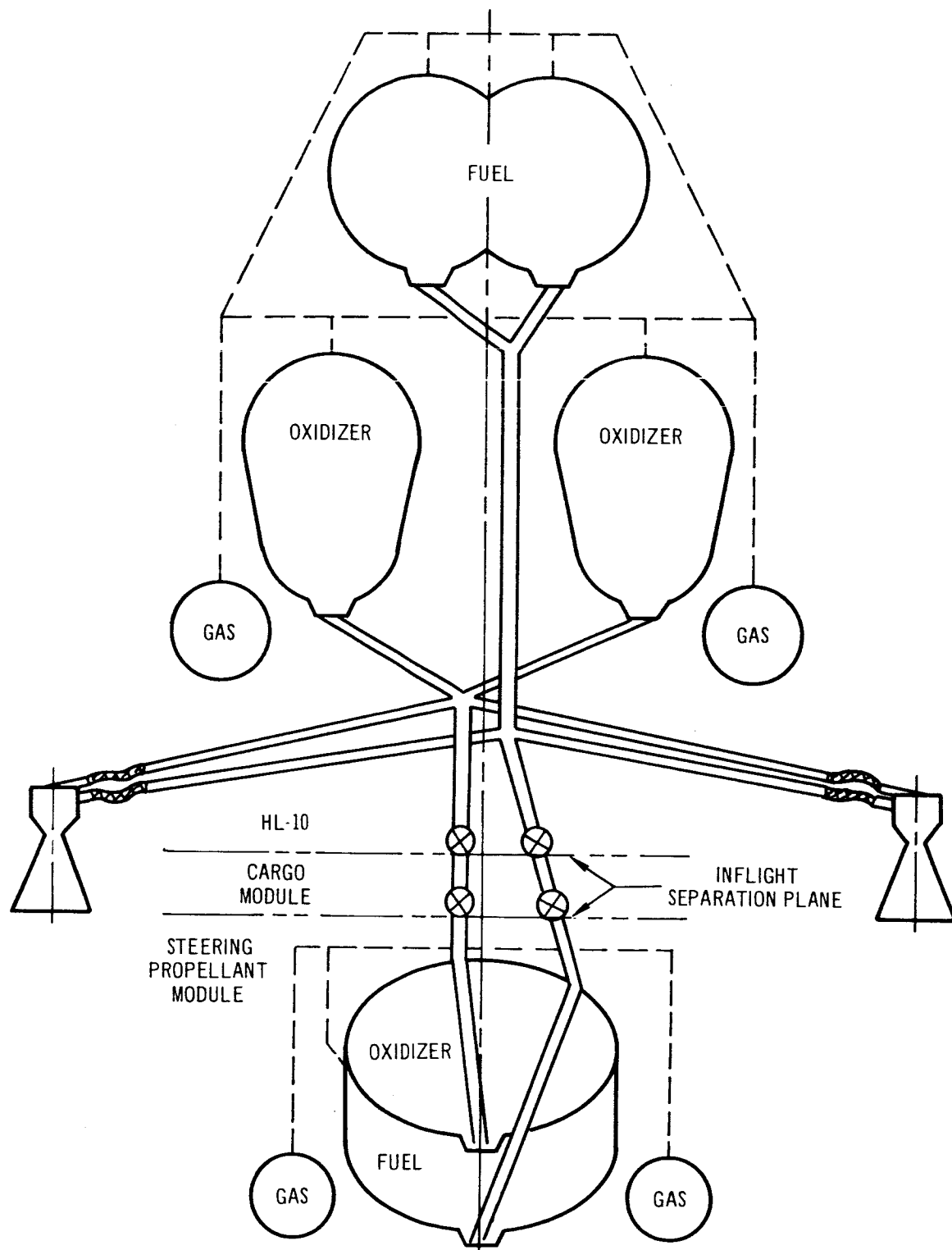
⊗ GUILLOTINE SHUTOFF VALVE
〰 FLEX HOSE
Ⅹ GIMBALING TURBOPUMP ROCKET ENGINE

Figure 5-6 Propulsion Subsystem Schematic

5.2.2.1 Steering Propulsion

The steering propulsion subsystem consists of the following major components:

1. A common bulkhead, storable, liquid-propellant tank;
2. A nitrogen gas-pressurization system;
3. Two gimbaled liquid-propellant turbopump-fed rocket engines.

This system provides thrust for steering the vehicle throughout the boost phase of the launch trajectory.

The propellants used are the Earth storable, hypergolic combination of Nitrogen Tetroxide, N_2O_4, as oxidizer, and Monomethyl Hydrazine, MMH, as fuel. The oxidizer-fuel mixture ratio of 2.2 is used to maximize energy. These propellants are stored in a common bulkhead-type aluminum tank located immediately above the third stage booster motor in the aft section of the adapter. These tanks, for preliminary design purposes, were sized on the basis of a 125 psia operating pressure to overcome distribution system losses and head losses during boost.

Pressurization is provided by means of two titanium, high-pressure nitrogen storage bottles located in the adapter that are connected to the propellant tanks by a pressure regulation and gas distribution system. Nitrogen storage pressure was assumed to be 3,000 psia for sizing purposes.

Propellant transfer lines pass through the propellant tankage, the forward cargo adapter, and across two inflight separation planes before connecting to the engines which are located on board the HL-10. Guillotine-type shutoff valves are located in the feed lines at both inflight separation planes to provide positive shutoff at separation. The engines are at the aft end of the HL-10 located outboard of the elevons. They are fed from a manifold located at the center of the HL-10, which is connected to both the steering propellant and onboard maneuver propellant tanks.

The rocket engines are of the turbopump-fed, regeneratively cooled type. The turbopump provides a chamber pressure of 800 psia. This high chamber pressure is required in order to provide minimal engine size for the steering thrust required. To reduce the physical size the nozzle expansion ratio is held at 10. An illustration of the engine used for layout and sizing purposes

is shown in Figure 5-7. This engine produces 50,000 lb. of thrust at vacuum conditions in order to meet the steering requirements of the vehicle. The delivered vacuum specific impulse is 284.5 sec. By incorporating thrust modulation capability in the engine design, the propellant weight required for steering is appreciably reduced. This saving in propellant and tankage weight is approximately 46,000 lb. For this vehicle configuration, thrust is modulated to approximately 32% of full thrust during second stage boost, and to 70% of full thrust during third stage boost. A gimbal capability of ±30° in yaw and in pitch can be provided by either of two gimbaling techniques. In both techniques, the turbopump is fixed to the thrust chamber so that only the low-pressure lines require flexing or sealing. In one technique, flex hoses of sufficient lengths and bend radii are arranged and utilized to provide adequate movement in any direction without applying torque to the flex hose. The flex hoses would be designed to fit the limited available space adjacent to the engines. The
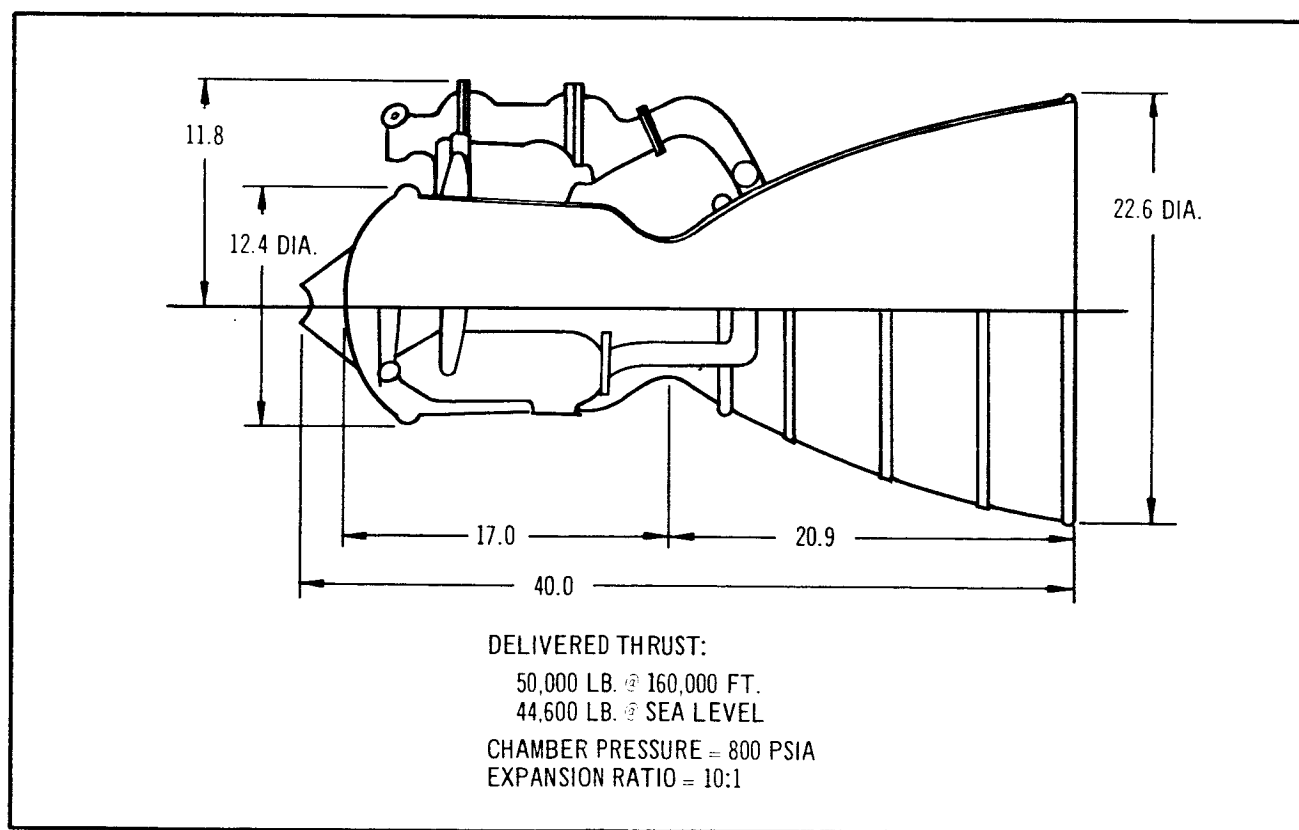
Figure 5-7 HES-2G Steering and Maneuver Rocket Engine

other technique requires dynamic seals so that the fuel and oxidizer can be passed through the gimbal bearings and quadrants of the gimbal ring into the turbopump inlet feed lines. Both of these techniques are feasible but would require sizeable development efforts to attain the large gimbal angles required by this system.

The rocket engines have partial shrouds to protect them from aerodynamic heating during the boost and re-entry phases. The shroud is designed so that it will not appreciably increase the outer wall temperature of the engine nozzle or chamber.

5.2.2.2 Maneuver Propulsion

The propulsion system used to provide maneuver capability, and those functions required other than steering, consist of:

1. One storable-liquid fuel tank
2. Two storable-liquid oxidizer tanks
3. A nitrogen gas pressurization system
4. Two gimbaled, liquid propellant, turbopump-fed rocket engines.

This system provides thrust for translation of the spacecraft throughout the mission subsequent to boost. It also provides thrust to supplement that of the abort system solid propellant rocket motors in the event that abort is required during the boost phase.

The propellants used in this portion of the propulsion system are the same type as those used for steering. The fuel, MMH, is stored in a single tank located in the HL-10 between the crew compartment and the cargo compartment. Its "Siamese", double-sphere shape allows utilization of a crawl-tube passageway between these two compartments without the large weight penalty associated with odd shaped pressure vessels. The oxidizer, N_2O_4, is stored in two tanks located aft of the cargo compartment. These tanks are conical in shape with hemispherical domes. Both the fuel and oxidizer tanks are sized for operating pressures of 50 psia in order to provide sufficient turbopump inlet pressures. The pressurization system consists of nitrogen gas, stored at ambient temperature at 3,000 psia, in two titanium, spherical pressure bottles. A pressure regulation and distribution system connects these bottles to the propellant tanks.

The propellants are carried through a distribution system to the same engines used to provide steering thrust. As shown in Figure 5-6, the oxidizer lines from both the steering propellant tanks and the maneuver propellant tanks are joined at a common manifold which feeds oxidizer to the engines. This is also true of the fuel feed lines. In this way, means are provided for eliminating the possibility of trapping gas in feed lines (a problem commonly associated with uphill feed systems), and also, means are provided for rapid transfer of the propellant source in case abort is required during the boost phase.

The timing of the translational thrust requirements for the various maneuvers dictates incorporation of stop-start capability in the rocket engine design. This can be used in conjunction with the throttling capability of the engines to provide the impulsive velocity increments and thrust-to-weight ratios required.

5.2.3 Stability and Control System

The SCS for all modes of flight (boost, orbit, rendezvous, re-entry, and landing) exhibits a commonality of electronics. This equipment will be located within the HL-10 and is, therefore, returned and can be reused. Within this electronics package will be the mode switching and circuit logic to accommodate all mission phases. Figure 5-8 is a simplified schematic showing salient features of the system.

During the powered portion of boost, HL-10 elevons and rudder will be locked in their null positions. Vehicle control will be accomplished through the use of two 50,000-lb. thrust engines, capable of being gimballed ±30° in pitch and yaw (see Figure 5-9). To obtain the necessary response to guidance commands, the boost control system was designed for natural frequency and damping of 0.15 cps and 0.7. The maintenance of these characteristics will involve discreet or continuous gain changes (adaptive gain control) in both the attitude and rate feedback loops due to large shifts in vehicle inertia and CG. From liftoff through third-stage burnout the approximate excursion of these two gains will be:

1. Attitude (64.0 to 5.03)
2. Rate feedback (94.2 to 7.42)
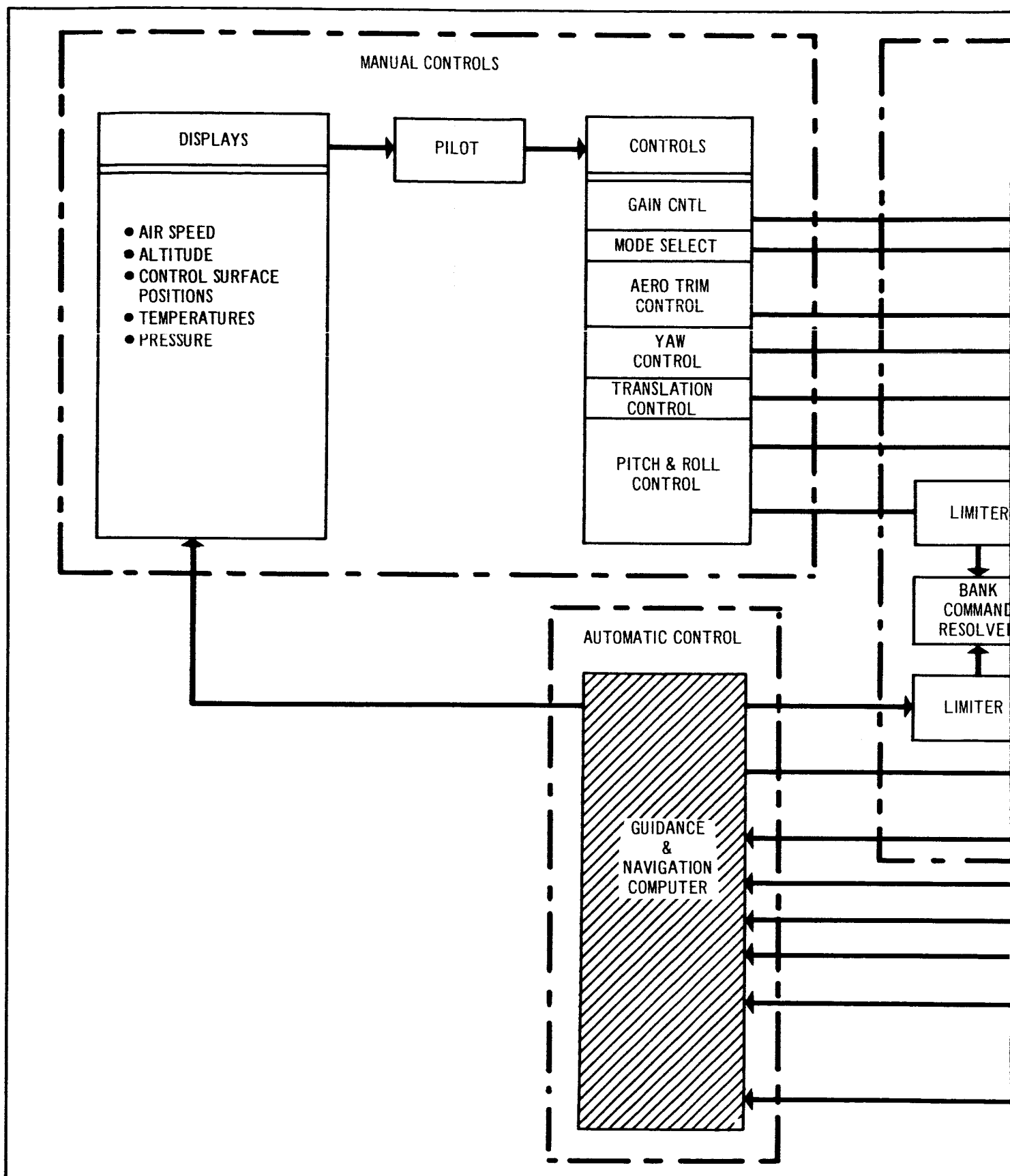
Figure 5-8 Stability and Control System Block Diagram

CONTROL ELECTRONICS

ADAPTIVE
GAIN
CONTROL

CONTROL
MECHANICS

CONTROL ENGINE
ACTUATORS

VARIABLE
GAIN
AMPLIFIER

CONTROL
SURFACE
ACTUATORS

MODE-
SWITCHING
ELECTRONIC

SWITCHING
DEADZONE

ATTITUDE
VALVE
DRIVERS

SUMMING
NETWORKS

MANEUVER
VALVE
DRIVERS

VAR. GAIN
AMPLIFIER

SENSORS

RATE
GYROS

INERTIAL
REFERENCE

CONT. ENG.
POSNS

ELEVON &
RUDDER
POSITIONS

PRESSURE
SENSOR

TEMP
SENSORS

2# (42)

NOTES:
REF. = NULL POS'N OF ENGINES
T_1 = NO. 1 ENGINE THRUST
T_2 = NO. 2 ENGINE THRUST
δ_{Y1} = YAW ANGLE – NO. 1 ENGINE
δ_{Y2} = YAW ANGLE – NO. 2 ENGINE
δ_{P1} = PITCH ANGLE – NO. 1 ENGINE
δ_{P2} = PITCH ANGLE – NO. 2 ENGINE
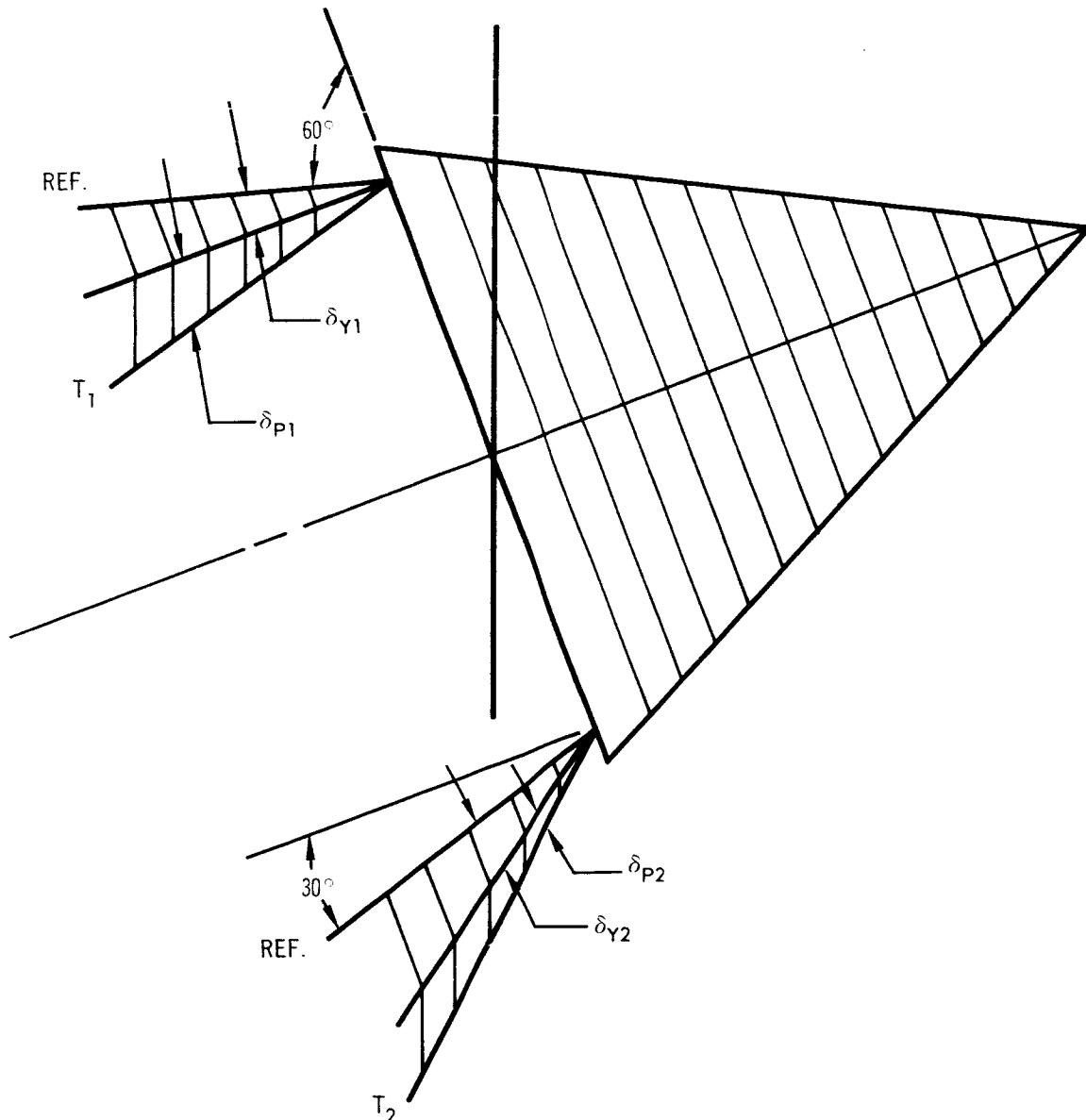
Figure 5-9 HL-10 Steering Engine Gimbal Coordinate Definition HES-2G

The booster control engines will be throttleable to take advantage of the reduced control moment demands of second and third stage operation. By so doing, a significant savings in steering propellant can be realized with attendant reductions in booster size. With continuous operation of steering engines, satisfactory control during separation of booster stages should be easily accomplished. A detailed analysis of the booster control system may be found in Section 5.5.

A reaction jet system aboard the HL-10 was sized to accomplish the following tasks, listed with their equivalent ΔV requirements:

1. Terminal rendezvous and docking - 50 ft./sec.
2. Attitude control - 150 ft./sec.
3. Separation from space laboratory - 50 ft./sec.

This information did not arise from efforts associated with the subject study, but rather extrapolations from Section 5.8, Reference 1. It is noted that the HL-10 boost steering engines are capable of performing orbit injection and mid-course rendezvous functions. They may also be used for in-orbit maneuvering, deorbit impulse, orbit maintenance, all as a portion of the abort propulsion, and perhaps as supplementary support in the re-entry and landing maneuver. Substantiation of the latter use would require a follow-on study.

Inasmuch as re-entry control was not a part of this study, no attempt to elaborate beyond the results indicated in Reference 1 will be shown here. It has been assumed that the HL-10 reaction jet system used in conjunction with rendezvous, docking, attitude control, and separation, would be capable of providing bank angle control during the hypersonic portion of re-entry. Aerodynamic surfaces would be fully active at the end of the re-entry guidance phase (approximately Mach 4); they would be employed in a system similar to those used in the X-15 and X-20 aircraft.

5.2.4 Onboard Checkout

A checkout system is provided onboard the spacecraft for the purpose of test and checkout of the various systems and for the detection of failure in the space-craft components. In order to maintain an overall approach to simplification in both the vehicle and in support operations, it was considered desirable for

the flight crew to assume a major role in preflight checkout procedures. The onboard checkout and malfunction detection system generic diagram is shown in Figure 5-10. This system has a test mode and an operational mode. In the case of the test mode, faults in the system may be isolated down to some predetermined level. The mission is allowed to proceed under known constraints or is held for corrective action. In the operational mode, the alternative to accepting mission constraints is to abort. The latter situation is, of course, mandatory for "life-critical" failures.

Table 5-3 classifies the effect of a given malfunction in order that the fault isolation level and corrective action requirements may be optimumly determined with respect to mission degradation and crew safety. A functional diagram of the checkout system is presented in Figure 5-11. The role of the pilot as test conductor, the concept of automatic and manual test, and the interface with remote testing are indicated in this figure.

5.2.5 Adapter Cargo Module

The primary structure is constructed of monocoque and waffled aluminum and designed for a maximum dynamic pressure condition of 1,000 lb./sq. ft. Spherical segment domes with a height-to-radius ratio of 0.2 were used for the cargo compartment. Due to the heavy sidewall weight and the low design pressure (20 psi), this type of dome is optimum. Docking structure with shock absorption provisions are mounted on the aft cargo compartment dome. An ablative coating protects the structure from exit heating and from the hot exhaust gases of the steering motors. The cargo compartment will be pressurized to 5 psia nominal. The pressurized cargo compartment size is based on providing sufficient volume for storage of 15,000 lb. of unpackaged cargo, access through the compartment, and provision of a docking control station in the compartment. The cargo volume required is based on an estimated average cargo and packaging density of 20 lb./cu. ft. with a volumetric loading efficiency of 75%. The cargo packaging was assumed to weigh 25% of the unpackaged cargo weight.
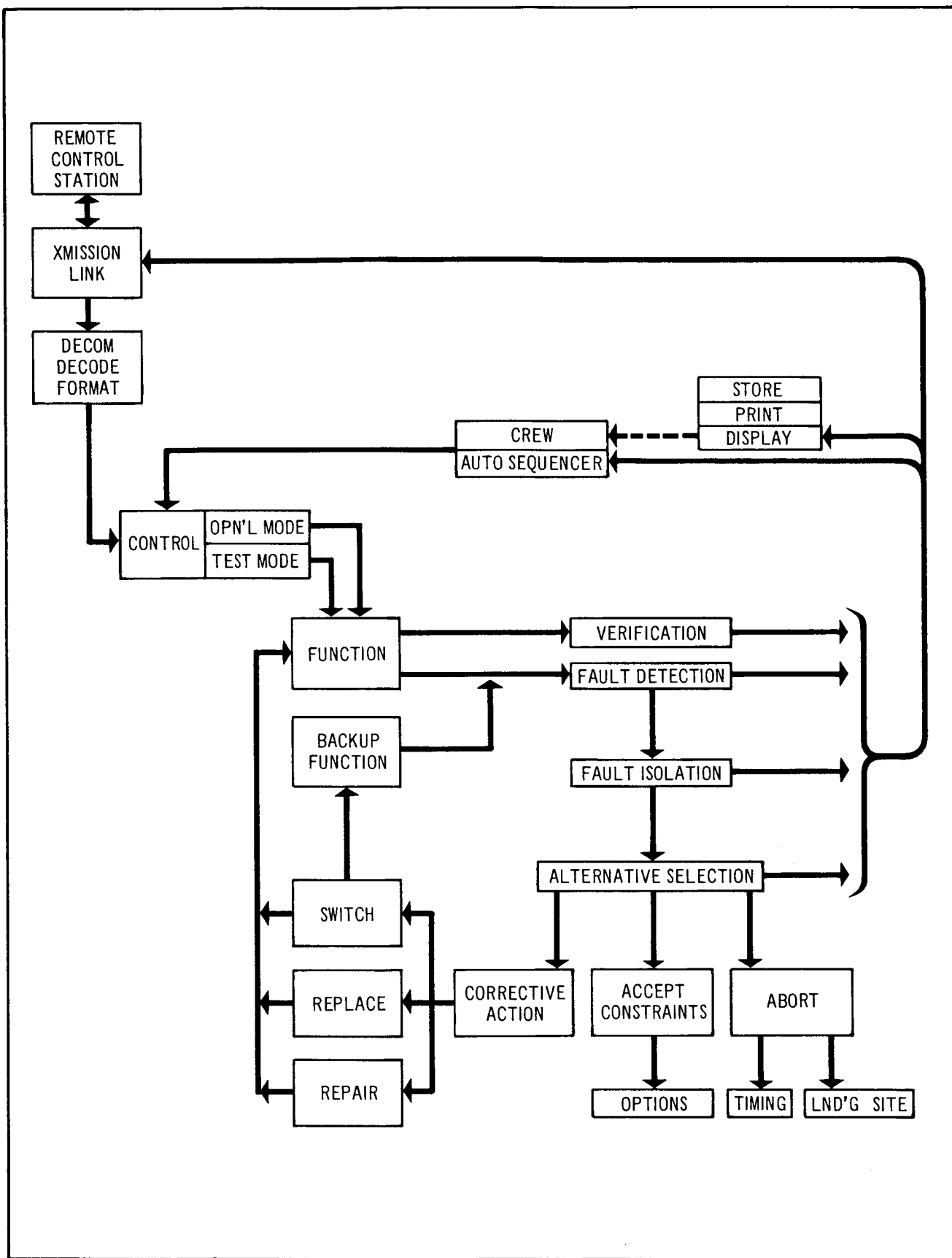
Figure 5-10 Generic Diagram – Onboard Checkout

Table 5-3

MALFUNCTION EFFECT CLASSIFICATION (Page 1 of 2)

System Function	Life Critical	Mission Critical	Non-critical
1. Structure			
Pressure compartment			X
Thermal protections	X		
2. Environmental Control			
Humidity control		X	
CO_2 control		X	
Temperature control		X	
Oxygen supply		X	
Cold plate temperature control	X		
Coolant supply	X		
NH_3 supply	X		
3. Crew system			
Suits	X		
Temperature control		X	
Water supply		X	
Back packs	X		
4. Electrical Power			
Main dc bus		X	
Actuator power bus	X		
ac bus		X	
Emergency bus	X		
5. Guidance and navigation			
Inertial reference		X	
Computer		X	
Star tracker		X	
Horizon scanning		X	
6. Communication-T/M-tracking			
Voice transmission and receiving		X	
Data acquisition and transmission			X
Beacon transponder			X
7. Onboard Checkout			
Data acquisition	X		
Program and compute	X		
Stimuli generation			X
8. Rendezvous and Docking			
Radar		X	
Television			X
Optics		X	
Attach mechanism		X	
Intervehicular seal		X	
Interconnects		X	

Table 5-3 (Page 2 of 2)

System Function	Life Critical	Mission Critical	Non- critical
9. Propulsion			
Thrust vectoring		X	
Orbit insertion and maneuvering		X	
Deorbit	X		
Attitude control and rendezvous translation	X		
10. Stability and Control			
Reaction control		X	
Attitude control and rendezvous translation	X		
Aerodynamic control	X		
11. Landing			
Wheel and skids		X	
Drag chutes		X	
Landing aids		X	
12. Abort			
Parachutes	X		
Flotation	X		
Sequential control	X		
Propulsion	X		
13. Displays			
Operational		X	
Onboard checkout		X	

5.3 THE BOOSTER VEHICLE

5.3.1 Booster Propulsion

Booster propulsion consists of three fixed-nozzle, large solid-propellant motors. Provision for thrust vector control is not incorporated in any of the booster motors. The motor design and performance of the booster motors reflect the technology which is currently being developed in the large solid motor demonstration program (Program 623A). The motor performance used in this study, however, is a modification of the 623A-program performance since the demonstration program requirements do not reflect the 260-in. motor potential when integrated into a particular flight system. Certain changes were made which improved performance, but in no case did these changes require extension of solid motor state-of-the-art beyond that which will be in
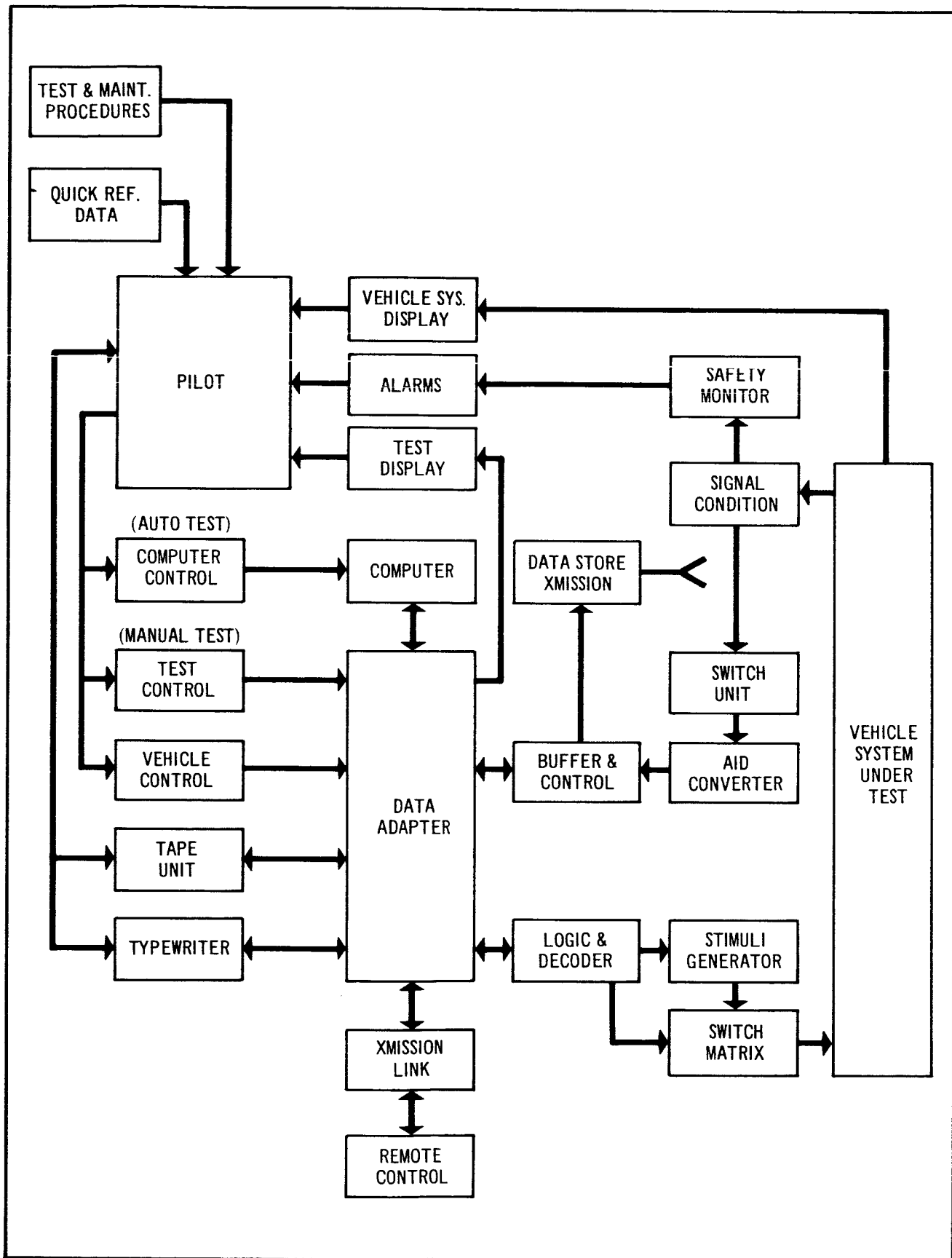
Figure 5-11 Functional Diagram – Onboard Checkout

existence during the time period of the 623A program. The nature and purpose of this study did not permit an extensive motor design optimization study of each of the stages. However, sufficient detail was pursued to ensure that the selected, motor performance parameters were within the physical limitations of each motor size and were consistent with the 623A-program technology.

The propellant used for all three motors of the boost vehicle is the terminally-carboxylated poly-butadiene type. It has a standard specific impulse of 250 sec. and a burn rate range capability of from 0.2 in./sec. to 0.8 in./sec. at 1,000 psia chamber pressure.

Burning of each of the three booster stages was represented by a simplified constant thrust time trace for the trajectory analysis. The web propellant which constitutes 93% of the total propellant burns at a constant rate for the duration of the web burn time. The remainder of the propellant, (the sliver) is assumed to burn in the tail-off portion of the pressure time trace. The tail-off pressure regresses at a constant rate until the sliver propellant is consumed.

The three booster motors have a port-to-throat ratio (ratio of grain port area to nozzle throat area) of 1.3.

A check on grain design confirmed that simple, star grain designs were obtainable for each motor based on a combination of the assumed value of sliver percent, port-to-throat ratio, and propellant burn rate limitations.

5.3.1.1 First Stage

A summary of the booster performance parameters are listed in Table 5-4. Overall motor dimensions are shown in the vehicle arrangement drawing, Figure 5-1. The first stage of the booster is a 260-in.-dia. solid-propellant rocket motor. The motor contains 4,000,000 lb. of propellant and develops 8,263,000 lb. of thrust at liftoff. The web burn time of 107 sec. was selected to obtain a liftoff thrust-to-weight ratio of 1.25. The nozzle exit diameter is limited to the maximum vehicle diameter of 260 in., resulting in an expansion ratio of 6.70. Though the nozzle is considerably under-expanded at this expansion ratio, a larger expansion ratio would require flaring of the aft skirt and would pose a number of design and handling problems. The nozzle

Table 5-4

BOOSTER VEHICLE PERFORMANCE SUMMARY

Stage	Propellant Weight (lb. x 10⁶)	Web Burn. Time (sec.)	Avg. Web Thrust (15 x 10⁶) (lb. x 10⁶) Vac	S.L	Specific Impulse (sec.) Vac	S.L	Mass Fraction	Length In.	Dia. In.	Chamber Pressure psia	ϵ *
1st	4.0	107	9.022	8.263	264	238	0.924	1897	260	644	6.3
2nd	1.35	110	3.24	2.43	284	213	0.905	812	260	644	20
3rd	0.526	100	1.429	1.070	292	218	0.904	674	156	775	25

* ϵ = nozzle expansion ratio

51

has a conical expansion section with a 17.5° half angle. The motor mass fraction is 0.924. The motor operating chamber pressure is 644 psia (corresponding to that used in the 623A program). Time limitation did not permit optimization of chamber pressure as well as other motor performance parameters. The first stage motor utilizes a launch-pad mounted, pyrogen-type ignition system mounted on the launch pad.

5.3.1.2 Second Stage

The second stage motor is a 260-in.-dia. motor with a propellant loading of 1,350,000 lb. This motor develops 3,240,000 lb. of thrust at vacuum conditions. The motor case is similar in design to the first stage, but with a shorter cylindrical section. The nozzle has a contoured expansion section. The exit diameter is limited to 260 in. which results in an expansion ratio of 20. The vacuum specific impulse is 284 sec. A web burn time of 110 sec. was selected for this motor. The motor mass fraction is 0.905, which is somewhat lower than the first stage mass fraction. This results from the fact that a heavier, high expansion ratio nozzle is used; in addition, the motorcase length is off-optimum. The motor will be ignited from the head end.

5.3.1.3 Third Stage

The third stage is a 156-in.-dia. motor with 526,100 lb. of propellant. The motor develops an average vacuum thrust of 1,429,000 lb. The motor uses a monolithic motor case and has a mass fraction of 0.904. The third stage motor has a contoured bell nozzle with an expansion ratio of 25. The vacuum specific impulse is 292 sec. The motor chamber pressure is 775 psia. The web burn time of 100 sec. was chosen to minimize steering propellant while staying within the allowable burnout acceleration limit. Head-end ignition is utilized.

5.3.2 Booster Thrust Misalignment

Thrust misalignment is a major factor in determining the feasibility of the head-end steering vehicle. The problem of estimating thrust misalignment

has been the subject of considerable investigation in a number of other system studies. All factors which contribute to thrust misalignment were considered in this study. They were:

1. Mechanical tolerances
2. Asymmetric throat erosion
3. Motorcase deflection due to flight loads
4. Asymmetric gas flow into the nozzle
5. Distortion of the motorcase upon pressurization
6. Motor center of gravity eccentricity.

Based on these considerations and on available quantitative data, the values of thrust misalignment angle and eccentricity used in the study are 0.10° and 0.88 in. respectively.

The principle propulsion contractors having experience with thrust misalignment in large solid rocket motors were consulted. Aerojet-General Corporation and Thiokol Chemical Corporation performed a design tolerance analysis of their respective 260-in. rocket motor design. The results of these analyses, along with other misalignment data, are presented in Table 5-5. Both the Aerojet and Thiokol numbers represent maximum possible mechanical misalignment and eccentricity values. The contribution of each of the individual component tolerances were assumed to be additive for maximization of these values. Considerable disagreement exists between the results of Aerojet and Thiokol, particularly in the angular misalignment tolerances. Upon consideration of their respective analyses, it was felt that the Thiokol number should be considered as a possible upper limit. The Thiokol misalignment angle is higher by 2.3 minutes than the value used in the study, but the study value is achievable through current state-of-the-art techniques of manufacturing and quality control. United Technology Corporation was consulted regarding the thrust misalignment of their 120-in. motor firings. Misalignment measurements were made during periods of no-thrust vector deflection. The maximum values of angular deflection and eccentricity of all firings are 0.133° and 2.8 in., respectively. Since the 120-in. motor fired in the UTC tests is segmented, larger thrust misalignment values would be expected than for a monolithic motorcase because of the additional tolerance build-up in the segment joints. While no quality control data was available for these motors, it would be expected that permissible nozzle alignment tolerances would be greater for nozzles using thrust vector control.

Table 5-5

THRUST MISALIGNMENT ANGLE AND ECCENTRICITY

| Type of Deviation | Value Used in Study | Tolerance Analysis* | | | 120-in. Firing** UTC |
		AGC260	TCC260	ZEUS	
Misalignment Angle (Min. of Arc)	6.0	2.23	9.3	13.0	14.0 Max 1.0 Min
Eccentricity	0.88	0.1	0.2	0.06	2.8 Max 0.6 Min

*Mechanical Tolerances   **Five Firings

AGC - Aerojet General
TCC - Thiokol Chemical
UTC - United Technology

The bending moments transmitted to booster motorcases in the head-end steering vehicle are less than in motors having aft-end steering or thrust vector control. Calculations showed that the deflections of the motorcase for this vehicle are insignificant.

A study made by Thiokol in connection with a preliminary design of a fixed-nozzle, solid-propellant vehicle indicated that asymmetric gas flow and case distortion upon pressurization can be neglected for large rocket motors.

The eccentricity of the motor CG was assumed to be 0.25 in. No conclusive information regarding this value is available at this time. The 0.25-in. value represents the motor manufacturer's best estimate. It can be seen that the ultimate choice of the thrust misalignment and eccentricity used in the study had to be, to a large extent, based on qualitative judgment.

5.3.3 Booster Steering

The booster steering propulsion system is described in Section 5.2.2. The stability and control function of the steering system is described in Section 5.2.3.

The propellant used for steering is contained in an adapter section located immediately above the third stage booster motor. The adapter primary structure is designed with aluminum monocoque and sheet-stringer construction. The propellant tankage is a common bulkhead tank designed for an operating pressure of 125 psia. The cassinian (ellipsoid-type) forward and aft domes are formed of aluminum. The hemispherical common bulkhead is of waffled aluminum construction designed to withstand reverse pressures equal to the operating pressure.

5.3.4 Interstage Structure and Fins

Interstage structure is required forward and aft of the motor skirts on all three stages. The second and third stages will utilize aluminum sheet-stringer construction. The first stage interstage structure will be constructed of monocoque aluminum, because the weight savings inherent in sheet-stringer construction do not justify its added cost on this stage. The first stage nozzle fairing will have provisions for attachment of four fins, each of which has an area of 100 sq. ft.

5.4 WEIGHT AND BALANCE

This section presents the weight breakdown for the HES-2G spacecraft, in-flight weight variations of the spacecraft with the corresponding CG locations, weight, and CG history of the HES-2G adapter and in-flight weight and CG history for the total vehicle. Included in this section is a discussion of the effect of HL-10 size on the HL-10 weights and wing loadings.

The HL-10 part of the HES-2G spacecraft has a length of 44.0 ft. and a gross weight at launch of 91,000 lb. This weight is broken down as shown in Table 5-6 with major subsystem weights summarized in the right column.

Table 5-6
HES-2G SPACECRAFT WEIGHT BREAKDOWN (HL-10 VEHICLE WITHOUT CARGO ADAPTER) (Page 1 of 2)

Structure and thermal protection		16,010
Pressure shell and internal stiffening	2,800	
Ablative thermal protection	6,450	
Backup structure	1,850	
Cargo compartment	1,400	
Aerodynamic surfaces	830	
Docking structures	200	
Windows and hatches	300	
Support and attachment provisions	2,180	
Landing gear and emergency recovery		2,840
Landing gear	1,160	
Emergency recovery	1,680	
Electrical and mechanical subsystems		6,030
Power and distribution	1,500	
Surface actuation	860	
Reaction control hardware	750	
Reaction control propellant	2,000*	
Guidance and flight control electronics	380	
Communications, tracking and rendezvous	190	
Steering motor actuation	250	
Onboard checkout	100	
Propulsion		3,540
Tanks and support structure	1,310	
Pressurization system	680	
Feed system	250	
Engines	1,300	
Life Support		2,100
Environmental control system	1,500	
Emergency survival gear	150*	
Food, water, and sanitation	450*	
Crew, furnishings, and displays		2,150
Crew and suits	1,750*	
Furnishings and displays	400	
Growth contingencies		5,830

*These items not included in dry weight.

Table 5-6 (Page 2 of 2)

Dry Weight		34, 150
Emergency survival gear	150	
Food, water, and sanitation	450	
Crew and suits	1, 750	
Cargo	5, 000	
Operating dry weight		41, 500
Reaction control propellant	2, 000	
Maneuver propellant	43, 900	
Abort rockets	3, 600	
Gross weight of spacecraft (HC-10)		91, 000

The structure and thermal protection comprise 56. 6% of the dry weight (less growth contingencies). This weight includes the pressure shell, internal stiffening, the ablative thermal protection and its backup structure, the cargo compartment, aerodynamic control surfaces, docking structure, and windows. Also included in this weight are support and attachment provisions for the landing gear, internal equipment, abort rockets, and aerodynamic control surfaces.

The power subsystem and its distribution network, actuation systems for the steering motors and control surfaces, the reaction control system, guidance, flight control, communications, tracking, onboard checkout, and rendezvous radar are included in the 6, 030 lb. allotted for electrical and mechanical sub-systems. The dry weight of these subsystems comprise 14. 2% of the total dry weight (less contingencies).

The propulsion system weight includes the tankage and its support structure, the pressurization and feed subsystems, and the two steering engines. The dry weight of this system is 12. 6% of the total dry weight (less contingencies).

The environmental control system, food and water supplies, personal hygiene, and emergency survival gear are included in the lift support subsystem.

The eight-man crew with their associated furnishings, seats and displays weigh 2, 150 lb.

The 5,000 lb. cargo weight includes 1,000 lb. for packaging.

The "maneuver propellant" is contained in the main propulsion tanks; additional velocity requirements for rendezvous, docking, and separation are supplied by the reaction control system.

A 20%-weight contingency factor was placed on the structure and thermal protection, landing gear, emergency recovery, electrical, mechanical, propulsion, and life support subsystems to provide for system growth.

Table 5-7 presents the weight and CG history for the spacecraft. The normal landing weight of 37,200 lb. results in a wing loading of 54 lb./sq.ft. In case of abort, the maneuver propellant and the burned-out abort rockets will be dumped; also part of the reaction control propellant will be expended, resulting in a landing weight of 43,000 lb. and a wing loading of 62 lb./sq.ft.

The forward adapter, with a cargo module that can hold 15,000 lb. of cargo plus 3750 lb. of packaging, weighs 3,900 lb. empty. The aft adapter section weighs 10,300 lb. dry; this weight does not include the skirt that connects the aft adapter section to the third stage motor.

The adapter weight and CG history is presented in Table 5-8. The mass properties of the total vehicle used for determining the steering requirements during boosted flight are presented in Table 5-9.

Figure 5-12 presents the spacecraft weights and wing loadings as a function of vehicle length. From purely volumetric considerations the spacecraft could have been shortened to between 41 ft. and 42 ft. resulting in a wing loading under abort conditions of as high as 70 lb./sq. ft. and under normal conditions of as high as 60 lb./sq. ft. The 44-ft. version was selected to reduce the abort wing loading to 60 lb./sq. ft., but the final weight estimate raised the wing loading above this value. To reduce the abort wing loading to 60 lb./sq. ft (see Figure 5-12) would require a spacecraft length of 45.3 ft. and an increase in gross weight of over 2,000 lb. A length of 51.2 ft. and an increase in gross weight of 14,000 lb. would be required to reduce the normal landing wing loading to 45 lb./sq. ft. The 51.2 ft. version would increase the adapter weight by approximately 1,000 lb. due to increased structural loads.

Table 5-7

HES-2G SPACECRAFT WEIGHT AND CENTER OF GRAVITY HISTORY (HL-10 VEHICLE WITHOUT CARGO ADAPTER)

	Weight (lb.)	CG (in. aft of Sta. 0)	
Spacecraft at launch	91,000	304	57.6
Two abort rockets ejected	(1,800)	(470)	(89.0)
S/C at 2nd stage ignition	89,200	301	57.0
Two abort rockets ejected	(1,800)	(470)	(89.0)
S/C at 3rd stage burnout	87,400	298	56.5
Maneuver and RCS propellant consumed	(44,400)	(313)	(59.3)
S/C at S/C burnout (also abort landing condition)	43,000	282	53.4
Ablatives, RCS propellant, and expendables consumed	(5,800)	(295)	(55.9)
S/C normal landing weight	37,200	280	53.0

( ) Parentheses indicate CG location of item noted.

The increases in spacecraft and adapter weight to obtain a 45 lb./sq. ft. loading would raise the total weight 15% above that of the third stage motor, thus significantly increasing the booster size. Effects of increased HL-10 plan area and gross weight on the steering requirements is discussed in Section 5.5.

Table 5-8

HES-2G ADAPTER WEIGHT AND CENTER OF
GRAVITY HISTORY (NO CARGO IN ADAPTER)

	Weight (lb.)	C.G. Relative to S/C Nose (in.)
Adapter at launch	102,600	773
Steering Propellant consumed during 1st stage burning	(43,200)	(763)
Adapter at 2nd stage ignition	59,400	779
Steering propellant consumed during 2nd stage burning	(14,400)	(787)
Adapter at 3rd stage ignition	45,000	777
Steering propellant consumed during 3rd stage burning	(28,200)	(805)
Adapter at 3rd stage burnout	16,800	730

Table 5-9

VEHICLE MASS PROPERTIES

	Weight (lb.)	Center of Gravity (in. aft of Sta. 0)	Pitch MOI* (Slug sq.ft. $\times 10^{-6}$)	Roll MOI* (Slug ft.$^2 \times 10^{-6}$)
Vehicle at launch	6,653,400	2,637	1,269.86	11.176
Vehicle at 1st stage burnout	2,610,200	1,826	347.41	3.860
Vehicle at 2nd stage ignition	2,243,900	1,579	106.66	3.210
Vehicle at 2nd stage burnout	879,500	1,193	37.74	0.728
Vehicle at 3rd stage ignition	721,000	1,047	16.59	0.465
Vehicle at 3rd stage burnout	166,700	672	8.03	0.107

*Moment of Inertia
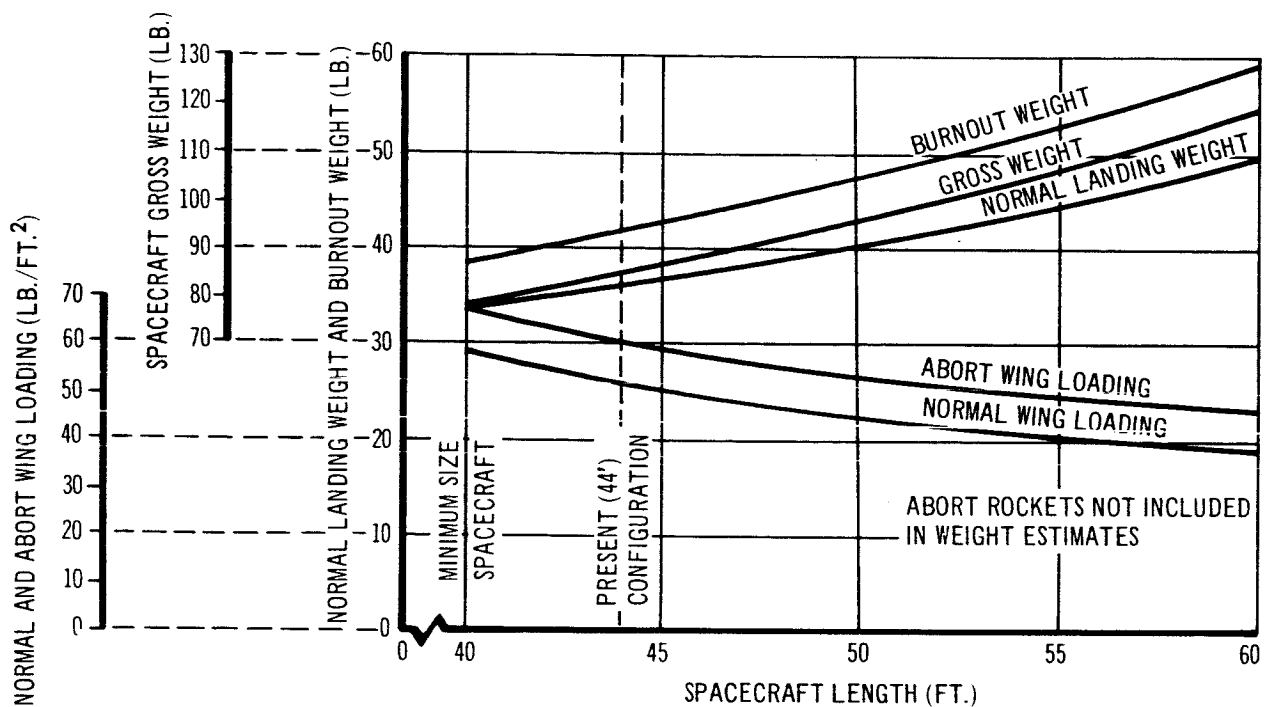
Figure 5-12 Configuration HES-2G Weights and Wing Loadings vs. Vehicle Length

5.5 STEERING ANALYSIS

5.5.1 Guidelines and Assumptions

The following guidelines and assumptions were used in the steering analysis of the HES-2G as a baseline vehicle. The assumptions are applicable to the baseline conceptual design and all other vehicles analyzed in the study.

Current design practices with respect to wind profiles with standard gusts for Saturn-launched vehicles, were used in this study. Figure 5-13 shows the 95% AMR-wind profiles which were used along with the standard gust definition shown in Figure 5-14. The steering system was sized assuming the wind profile to be omnidirectional, i. e., both head winds and side winds were investigated.
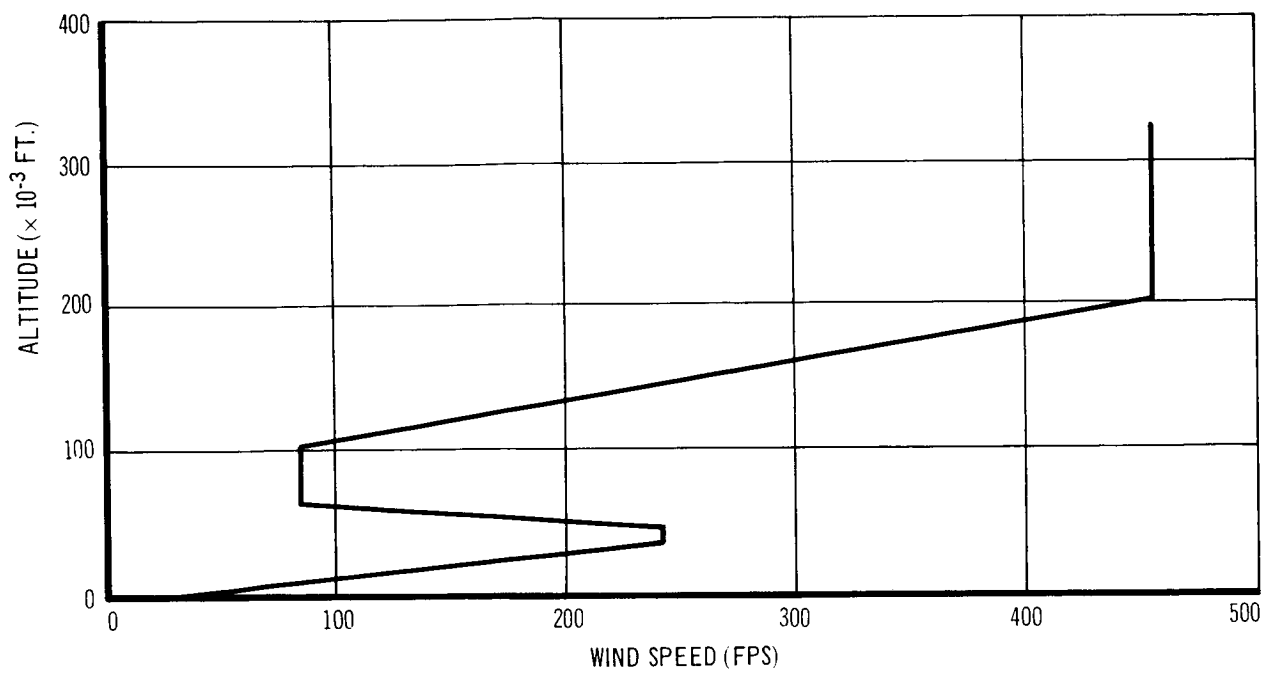
Figure 5-13 Atlantic Missile Range Wind Profile
(Ninety-Five Percent Probability of Occurrence)
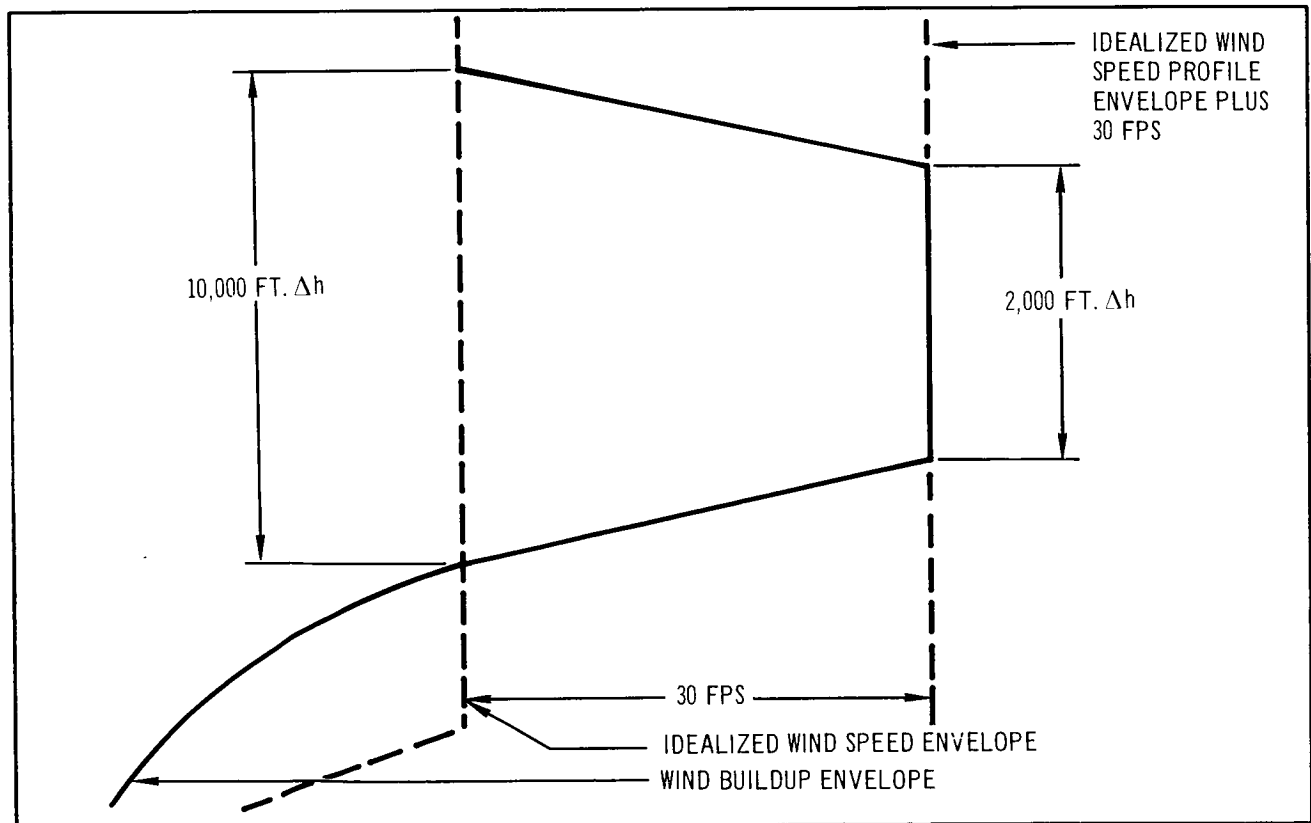
Figure 5-14 Gust Profile

Steering response capabilities are those corresponding to an equivalent second-order system with a natural frequency and damping of 0.15 cps and 0.7 cps, respectively. These characteristics are based on considerable experience with booster steering systems and are identical to those employed in the Saturn system.

All steering systems sized in this study have, in addition to statically balancing all disturbing moments, the capability for proportionally (without system saturation) following step changes in attitude rate commands of 0.35° and 0.1°/sec. in pitch and yaw respectively. The pitch rate command of 0.35°/sec. represents typical requirements for the gravity turn trajectories used in the study. The allowance for yaw of 0.1°/sec. considers the possible use of dog-leg maneuvers.

The predominant influences on the steering system thrust and torque level requirements are the disturbing moments. The entire concept of steering feasibility rests on a satisfactory control of these influences. Listed below are all sources considered and their levels of uncertainty:

1. Aerodynamic coefficients are known to ±5%

2. Booster stabilizing fins are aligned to within ±6 min. of arc to the design nominal position.

3. Misalignment of stages with respect to a reference centerline is ±0.03°

4. Misalignment of solid motor thrust is ±6 min. of arc (see Section 9.3)

5. Eccentricity of solid motor thrust is ±0.88 in.

6. Lateral CG tolerance is ±1.0 in. referenced to a geometrical centerline position.

The uncertainties listed above represent the best information available at the time of the study. The influence on steering system design due to deviations of these values are shown in Section 5.4.3.4.

5.5.2 Steering Engine Layout

The steering engine layout described in Section 5.2.2 was provided to accommodate required steering torque levels and HL-10 design constraints. This propulsion arrangement provides an optimal balance between thrust level and

gimbal throws. The engines will be centered at 30° out from the vehicle centerline in yaw to reduce plume-impingement heating problems on the aft adapter. A pitch throw of ±30° requires but minor modification to the spacecraft geometry.

To eliminate pitch-roll cross-coupling, the gimbal arrangement (see Figure 5-9) provides for the generation of yaw- and pitch-roll torques by rotating about the outer and inner gimbal axes, respectively. There is a cross-coupling of pitch-roll into yaw but it would not be significant unless large demands for pitch and roll occurred simultaneously. A detailed analysis of steering torque requirements has shown that such a condition will not occur.

Control system logic dictates that neutral condition in yaw be 30° outboard rather than parallel to the centerline in keeping with aft adapter heating considerations. Maximum expected gimbal rates are 12°/sec. in pitch and yaw. They represent a capability for returning vehicle attitude to its desired orientation within 2 sec. after liftoff while subjected to thrust misalignment and aerodynamic disturbance moments.

Alternate engine layouts are shown and described in Section 9.2.

5.5.3 Steering Requirements

To adequately specify a set of steering system parameters it is necessary to develop an accurate representation or model of the vehicle. Following is a detailed discussion of the booster control system model and the salient results of a detailed digital simulation.

5.5.3.1 Aerodynamic Representation

For purposes of determining aerodynamic loads, the vehicle was broken into six segments, A through F as shown in Figure 5-15. Each segment was considered to act independently of the others with the exception of E and F where control engine thrust effects on body aerodynamics were omitted. Final selection of booster stabilizing fins would be preceded by extensive wind tunnel and flight test analysis. These tests would be expected to show the aerodynamic-control engine thrust composite characteristics within plus
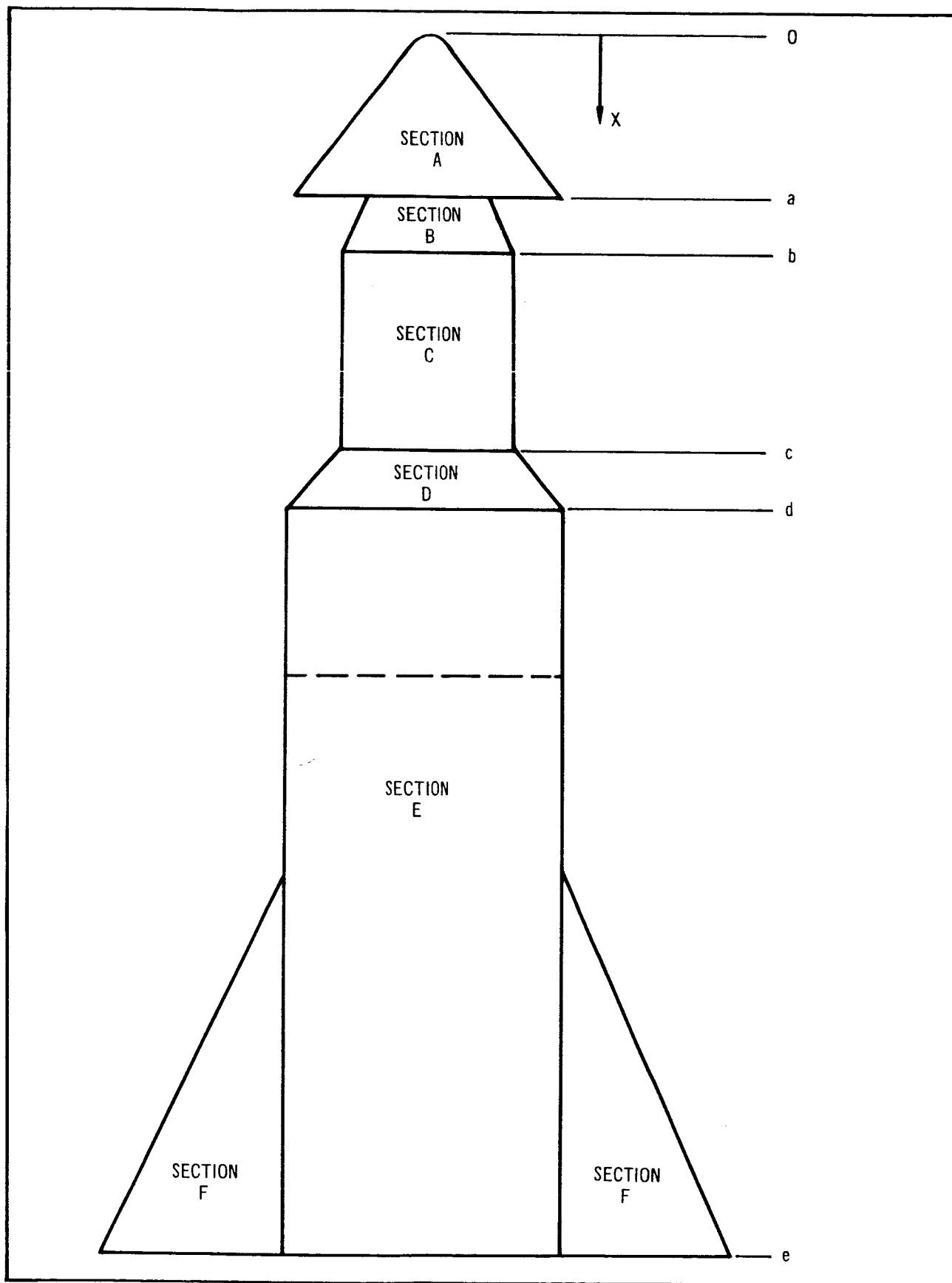
Figure 5-15 HES-2G Vehicle

or minus 5%. Some deviation in nominal aerodynamic coefficients with respect to those used in this study will undoubtedly result. To gain insight into these influences, the sensitivities of minimal control thrust to both nominal and uncertain deviations in aerodynamics are discussed in Section 5.5.3.4.

Analysis of booster flight has shown that the predominant aerodynamic influences on the required control engine thrust level occur in the transonic flight regime. Below and above this regime, vehicle disturbing moments result primarily from solid motor thrust. In view of this characteristic, all aerodynamic parameters are represented with their transonic values. The following list quantitatively specifies the values used in the study. HL-10 data were obtained from wind tunnel analyses, Section 5.8, References 3 and 4. In all cases, α and β are assumed to be less than 10°.

Segment A

$$C_{n\alpha} = 0.022 \text{ deg.}^{-1}$$

$$C_{n\beta} = 0.015 \text{ deg.}^{-1}$$

$$Cp = \frac{2X_a}{3}$$

Segment B

$$C_{n\alpha} = C_{n\beta} = 0.035 \text{ deg.}^{-1}$$

$$Cp = \frac{X_a + 2X_b}{3}$$

Segment C

$$C_{n\alpha} = C_{n\beta} = \frac{16\ell \, |\alpha \text{ or } \beta|}{3\pi (57.3)^2 d} \text{ deg.}^{-1}$$

where ℓ = length of segment C

d = diameter of segment C

$$Cp = \frac{X_b + X_c}{2}$$

Segment D

$$C_{n\alpha} = C_{n\beta} = 0.035 \text{ deg.}^{-1}$$

$$Cp = \frac{X_c + 2X_d}{3}$$

Segment E

$$C_{n\alpha} = C_{n\beta} = \frac{16 \, \ell \, |\alpha \text{ or } \beta|}{3 \, \pi \, (57.3)^2 d} \text{ deg.}^{-1}$$

$$Cp = \frac{X_d + X_e}{2}$$

Segment F

$$\left.\begin{array}{c} C_{n\alpha} \\ \\ C_{n\beta} \end{array}\right\} \quad \left\{\begin{array}{c} \text{fin in presence} \\ \text{of body} \end{array}\right\} = 0.053 \text{ deg.}^{-1}$$

$$\left.\begin{array}{c} C_{n\alpha} \\ \\ C_{n\beta} \end{array}\right\} \quad \left\{\begin{array}{c} \text{body in presence} \\ \text{of fin} \end{array}\right\} = 0.038 \text{ deg.}^{-1}$$

$$C_{n\delta} \quad \left\{\begin{array}{c} \text{fin in presence} \\ \text{of body} \end{array}\right\} = 0.035 \text{ deg.}^{-1}$$

$$C_{n\delta} \quad \left\{\begin{array}{c} \text{body in presence} \\ \text{of fin} \end{array}\right\} = 0.023 \text{ deg.}^{-1}$$

where δ = incidence angle between fin and body

$C_{n\delta}$ is used for determining fin misalignment effects.

The lift coefficients given for Segment F reflect the interaction effects of the fin-body combination. Linearized potential flow theory has been applied to this type of problem in Section 5.8, Reference 5. The results provide normal force derivative coefficient ($C_{n\alpha}$) ratios which have been normalized with respect to the fin-alone derivatives.

$$K_{B(w)} = \frac{(C_{n\alpha})_{B(w)}}{(C_{n\alpha})_w}$$

$$K_{w(B)} = \frac{(C_{n\alpha})_{w(B)}}{(C_{n\alpha})_w}$$

where the subscript B(w) means body in the presence of a wing, etc.

$C_{n\alpha}(\text{total}) = (K_{w(B)} + K_{B(w)}) (C_{n\alpha})_w$

Two separate cases must be considered:

1. Fins fixed on body at zero incidence with the combination at some angle-of-attack, a .

2. Body at zero angle-of-attack with fins at some incidence angle, δ .

A thorough discussion of the various ratio factors K for Case 1 and k for Case 2 is provided in Reference 5. These factors are in turn plotted versus the radius - semispan ratio in the reference. Inasmuch as pitch and yaw fins were of approximately the same areas, identical ratios were used for each. $C_{n\alpha}$ for the fin pair alone was assumed to be $\pi/2$ times the aspect ratio for delta wings.

A determination of aerodynamic torques about the vehicle roll axis was accomplished using HL-10 wind tunnel data and analytical techniques appropriate for describing fin-body contributions. The HL-10 $C_{\ell\beta}$ was 0.0015 deg.$^{-1}$. It was assumed that this moment could be counteracted by judiciously sizing the booster tail fins to a slight degree of asymmetry of planform area in pitch and yaw.

An estimation of the $C_{\ell\beta}$ effect of the fin-body combination was obtained by a modification of the results of Section 5.8, Reference 6. The data from this source provided the $C_{\ell\beta}$ contribution of the fins themselves. In order to obtain the carry-over effect of the fins on the body, it was assumed the 23% of the fin-alone normal force is reflected onto the body and is acting at point 1/3 the distance of the fin semispan, measured inboard from the outside of the booster. The fin and carry-over contribution are then summed to obtain the total $C_{\ell\beta}$.

The respective areas of the pitch and yaw fins are chosen to locate, at a specified time of flight, the CP of HL-10 booster combination at the CG of the same. Triangular planforms were assumed for the fins. The span of the fins were chosen to eliminate any consideration of fin-to-fin interference.

Reference 5 indicated that the fins themselves would be approximately 183% effective. Given below are the subincrements forming this total

$$100\% \quad (1.0 \quad C_{n\alpha} = \text{fins alone})$$
$$60\% \quad (0.6 \quad C_{n\alpha} = \text{effect of booster on the fins})$$
$$23\% \quad (0.23 \quad C_{n\alpha} = \text{effect of fins on the booster})$$

The body carry-over effect of a fin, given earlier as 23%, was obtained from the data above. Fin and body contributions (per fin pair) to $C_{\ell\beta}$ were -6.78×10^{-4} (α or β) and -0.382×10^{-4} (α or β) respectively. Both values are referenced to the fin pair area and semibasespan of the fin body combination.

5.5.3.2 Steering System Simulation Program

Preliminary steering system analysis established the probable range of control thrust levels to be encountered for the expected payload weights. Subsequent detailed investigations have substantiated these predictions. Based on these early studies, a decision was made to proceed on the basis of proportional steering system philosophy. Alternate schemes (on-off, spin stabilization, and weathercocking) were investigated and their characteristics are discussed under Section 9.2.4.

In order to accurately represent the multiple combinations of boosters, spacecraft, trajectories, and steering arrangements within the time span of the study, a comprehensive Fortran program was written. The primary objective of the program was to determine, as a function of flight time, minimal steering control thrust and gimbal angle requirements. To effect a high confidence level in the program's output, effort was spent in developing methods for ensuring that critical design values would be specified for every second of flight time from lift-off through 1st-stage burnout. To accomplish this, the program accurately accounts for the following influences:

1. Omnidirectional winds with gusts

2. Nominal trajectory characteristics (altitude, velocity, flight path angle, attitude, dynamic pressure) versus flight time

3. Six-segment breakdown of aerodynamic coefficients (pitch, yaw and roll)

4. Position, number, and allowable gimbal throws for steering engines

5. Solid motor thrust variation with altitude

6. Solid motor thrust eccentricity

7. Solid motor thrust misalignment

8. Uncertainty in aerodynamic characteristics

9. Uncertainty in lateral position of vehicle CG

10. Misalignment of stabilizing fins

11. Vehicle CG location versus flight time

12. Vehicle pitch, yaw, and roll moments of inertia versus flight time

13. Steering requirements over and above a static balance of disturbing moments

Nominal trajectory characteristics are curve-fitted with straight line segments to the desired degree of accuracy. Wind profiles are entered in a similar manner. To account for an omnidirectional wind profile the program simultaneously solves the steering problem with head winds and side winds. Standard gust profiles were superimposed on the wind shears at maximal (jet stream) level of the latter and the corresponding altitude shifted to that which centers over peak dynamic pressure. Dynamic pressure is adjusted to account for relative wind for both the head- and side-wind conditions.

For every second of the trajectory, the program computes the nominal aerodynamic torques on each segment. Since all of the trajectories considered were gravity turn, aerodynamic pitching and yawing torques result solely from the influence of head winds and side winds, respectively. These torques are initially used to determine aerodynamic uncertainties and are subsequently summed and stored. Following this procedure, every other source of disturbing torque uncertainty is computed (motor misalignment and eccentricity, fin misalignment, vehicle CG tolerance) and root summed squared. The RSS value is both added and subtracted from the nominal conditions and stored for both head and side wind conditions. This may be expressed as follows:

$$\text{Head Winds} \begin{cases} M_{DPH1} = M_{DPN} + M_{DPH} \text{ (rss)} \\ M_{DPH2} = M_{DPN} - M_{DPH} \text{ (rss)} \\ M_{DYH} = M_{DM} \text{ (rss)} \end{cases}$$

$$\text{Side Winds} \begin{cases} M_{DYS1} = M_{DYN} + M_{DYS} \text{ (rss)} \\ M_{DYS2} = M_{DYN} - M_{DYS} \text{ (rss)} \\ M_{DPS} = M_{DM} \text{ (rss)} \end{cases}$$

where

M_{DPH1} = Head wind pitching torque using nominal plus uncertainties

M_{DPH2} = Head wind pitching torque using nominal minus uncertainties

M_{DYN} = Head wind yawing torque due to motor uncertainties

M_{DYS1} = Side wind yawing torque using nominal plus uncertainty

M_{DYS2} = Side wind yawing torque using nominal minus uncertainty

M_{DPS} = Side wind pitching torque due to motor uncertainties

M_{DPN} = Nominal pitching torque

M_{DPH} (rss) = R. S. S. pitching torque due to all uncertainties - headwind

M_{DM}(rss) = R. S. S. pitching or yawing torque due to motor uncertainties

M_{DYN} = Nominal yawing torque

M_{DYS} (rss) = R. S. S. yawing torque due to all uncertainties - sidewind

Only the nominal values of induced aerodynamic rolling torque (head- and side-winds) are computed, in that associated uncertainties do not constitute significant contributions. Realistic roll torque levels are insured by letting α and β assume 1° values for side winds and head winds respectively.

The remaining demand on control torque, beyond the disturbances outlined above, arises from the need for following a prescribed vehicle attitude time history. Attitude step rate changes from 0.1°/sec. to 0.4°/sec. are typical of the requirements imposed on the class of boosters involved in this study. In order to guarantee acceptable lag times (≈ 2.0 sec.) and overshoots in accomplishing the commanded rate histories, the control system was designed with natural frequency and damping of 0.15 cps and 0.7 respectively. This simulation required a capability for following at all flight times, attitude step rate changes of 0.35°/sec. in pitch and 0.1°/sec. in yaw. The latter was included to provide for dog-leg types of maneuvers if they should arise. When these values are converted into peak angular acceleration requirements (assuming no system saturation) the control system must provide 0.148° and 0.043°/sec.^{2} in pitch and yaw, respectively. The program takes these requirements and, using computed vehicle inertias, converts them into steering torques. These are combined with the disturbing torques forming the total demand on the steering system.

Two proportional steering system arrangements were built into the program:

1. Four engines symmetrically positioned on the HL-10 aft adapter
2. Two engines placed in the aft-outboard region of the HL-10.

System 1 required two engines for pitch, two for yaw, and all four for roll. System 2 required both engines in pitch, yaw, and roll. The desirability for recoverable engines led to a choice of System 2 for the recommended HES-2G configuration.

The technique to ensure that adequate control thrust was specified for every time point was to seek out the combination of disturbing and steering torques that produced a maximum demand for control thrust. Using M_{SP} and M_{SY} to define the required pitch and yaw steering torques (those required to follow steering commands) beyond a static balance of disturbances, this combination may be written as:

$$
\text{Head}\atop\text{Winds}
\left\{
\begin{aligned}
\text{Max. } M_{TP1} &= M_{DPH1} \pm M_{SP} \\
\text{Max. } M_{TP2} &= M_{DPH2} \pm M_{SP} \\
\text{Max. } M_{TYH} &= M_{DYH} \pm M_{SY} \\
M_{DRH} &= M_{DRH}
\end{aligned}
\right.
$$

$$
\text{Side}\atop\text{Winds}
\left\{
\begin{aligned}
\text{Max. } M_{TY1} &= M_{DYS1} \pm M_{SY} \\
\text{Max. } M_{TY2} &= M_{DYS2} \pm M_{SY} \\
\text{Max. } M_{TPS} &= M_{DPS} \pm M_{SY} \\
M_{DRS} &= M_{DRS}
\end{aligned}
\right.
$$

where M_{TP1} and M_{TP2} are the two possible total pitch torque requirements for head winds

M_{TYH} is the total yaw torque requirement for head winds

M_{DRH} is the total roll torque requirement for head winds

M_{TY1} and M_{TY2} are the two possible total yaw torque requirements for side winds

M_{TPS} is the total pitch torque requirement for side winds

M_{DRS} is the total roll torque requirement for side winds

The four possible levels of control thrust that satisfy the combinations of torques for head- and side-winds are computed, and the maximal value of the four is the minimal allowable control thrust at the time point in question.

A detailed flow diagram of the digital program is shown in Figure 5-16.

5.5.3.3 Control Thrust Requirements

In subsequent discussions, the focal point of concern regarding the steering system will be its minimal thrust level requirements. To appreciate the emphasis placed on this parameter it is necessary to realize its influence

Figure 5-16 Steering System Digit[...]

NOTE:
U = UNCERTAINTY
SW = SIDEWIND
HW = HEADWIND
S.M.T = SOLID MOTOR THRUST
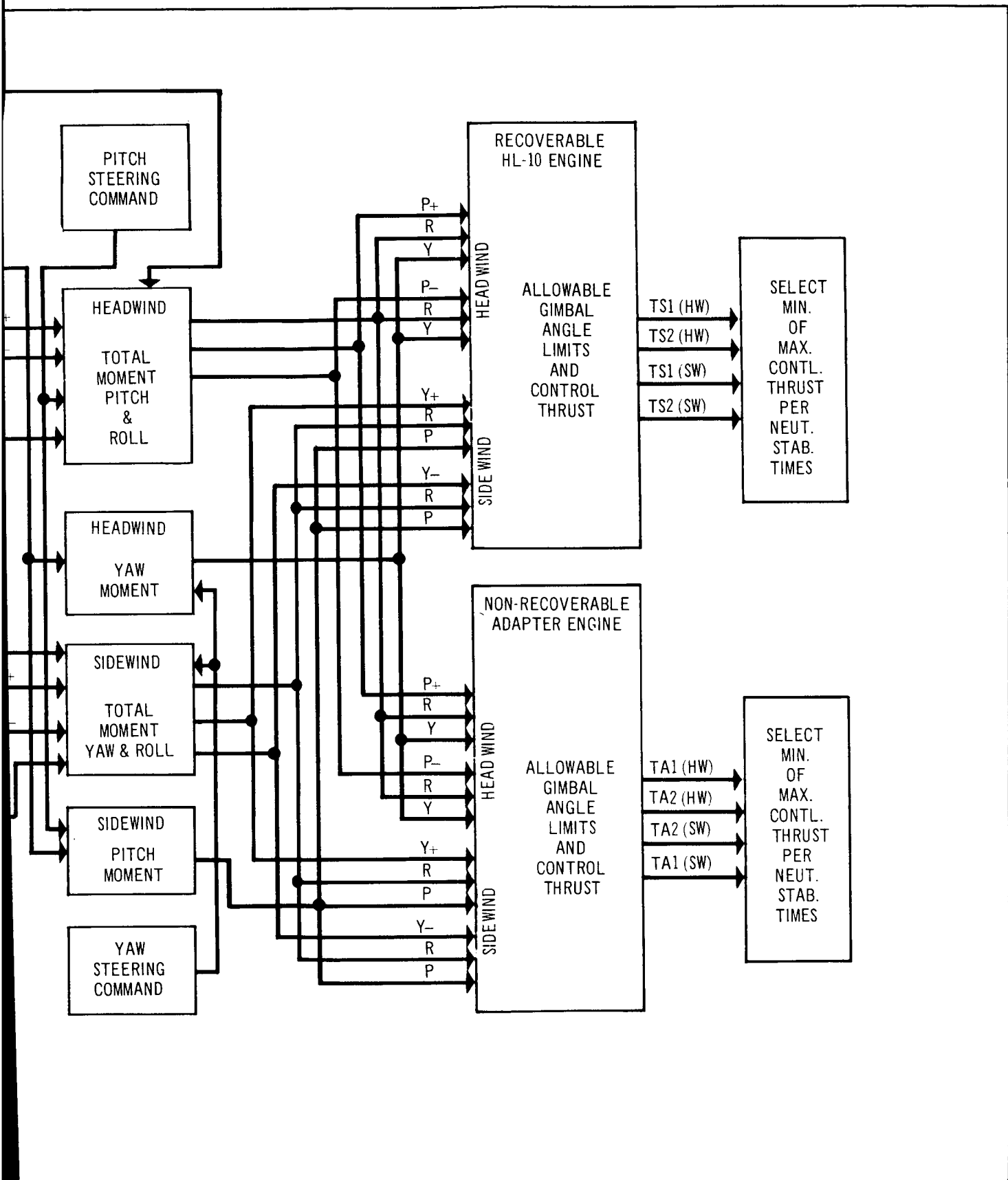
Program Flow Diagram

on feasibility. Significant increases from the present vacuum thrust level of 47,300 lb./engine would necessitate a larger HL-10 engine envelope volume, which would possibly require additional modifications of HL-10 external geometry. This is, of course, to be avoided if at all possible. If larger (higher thrust) engines were employed, they would require greater amounts of steering propellant and, hence, heavier steering tankage. The added weights required of the steering system would be magnified by the vehicle growth factor resulting in larger booster sizes. To maintain the liftoff thrust-to-weight ratio of 1.25, higher first stage thrust levels would be necessary. These, in turn, generate greater disturbing moments which impose additional demands on the steering system (see Section 5.5.3.4). A further demand arises from the need for following attitude rate commands in the face of higher vehicle inertias brought about by increased booster size.

This sequence of events does not necessarily mean a divergent design situation, but rather illustrates the influence on booster size and the reinforcing growth demands placed on steering thrust once an upward departure in steering thrust is initiated.

To minimize the influence of aerodynamic loading on steering thrust requirements, it was desirable to constrain peak dynamic pressure during the first stage of flight. This was done with virtually no loss in performance by maintaining a liftoff thrust-to-weight ratio of 1.25. Resultant peak dynamic pressure was 723 psf. An equally important step in minimizing these influences was the optimal sizing of booster stabilizing fins. The single most important feature of the digital program discussed in the previous section was its ability to extract the most desirable pitch and yaw fin areas from an arbitrary number of candidates chosen by the engineer. The mechanism for choosing a candidate was to select the time of flight where neutral aerodynamic stability was to be achieved. The program would then compute the corresponding fin areas and fly the entire trajectory, determining the minimal allowable steering thrust for every second of flight.

Figure 5-17 illustrates three flight time histories of minimum steering thrust. The values of N noted as 43, 68, and 93 correspond to fin sizes which result in neutral stability at flight times of 43, 68, and 93 sec. respectively.
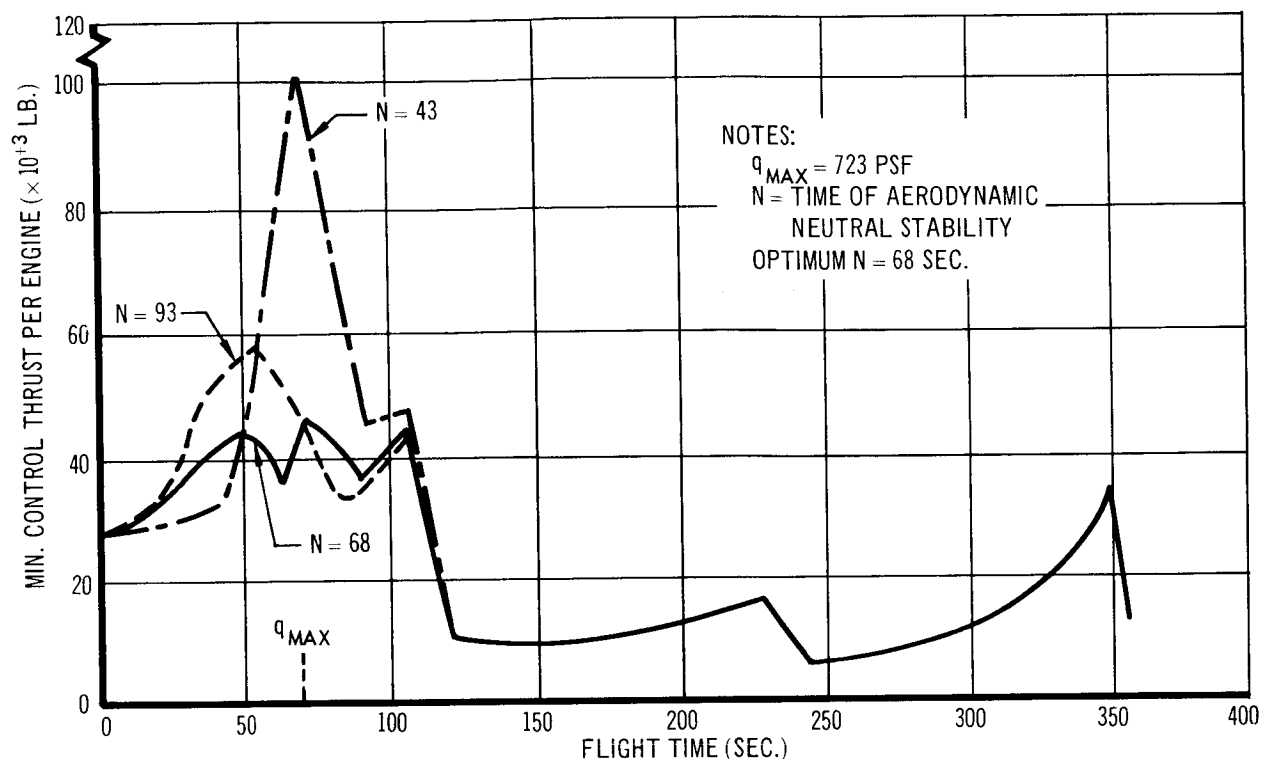
Figure 5-17 Minimum Control Thrust Vs Flight Time – HES-2G

These three values represent the extremes and optimal choices of fin size.
To preserve clarity in the figure, interim values of N were omitted. It is
seen that choices of neutral stability at 93 seconds and 43 seconds result in
minimum steering thrusts of 56,000 lb. and 102,000 lb., respectively. These
levels are not vacuum, but occur at the flight times shown. Extrapolating to
vacuum conditions results in 59,000 lb. and 104,000 lb. of thrust.

Figure 5-18, which shows a locus of minimal allowable steering thrust/engine as
a function of the time of neutral stability, (N), illustrates the optimal design
point (N = 68) used in this study. Figure 5-19 indicates pitch and yaw fin
areas (per pair) versus N.

Close examination of Figure 5-17 reveals that for optimal fin sizing, control
thrust level at web burn time of the first stage (107 seconds) is very close
to the maximum level which occurs at 73 seconds (maximum dynamic pres-
sure). This is the result of forward motion of the CG and represents the
point in first stage operation where lever arms for solid motor thrust
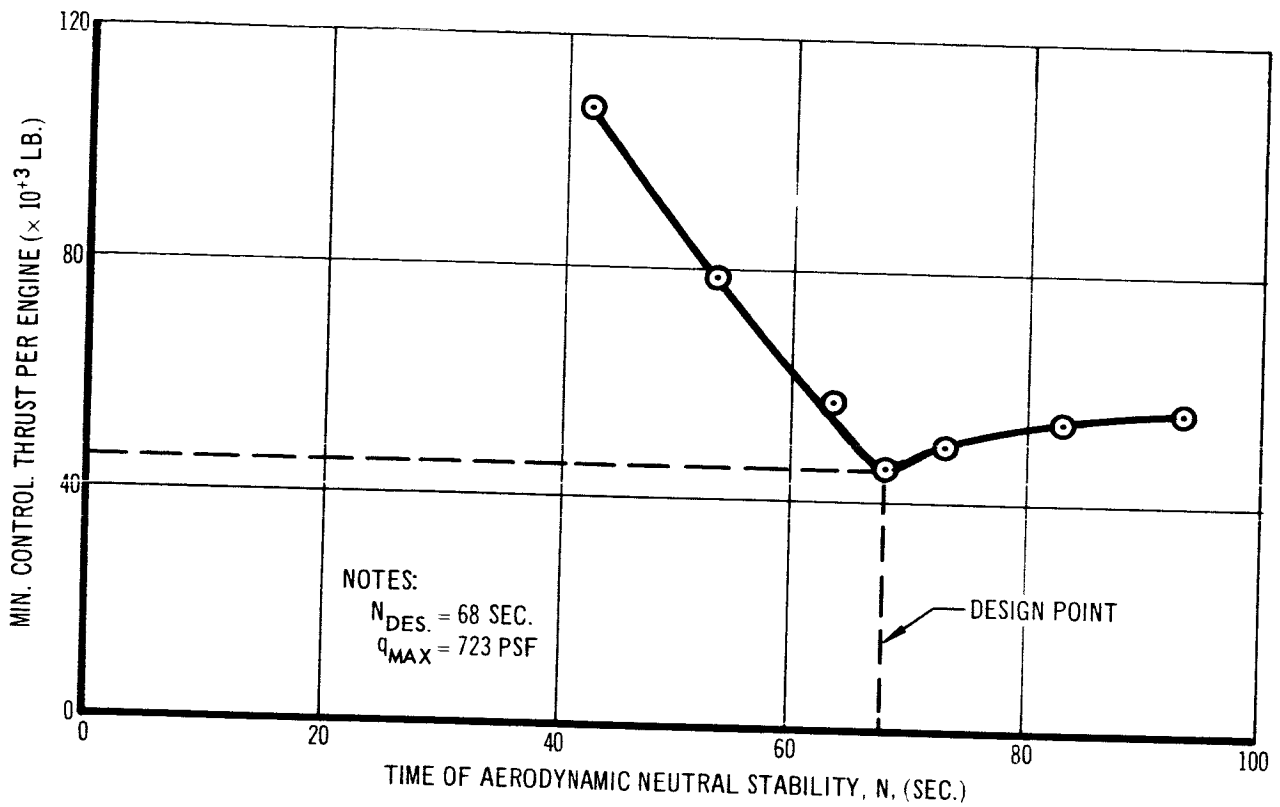
Figure 5-18 Minimum Control Thrust Vs. Time of Aerodynamic Neutral Stability – HES-2G
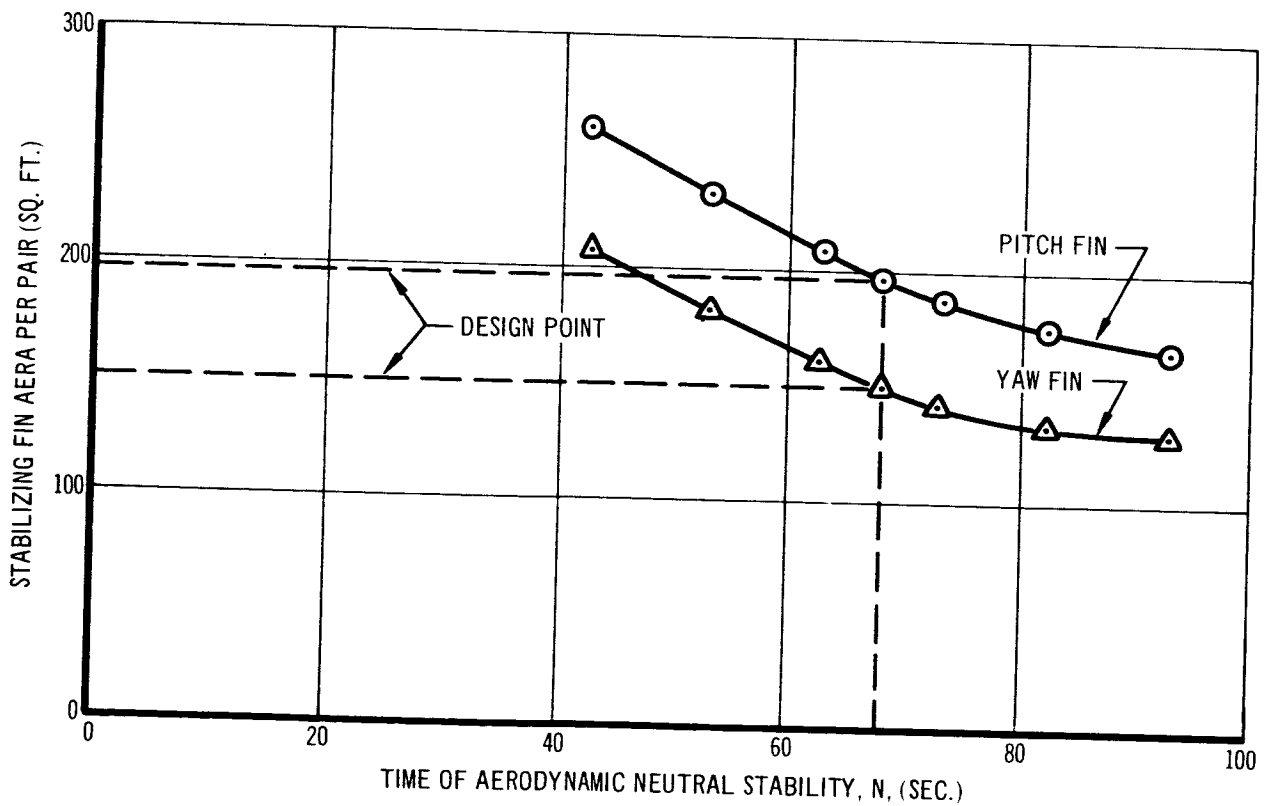
Figure 5-19 Stabilizing Fin Area Vs. Time of Aerodynamic Neutral Stability – HES-2G

misalignment and control thrust are maximized and minimized, respectively. Aerodynamic influences have become relatively small at 107 seconds. The component makeup of control thrust for these two time points is shown in Table 5-10. The important conclusion to be drawn is that for optimal fin sizing, minimal control thrust level is largely dictated by disturbing moments emanating from the solid motor at completion of the web burning of the first stage. Removal of all aerodynamic torques throughout the flight would not substantially alter minimal control thrust levels. For this reason, the aerodynamic control surfaces of the HL-10 were not used for control during boost. Had they been used, the accuracy of predicting their effectiveness, and taking cognizance of the interaction effects of control engine thrust and the aft adapter would be less than satisfactory.

Table 5-10

HES-2G CONTROL THRUST REQUIRED TO OVERCOME
DISTURBING MOMENTS
(Q MAX AND 1ST STAGE BOOSTER BURN OUT)

Source of Disturbing Moment	Steering Thrust (vac) Per Engine ($\times 10^3$ lb.)	
	Flight Time	
	Maximum Dynamic Pressure (73 sec.)	First Stage Booster Burnout (107 sec.)
1. Nominal aerodynamic	15.2	3.7
2. Aerodynamic uncertainty	7.3	0.4
3. Solid motor thrust misalignment	13.3	28.0
4. Solid motor thrust eccentricity and vehicle CG offset	5.6	9.5
5. Stabilizing fin misalignment	0.4	0.2
6. Response to steering command	5.5	3.2
TOTAL THRUST	47.3	45.0

Figure 5-17 shows control thrust histories for the entire powered phase of boost (360 seconds). The low thrust levels during second stage (123 seconds to 245 seconds), afford the opportunity for throttling, thereby reducing steering propellant and associated tank weight. Third stage operation requires a minimum of 34,000-lb. control thrust. Again, throttling proves to be beneficial. The design of the HES-2G reflects throttle ratios of 0.32 and 0.70 for the second and third stages.

The sharp upswing in control thrust requirements at the completion of web burning of the third stage (349 seconds) is indicative of progressively closer proximity of vehicle CG and steering control station. The significant factor in determining the nature of the control situation during third stage is the empty-case weight of the 156-in. motor. Clearly, there are additional influences, namely, adapter cargo module and steering tankage. The following section will present the sensitivities of control thrust to these, and other influential parameters.

5.5.3.4 Control Thrust Sensitivity Analysis

A feasibility study is never completely free of errors when estimating involved parameters. In order to place a practical value on the study's results it is necessary to show that the conclusions pertaining to feasibility of head-end steering would not be violated by possible variations of more significant design parameters. It is the purpose of this section to show how a variation in some design parameters could affect the feasibility of the concept.

The most influential variable on steering thrust is the misalignment angle of fixed-nozzle solid motor thrust. Figure 5-20 shows the minimal control thrust required as a function of misalignment angle. The design point chosen for the study (Section 9.3) was 6 minutes of arc representing the best current estimation of the state-of-the-art capability in large solid motor construction. Progressing upwards from 6 minutes results in rapidly growing steering thrust requirements. The flattening of the curve as misalignment approaches zero is indicative of the influence of aerodynamic loads and the basic requirement for following steering commands. It is clear that effort should be expended to control the maximum misalignment angle to within the tolerance of 6 minutes of arc.
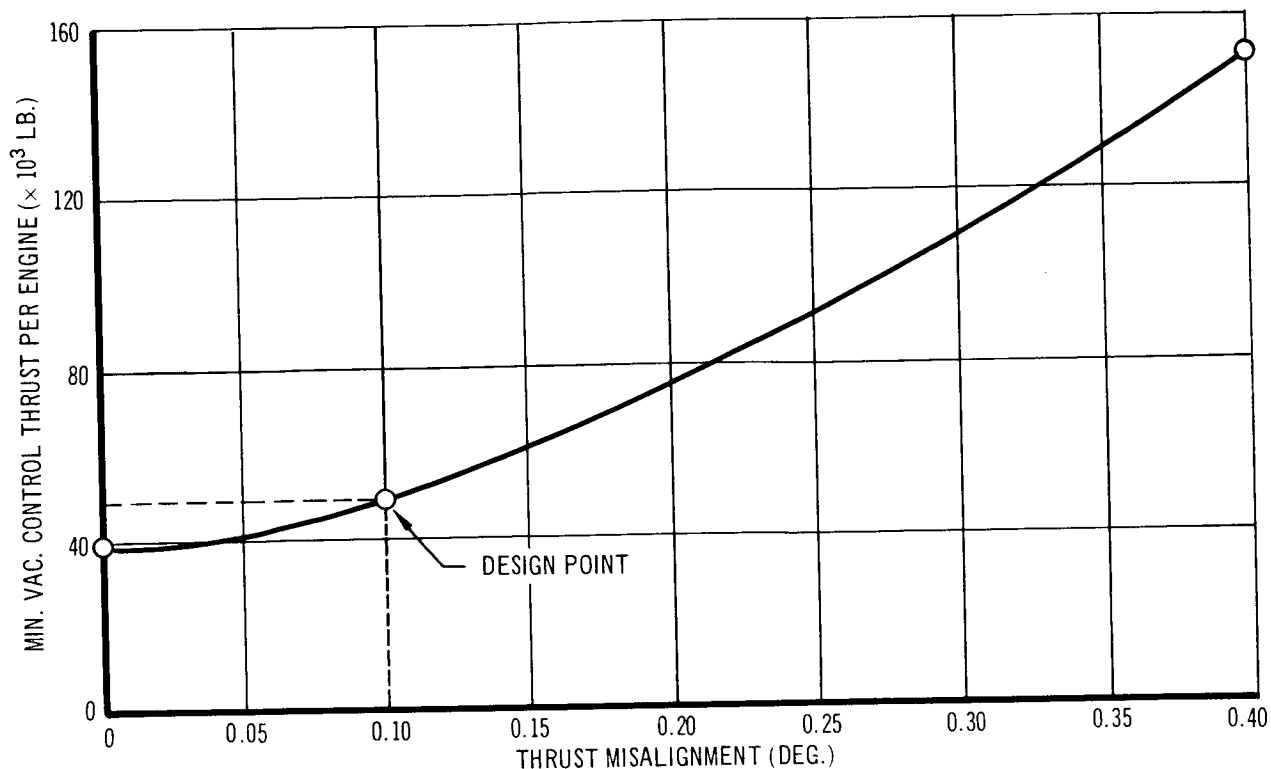
Figure 5-20 Minimum Control Thrust Vs. First Stage
Thrust Misalignment – HES-2G

Figure 5-21 shows a relatively insensitive control thrust to solid motor eccentricity. It is noted that a 1-in. lateral offset of vehicle CG has been assumed for the basic HES-2G vehicle. Inasmuch as this effect is root summed squared with motor eccentricity, its influence tends to be mitigated.

The effect of errors in predicting nominal aerodynamic coefficients is shown in Figure 5-22 where the effect is shown on control thrust of variations in nominal aerodynamics of up to 50%. It is significant to note that 50% errors would result in only a 7,000-lb. thrust increase relative to the chosen level of 50,000 lbs. The 50,000-lb. thrust level provides a 2,700-lb. pad over the nominal steering system requirement (design point) of 47,300 lb.

Figure 5-23 shows the sensitivity of control thrust to an uncertainty in estimating aerodynamic characteristics. It is possible to tolerate a 15% uncertainty without exceeding a 10,000-lb. increment (60,000 lb.) over the thrust design level. Improved accuracies beyond those assumed (±5%) do not significantly reduce control thrust.
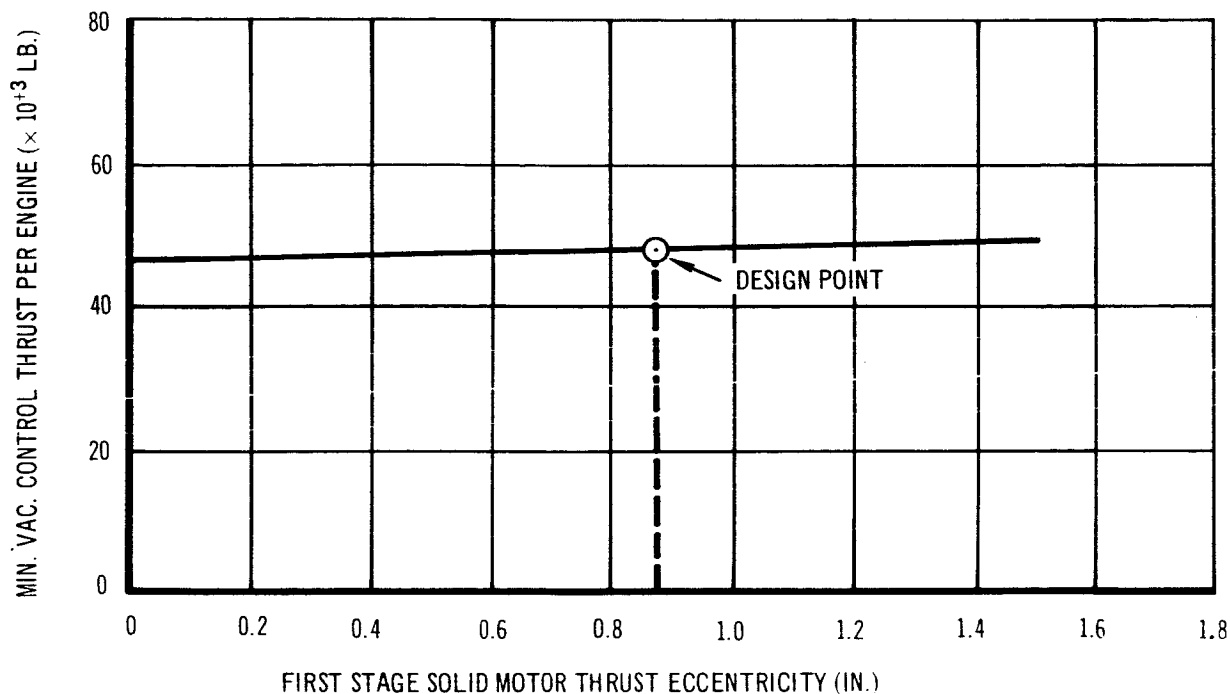
Figure 5-21 Minimum Control Thrust Vs. First Stage
Thrust Eccentricity HES-2G

The effect of variations in booster fin misalignment is shown in Figure 5-24.
A misalignment as high as three degrees would require an additional 3,500 lb.
of control thrust per engine. While this variation is far in excess of manufac-
turing tolerances, such an effective misalignment might be representative of
the effect of interference flows from the steering engine jet wake.

Figure 5-25 presents the sensitivity of required control thrust to first stage
motor length. This variation is based on a constant HES-2G payload. It can
be seen that an increase in first stage motor size from a 120% full length to
a 140% full length motor can be handled by an additional 10,000 lb. of steering
thrust.

As mentioned in Section 5.5.3.3 substantial control thrust requirements
occur at the web burnout time of the third stage 156-in. motor. Control
in yaw is critical due to vehicle-engine geometry and the proximity of CG to
the control station. The CG is most sensitive to HL-10 weight and 156-in.
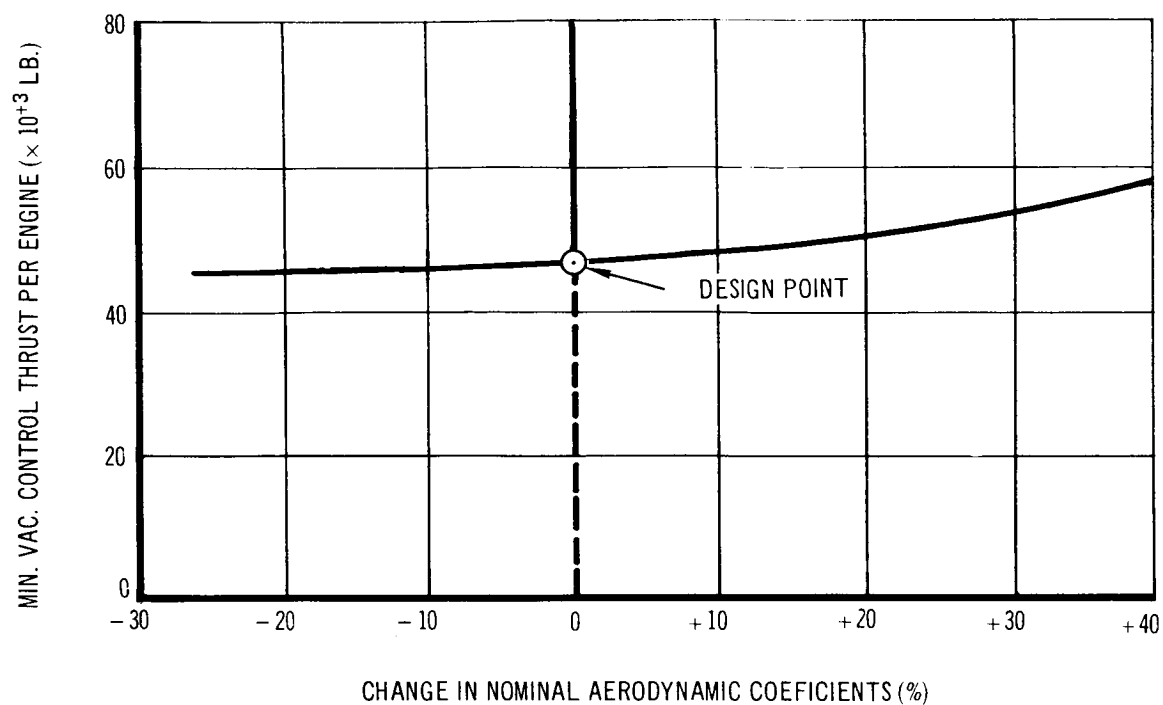
Figure 5-22   Minimum Control Thrust Vs. Nominal Aerodynamic Conditions
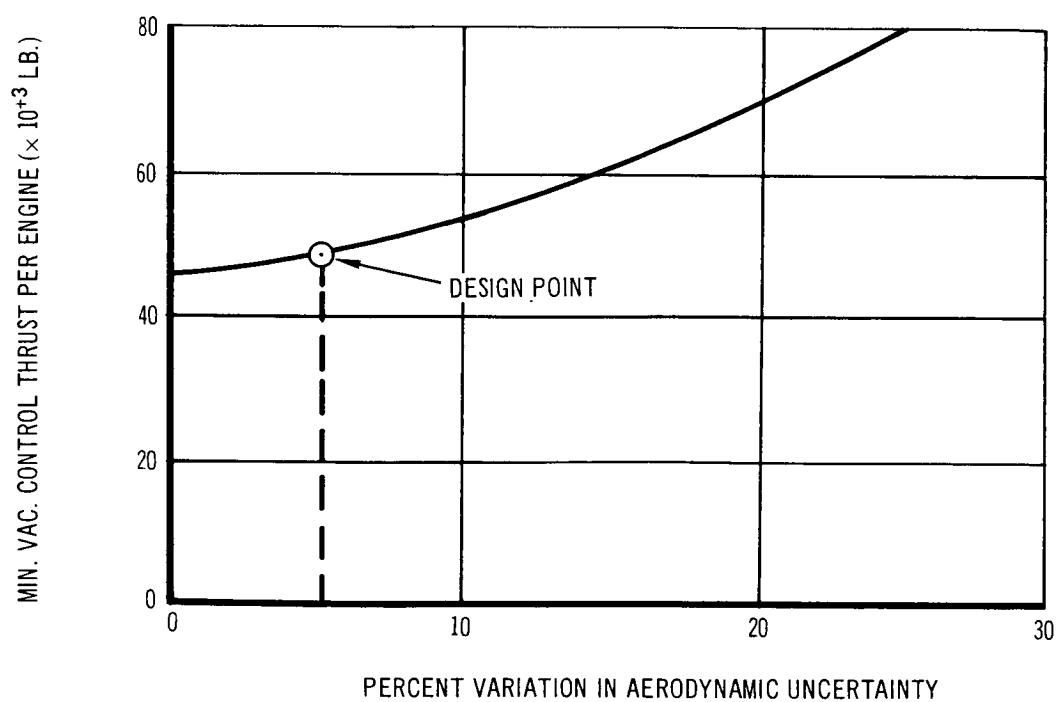
Figure 5-23   Minimum Control Thrust Vs. Uncertainty in Aerodynamic Characteristics
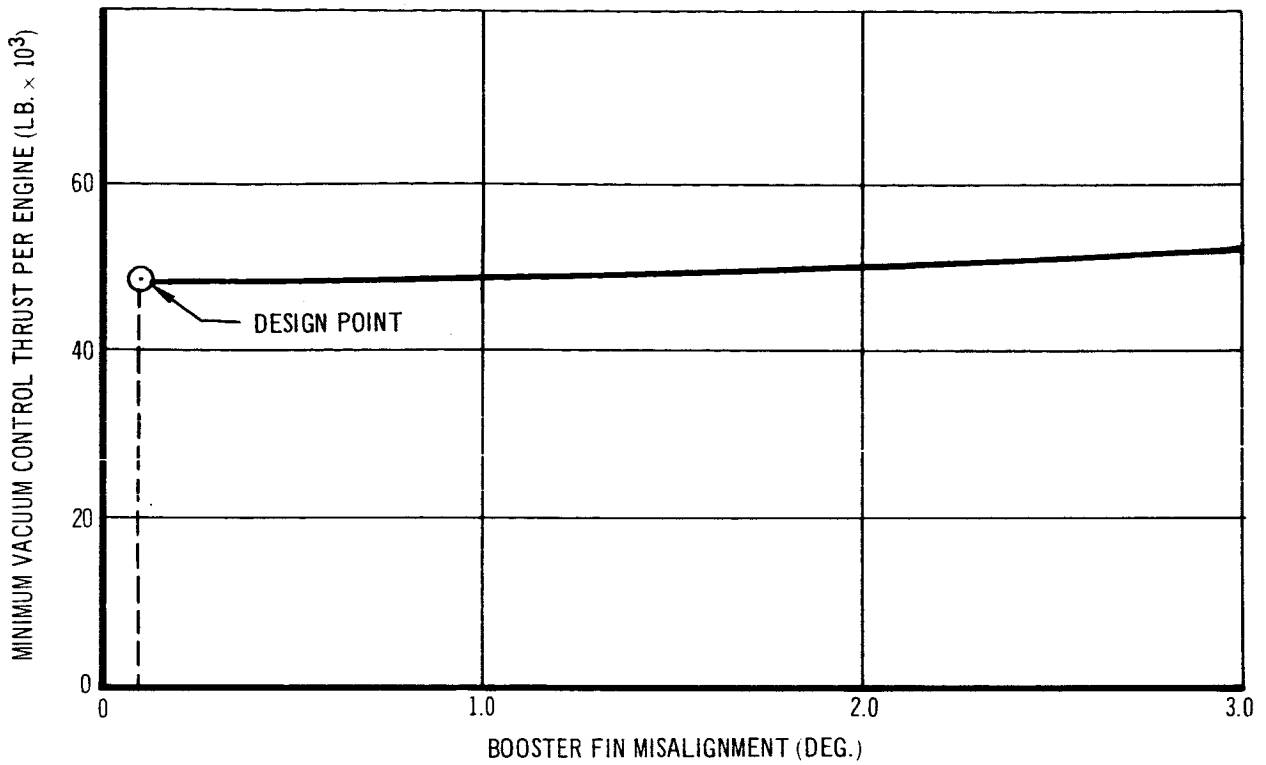
Figure 5-24 Minimum Control Thrust vs. Booster Fin Misalignment – HES-2G
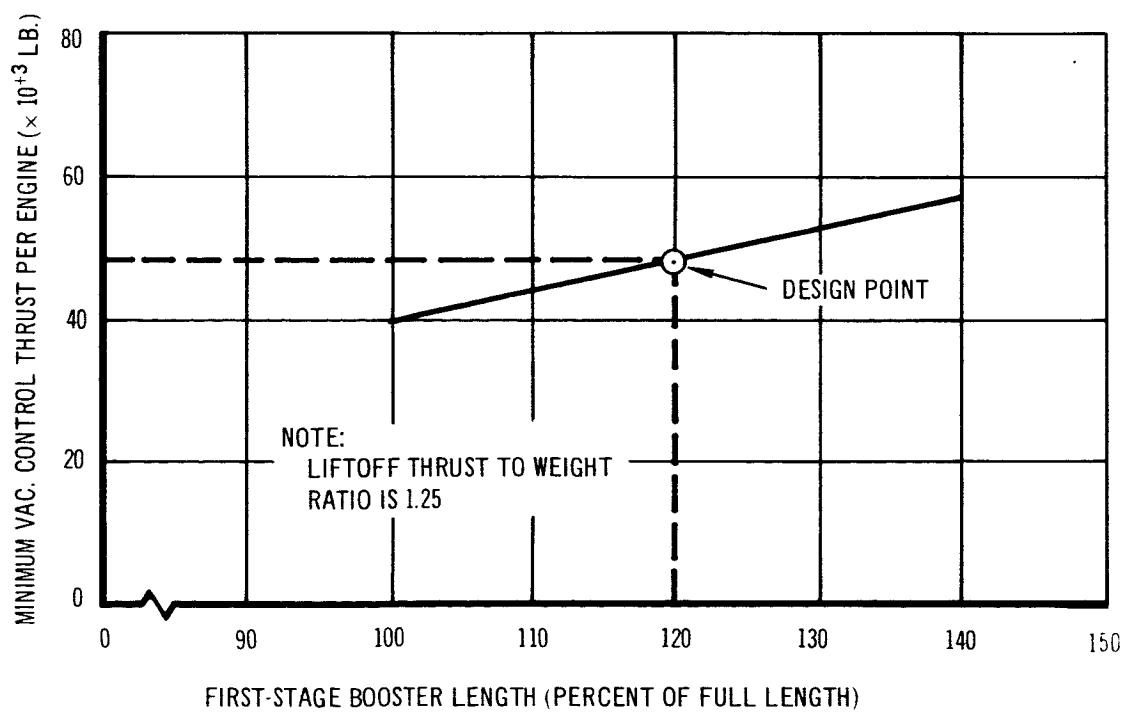
Figure 5-25 Minimum Control Thrust Vs. First Stage Length

motor case weight and, to a lesser degree, the adapter length and the steering tankage weight. Figure 5-26 illustrates the influence on the third stage burnout control thrust of all the significant parameters, Figures 5-27 and 5-28 show the sensitivities of steering thrust to spacecraft weight and gross steering propellant weight (steering tank weight) as a function of 156-in. motor size. Inasmuch as third stage burnout control thrust is only 0.7 of the capability, sizeable deviations of influence parameters could be tolerated.

5.6 MISSION AND PERFORMANCE CAPABILITY

The performance capability of the HES-2G spacecraft is based on the ideal impulsive velocity budget shown in Table 4-1 of Section 4.1. This budget shows a requirement of 2,250 fps of impulsive velocity in order to perform the necessary mission maneuvers and an additional allowance of 4,000 fps for discretionary maneuvering capability. The impulsive velocity equivalent of the separate attitude control system is 250 ft./sec. This attitude control requirement allows for docking, separation, and attitude control throughout the flight profile. As a consequence of this budget, the propulsion system on board the HL-10 was designed to provide 6,250 fps with 5,000 lb. of cargo (including packaging) on board throughout the flight profile.

The curves shown in Figure 5-29 describe the tradeoff between impulsive velocity capability and cargo-carrying capability for the HES-2G spacecraft. As noted, curve (1) refers to the condition in which 4,000 lb. of unpackaged cargo is carried along with the cargo module through rendezvous and docking, and then left at the orbiting space station. The expended ΔV requirement of 1,940 fps is based on those maneuvers listed in the budget, and accomplished prior to docking, plus an additional 150 ft./sec. orbital injection allowance for this vehicle configuration. This is over and above the 350 fps allowed for injection in the ideal budget. The 4,000 lb. of cargo on board the HL-10 is carried throughout the flight. Curve (3) shows the effect of carrying more than 4,000 lb. of unpackaged cargo, along with the adapter cargo module, throughout the flight profile. All of the curves are based on the HES-2G spacecraft as previously described. As can be seen from curve (1), the spacecraft is capable of providing approximately 6,300 fps with 4,000 lb. of
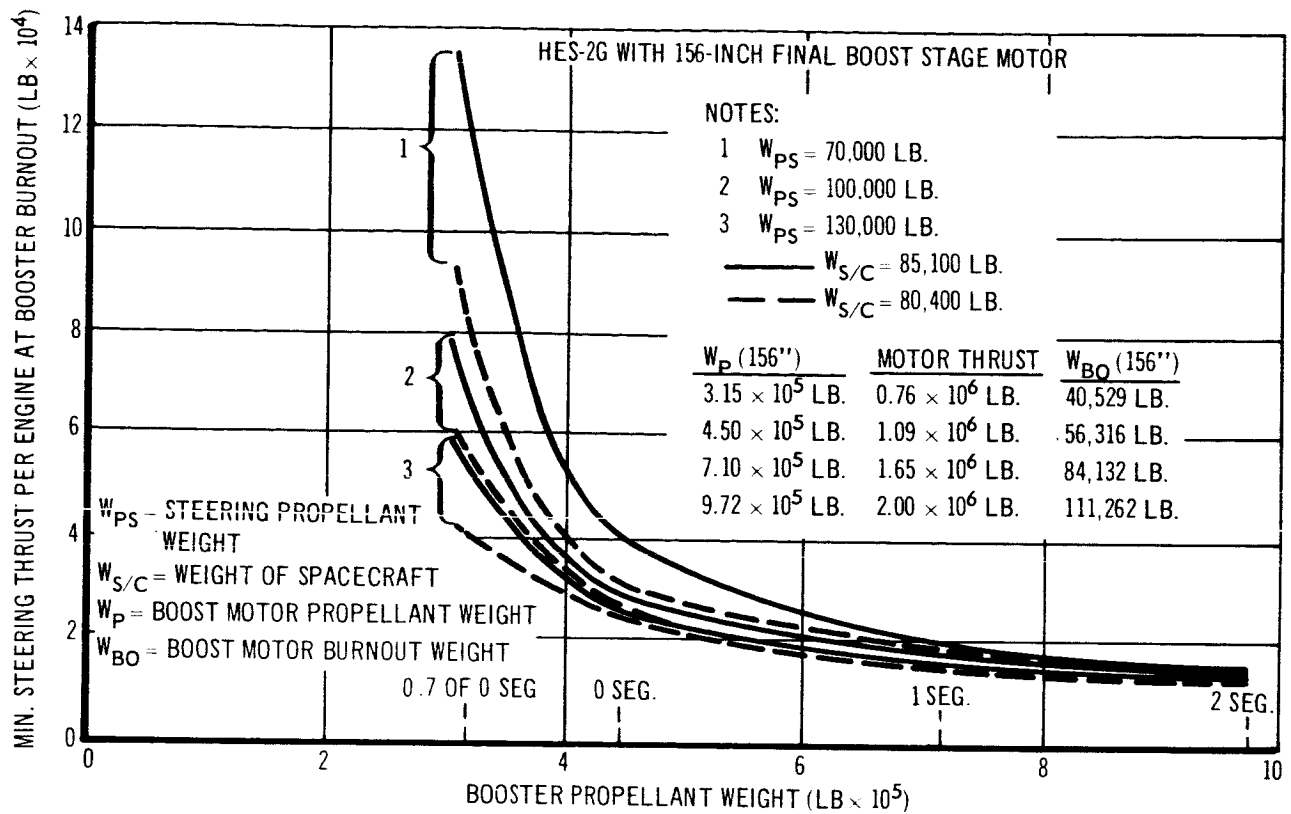
Figure 5-26 Minimum Steering Thrust at Final Boost Stage
Burnout Vs. Booster Motor Size
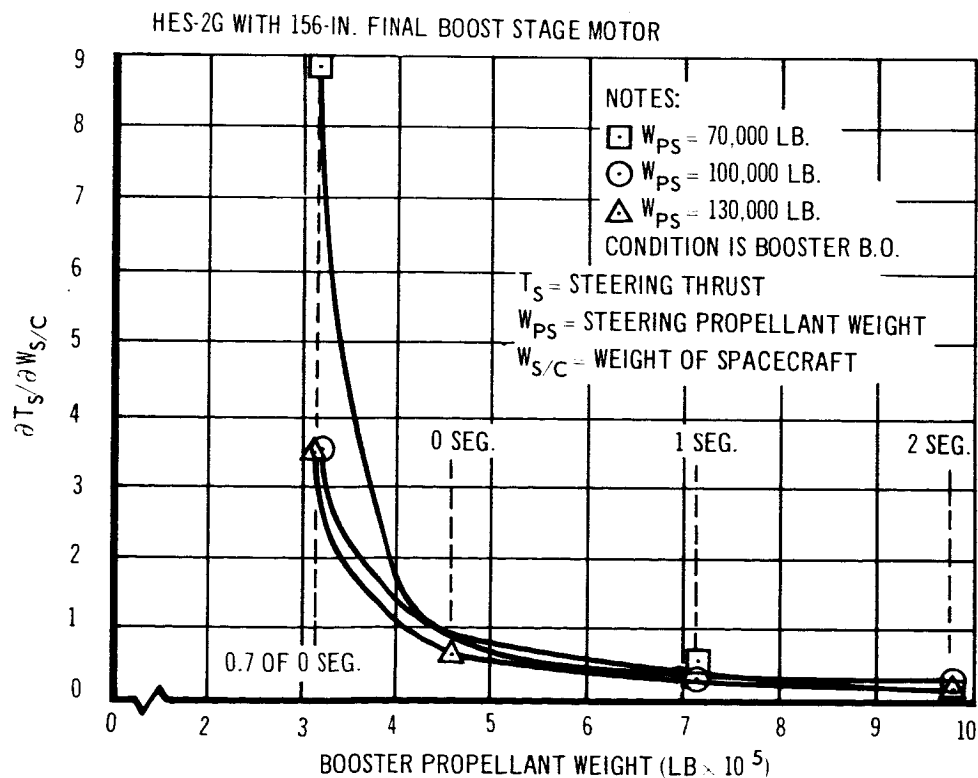
Figure 5-27 Sensitivity of Steering Thrust at Booster Burnout
to HL-10 Weight (HES-2G)
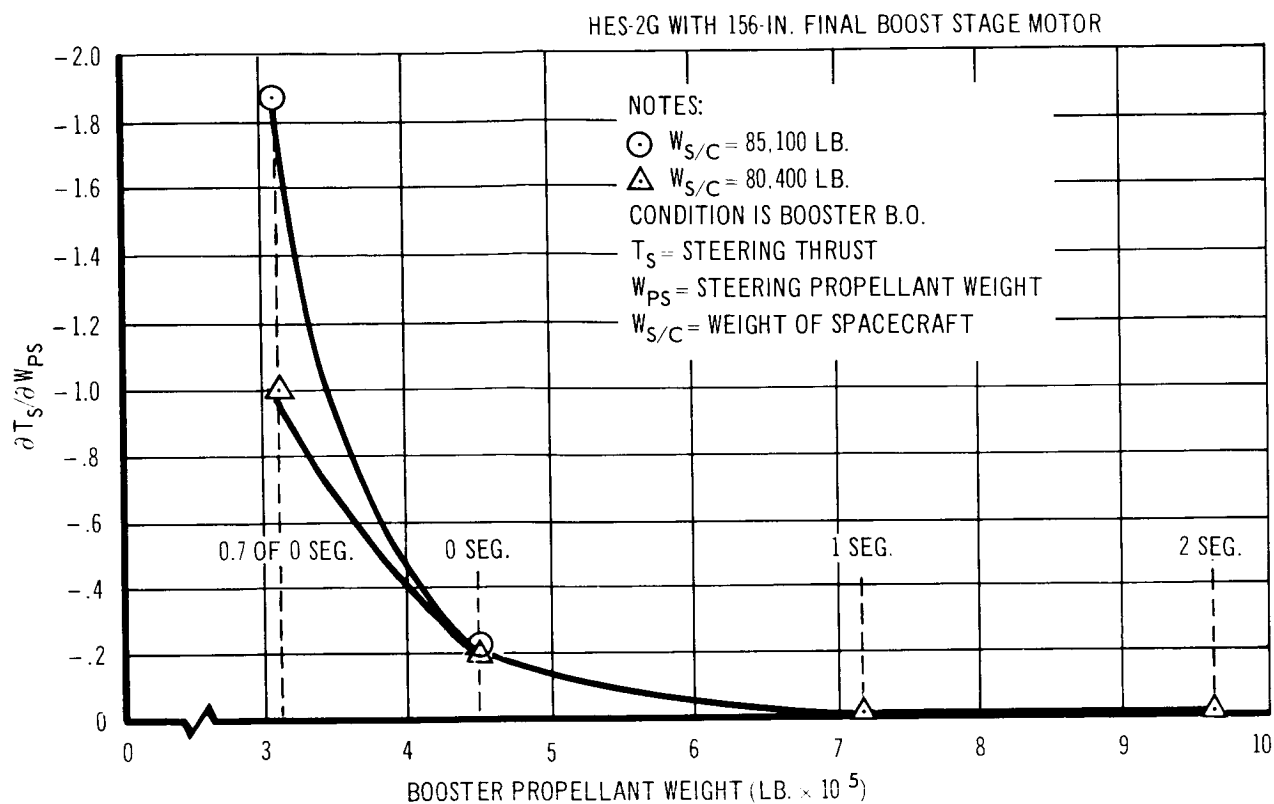
Figure 5-28 Sensitivity of Steering Thrust at Booster Burnout to
Gross Steering Propellant Weight
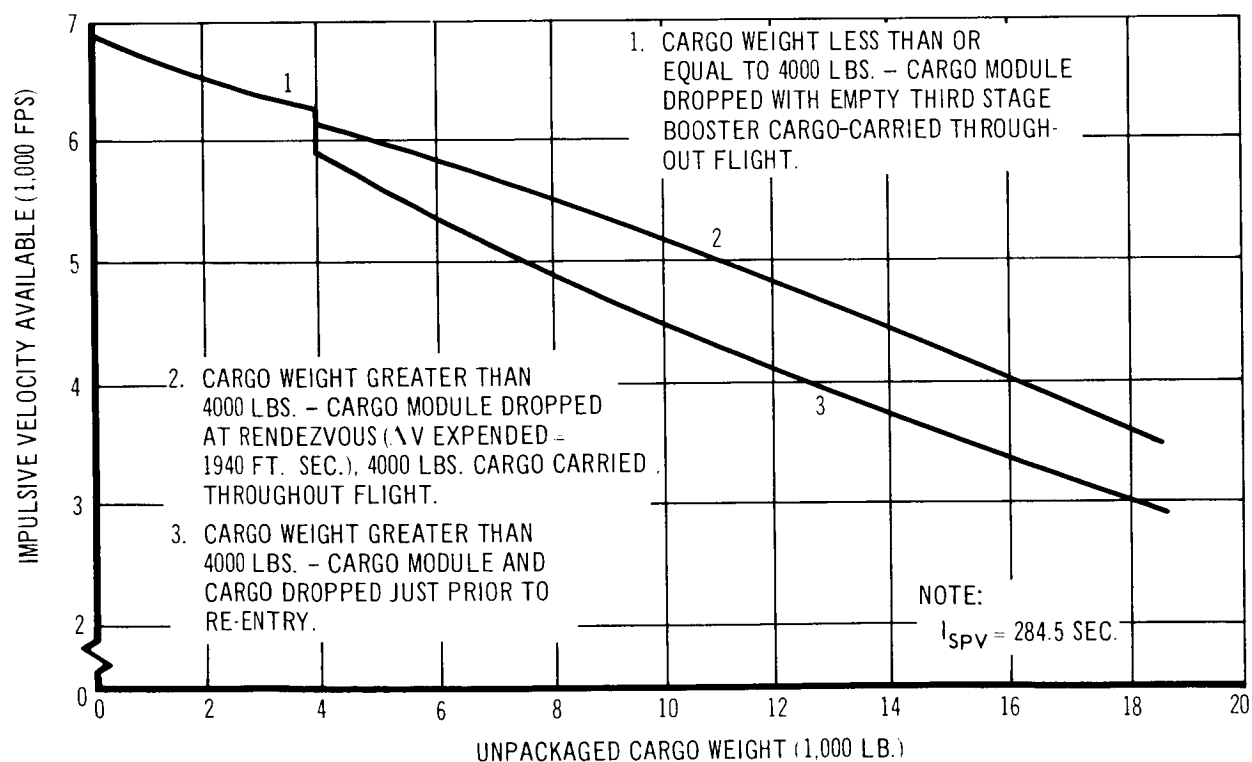
Figure 5-29 Spacecraft Impulsive Velocity Capability
Vs. Cargo Carrying Capability

unpackaged cargo on board. This is slightly higher than the 6,250 fps budgeted, because of the detail weight analysis performed subsequent to preliminary sizing. For the purpose of determining these tradeoffs, the gross weight of the spacecraft and, consequently, the booster payload weight was kept constant for cargo weights greater than 4,000 lb. Propellant on board the HL-10 was considered to be offloaded as cargo weight was increased. For cargo weights less than 4,000 lb. propellant weight on board was held constant and payload weight was decreased.

Final trajectory analysis for this vehicle shows that an additional impulsive velocity increment of approximately 610 fps is required in order to achieve satellite velocity at a 300 n. mi. altitude. The velocity allowed for this requirement in the ideal budget, shown in Table 4-1, is 350 fps. It is felt that detailed trajectory shaping would decrease this discrepancy of 260 fps. The balance would be provided out of the 4,000 fps allowed for discretionary maneuvering capability.

A number of alternate missions were investigated with respect to their effects on impulsive velocity requirements and cargo-carrying capability. The results, along with the mission descriptions are shown in Table 5-11. The impulsive velocity requirements shown for Loading Conditions 1, 4, and 5 are based on the budget and figures shown in Section 4. The impulsive velocity requirements shown for loading conditions 1, 4, and 5 are based on the budget and figures shown in Section 4. The impulsive velocity requirements of Conditions 2, 3, 6, and 7 are based on the cargo-carrying requirements of those missions. Condition 8 shows the maximum capability for this mission. For all conditions, it is assumed that the cargo, and cargo module if required, are carried throughout the flight profile.

5.7 SENSITIVITY OF VEHICLE PERFORMANCE TO DESIGN PARAMETERS

The sensitivity of booster performance to various vehicle design parameters was determined and is presented in Table 5-12. With the exception of the derivatives with respect to steering system specific impulse and thrust, all the sensitivities were computed using the impulsive velocity equation. The derivatives were determined by making perturbations in the nominal three stage vehicle and computing the impulsive velocity. The difference between the resultant impulsive velocity and the nominal impulsive velocity divided by the variation produced the appropriate sensitivity.

Table 5-11

MISSION CAPABILITY - BASELINE VEHICLE

Loading Condition	Number of Passengers	Total Cargo* (Unpackaged)	Impulsive Velocity ΔV	Mission Description
1	6	29,900	1,140	Max. cargo with min. ΔV. Rendezvous at 300-n. mi. circular orbit i = 31°
2	6	19,000	2,860	Extended MORL resupply rendezvous at 200-n. mi. orbit i = 28.7°
3	9	0	6,530	Extended MORL - Rescue search capability is Δi_{REL} = 13.8°
4	6	8,400	4,920	Rendezvous with space station launched at max. azimuth of 40° at AMR at 200-n. mi. altitude (53° inclination)
5	6	23,000	2,190	Polar orbit (minimum energy ascent)
6	6	0	6,880	Maximum altitude of 2,000-n. mi.
7	6	0	6,880	Multiple rendezvous with 4 equally-spaced coplanar targets at 860 n. mi. i = 28.5°
8	6	0	6,880	Reconnaissance with one over-fly assurance. i = 78.5°

*Maximum available cargo volume based on a packaging weight of 25% of unpackaged weight with 12,750 lb. of dry cargo at an average density of 20 lb./cu. ft. and volume efficiency of 75%, and on 6,250 lb. of propellant at a density of 75.1 lb./cu. ft. and volume efficiency of 50%.

The sensitivities for the steering system specific impulse and thrust were determined by trajectory simulations. The trajectories were flown to a 300-n. mi. apogee with different payloads, steering specific impulses, and steering thrusts. Plots of total booster impulsive velocity and apogee velocity were made as a function of payload for constant steering specific impulse or steering thrust. From the apogee velocity plot for a particular specific impulse or thrust, the payload was selected that corresponded to an apogee velocity of 24,277 ft./sec. (apogee velocity of the baseline trajectory). From the total impulsive velocity/payload plot, the impulsive velocity was determined for the payload selected. The sensitivities were then computed for the steering system specific impulse and thrust and are included in Table 5-12.

Generally speaking, the data of Table 5-12 reflect sensitivities typical of three stage vehicles designed to near-optimum ratios of liftoff to payload weight ratios. It will be noted that the payload weight is relatively insensitive to changes in steering engine impulse and steering engine thrust.

5.8 REFERENCES

1. A Lifting Re-Entry, Horizontal-Landing-Type Logistic Spacecraft. Boeing Report D2-22921, 3 February 1964.

2. ASTRO - An Available Economical Solution to the High Cost of Space Flight. Douglas Engineering Paper No. 1651, 18 June 1963.

3. R. W. Rainey and C. L. Ladson. Aerodynamic Characteristics of a Manned Lifting Entry Vehicle at Mach Numbers from 0.2 to 1.2. NASA Report L-3965 (Review Copy), Langley Research Center, Hampton, Virginia.

4. Transmittal of Preliminary HL-10 Data. Letter from Langley Research Center, Hampton, Virginia, 18 January 1964.

5. W. C. Pitts, J. N. Nielsen, and G. E. Kaattari. Lift and Center of Pressure of Wing-Body-Tail Combinations at Subsonic, Transonic, and Supersonic Speeds. NACA Report 1307, 1959.

6. J. R. Spahr. Contributions of the Wing Panels to the Forces and Moments of Supersonic Wing-Body Combinations at Combined Angles. NACA Technical Note 4146, January 1958.

Table 5-12

BOOSTER SENSITIVITIES

X	$\dfrac{\partial \Delta V}{\partial X}$		$\dfrac{\partial W_{pl}}{\partial X}$	
Specific Impulse, First Stage	+30.11	ft./sec./sec.	+585.90	lb./sec.
Specific Impulse, Second Stage	+30.14	ft./sec./sec.	+586.56	lb./sec.
Specific Impulse, Third Stage	+47.11	ft./sec./sec.	+916.76	lb./sec.
Propellant Weight, First Stage	+ 0.00125	ft./sec./lb.	+ 0.02439	lb./lb.
Propellant Weight, Second Stage	+ 0.00212	ft./sec./lb.	+ 0.04127	lb./lb.
Propellant Weight, Third Stage	+ 0.00474	ft./sec./lb.	+ 0.09216	lb./lb.
Inert Weight, First Stage	- 0.00195	ft./sec./lb.	- 0.03787	lb./lb.
Inert Weight, Second Stage	- 0.00826	ft./sec./lb.	- 0.16073	lb./lb.
Inert Weight, Third Stage	- 0.05145	ft./sec./lb.	- 1.00000	lb./lb.
Payload Weight	- 0.05139	ft./sec./lb.	-	
Specific Impulse, Steering Engines	- 0.36364	ft./sec./sec.	+ 65.45	lb./sec.
Thrust, Steering Engines	+ 0.00092	ft./sec./lb.	- 0.01760	lb./lb.

ΔV = increment in impulsive velocity, ft./sec.

W_{pl} = payload weight, lb.

Section 6
MANNED SPACE VEHICLE SYSTEM CHARACTERISTICS

6.1 PREPARATION FOR LAUNCH AND LAUNCH OPERATIONS

This section deals with those system operational characteristics which require some definition to establish total system feasibility. These were, (1) the prelaunch and launch operations, (2) the mission ascent-trajectory, (3) the abort provisions, (4) rendezvous and docking, and (5) crew cargo ingress and egress. The deorbit, re-entry, and landing phases of the mission were investigated only to the extent that allowances for impulsive velocity requirements were made in the total mission energy budget.

6.1.1 Introduction

The purpose of this section is to describe the operations preparing the HL-10 vehicle and boosters for launch. These operations consist of the following events:

1. Transportation from manufacturing site to launch pad
2. Handling and erection of the boosters at the pad
3. Assembly of the boosters, HL-10 spacecraft and adapters
4. Integrated system checkout and countdown prior to launch
5. Scheduling of the entire operation from receipt and inspection of hardware components to final countdown.

Additional facilities are required to cope with the problem involved in handling large solid boosters because of their extreme size and weight. For example, new transportation methods must be provided to move the boosters from the manufacturer to the launch pad, erection methods must be devised to hoist more than 4 million lb. to heights of several hundred feet, and new methods are also needed for assembling large stages weighing from 500,000 lb. to 4 million lb.

Although these handling problems are significantly greater than those posed by current systems, their solution is not beyond the current state-of-the-art. However, it is outside the scope of this study to deal in any great detail with the problems involved in transporting and handling these large solid boosters, except in the area of feasibility.

6.1.2 Transportation to the Launch Area

Figure 6-1 shows the relationship of the two alternate manufacturing sites (Aerojet General Corporation at Dade County, Florida and Thiokol Chemical Corporation at Brunswick, Georgia) to each other and to the Cape Kennedy launch facilities. Barges containing the booster motors can be towed by ocean-going tugs from either of the manufacturing sites to Cape Kennedy (200 miles). The towing operation can be accomplished via the ocean (off coast) or via one of the many sheltered waterways along the Florida coast. It is estimated that loading a motor on the barge and towing it to the ocean will take about one day; two more days should be allowed for the trip to Cape Kennedy.

Steps and times involved in the major events of the logistics sequence from factory to launch area are shown in Figure 6-2.

6.1.3 Handling and Erection of Boosters at the Launch Pad

Two methods have been considered for transporting the booster to the launch area after arrival at Cape Kennedy. First, the barge can be towed down a canal linking the ocean to a buoyant handling pit located at the launch pad area. Towing the barge down the canal and erecting it in the pit will take approximately two days. Second, if no canal linking the ocean with the pad is available, the barge can be towed directly to an off-loading dock. The booster can be transferred to either a railroad transporter or road crawler and moved to the launch area for erection. The distance from the dock to the launch pad area is about five miles. It is estimated that this handling and erection operation will, as in the first method, require two days including one day for erection.

Erection is accomplished with a tower, step jack, and truck. However, there are many other alternate methods described in Section 6-6, Reference 1.

GEORGIA

THIOKOL CHEMICAL CORPORATION
BRUNSWICK, GEORGIA

200 MILES

INTRACOASTAL WATERWAY
(THIOKOL TO MILA)

CAPE KENNEDY
MISSILE LAUNCH FACILITY
MILA

FLORIDA

200 MILES

INTRACOASTAL WATERWAY
(AEROJET GENERAL
TO MILA)

AEROJET-GENERAL CORPORATION,
DADE COUNTY FACILITY
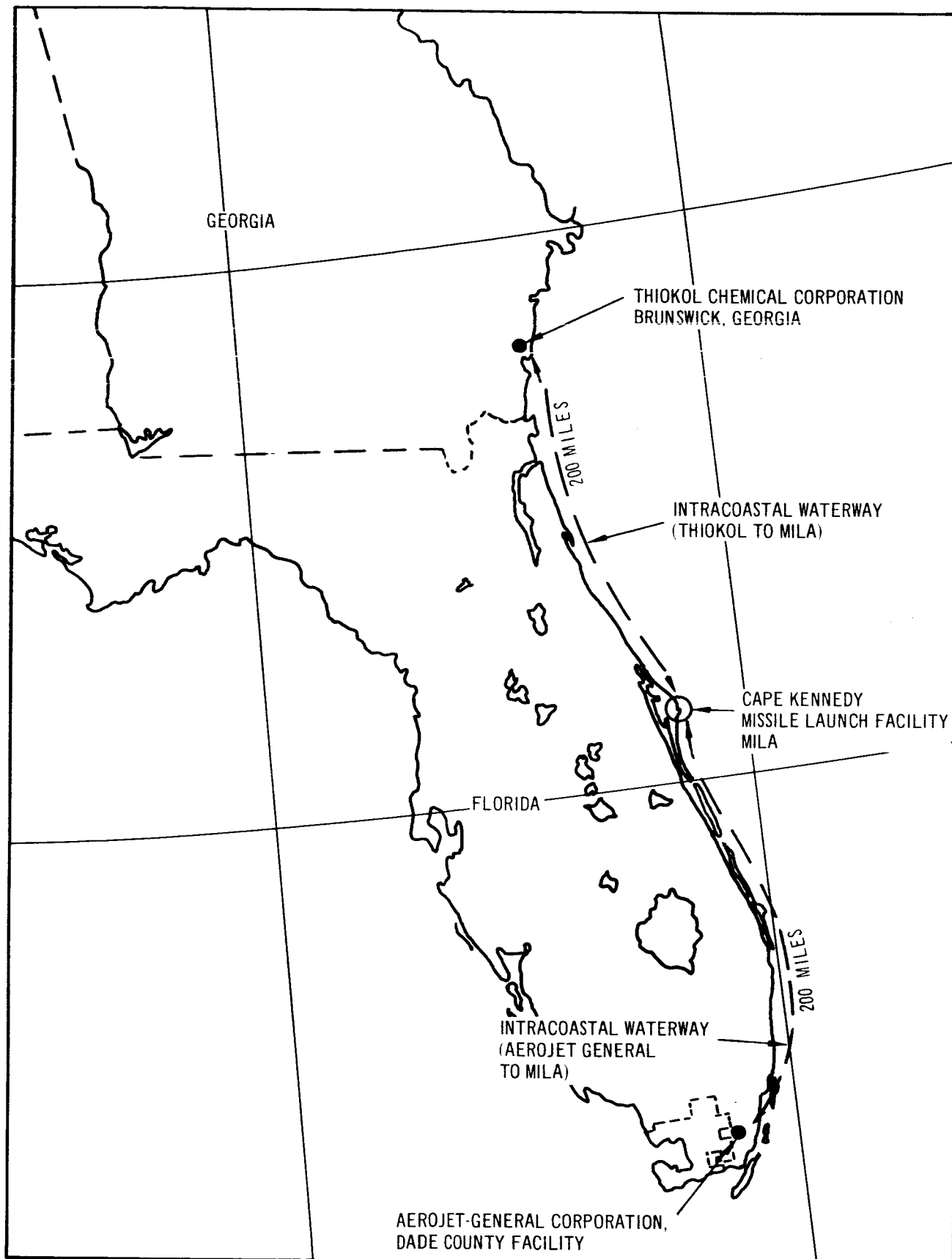
Figure 6-1 Manufacturing Locations and Water Routes to
Cape Kennedy Launch Site
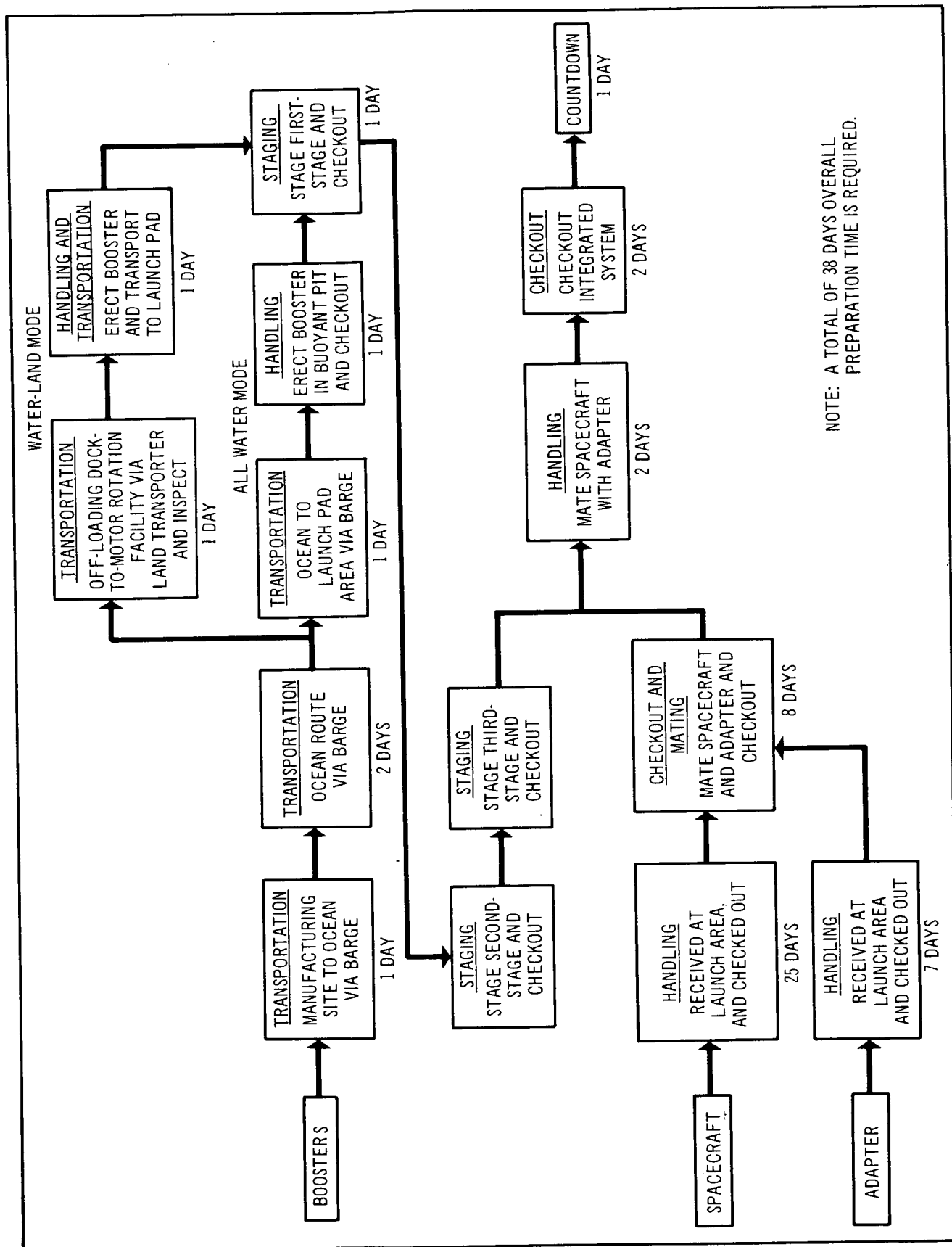
Figure 6-2   Major Operational Events and Times for Logistic
Support of HES-2G   HL-10 Spacecraft System

It is sufficient for the purposes of this study to state that a solid motor erection and rotation facility.is well within the state-of-the-art of present engineering practice and does not present a problem. Figure 6-3 illustrates the tower method of erection.

A typical launch area is shown in Figure 6-4 (proposed in Reference 1) as a future base of operations for large solid motors launch vehicles.

6.1.4 Stage Assembly

After the first stage is erected, it is ready for assembly with the upper stages. This may be accomplished using derricks, cranes, and roll-ramps. The booster stages weigh approximately 4.33 million lb., 1.5 million lb., 0.58 million lb., for the first, second, and third stages, respectively. The spacecraft (including adapter, fuel, abort rockets, etc.) plus fueled steering tankage weighs approximately 194,000 lb. The boosters and spacecraft at liftoff weigh 6.6 million lb. These are the weights that must be handled during staging.

STAY

ERECTION TOWER

TRUCK

ELEVATION OR LIFTING OPERATION
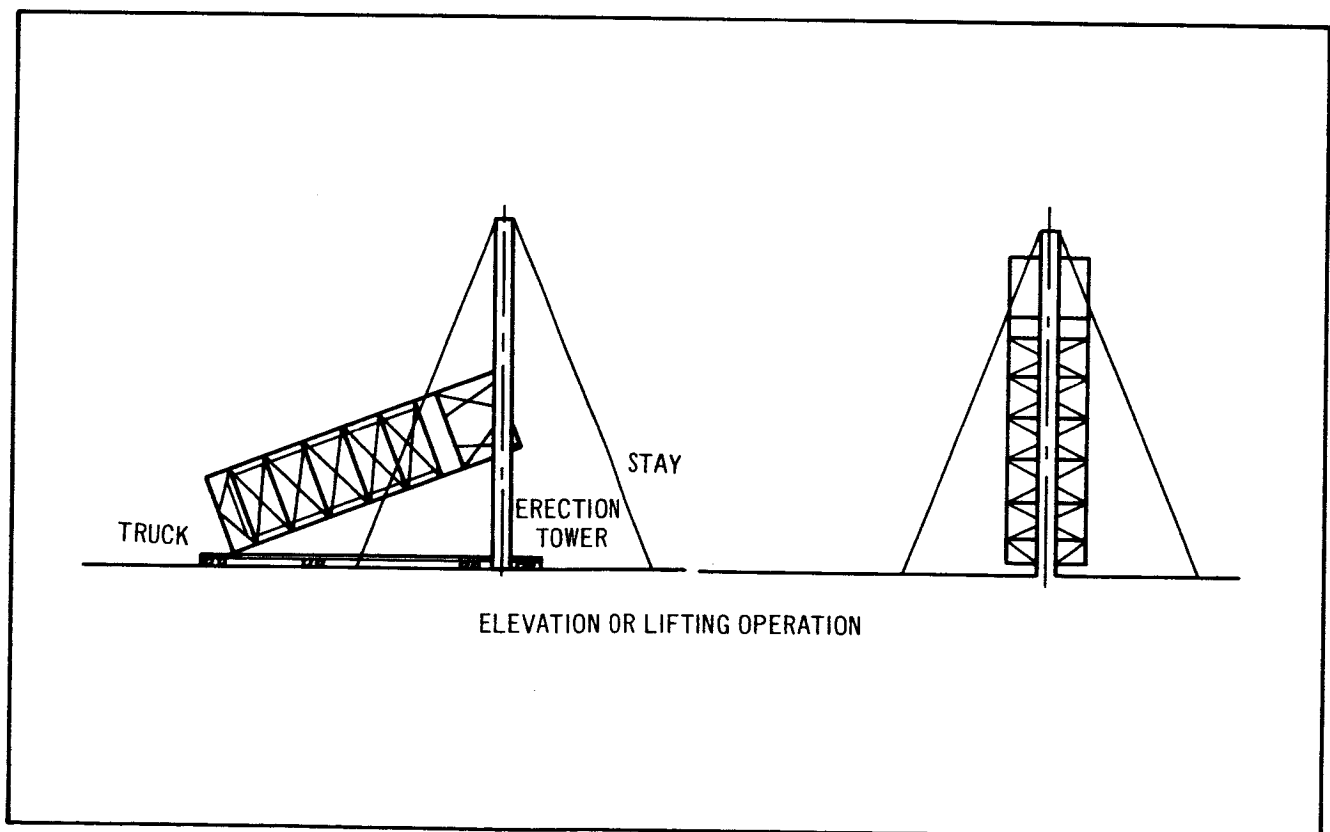
Figure 6-3 Typical Erection Tower, Step Jack, and Truck for Erecting Boosters
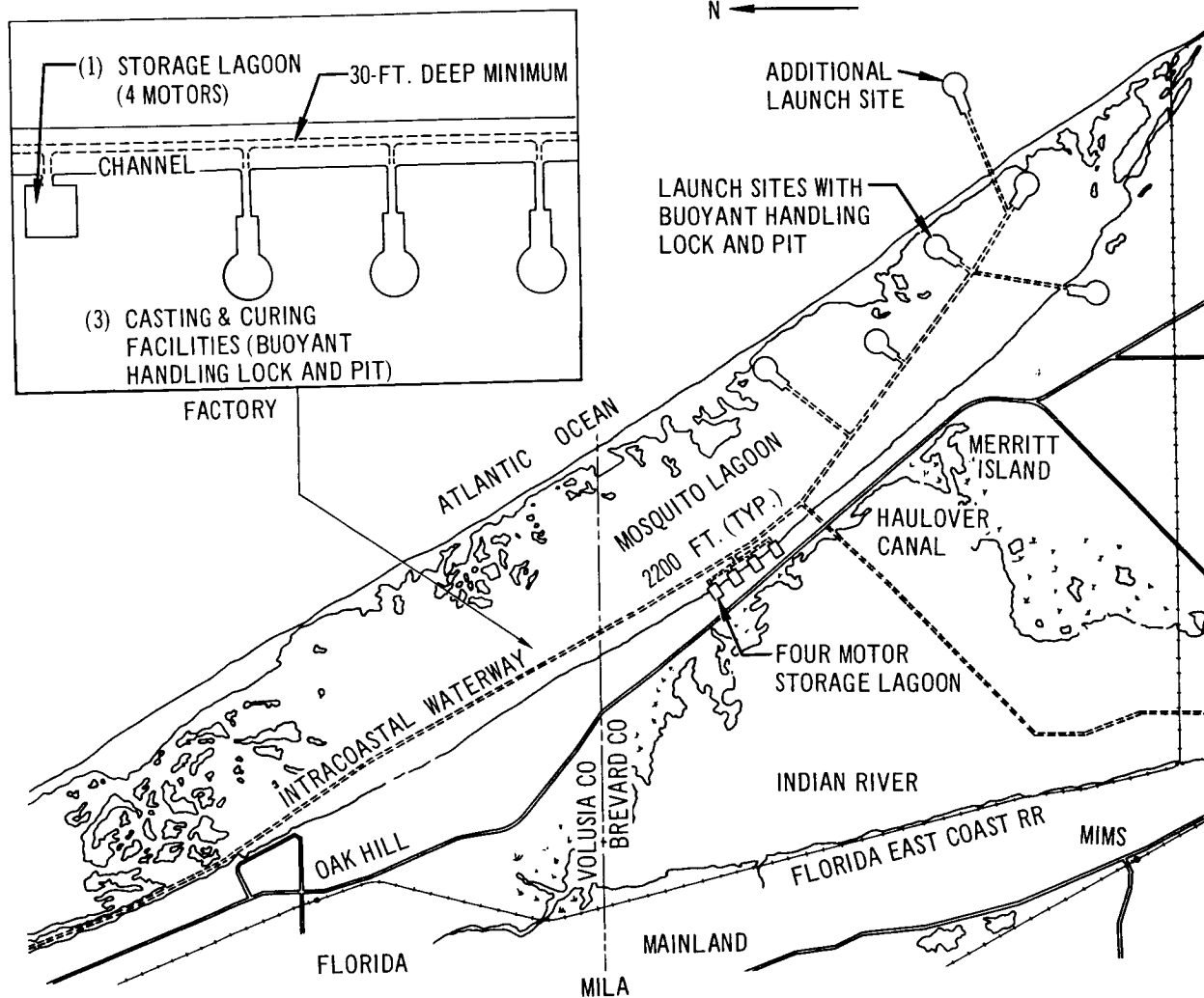
Figure 6-4 Proposed Merritt Island Large Solid Booster Launch Area

A roll-ramp installation presents a possible solution to the handling of large stage weights. Such an installation is shown in Figure 6-5; it is used to raise and lower the stages during, and after, the assembly operation. The system consists of a pedestal and a platform which can be positioned relative to the pedestal. It can be designed to handle as much as 20 million lb.; this is more than sufficient to handle the boosters and spacecraft system. Cranes can be built capable of lifting 10 million lb., so that, a roll ramp and crane system, in conjunction with a handling and staging pit (see Figure 6-5) can be used to stage the HES HL-10 system. Using the roll-ramp and pit allows the staging to be done below ground level and eliminates the problem of lifting stages several hundred feet. The boosters are positioned on the roll ramp platform and the platform lowered into the pit. Succeeding stages are similarly staged. The roll-ramp platform may also serve as the launch pad. Igniters and the deflection shield are positioned after staging is complete. For details of this phase, see Section 6.1.5. Figure 6-5 shows that a pit, 350 ft. deep and 50 ft. in dia. would be more than sufficient to allow all handling and assembly below ground. Caissons of several sections can be used, and annularly positioned, (one inside the other like a sleeve), and "bulkheaded" along the length of the pit (at regular intervals) to provide strength and prevent buckling. The large motor manufacturers have had extensive experience with pit construction in the 623A large motor development program. The roll-ramp stems (e.g., Figure 6-5) can be formed in sections also. The stems may be connected at intervals with adapters. This will provide the means to lift the entire staged system above ground level prior to countdown. Work and maintenance platforms may be located along the length of the pit in a peripheral arrangement. This will provide ready access to the stages as well as stiffness to the caisson, pit, and integrated roll-ramp system. These platforms may be made so that they can be moved to different heights. Details of this system qualify as a proper subject for a subsequent study.

6.1.5 Schedule for Operations

The event and time schedule of all systems of the HES-2G (1.2-0.4-0)logistics spacecraft is presented in Figure 6-6. The overall time from "receive
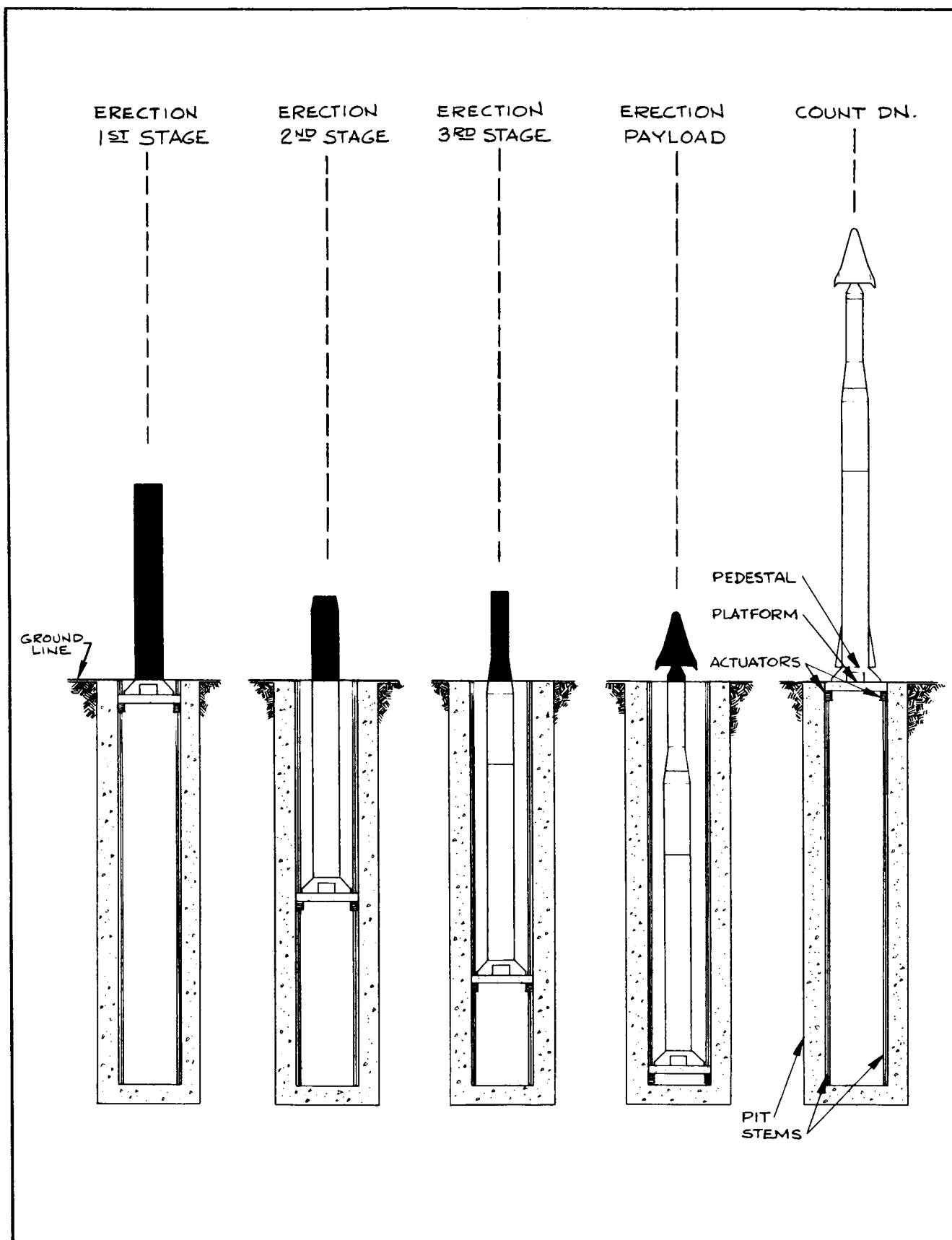
Figure 6-5 Spacecraft and Booster System Assembly Sequence Diagram
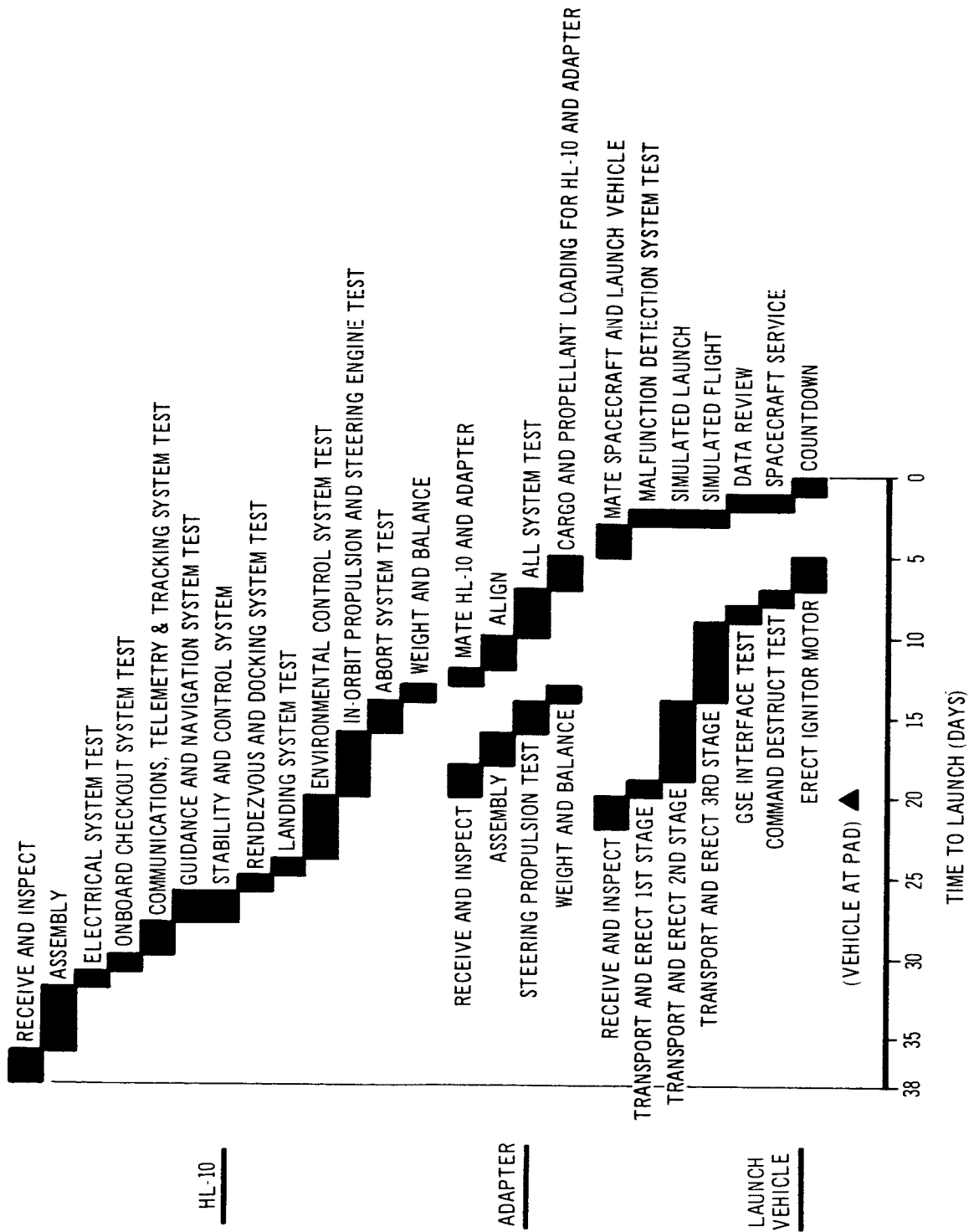
Figure 6-6 HES-2G Spacecraft/Solid Booster Launch Preparation Schedule

and inspect" of the HL-10 through final launch-countdown is about 38 days. This includes a countdown of 560 minutes; the countdown schedule is shown in detail in Figure 6-7.

The HL-10 is received early in the schedule; the solid boosters are received at about midpoint. A schematic showing crucial times for erecting and assembling the 3 stages, and staging the spacecraft are shown in Figure 6-8. The assembly of the boosters is done in parallel with spacecraft and adapter-oriented operations. All cargo and propellant are loaded prior to the staging of the spacecraft (HL-10 plus adapter) to the booster. Approximately 5 days before countdown the spacecraft and booster systems are mated.

The last 5 days are spent in final system checkout; details are noted in Figure 6-6. The countdown schedule of events is shown in Figure 6-7. These data are based on a review of existing systems (Section 6-6, References 2, 3, and 4) and also on discussions with large solid-motor manufacturers' representatives.

A relatively large portion of the time in countdown is spent installing the launch vehicle ordnance components, such as squibs, ignition system, etc.; for other details refer to Figure 6-7.

6.1.6 Liquid Booster Effect on Launch Preparation Schedule

In order to evaluate the soundness of the previously discussed prelaunch and launch operation time table for the large solid booster vehicle, a comparison was made with existing systems. The systems chosen were a large liquid fueled vehicle, the Saturn I, and a vehicle using composite propellants, the Titan IIIC. Schedules based on utilization of these boosters are presented in Figures 6-9 and 6-10 for Saturn I and Titan IIIC, respectively.

The Saturn I schedule requires 56-days prelaunch operations whereas the Titan IIIC requires 55 days. The solid boosters have about an 18-day schedule time advantage over the corresponding liquid or composite boosters. The basic reason for this difference is due to the relatively longer time required to check out liquid booster systems. The data upon which the liquid booster checkout schedule is based are given in Section 6-6, References 2, 3, and 4.
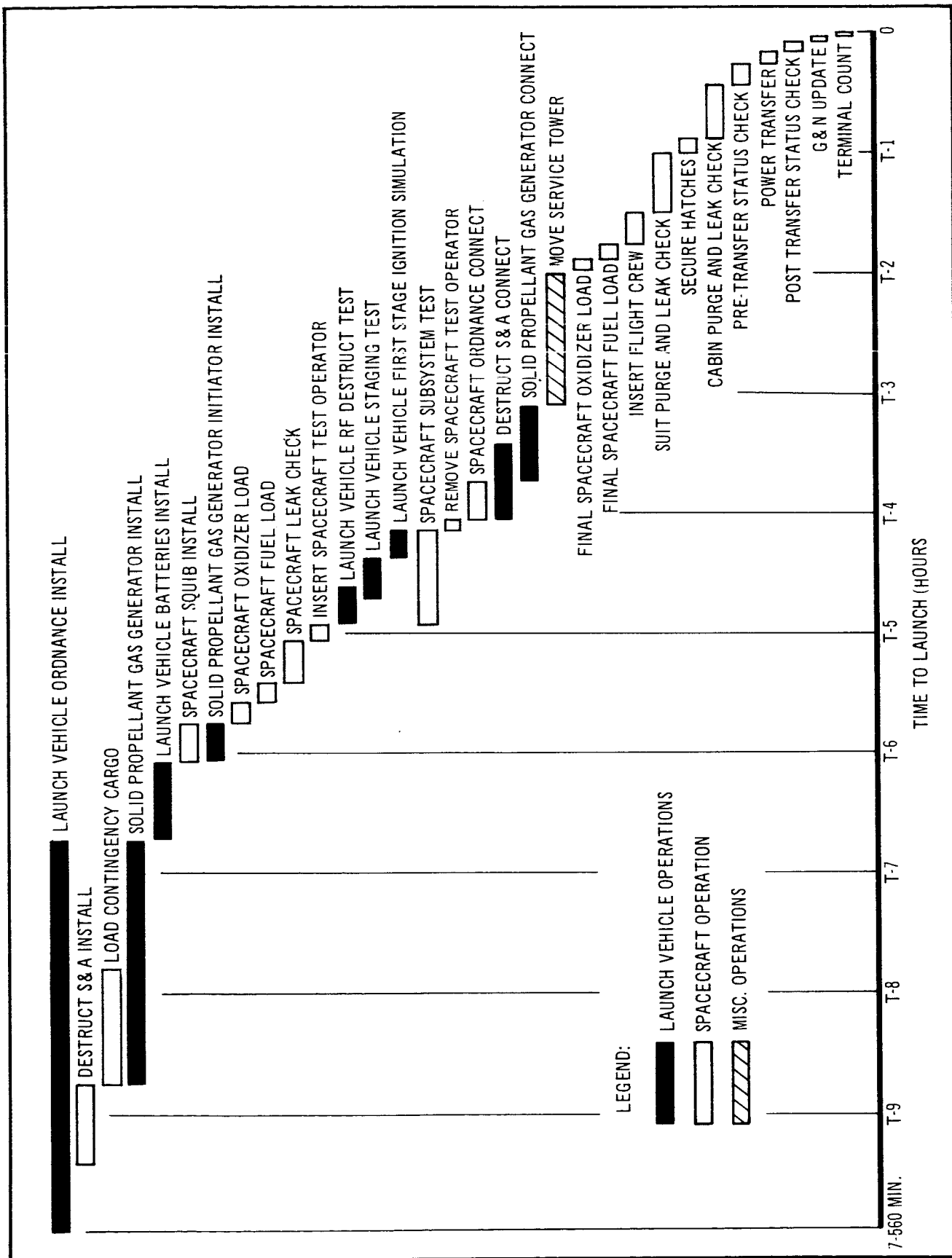
Figure 6-7 HES-2G Spacecraft/Solid Booster Countdown

Figure 6-8 Major Events In Launch Preparation Schedule

RECEIVE AND INSPECT FIRST ITEM

TRANSPORT & ERECT 1ST. STAGE

TRANSPORT & ERECT 2ND. STAGE

TRANSPORT & ERECT 3RD STAGE

38 37 36 31 30 29 28 27 26 25 24 23 22 21 20 19 18 17 16 15 14

DAYS

1#   (102)

MATE HL-10 & ADAPTER

HL-10 SPACECRAFT

ADAPTER

3RD STAGE

2ND STAGE

MATE SPACECRAFT SYSTEMS TO LAUNCH VEHICLE

1ST STAGE

G.S.E TEST, ET AL

SCALE 1 INCH = 200 INCHES

13 12 11 10 9 8 7 6 5 4 3 2 1 0

2 #   (102)

560 MINUTES

COUNTDOWN
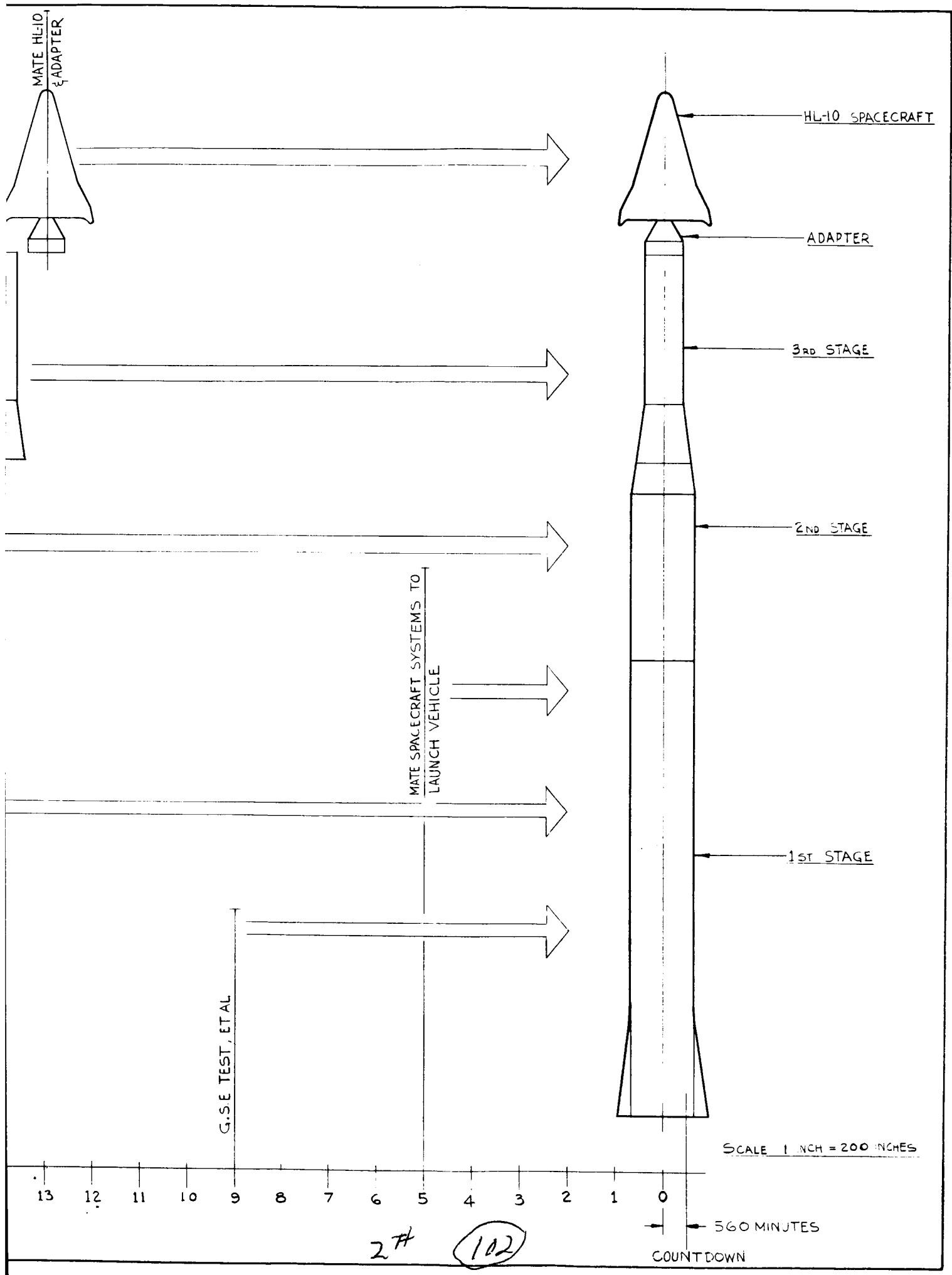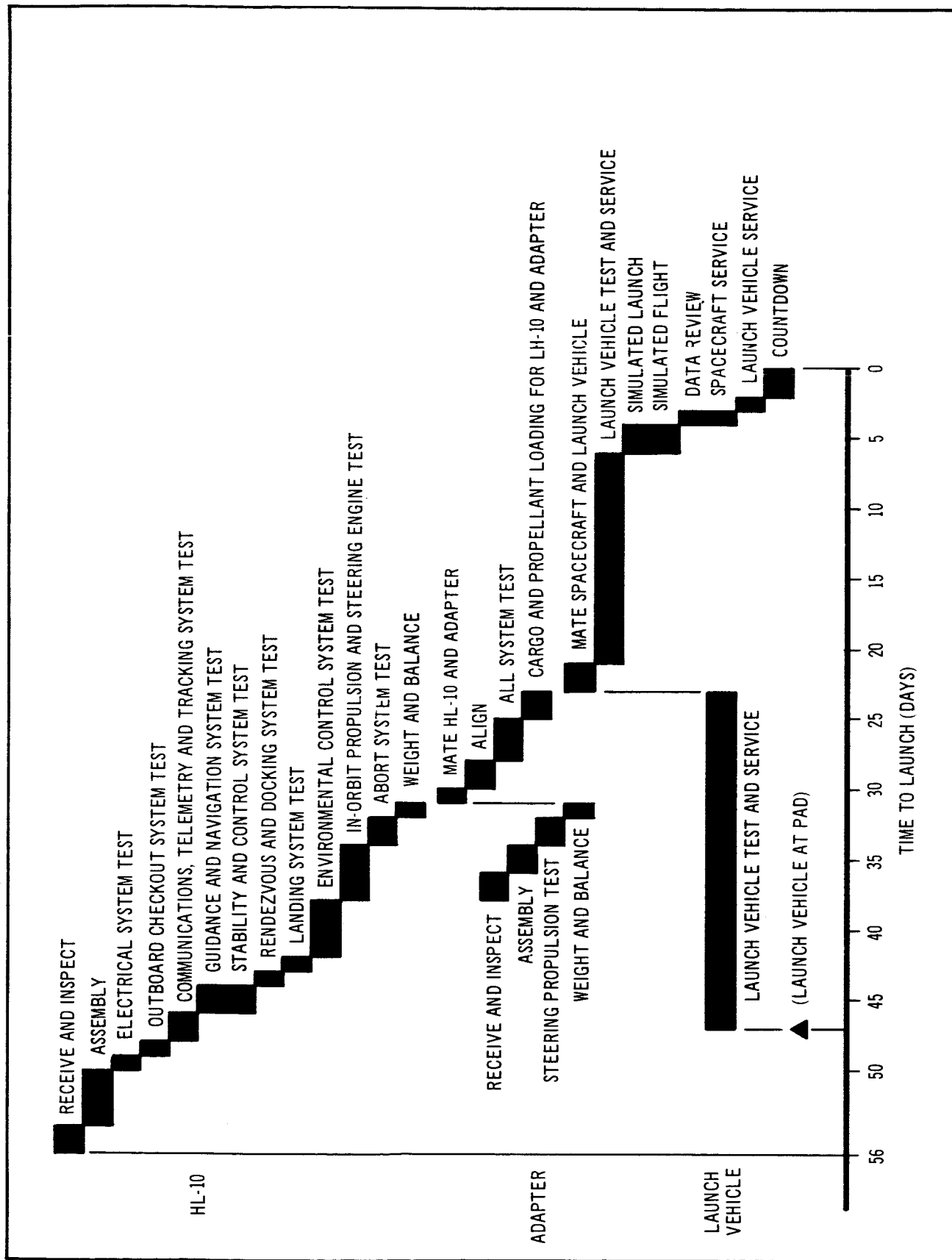
Figure 6-9 HES-2G Spacecraft/Saturn I Launch Preparation Time
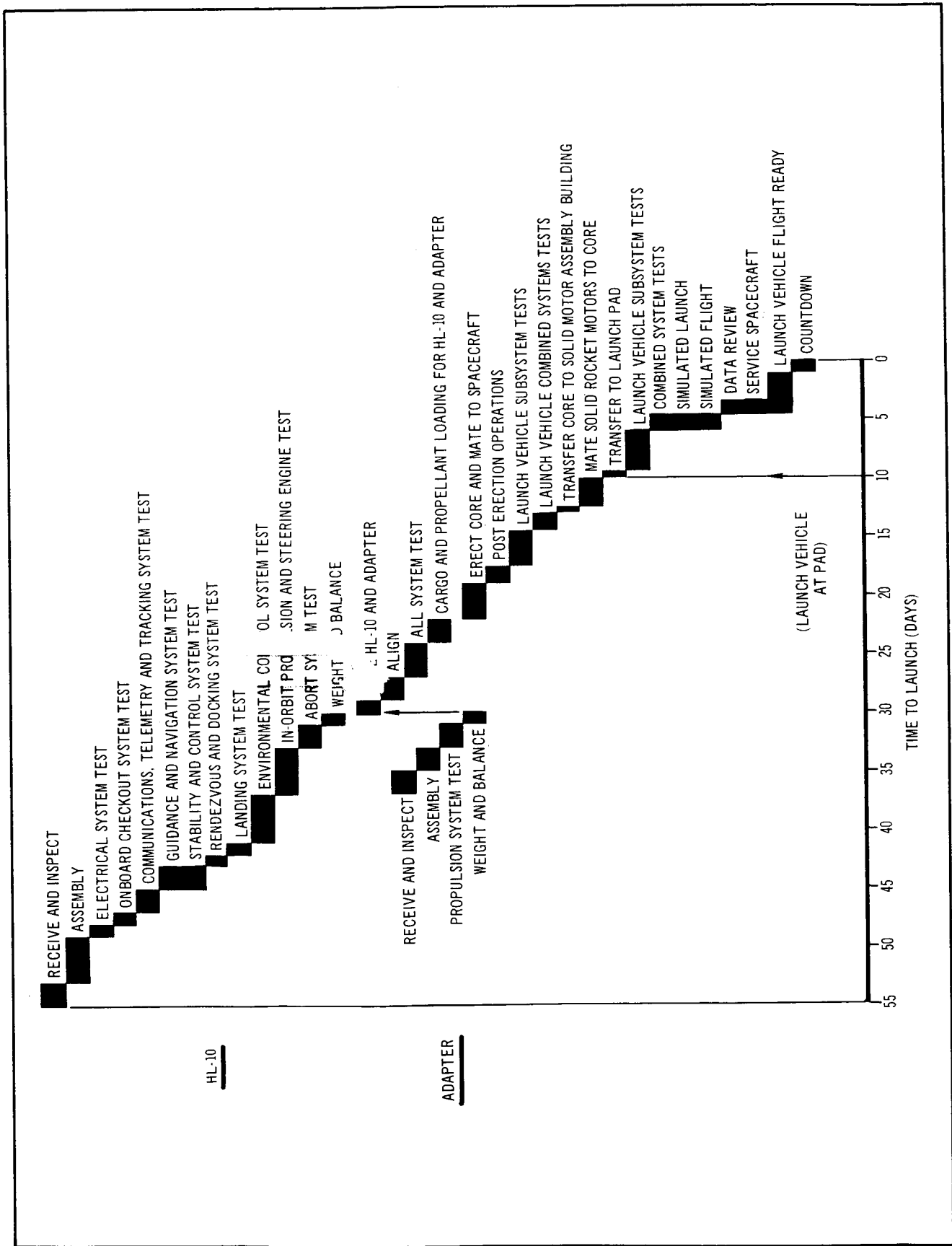
Figure 6-10 HES-2G Spacecraft/Titan IIIC Launch Preparation Time

However, the corresponding schedule for the solid booster is not based on actual operational data, since none exists for this size booster. The schedule is based upon judgment coupled with related experience, which indicates an attractive operational potential for the all-solid booster system.

6.1.7 Spacecraft Internal-Arrangement Effect on Preparation Schedule

Several alternate spacecraft internal arrangements are described in Section 9.1. The effect of these arrangements on launch preparation schedule are described in this section.

The selected spacecraft system arrangement (designated HES-2G) is shown in Figures 5-2 and 5-4, Section 5.1. This spacecraft arrangement locates the consumable cargo and steering propellant in the adapters, and the in-orbit propellant, selected cargo, and steering engines in the HL-10. The preparation schedule for this arrangement is shown in Figure 6-6, and indicates a requirement of about 38 days for prelaunch preparation.

Locating everything in the spacecraft (HES-2A) decreases the preparation time by only one day (37 rather than 38 days).

Locating all cargo, in-orbit propellant, steering propellant, and steering engines in the adapter (HES-8) decreases preparation time by about 4 days (34 days total).

Locating all cargo, in-orbit propellant, and steering engines in the spacecraft, and steering propellant in the adapter (HES-2B) does not change the preparation time from that required for the HES-2G vehicle.

Similarly, locating the propellants and steering engines in the spacecraft and all the cargo in the adapter (HES-2D) decreases the preparation time by one day (37 rather than 38 days).

The other vehicles which were studied, i.e., HES-2C, -2E, and -2F, were essentially the same as the HES-2G vehicle.

A comparison of overall launch operations, preparation times using solid boosters as launch vehicles, is presented in Figure 6-11. Change in external arrangement has minimal effect on the overall spacecraft system launch preparation time (34 to 38 days, a saving of only four days). This difference is independent of solid or liquid booster usage for launch of the HES-2G spacecraft.

The basis for selecting and adopting the HES-2G system is discussed in detail in Section 9, since internal arrangement did not significantly affect system operations, selection can be made independent of system operations.

6.1.8 Effect of Launch Pad Tie-Up and Refurbishment Time on Launch Schedule and Number of Pads

The pad tie-up and refurbishment times influence the number of launch pads required to sustain a mission. For an operational environment requiring 10 launches/year, a launch must be made on the average of once every 36 days. To sustain this operation, Saturn I liquid boosters would require two
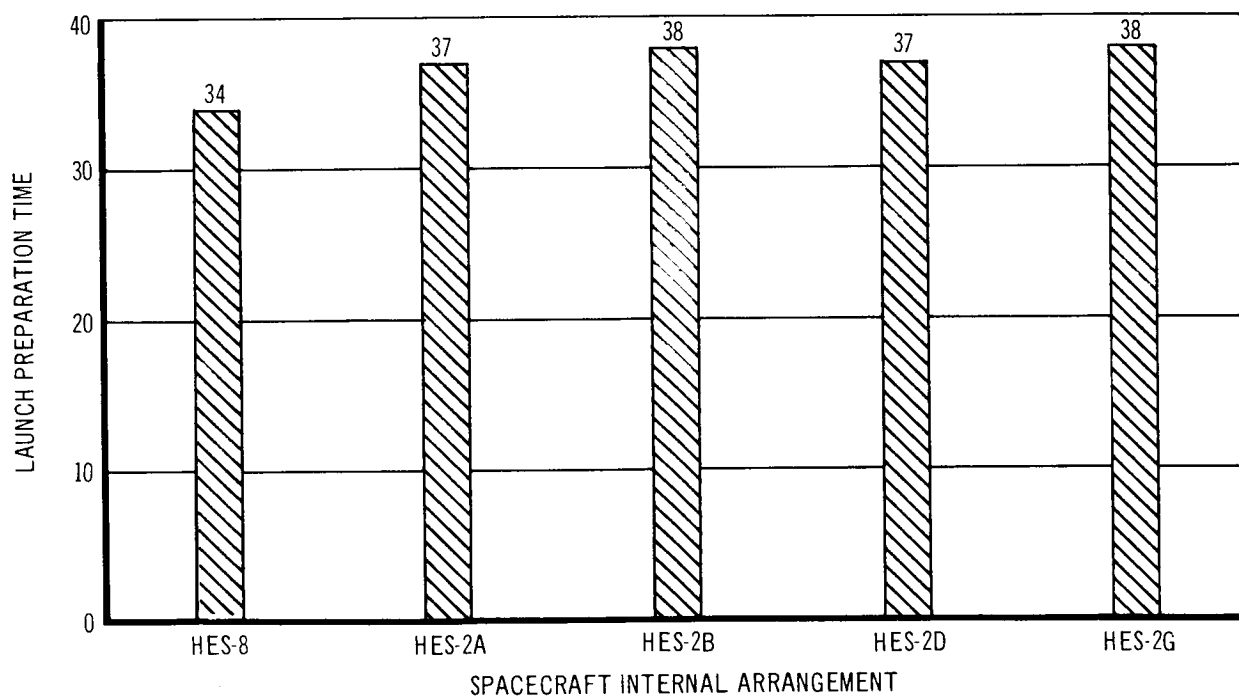
Figure 6-11 Effect on Total Launch Preparation Time Based on Variation of Spacecraft and Adapter Internal Arrangements

operational pads plus one stand-by. For a solid booster, however, only two pads are required, one operational and one stand-by.

Table 6-1, presents the data upon which these requirements are based. It is assumed vehicle-cycle time is about 110 days. (See Section 8.4.3.)

Table 6-1

BOOSTER PAD-TIME REQUIREMENTS

Booster	Pad Tie-Up * Time, Days	Pad Refurbishment Time, Days	Total Days	Required Number of Pads
Solid	20	less than 16 **	- 36	2
Titan IIIC	10	approximately 4 ***	- 14	2
Saturn I	47	approximately 5****	- 52	3

    * Taken from Figures 6-7, 6-9, and 6-10.
   ** No information available, based on manufacturer's judgment.
 *** Section 6.6, Reference 4.
**** References 2 and 3.

6.2 BASELINE TRAJECTORY

The baseline launch vehicle for the HES-2G arrangement consists of three large, solid-propellant booster motors:

    1.   A first stage, 260 in., with 4,000,000 lb. of propellant
    2.   A second stage, 260 in., with 1,350,000 lb. of propellant
    3.   A third stage, 156 in., with a propellant loading of 526,100 lb.

This vehicle has a gross weight of 6,653,141 lb. at liftoff from Cape Kennedy. The vehicle lifts off with a thrust-to-weight ratio of 1.25 and flies down a 90° launch azimuth using a gravity turn (zero angle-of-attack) trajectory. The launch vehicle uses a throttling program on the steering system thrust consisting of 100,000 lb. during first stage flight, 32,000 lb. during second stage, and 70,000 lb. during third stage flight.

The baseline trajectory has a maximum dynamic pressure of 721 lb./sq.ft. at 20 sec. after liftoff, and the dynamic pressure at first stage separation is 38 lb./sq.ft. The maximum acceleration during flight is 7.18 g's, which occurs during third stage flight 350 sec. after liftoff. At third stage burnout the vehicle has an altitude of 584,643 ft. above the Earth's surface and an inertial velocity of 25,707 ft./sec. at an inertial elevation flight path angle of 2.7°. After third stage burnout, the launch vehicle coasts to an apogee altitude of 300 n.mi. with a payload of 106,000 lb. At apogee the velocity is 24,277 ft./sec. which is 608 ft./sec. less than circular satellite velocity at that altitude. Figures 6-12 through 6-14 show important trajectory parameters plotted as a function of time.

6.3 ABORT PROVISIONS

A comprehensive analysis of the emergency detection and escape-initiation system must include procedures for dealing with malfunctions in the following subsystems (See Reference 5). These malfunctions are listed in the descending order of expected frequency.

1. Spacecraft

    A. Inertial navigation
    B. Secondary power
    C. Flight control
    D. Environmental control
    E. Communications
    F. Structure
    G. Steering engines
    H. Landing gear

2. Booster

    A. Body heating
    B. Structural failure
    C. Staging disconnects
    D. Motorcase rupture
    E. Nozzles

Of the above items, only two are crucial in demonstrating the feasibility of the head-end steering concept. These are malfunctions of the steering engines and motorcase rupture. In this study, only motorcase rupture was investigated.
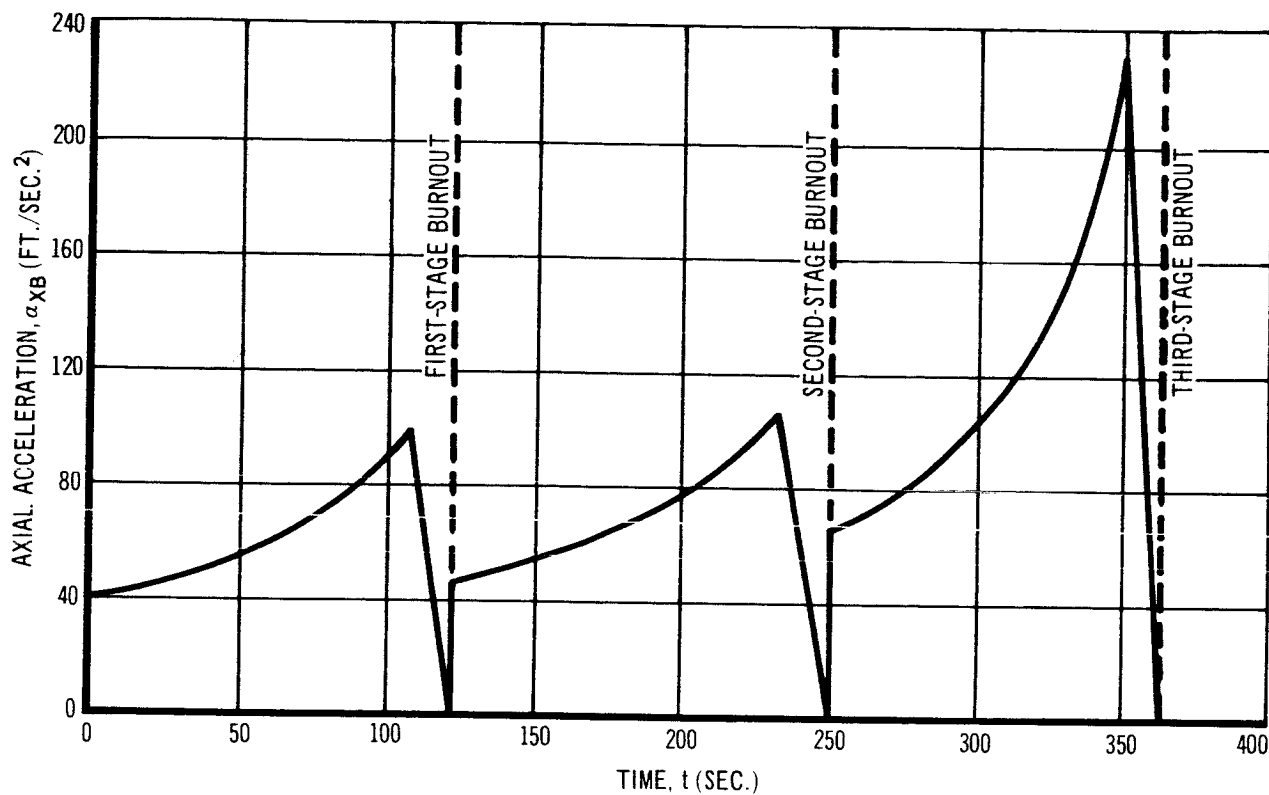
Figure 6-12 Axial Acceleration vs. Flight Time
HES-2G VEHICLE
(1.2-0.4-0)
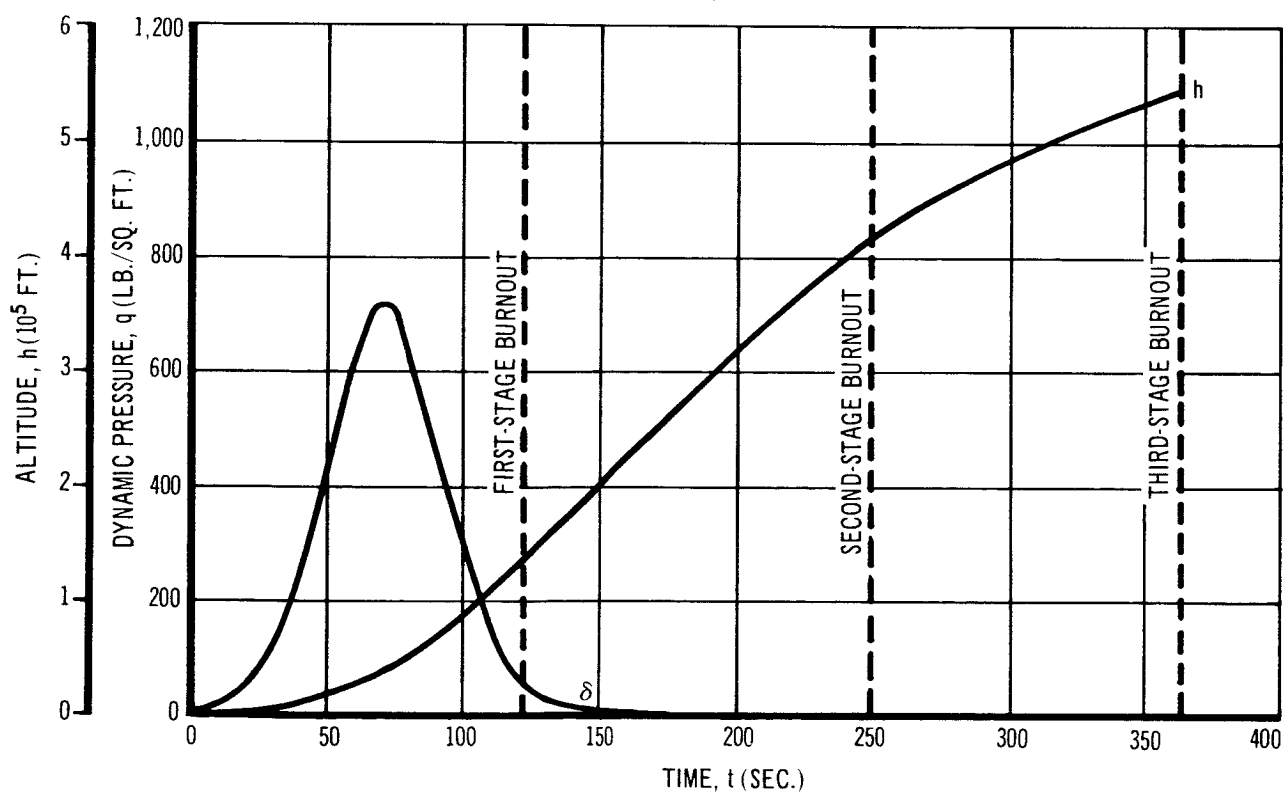
Figure 6-13 Altitude and Dynamic Pressure vs. Flight Time
HES-2G VEHICLE
(1.2-0.4-0)
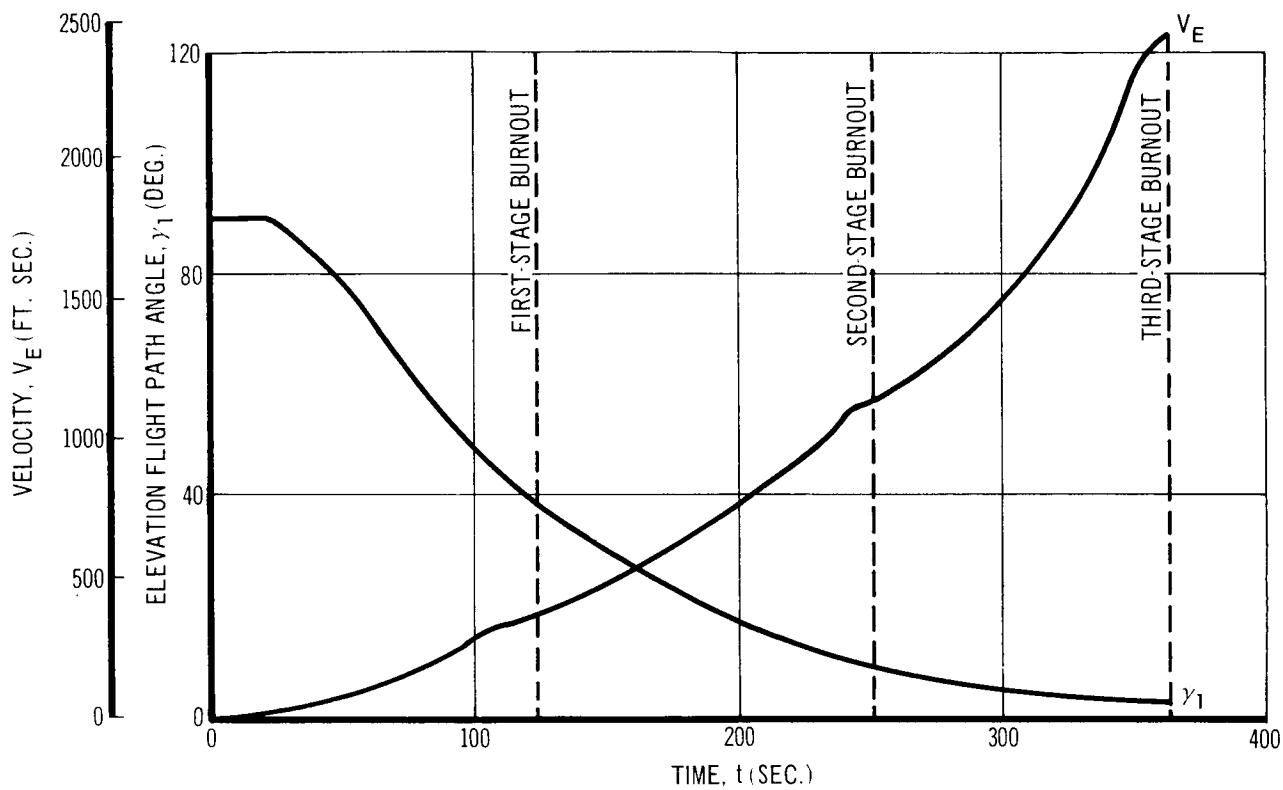
Figure 6-14 Velocity and Flight Path Angle vs. Flight Time
HES-2G VEHICLE
(1.2-0.4-0)

In order for the spacecraft to escape the booster in the event of a stage explosion, the sizing of the abort rocket system was based on the following criteria:

1. A TNT equivalent of 2% of the propellant weight of the operating stage.
2. A warning time of 4 sec.
3. A delay of 0.5 sec. in escape initiation.
4. A maximum overpressure at the spacecraft of 10 psi.

The TNT-equivalent and overpressure criteria were specified in the study guidelines. The 4-sec./ warning time figure is based on an analysis of motor-case rupture modes (Reference 6). The half-second initiation delay time results from a survey of previous study results.

The possibility of a motorcase rupture during second or third stage operation at high altitudes does not present a critical hazard. The most severe conditions to which the abort rocket system must be designed are those for an on-the-pad explosion. Figure 6-15 shows the required spacecraft thrust-to-weight ratio for abort versus TNT equivalent and various warning time. In the figure, the warning time is the net warning time; that is, the 4-sec. warning time in the case of the head-end steering concept minus the half-second initiation delay time. For a full length, 260-in. dia. first stage motor the 2% equivalent TNT is approximately 67,000 lb., but for the case of an on-the-pad abort, twice this value must be used to account for the reflection effect of the ground plane. Thus, the design point taken from Figure 6-15 is a thrust-to-weight ratio of 2.8. Figure 6-16 shows the corresponding propellant weight requirement in percent of gross-weight-aborted, which results in a value of 4.3% of the aborted gross weight.

The abort rocket system necessary to meet the imposed requirements consists of four solid-propellant motors, each generating a sea level thrust of 44,000 lb. and burning for a period of 3.75 sec. Figure 6-17 shows a sketch of the abort motor designed for this case.

Before the actual completion of the abort analysis, the possibility of lighting off the second or third stage to escape from an exploding first stage was recognized. However, the initial thrust-to-weight ratio of the second stage
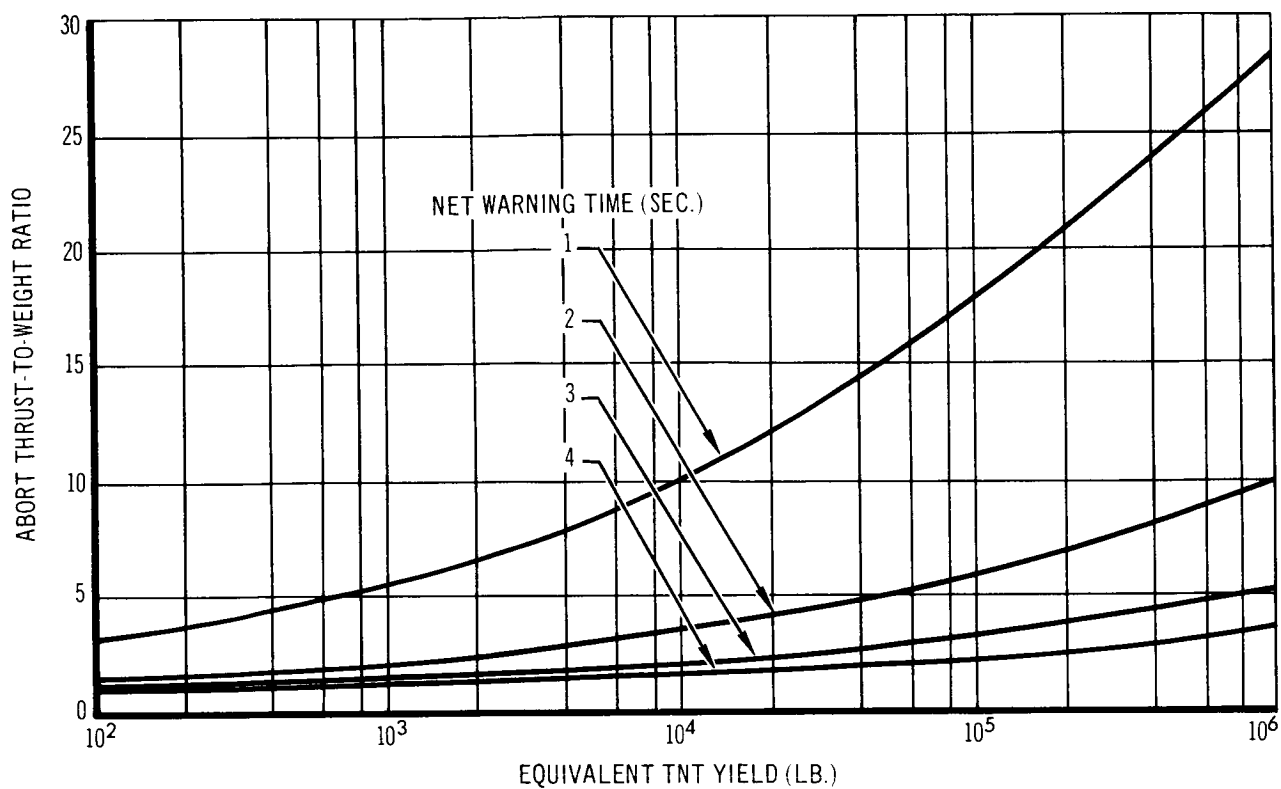
Figure 6-15 Pad Abort Design Data
(10 PSI Overpressure)
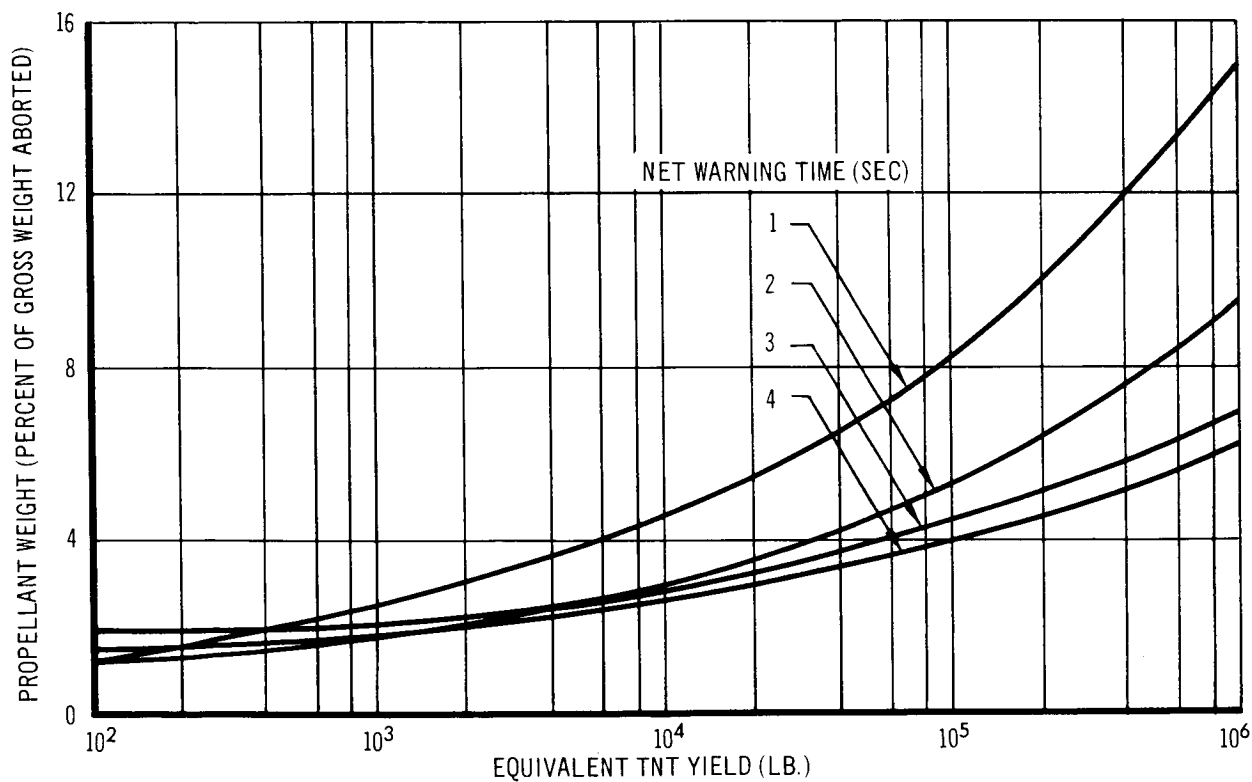
Figure 6-16 Pad Abort Design Data (10 PSI Overpressure)

SEA LEVEL THRUST = 44,000 LB.
VACUUM THRUST = 48,000 LB.
BURN TIME = 3.75 SEC.
PROPELLANT WEIGHT = 660 LB.
TOTAL WEIGHT INCL.
   THERMAL PROT. = 900 LB.
EXPANSION RATIO = 9.9
CHAMBER PRESSURE = 1,000 PSIA

NOTE:
   NOZZLE TO BE CANTED AT
   ANGLE DEPENDENT ON
   MOTOR-MOUNTING LOCATION.
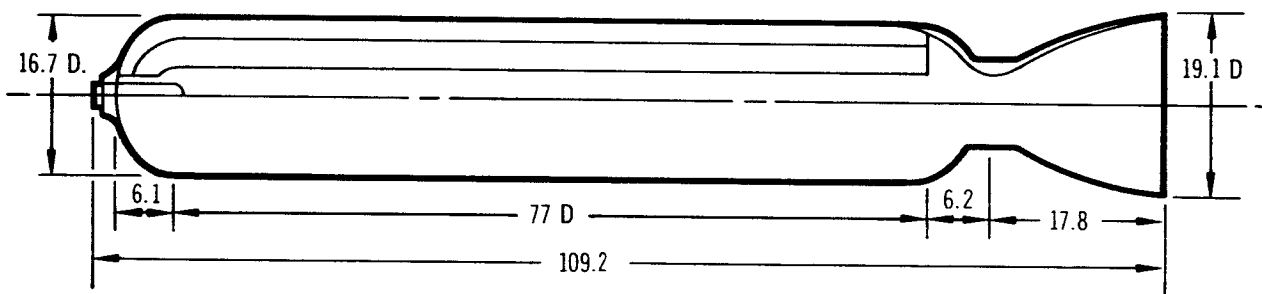
Figure 6-17 HES-2G Abort Motor (4)

is 1.46 and that of the third stage is 2.06. Thus, it is seen that neither of these abort techniques meet the 2.8-g requirement for a successful escape.

Although other failure modes were not investigated to establish the various emergency subsystem weights, these weights were nevertheless estimated from data obtained from other studies (Reference 7). Consideration was given to the following emergency subsystems:

1. Parachutes
2. Flotation
3. Shock absorption
4. Survival gear
5. Propulsion
6. Sensors
7. Electronics
8. Staging

Since only a first order analysis was made on a single possible malfunction event, and since a reasonably comprehensive analysis of abort modes is necessary to evaluate the feasibility of a manned vehicle concept, it is recommended that further study be initiated on the subject of emergency detection and escape--particularly the possible mode of a single steering engine failure. This latter condition could be extremely severe near the burnout of any one of the three stages where the burnout g's for the first stage are 3.1, for the second, 3.4, and for the third, 7.1. Clearly in the case of separation from an active third stage, a thrust-to-weight ratio in excess of 7.1 is necessary, unless a water-quenching system is available on board the third stage. Still another possible hazard is the leakage of the hypergolic fuels on board the spacecraft. In this event, the only escape system visualized is an ejection capsule containing the crew and occupants.

6.4 RENDEZVOUS AND DOCKING

6.4.1 Rendezvous

As discussed in Section 4.1, the baseline ascent trajectory uses a parallel-launch technique which requires a plane change to accomplish the proper phasing with the space station. It was assumed for the purposes of this study that a guidance system similar to one investigated in Reference 7 would

provide the correction for the position and velocity errors accumulated during the boost phase, the mid-course correction phase, and the terminal rendez-vous phase. Such guidance system would include an inertial measurement unit, a digital computer, a horizontal scanner, a rendezvous radar, and a television camera with displays. The use of the parallel-launch technique requires no phasing in a parking orbit, and hence, probably no updating of position and rate information.

6.4.2 Docking

The configuration of the spacecraft before and during docking operations may or may not include the cargo module. In either case the orientation of the HL-10 for docking is a back-in orientation rather than a nose-in one.

6.4.2.1 Docking the HL-10 with the Cargo Module Attached

Provisions have been made for the use of either a television mode of observation or a direct vision mode. The television mode may be used at a remote station such as the HL-10 crew station or at an aft station in the pressurized cargo module. The latter station can also be provided with direct vision parallel to and slightly offset from its docking probe centerline. Figure 6-18 shows the arrangement of the spacecraft and space station. The space station is the MORL and the docking mechanism is one similar to the Apollo probe and drogue investigated for the MORL (see Reference 8). A 28-in. minimum-dia. hatch is located at the aft end of the HL-10; it provides crew and passenger access into the adapter section for transfer to the space station. The cargo adapter, Figure 5-4, is a simple pressurized compartment for storage of the prepackaged (solid) type of cargo. Approximately 1,000 cu.ft. is provided for both the cargo and the aft crew docking station. A separation plane is located at station 528.

After obtaining the proper alignment with the space station, the pilot backs the spacecraft toward the space station until contact is made, and the probe and drogue are engaged and latched. Rigidizing the probe pulls the space-craft to the space station structure, where it meets the cargo module docking cone and the docking seal on the space station. An expandable lock ring is
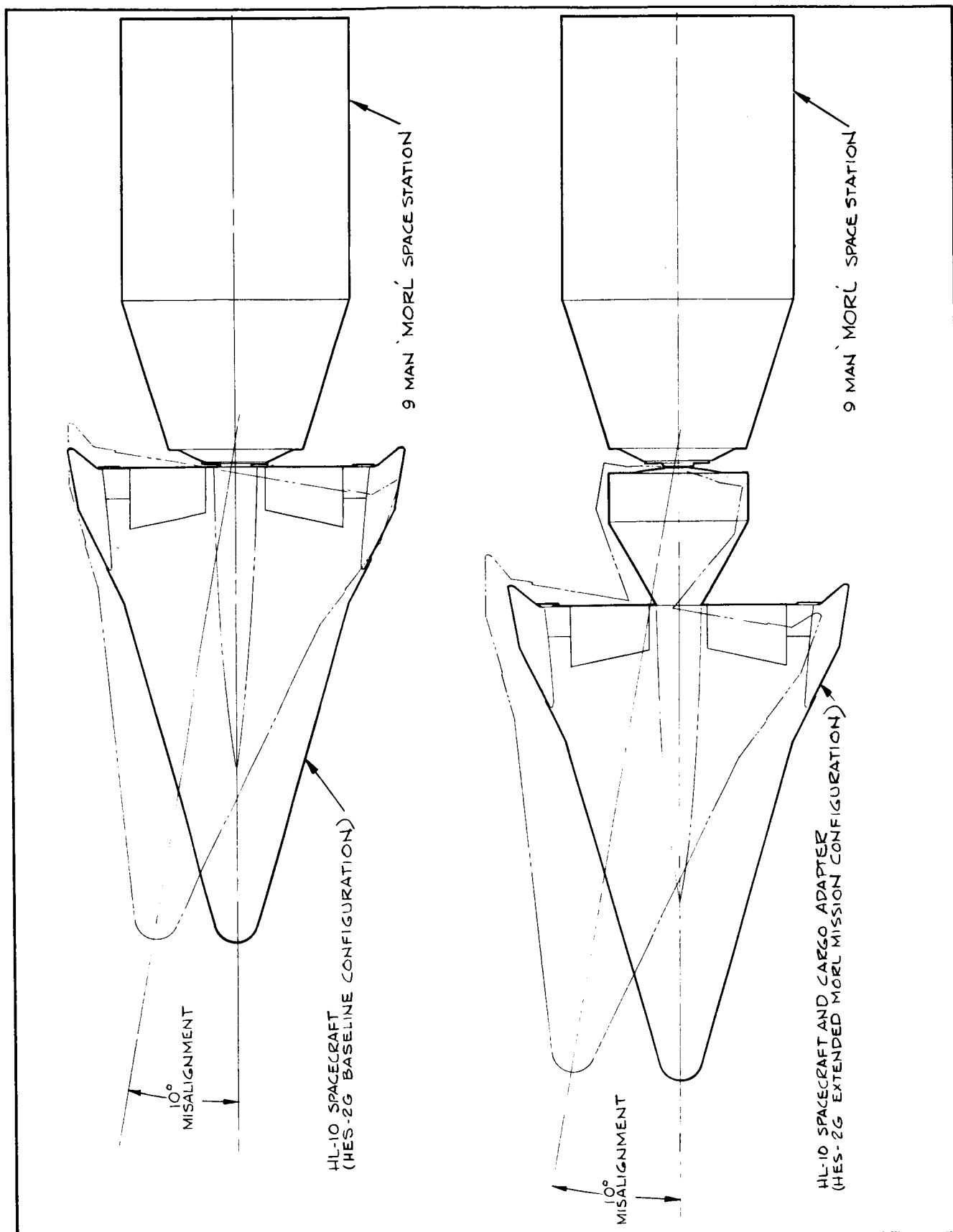
Figure 6-18 Docking Diagram – HES-2G with 'MORL'

9 MAN 'MORL' SPACE STATION

9 MAN 'MORL' SPACE STATION

10° MISALIGNMENT

10° MISALIGNMENT

HL-10 SPACECRAFT (HES-2G BASELINE CONFIGURATION)

HL-10 SPACECRAFT AND CARGO ADAPTER (HES-2G EXTENDED MORL MISSION CONFIGURATION)

engaged and the seal is inflated, which locks and seals the spacecraft to the space station. Once docked, the HL-10 crew performs the connection of the umbilicals necessary to transfer data between the two vehicles.

Before the astronauts leave the HL-10 and enter the space station, the connecting tunnel must be pressurized. The cargo hatch is then opened and stowed in the cargo module. The astronauts on board the space station remove and store the docking drogue and support structure inside the experimental area of the space station. Locking pins are then pulled and the docking probe and support structure is removed and stored in the space station. Astronauts may now leave the HL-10 and enter the space station in a pressurized shirtsleeve environment. Following crew transfer, the vehicle is in a position for cargo transfer. The aft dock technique enables the HL-10 to return to Earth before, during, or following cargo transfer. While the spacecraft remains locked and sealed to the space station, the return crew and passengers enter the HL-10 and load and stow whatever return cargo is required in the HL-10 cargo hold. The aft hatch on the HL-10 is then closed as is the forward hatch on the cargo module. Following checkout and countdown, the HL-10 is separated from the cargo module and oriented for the deorbit impulse.

Upon separation of the HL-10, the cargo module may be unloaded and stowed at the space station in much the same manner as the Apollo command module is stowed in the current MORL studies (see Reference 8).

An alternate procedure would involve the reinsertion of an empty cargo module (or one containing waste materials) in place of the newly arrived, loaded cargo module. This would be done while the HL-10 is still docked, and the replacement would be handled by booms similar to ones currently used for MORL. This would enable the HL-10 to provide the deorbit impulse for the empty cargo container which would then be separated from the HL-10 during re-entry.

For cargo module stowage, the cargo hatch is replaced, and the docking drogue structure is placed back into its normal position and locked. The seal is deflated and the locking pins are disengaged. A preselected stowage arm is attached to the module, and the carriage is activated, which moves the module

away from the space station seal. The module is then rotated to a stowage position around the outside periphery of the space station.

An alternate crew transfer technique is provided for in the design of the spacecraft. This technique allows initial manning of the space station, or else crew transfer, without assistance from the space station crew. After docking has been accomplished and the vehicle is locked and sealed, the connecting tunnel between the logistics vehicle and the space station is pressurized. Then the cargo hatch is removed and stowed in the cargo module. The probe head is unlatched from the drogue and support, and the probe mechanism is removed to the cargo module and stowed. The docking drogue pins are pulled and the drogue is also removed to the cargo module. The astronaut now proceeds to open the door in the center of the docking drogue support structure. All astronauts may now leave the HL-10 and enter the space station in a shirtsleeve environment. Following the crew transfer it is necessary to transfer the docking drogue from the cargo module to the space station to prepare for the next logistics vehicle operation. Following cargo transfer, the large drogue support structure may be rotated and cargo transfer operations started.

6.4.2.2 Docking the HL-10 Directly to the Space Station

Docking directly to the space station is accomplished in the same way as it is when the cargo module is attached. The aft crew station is, in this case, in the crawl tube just forward of the hatch. The locking and sealing operation is the same as described in Section 6.4.2.1. Cargo unloading for the HL-10 without the adapter must be done through the personnel hatch. This precludes the use of the HL-10 alone for an initial manning situation (as described in Section 6.4.2.1) when the use of the cargo module permits docking and egress into the space station before anyone is on board the space station.

Figure 6-18 shows the HL-10 docked directly to the space station. It will be noted in this sketch that a 10° misalignment may be incurred without physical interference between the space station and the HL-10. The critical points of contact are with the probe components rather than with the trailing edge of the HL-10.

6.5 CREW AND CARGO INGRESS AND EGRESS

The spacecraft personnel and cargo ingress and egress flow patterns are shown on the diagram in Figure 6-19. Provisions are shown for both the loading of personnel and cargo on the launch pad and the unloading and transfer operations at the space station.

A single overhead hatch is located above the crew compartment for crew and passenger loading on the launch pad and for the exit on the ground after landing. Two circular overhead hatches are located above the cargo compartment for the loading of cargo and for crew access into the HL-10 during prelaunch operations.

Crew and passenger movement during space station operations is directly aft through the cargo compartment into the cargo module and into the space station. Hatches are located just ahead of the HL-10 trailing edge station, and in the forward and aft domes of the cargo module.

6.6 REFERENCES

1. Solid Motor Logistics Study. Volume III. Martin Technical Report, NASA-CR-63-111, January 1964. (Unclassified)
2. Daily Work Schedule for SA-7. 27 June 1964 through 18 August 1964.
3. Saturn I Countdown Manual. SA-5, Test No. 7 - LLUT-100, 16 January 1964.
4. Program 706 Phase Zero Study Final Report. Martin-Marietta (Denver) (AF04(695)-396) for Air Force Space Systems Division SSD-TDR-63-333. Vol. 5, November 1963.
5. Emergency Detection and Escape Initiation System. Part II. ASD-TDR-62-276, Part II, November 1964.
6. Time Between Malfunction Warning and Failure in 260-inch Solid Propellant Rocket Motor. Letter from Aerojet-General Corp. 3 August 1964.
7. A Lifting Re-Entry, Horizontal-Landing Type Logistics Spacecraft. Boeing Report No. D2-22921. 3 February 1964. (NASA Contract NAS9-1689)
8. Report on the Optimization of the Manned Orbital Research Laboratory (MORL) System Concept. Volume XI Laboratory Configuration and Interiors. Douglas Report SM-46082. September 1964.
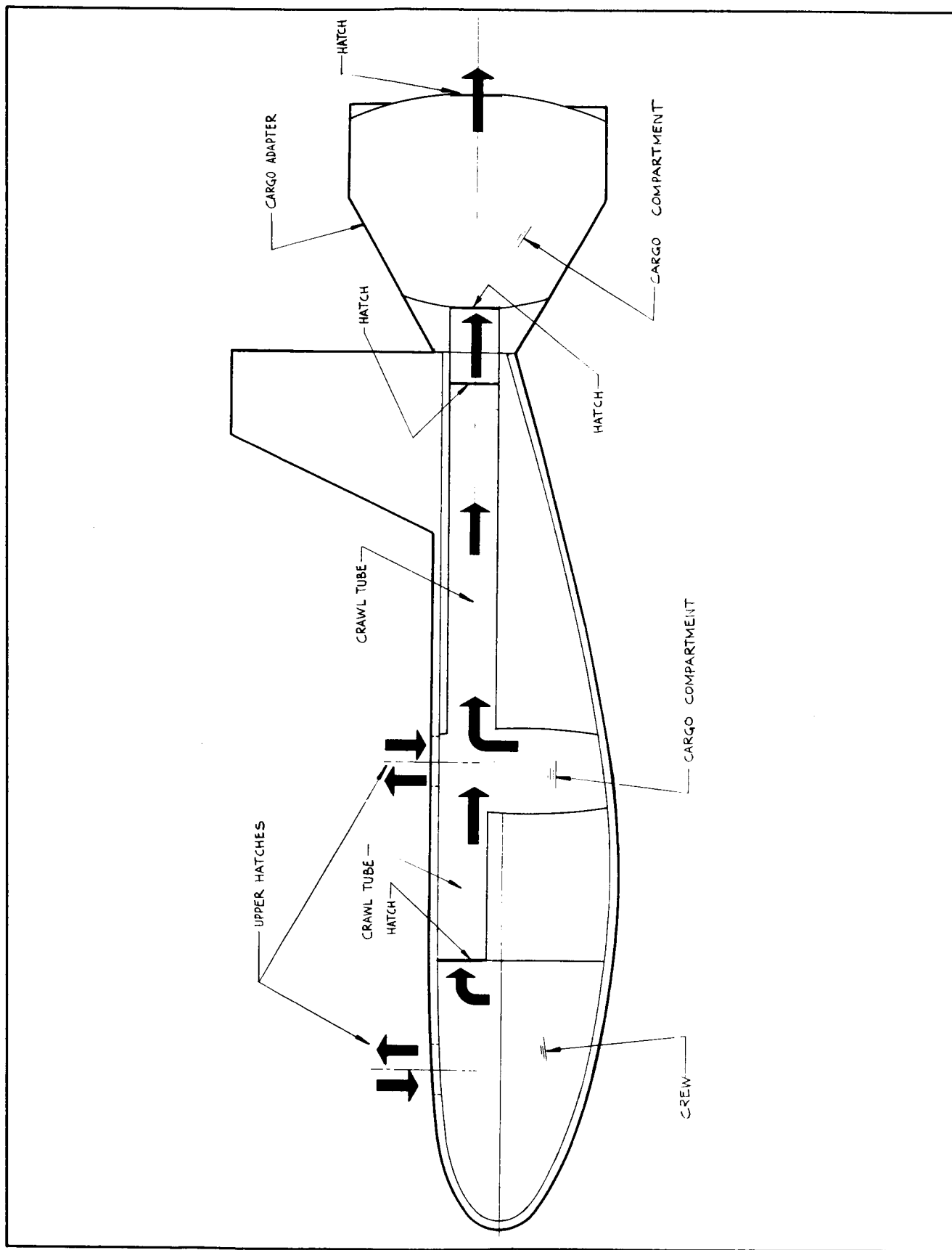
Figure 6-19 Crew-Passenger-Cargo Ingress and Egress Diagram

Section 7
DEVELOPMENT PLAN

7.1 MAJOR ELEMENTS IN BASELINE CONCEPT

This section will present the major elements required in a development program for the baseline concept defined in this study. The development program discussed in the following paragraphs will include the numbers and types of hardware which would be involved and the scheduling of the various program phases.

There are two major phases to the RDT&E program outlined herein for the HES-2G vehicle. These are the engineering development phase and the development test phase. The first phase consists of the engineering development and manufacturing of the prototype items which are to be delivered to the development test program. The details of this phase are covered in Section 7.3. The second phase consists of the development testing required to man-rate and integrate the spacecraft, booster, steering, and adapter systems. This part of the RDT&E program is described in Sections 7.4 and 7.5. In the testing phase it is estimated that seven development flight test vehicles and one acceptance test vehicle will be launched. It is pointed out that all facilities used during the man-rating test program will also be used for logistics launches during the operational phase.

It is estimated that the engineering development and manufacturing phase will take three years while the development test program is also allowed three years plus another year for slippage, i.e., seven years.

Figure 7-1 shows how the HL-10 HES development plan and operational schedule may be phased in with the development and operational schedules of (1) the baseline MORL program and (2) the extended MORL program. The RDT&E for the HL-10 program should be started at the same time as the baseline MORL program. However, to be compatible with the extended MORL program, the HL-10 HES development schedule should be initiated a year earlier than the extended MORL development schedule. Figure 7-1 shows that the boosters will be scheduled as needed.

7.2 TOTAL PROGRAM PHASES

The scheduling and programming phases for the head-end steering configuration are shown in Figure 7-2. These phases are:

1. RDT&E
   A. Engineering, development, and manufacture of prototype items
   B. Development of man-rating test schedule.
2. Operational Program.

A separate block represents the manufacture of the various components for direct support of the operational program.

7.3 ENGINEERING, DEVELOPMENT, AND MANUFACTURING SCHEDULE OF PROTOTYPE

The schedule for the engineering, development, and manufacture of the head-end steering prototype systems and subsystems as well as for systems integration is shown in Figure 7-3.

The HES-2G spacecraft head-end steering and control unit and the various subsystems will take 2 years for development and manufacture. The qualification testing of the subsystems will be completed by the end of the second year; systems integration activity will start at the beginning of the tenth month. The adapter will take 1 year and will be ready for system integration at the middle of the second year of the program.

YEAR

| 1963 | 1964 | 1965 | 1966 | 1967 | 1968 | 1969 | 1970 | 1971 | 1972 | 1973 | 1974 | 1975 | 1976 | 1977 | 1978 | 1979 | 1980 |

LIQUID-SOLID BOOSTERS

BASELINE MORL DEVELOPMENT PROGRAM

BASELINE MORL OPERATIONAL PERIOD

△ FIRST BASELINE SPACE STATION

EXTENDED MORL DEVELOPMENT PROGRAM

EXTENDED MORL OPERATIONAL PERIOD

ENGINEERING & DEVELOPMENT (PROTOTYPE)

MAN-RATING TEST PROGRAM

HEAD-END STEERING SPACE-CRAFT OPERATIONAL PERIOD

Figure 7-1 Scheduling and Phasing of MORL Space Station Logistics Support System: Head-End Steering Spacecraft

DELIVER PROTOTYPE

DELIVER MAN-RATED SYSTEM

ENGINEERING, DEVELOPMENT, AND MANUFACTURE OF PROTOTYPE SYSTEMS

DEVELOPMENT MAN-RATING TEST SCHEDULE

OPERATIONAL PROGRAM

DIRECT SUPPORT OF PROGRAM
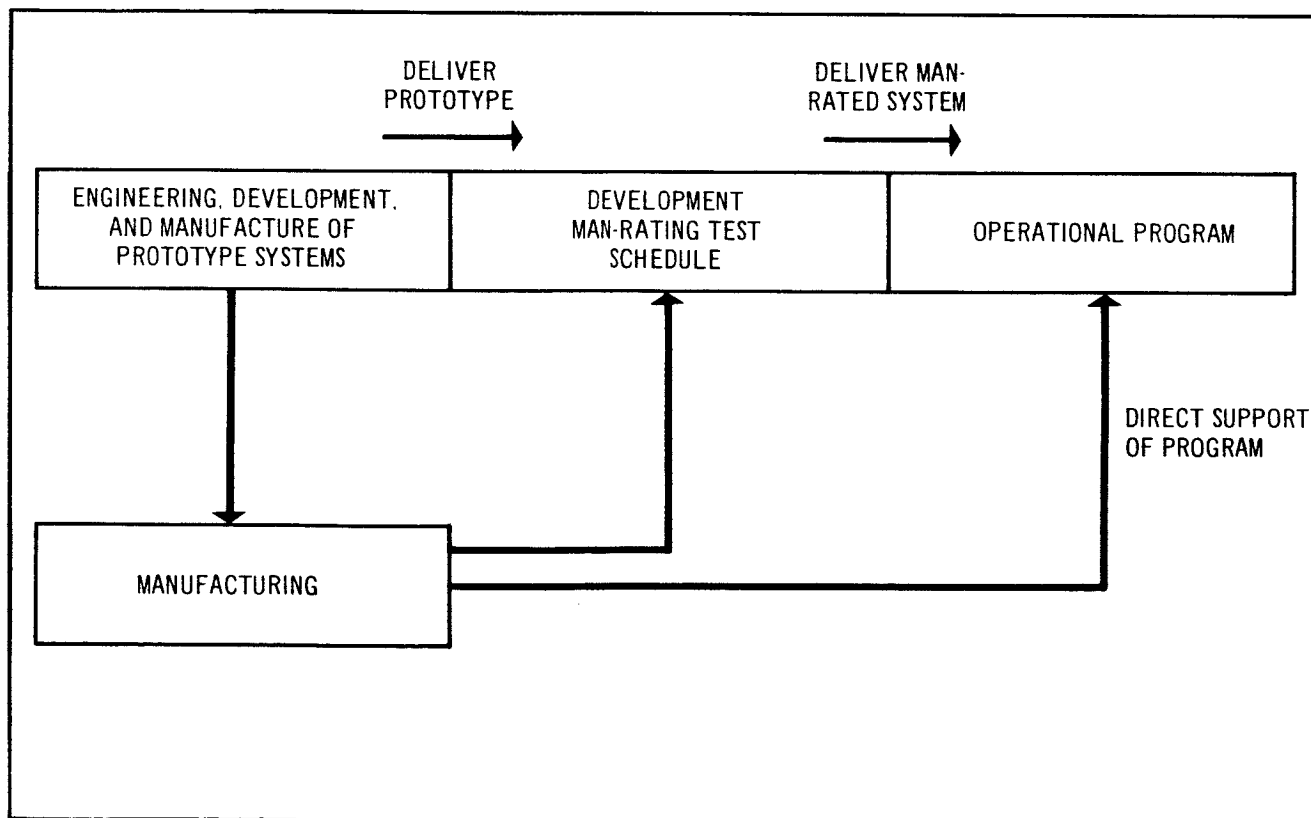
MANUFACTURING

Figure 7-2 Total Program Phases of the Head-End Steering Spacecraft
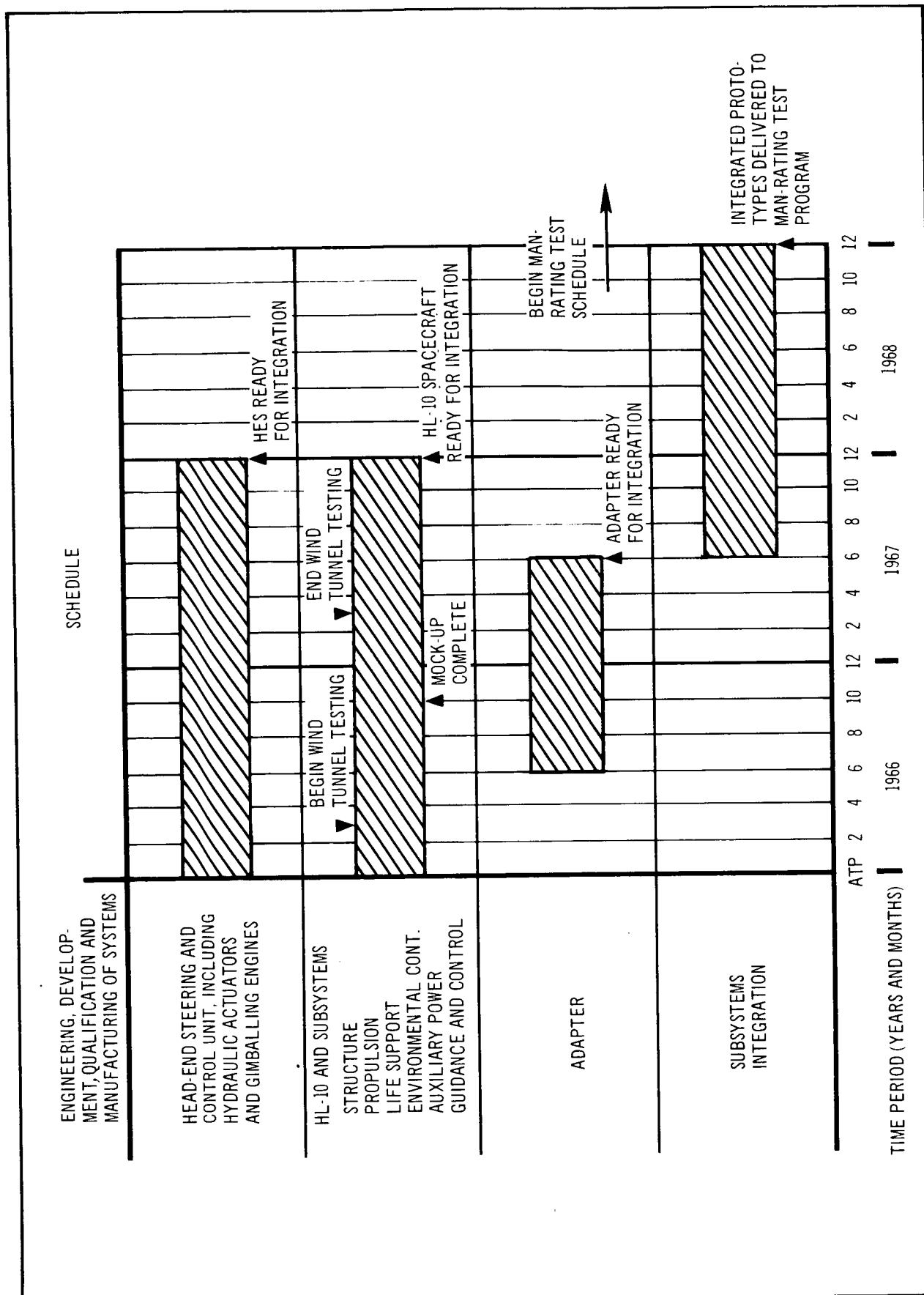
Figure 7-3 Engineering, Development & Manufacturing Schedule

124

Wind tunnel testing will be started at the beginning of the fourth month and will be completed by the end of the sixteenth month; 1 year will be allowed for the testing period.

The full-scale mockup will be completed by the end of the tenth month.

Integrated prototype spacecraft and adapters will be delivered to the Man-Rating Test Program at the end of the third year, which will be the beginning of 1969.

7.4 DEVELOPMENT MAN-RATING TEST SCHEDULE, NOMINAL

A nominal man-rating 4-year test schedule is shown in Figure 7-4. The first 3 years are for the actual testing and the fourth year is allowed for events not foreseen at this time.

Eight integrated vehicles will be launched during the test period with the eighth launch being an acceptance launch. The acceptance launch will employ all production subsystems.

The first column on the left in Figure 7-4 lists the various tests that will be made and evaluated for each of the subsystems and for the integrated system. Environmental tests will be performed to determine the effects of temperature, noise, vibration, altitude, radiation, etc., on the crew members. These tests will be made in a space simulator. Engine rating tests will be performed to check the manufacturer's engine rating, and to determine the engine characteristics over a range of thrust and gimbal angle, using control actuators. These tests will be made under static firing conditions in pits, as well as under dynamic conditions using sleds. Water submersion tests will be performed to check the structure and pressure characteristics of the spacecraft and adapter system.

In addition, two drop tests will be made to check the impact and structural characteristics of the spacecraft system. An air launch, or drop test will be made to check the stability, aerodynamic, and landing capability of the spacecraft. It is planned to drop the craft from a B-52 which will be specifically modified to make the launch. Only subsystem characteristics will be demonstrated as a result of this test.
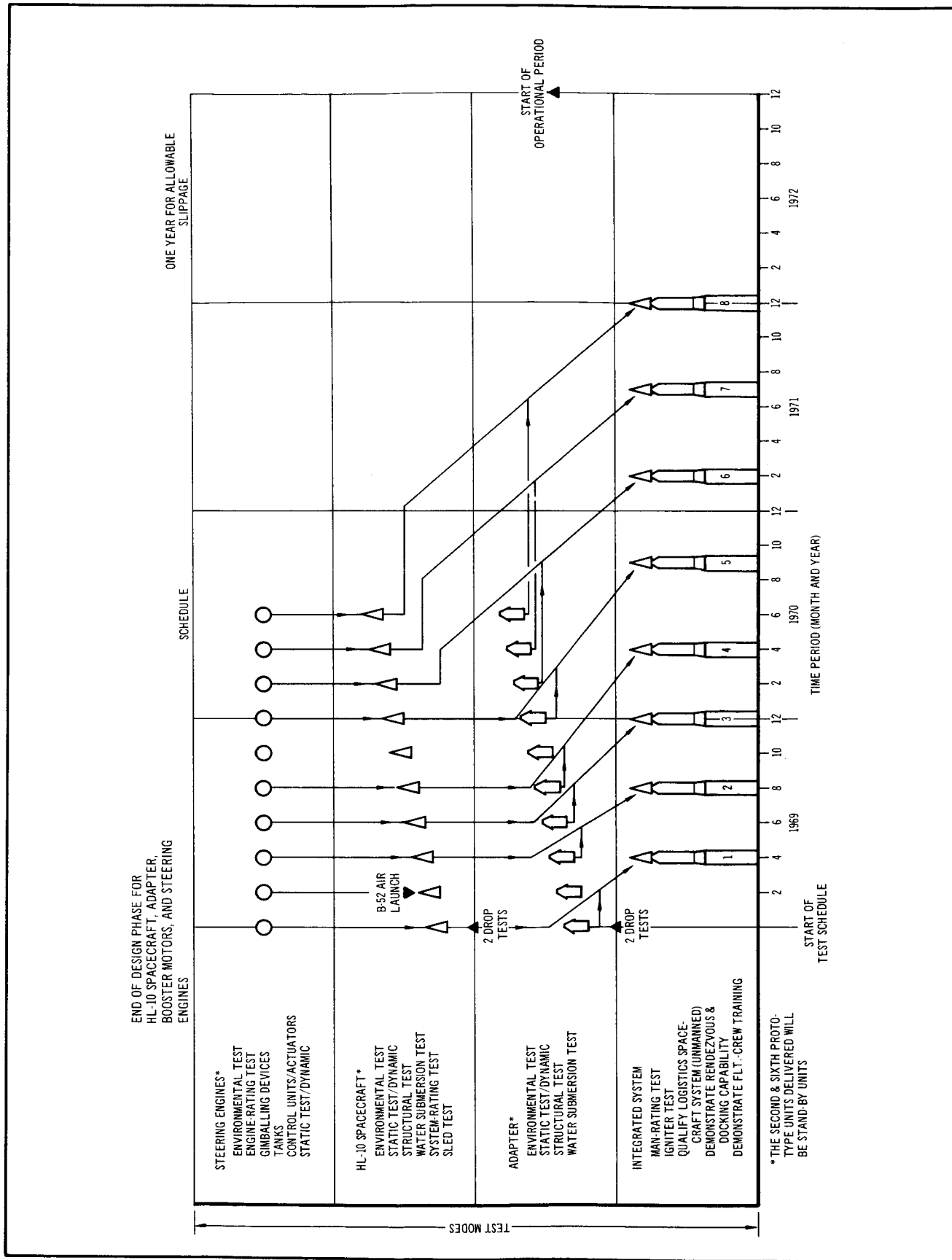
Figure 7-4 Development Man-Rating Test Schedule

Ten complete systems of the prototype HL-10 spacecraft, adapters, and steering engines will be required for the program intervals. Eight are scheduled for launch and two for standby.

7.4.1 Test Characteristics

Table 7-1 describes the test characteristics of the eight integrated launches. The first three launches are suborbital; the last five are orbital. The last four include rendezvous with an orbiting space station; a full crew complement will be carried. These tests serve as a training program as well as a program to develop rendezvous capability. All tests carry autopilot test equipment to serve as both primary and backup control. The autopilot serves as primary control for the first series of four launches, and secondary control for the last 4 launches. The eighth launch is planned as a flight verification test; it marks the beginning of the operational program.

7.4.2 Required Number of Test Articles

The required number of test articles are summarized in Table 7-2. Figure 7-4 presents the Test Plan which is the basis for Table 7-2.

The effect of spacecraft reusability is reflected in this plan by reusing spacecraft for the air launch, drop, and sled tests in the orbital and suborbital shots. This way the spacecraft is refurbished and failure modes are isolated and provided for as the program progresses. Also, fewer test articles will be required than if entirely new articles are used for each test. This practice will cut the costs of the adopted test program. Table 7-3 shows the number of test articles which would be required if new articles were used for each test. For example, instead of 10 spacecraft (8 + 2 standbys), 15 would be required. There would be no change in the required number of boosters (10, including 2 standbys), since the number of launches would remain constant. The cost of the development plan (presented in Section 8) represents about 40% of the total program cost. The development plan was designed to realize its objective at as low a cost as possible. Plans to reuse test articles and to measure the effect of reuse on system reliability were also developed on this basis.

Table 7-1

TEST CHARACTERISTICS

Development Test Flight No.	Spacecraft		Adapter	Steering Engine	Telemetry	Booster Test	Suborbital
	Stripped Down	Complete	Prototype				
1	X		X	X	X	X	X
2	X		X	X	X	X	X
3	X		X	X	X	X	X
4	X		X	X	X	X	
5		X	X	X	X	X	
6		X	X	X	X	X	
7		X	X	X	X	X	
8		X	X	X	X	X	

Development Test Flight No.	Orbital	Ablative Test	Deorbit	Guidance System	Autopilot	Rendezvous	Crew	Acceptance
1		X		X	X			
2		X		X	X			
3		X		X	X			
4	X	X	X	X	X			
5	X	X	X	X	X	X	X	
6	X	X	X	X	X	X	X	
7	X	X	X	X	X	X	X	
8	X	X	X	X	X	X	X	X

Table 7-2

REQUIRED TEST ARTICLES
(Test Article Reused)

	Required Test Articles	Stand-by Test Articles	Total	Notes
HES-2G Spacecraft	8	2	10	Includes drop tests, sled tests, and B-52 air launches.
Adapter	8	2	10	
Steering Engines	8	2	10	
Boosters				
1st Stage 260-in.	8	2	10	Required for both suborbital and orbital launches.
2nd Stage 260 in.	8	2	10	
3rd Stage 260 in.	8	2	10	

Table 7-3

REQUIRED TEST ARTICLES
(Test Article not Reused)

	Required Test Articles	Stand-by Test Articles	Total	Notes
HES-2G Spacecraft	13	2	15	Includes drop tests, sled tests, and B-52 air launch
Adapter	10	2	12	
Steering Engines	10	2	12	
Boosters				
1st Stage 260 in.	8	2	10	Required for both suborbital and orbital launches.
2nd Stage 260 in.	8	2	10	
3rd Stage 156 in.	8	2	10	

Section 8

ECONOMIC FEASIBILITY

The purpose of this section is to present a gross cost assessment of the selected manned space vehicle and support systems concept. This section includes an assessment of system research, development test and evaluation, manufacturing, and operations costs for a 5-year operational period. These costs have been assessed on the basis of 4, 10, and 20 launches per year. The costs for other logistics spacecraft systems as given in Section 8.7, Reference 5, are to establish the relative economic feasibility of the subject system concept.

This study is limited to assessing gross costs only. This means that cost items such as subsystems components, operating spares, storage, etc. are not included. All subsystems, with the exception of the steering engines, are lumped together and considered to be state-of-the-art. The cost of state-of-the-art subsystem development is relatively small--about 2 to 3% of the system integration cost. Therefore, only development which is required to test and evaluate the integrated spacecraft and booster systems is costed. The steering engines are also state-of-the-art; they require, however, a basic development program in addition to test and evaluation for systems integration. This is costed as a separate item in the development plan.

Many of the large cost items indicated, such as space vehicle development, are to be regarded as gross order of magnitude estimates only, based on best available information, and should not be construed to represent exact costs. How variations in large cost items affect total cost is discussed in Section 8.4.

Cost assessment has been done for the nominal case in which a reusable HL-10 vehicle is employed in a 5-year logistics support program. The nominal vehicle cycle time (the sum of mission time, recovery-refurbishment time, and pad preparation time) is 110 days. The recovery-refurbishment cost for each reuse is estimated to be 10% of the unit production cost of the HL-10 spacecraft

and steering engines. Only the HL-10 spacecraft and steering engines are recoverable. All other stage components such as boosters and adapters are used only once and are not recovered.

No attempt has been made to incorporate into the HL-10 development and production cost any variation of cost that would be incurred when designing and proving different reuse levels of the spacecraft. How development and production cost varies specifically with different levels of vehicle life is not known; this requires further study beyond the scope of this report. Reliability also was not included as a constraint on cost assessment. Therefore, the nominal case assumes a reliability of 1.0.

8.1 SUMMARY OF TOTAL PROGRAM COSTS

Total program costs are as follows:

$$\begin{bmatrix} \text{Total} \\ \text{Program} \\ \text{Costs} \end{bmatrix} = \begin{bmatrix} \text{RDT\&E Costs for} \\ \text{HL-10 and Steering} \\ \text{Engines} \end{bmatrix} + \begin{bmatrix} \text{Operations} \\ \text{Costs} \end{bmatrix} + \begin{bmatrix} \text{Training} \\ \text{Costs} \end{bmatrix}$$
$$+ \begin{bmatrix} \text{Launch Complex} \\ \text{Construction Cost} \end{bmatrix}$$

Table 8-1 shows a breakdown of total program costs under the major categories shown above. (For the purposes of this report, RDT&E, training, and launch complex construction cost are defined as nonrecurring costs, while operations are a recurring cost.) Those costs are based on an HES-HL-10 vehicle making logistics launches at frequencies of 4, 10, and 20 launches per year over a period of 5 years.

The RDT&E costs are as follows:

1. Development engineering--cost required to deliver the HL-10 prototypes to the development test program.
2. Development testing--cost required to man rate and integrate the spacecraft, booster, steering, and adapter systems.

The operations cost consists of the following:

1. Unit costs for spacecraft and booster hardware production plus recovery-refurbishment costs for the HL-10.

Table 8-1

PROGRAM COST BREAKDOWN FOR A 5-YEAR LOGISTICS
LAUNCH OPERATION

Cost Item	4 Launches/Year		10 Launches/Year		20 Launches/Year	
	Cost ($ million)	Percent of Total Cost	Cost ($ million)	Percent of Total Cost	Cost ($ million)	Percent of Total Cost
Dev. engineering	110	10.7	110	8.0	110	5.6
Dev. testing	279	27.1	279	20.2	279	14.2
Steering engine RDT&E	40	3.9	40	2.9	40	2.0
SUBTOTAL RDT&E	429	41.7	429	31.1	429	21.8
Training	100	9.75	100	7.2	100	5.1
Launch complex	100	9.75	100	7.2	100	5.1
SUBTOTAL OTHER	200	19.5	200	14.4	200	10.2
Hardware production and Recovery refurbishment	279	27.1	634	45.8	1220	61.9
Launch support	120	11.7	120	8.7	120	6.1
SUBTOTAL OPERATIONS	399	38.8	754	54.5	1340	68.0
TOTAL PROGRAM COST	1028	100.0	1383	100.0	1969	100.0

2. Launch support cost--this includes the cost of ground support equipment and the handling and transportation of the big boosters.

Training costs are those costs required to support training of the HL-10 crew and support personnel. This includes the cost of special simulators, training aids, and schooling.

Launch complex construction costs include construction of the receiving area, storage warehouses, assembly area, access roads and canals, and the launch pads.

References for these costs are given, as appropriate, in succeeding sections where cost breakdown is discussed in more detail. A list of references is presented in Section 8.7.

The total cost of a 5-year logistics launch program is about $1 billion if only 4 launches per year are made. The cost increases to almost $1.4 billion if 10 launches per year are made. If 20 launches per year are needed, the total program costs become approximately $2 billion. This is a 100% increase over the cost of four launches annually, but represents 5 times the cargo and/or personnel delivered to orbit. Table 8-1 also shows a distribution of program cost as a percentage of total cost for the cases of 4, 10, and 20 launches per year. In the case of four launches per year, RDT&E and operations each contribute about 40% or a total of 80% to the total cost. Since operations cost is a function of the number of launches, and RDT&E costs remain constant, it can be understood why operations costs are nearly double RDT&E costs for 10 launches per year and three and a half times RDT&E costs for 20 launches per year.

The largest part of RDT&E cost is development testing. This accounts for over 65% of the total RDT&E cost; steering-engine development is only 9.4% of the total RDT&E cost.

Booster cost is the largest part of the operations cost. It accounts for 46%, 55% and 60% of the operations cost for 4, 10, and 20 launches per year, respectively. Production cost of the HL-10 spacecraft amounts to less than 10% of the operations cost, regardless of launch frequency.

Table 8-2 shows a summary of launch and cargo costs based on a 5-year launch operation. It is interesting to note that cost/launch and cost/lb. of unpackaged cargo delivered is less expensive including development cost for 20 launches/year, than the cost/launch and cost/lb. of cargo for 4 launches/ year without development cost.

Table 8-2

LAUNCH AND CARGO COSTS BASED ON A

5-YEAR OPERATION

	Operations Cost Basis			Total Cost Basis		
Launches/ Year	Cost/ Launch ($ million)	Cost/lb.	Total Operations ($ million)	Cost/ Launch ($ million)	Cost/lb.	Total Program Cost* ($ million)
4	20.0	1,050	399	50.0	2,700	1,028
10	15.1	793	754	27.0	1,450	1,380
20	13.4	705	1,340	19.4	1,035	1,970

*Cost/lb. of unpackaged cargo delivered (excluding people) based on a 19,000 lb. (unpackaged) cargo payload capacity each launch.

8.2 NONRECURRING COST

8.2.1 RDT&E Cost

The research, development, test, and evaluation costs are defined as:

$$\begin{matrix} \text{RDT\&E} \\ \text{Costs} \end{matrix} = \begin{bmatrix} \text{Development \& manu-} \\ \text{facturing of the proto-} \\ \text{type HL-10 vehicle} \end{bmatrix} + \begin{bmatrix} \text{Development} \\ \text{testing of} \\ \text{HL-10 vehicle} \end{bmatrix} + \begin{bmatrix} \text{Development} \\ \text{cost for} \\ \text{steering} \\ \text{engines.} \end{bmatrix}$$

The principal RDT&E cost elements in the HL-10 logistics vehicle program cover development and manufacturing of the prototype HL-10 vehicle, development testing needed to man-rate the spacecraft and to integrate the HL-10,

booster, steering, and adapter systems. The development cost for the steering engines is also included. An estimated cost breakdown is as follows:

1. Development and manufacturing of the prototype HL-10 vehicle.

A.	Engineering	$ 25 million
B.	Subsystem testing	35 million
C.	Integration	10 million
D.	Tooling	17 million
E.	Manufacturing	23 million
	TOTAL	$110 million

2. Development testing of HL-10 vehicle.

    A. Test vehicle requirements

(1)	Seven experimental HL-10 vehicles + steering engines at $19 million each	$133 million
(2)	One acceptance test HL-10 vehicle + steering engines at $19 million each	19 million
(3)	Two backup HL-10 vehicles + steering engines at $19 million each	38 million
(4)	Eight three-stage boosters at $9 million each	72 million
(5)	Ten cargo adapters at $0.8 million each	8.0 million
	Subtotal for launch vehicles costs	$270 million

    The unit costs for the HL-10, boosters, cargo adapter, and steering engines are covered in Section 8.3.1. It should be mentioned here, however, that the unit costs given in the development test program are taken to be the same as the unit costs used in the operational phase, and should be considered as representing the average cost/unit for the total production run.

    The development and manufacturing cost estimate is based on data given in the MORL report (Reference 1) and modified to reflect the particular requirements of the HL-10. The number of launch vehicles required in the development testing phase is taken from Section 7 (Development Plan) of this report.

    B. Test Support Personnel

    It is estimated that 100 support personnel will be needed for at least 3 years to support the test phase.

100 x $30,000/yr. x 3 yr.	$ 9 million
HL-10 Development Test Total	$279 million

3. Development cost for steering engines

It is estimated that steering engine development cost, based on un-published engine manufacturer's cost data, will be on the order of:

$1,000/lb. of thrust x 40,000 lb. $40 million

This includes hardware, facilities, and propellant cost through PERT, including acceptance testing.

The numbers of support personnel needed in the HL-10 test phase and the cost/lb. used in the costing of the steering engine development are based on best judgment estimates.

It is assumed that test equipment and support facilities, normally included under RDT&E costs, will also be used in the operations phase. Hence, these items are costed separately in Section 8.4 (Operations Costs).

$$\text{(Total RDT\&E Costs)} = \$(110 + 279 + 40 \times 10^6) = \$429 \times 10^6$$

It should be noted that steering engine development comprises only 9.4% of total RDT&E costs.

8.2.2 Training Cost and Launch Complex Cost

1. Training Cost

The following training costs are taken from the MORL report (Section 8.7, Reference 1). These costs are for the training of logistics vehicle personnel only:

A. Logistics System Simulators, Training $ 60 million
   Aids and Miscellaneous Equipment

B. Training Schooling   40 million
   (12 crewmen for a 3 yr. training program)

         TRAINING TOTAL COST $100 million

2. Launch Complex Cost

Launch complex cost consists of the cost involved in constructing the receiving and unloading areas for the boosters, storage ware-houses, assembly area, access roads and canals, and launch pads (this includes electrical, mechanical, hydraulic, etc. supporting subsystems). Based on data from the Titan IIIC and Saturn IB programs, it is estimated that this cost would be on the order of $100 million. A discussion of a typical launch complex system is contained in Section 6.

8.2.3 Total Nonrecurring Cost

The nonrecurring cost factors consisting of RDT&E, training, and launch complex are summed as follows:

$$\text{Total Nonrecurring costs} = \$(429 + 100 + 100) \times 10^6 = \$629 \times 10^6$$

8.3 OPERATIONS COSTS

8.3.1 Total Hardware Production Cost

1. Hardware Production Cost for the HL-10 Vehicle (Recoverable)

    A description of the HL-10 vehicle is given in Section 5 of this report. The estimate for unit production cost of an HL-10 is based on data from other programs such as Apollo, Gemini, and MORL. These data were modified to reflect HL-10 vehicle requirements. The spacecraft average cost/lb. was determined by examining the cost of spacecrafts such as Apollo and Gemini. A correlation of these costs was made as a function of craft weight. The Apollo cost was \$825/lb., the Gemini, \$600. Considering such factors as relative complexity, available volume, and expected experience gained in spacecraft systems, an average cost of \$650/lb. was adopted for the HL-10 spacecraft. For the purposes of this feasibility study this assessment is justified; when the system is better defined, as a result of subsequent studies, a more accurate cost may be determined (see Section 8.5 on sensitivity). The dry weight of the vehicle, using configuration HES-2G, is about 28,300 lb. Thus, a gross production cost assessment of the HL-10 vehicle can be taken as:

    $$\$650/\text{lb.} \times 28,300 \text{ lb.} = \$18.5 \times 10^6$$

    This includes the structure, thermal protection and subsystem, excluding steering engines and abort rockets.

2. Steering Engines and Accessories (Recoverable)

    On the basis of engine production costs in other programs, it is estimated that each steering engine will cost about \$4.00/lb. of thrust. An engine capable of 40,000 lb. of thrust will therefore cost around \$160 thousand to produce. Since each vehicle has two steering engines, this results in a total cost of \$320 thousand. The cost of fuel tanks and fuel will amount to \$200 thousand.

Engine cost per HL-10	\$0.320 million
steering propellant and tanks	0.200 million
abort rockets per HL-10 \$12.00/lb. x 3,600 lb.	0.043 million
TOTAL	\$0.56 million

The HL-10 vehicle, steering engines, and accessories are recoverable items and will be taken to be a complete unit and costed out at $19 million.

3. Cargo Adapter Cost (Nonrecoverable)

The cargo adapter is essentially an aluminum structural system. It is costed on the basis of nominal aerospace structure, i.e., $200/lb. The adapter weighs 4,000 lb.

	Weight	Cost/lb.	Unit Cost
Cargo Adapter	4,000 lb.	$200	$0.8 million

4. Interstage Structure Cost (Nonrecoverable)

The interstage structure consists of the adapters and connectors used to integrate the various booster stages and the HL-10 capsule into a single logistics vehicle. This cost is based on the booster structure cost of $7.15/lb. taken from Section 8.7, Reference 2.

	Weight	Cost/lb.	Gross Cost
Interstage Structure	70,000 lb.	$7.15	$0.5 million

5. Booster Production Cost (Nonrecoverable)

The data upon which the booster production cost estimates are based is taken from Aerojet and Thiokol reports (References 2 and 3). These data were modified to reflect the three stage booster configuration used for the baseline vehicle concept. Figure 8-1 is a graph of cost per pound of total motor weight versus the number of fixed nozzle motors manufactured. Curves for the 156-in. third stage, 260-in. second stage and 260-in. first stage motors are shown in Figure 8-1. Depending on whether the launch schedule is 4, 10 or 20 launches per year, the number of three stage boosters that will be required over a 5-year operational period are 20, 50, and 100 units, respectively. Table 8-3 shows stage by stage booster costs and weights as a function of launch schedule. The extra eight boosters added on to each schedule in Table 8-3 are to allow for the extra boosters required during the development testing phase. Three stage booster costs are summarized in Table 8-4.

Table 8-5 presents a production cost summary for the first operational launch, as a function of launches per year. Production cost for the first launch is not very sensitive to launch schedule because only booster cost varies with the number of launches. No progress curve was applied to the spacecraft hardware costs; this resulted in rather conservative cost levels.

In terms of recoverable and nonrecoverable items (since only the HL-10 vehicle and steering engines are used over again), it is clear that at least $8 to $9 million worth of hardware is bought for each launch.
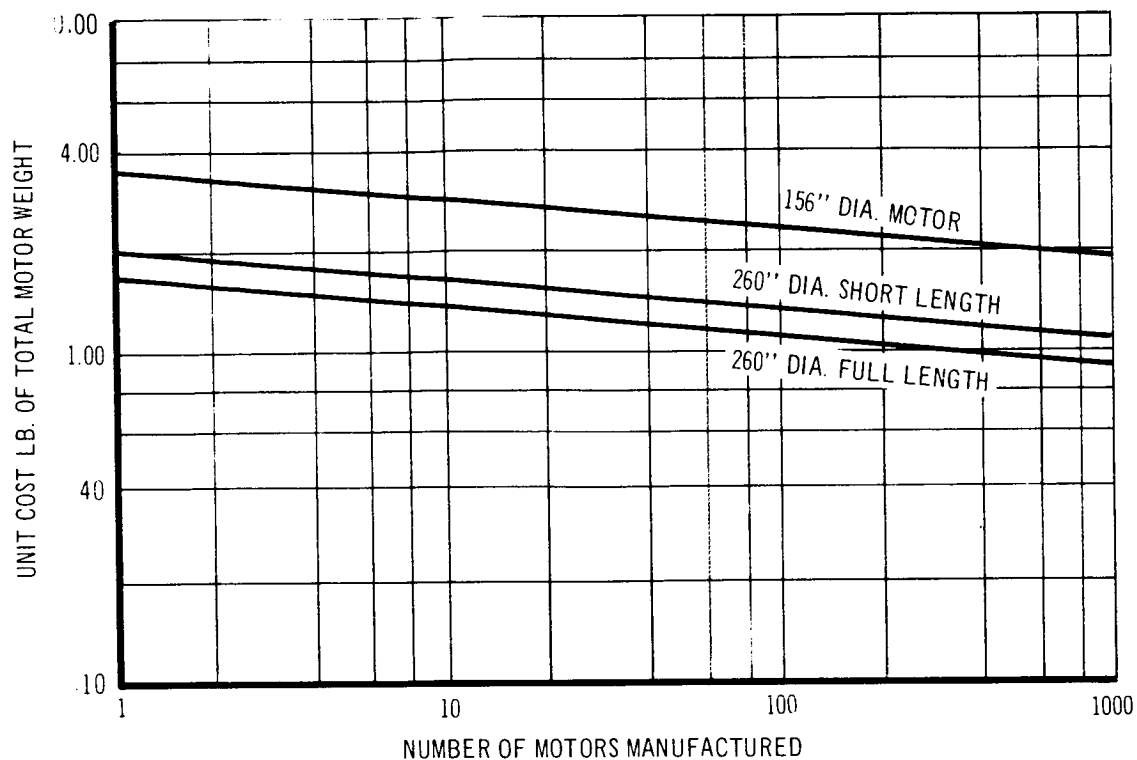
Figure 8-1 Cost/Lb. of Total Motor Weight vs. Number of Motors Manufactured (Fixed Nozzle)

8.3.2 Launch Support Costs

Launch support costs are defined as:

$$
\begin{bmatrix} \text{Logistics} \\ \text{Operations} \\ \text{Costs} \end{bmatrix} = \begin{bmatrix} \text{Total Hardware Production Costs} \\ \text{of HL-10, Boosters, Etc. +} \\ \text{Recov. -Refurb. Costs of HL-10} \end{bmatrix} + \begin{bmatrix} \text{Launch} \\ \text{Support} \\ \text{Costs} \end{bmatrix}
$$

The first term on the right hand side is a function of the number of launches and will be dealt with further in Section 8.3.3. However, the second term on the right, launch support costs, may or may not be a function of the number of launches. This depends on how it is defined. In connection with the HL-10 vehicle, launch support costs will be defined as:

$$
\begin{bmatrix} \text{Launch} \\ \text{Support} \\ \text{Costs} \end{bmatrix} = \begin{bmatrix} \text{Cost of Support} \\ \text{Facilities and} \\ \text{Equipment} \end{bmatrix} + \begin{bmatrix} \text{Labor Costs for Booster and Vehicle} \\ \text{Transportation, Erection, Staging} \\ \text{and Launching} \end{bmatrix}
$$

140

Table 8-3

BOOSTER COSTS AND WEIGHTS

| Stage | Motor Dia. | Gross Wt. (million lb.) | Number of Launches | | | | | |
| | | | 28 | | 58 | | 108 | |
			Estimated Cost/Lb.	Unit Cost ($ million)	Estimated Cost/Lb.	Unit Cost ($ million)	Estimated Cost/Lb.	Unit Cost ($ million)
1st	260 in.	4.33	$1.23	5.32	$1.15	4.97	$1.09	4.72
2nd	260 in. (40% Length)	1.50	$1.50	2.25	$1.40	2.10	$1.31	1.97
3rd	156 in.	0.58	$2.58	1.50	$2.40	1.39	$2.27	1.32
	TOTAL	6.41	$1.42	9.07	$1.32	8.46	$1.25	8.01

Table 8-4
SUMMARY OF BOOSTER MOTOR COSTS

3 Stage Booster	Lb. (million)	Cost/lb.	Gross Cost ($ million)
4 launches/yr.	6.41	$1.42	9.07
10 launches/yr.	6.41	$1.32	8.46
20 launches/yr.	6.41	$1.25	8.01

Table 8-5
PRODUCTION COST SUMMARY FOR FIRST
OPERATIONAL LAUNCH

	Production Item	4 Launches/ Year ($ million)	10 Launches/ Year ($ million)	20 Launches/ Year ($ million)
Recoverable	HL-10 Vehicle	18.5	18.5	18.5
	Steering Engines and Accessories	0.5	0.5	0.5
	Total Recoverable	19.0	19.0	19.0
Nonrecoverable	Three-Stage Booster	9.07	8.46	8.01
	Cargo Adapter	0.80	0.80	0.80
	Interstage Structure	0.50	0.50	0.50
	Total Nonrecoverable	10.37	9.76	9.31
	Total Production Cost for the First Operational Launch	29.4	28.8	28.3

Launch support costs will reflect investment in both men and equipment and will be considered, for the purposes of this study, to be independent of launch frequency over a 5-year operational period (see below).

1. Support Facilities and Equipment Cost

Checkout equipment costs for HL-10 and boosters = $25 x 10^6

This number is obtained from modifying the data in the MORL report (Reference 1) to reflect HL-10 requirements. It should be emphasized that this is an order of magnitude estimate only.

HL-10 and Booster Support Facilities and
Equipment Cost (Excluding Checkout   = $80 x 10^6
Equipment)

The HL-10 and booster support cost given above includes the cost of HL-10 vehicle and booster transportation from factory to launch area, vehicle transporters, such as crawlers to transport the flight vehicle from the assembly building to the launch pad, vehicle staging and erection equipment costs, other ground support equipment, vertical assembly building, cranes, gantries, etc. The data upon which this cost is based comes from Reference 3.

It should be noted that the cost of recovery of the HL-10 vehicle and its transportation back to Cape Kennedy is included in the recovery-refurbishment cost which is taken to be 10 percent of the HL-10 and engine unit production cost.

2. Labor Cost

Labor cost for booster and
vehicle transportation,   = 100 men x $30,000/man x
erection staging and   5 yrs. = $15 x 10^6
launching operations

Equipment costs can be considered to be independent of the number of launches because equipment is bought and paid for only once, regardless of the launch schedule. On the other hand, labor costs are sensitive to launch schedule. It is certainly true that more men working longer hours may be required to sustain a launch rate of 20 shots per year (one launch every 18-1/4 days) than are needed to support 4 shots per year (one launch every 90 days or so). Unfortunately, it is not known how many more men will be required. 100 men may be too many for 4 launches per year, not enough for 20 launches per year and just the right number to sustain 10 launches per year. The $30,000 per man includes salary, overhead and overtime costs for a year. No overtime may be necessary to sustain 4 launches per year while more overtime than is reflected in the $30,000 annual figure given, may be required to support a 20 per year launch schedule. Therefore, the 100 men and $30,000 per man

year should be considered to represent average figures of merit which reflect launch requirements ranging from 4 launches per year to 20 launches per year over a 5-year operations period.

3.   Launch Support Cost Summary

Total Launch Support Costs Over a 5-Year Operations Period $= \$(25 + 80 + 15) \times 10^6 = \$120 \times 10^6$

8.3.3   Logistics Cost to Support a Manned Space Station

We are now in a position to assess the logistics operations cost involved in supporting a manned space station using an HL-10 vehicle. Three different launch schedules will be considered:

1.   4 launches per year or 20 launches over a 5-year period (equally spaced)

2.   10 launches per year or 50 launches over a 5-year period (equally spaced)

3.   20 launches per year or 100 launches over a 5-year period (equally spaced).

The vehicle cycle time will be taken to be on the order of 110 days. This cycle time is broken down in Table 8-6.

Table 8-6

MISSION CYCLE TIME

Mission time	7 days
Transportation from recovery area to refurbishment area	5 days
Refurbishment time	60 days
Prelaunch preparation time	38 days
TOTAL CYCLE TIME	110 days

The vehicle cycle time, then, is the time that elapses from vehicle launch to the time when the vehicle is ready to be relaunched. However, the vehicle is not actually relaunched until the next scheduled launch which may or may not coincide with the time that the vehicle is ready to be launched. This is shown in Table 8-7.

Table 8-7

LAUNCH TIME CHARACTERISTICS

Number of Equally Spaced Launches/Yr.	Launch Interval (days)	Vehicle Cycle Time (days)	Waiting Time to Next Scheduled Launch (days)	Total Time Elapsed Between Launches Using the Same Vehicle (days)
4	91.0	110	73	183
10	36.5	110	0	110
20	18.0	110	0	110

The number of HL-10 vehicles required to support a given launch schedule will depend on the total time elapsed between launches using the same vehicle (i.e., vehicle cycle time + waiting time to next launch):

$$\begin{array}{l}\text{Number of}\\\text{Vehicles}\\\text{Required}\end{array} = \left(\begin{array}{l}\text{Number of}\\\text{Launches}\\\text{per Year}\end{array}\right) \times \left(\frac{\text{(Vehicle Cycle Time + Waiting Time to Next Launch)}}{365}\right) \qquad (1)$$

The number of vehicles required will then put a constraint on the number of times the HL-10 is to be recovered and reused:

$$\begin{array}{l}\text{Number of Times}\\\text{HL-10 is Used}\end{array} = \frac{\left(\begin{array}{l}\text{(Number of Launches}\\\text{per Year)}\end{array}\right) \times \left(\begin{array}{l}\text{(Number of Years}\\\text{of Operation)}\end{array}\right)}{\text{(Number of Vehicles Required)}} \qquad (2)$$

It should be pointed out that the terms "vehicle use" and "vehicle reuse" are not used interchangeably.

If we make use of equations (1) and (2) we can obtain the number of HL-10 vehicles required, for a vehicle cycle time of 110 days, to support a 4, 10 and 20 annual launch schedule over a 5-year operational period. This information is summarized in Table 8-8.

Table 8-8
REUSE REQUIREMENTS

Annual Launch Schedule	Number of HL-10 Vehicles Required Over a 5-Year Operational Period	Number of Times HL-10 Will be Used Over a 5-Year Operational Period
4	2	10
10	3	17
20	6	17

Table 8-9 shows the total hardware production cost expended, in order to support an annual launch rate of 4, 10, and 20 launches per year, respectively, for a 5-year operational program. The items are listed in two categories: recoverable and nonrecoverable hardware. The recoverable items consist of the HL-10 capsule, steering engines and engine accessories. The nonrecoverable items consist of the three stage booster, cargo adapter and interstage structure. The table shows that the percentage of total hardware production cost contributed by the recoverable and nonrecoverable items, respectively, is almost independent of launch frequency. Thus the recoverable hardware production cost (including recovery refurbishment) contributes about 25 percent to the total cost, whereas 75 percent of the total production cost is contributed by the cost of producing nonrecoverable hardware. The booster cost alone accounts for 65 percent of the total cost.

The HL-10 and steering engine recovery-refurbishment cost is assumed to be 10 percent of the 19×10^6 unit production cost of the HL-10 and steering engine group. This cost (1.9×10^6 for each reuse) is listed in the table under the recoverable item category. The number of reuses is easily calculated:

$$\begin{pmatrix} \text{Number of} \\ \text{HL-10 Reuses} \end{pmatrix} = \begin{pmatrix} \text{Total Number of} \\ \text{Launches Over} \\ \text{5-Year Period} \end{pmatrix} - \begin{pmatrix} \text{Number of HL-10} \\ \text{Vehicles Required} \\ \text{Over a 5-Year} \\ \text{Operational Period} \end{pmatrix}$$

No attempt has been made to include in the production cost presented in Table 8-5 any additional cost that would be incurred in building reuses into

	Item	Breakout	4 Launches/Yr* Cost x 10^6	Percent Total Prod. C
Recoverable	HL-10	2 x 18.5 x 10^6	37.0	13.3
	Steering Engines & Accessories	2 x 0.5 x 10^6	1.0	0.4
	HL-10 Recov. - Refurb.	18 x 1.9 x 10^6	34.2	12.2
	TOTAL	Recoverable	72.2	25.9
Nonrecoverable	Three Stage Booster	20 x 9.07 x 10^6	181.0	64.8
	Cargo Adapter	20 x 0.8 x 10^6	16.0	5.7
	Interstage Structure	20 x 0.5 x 10^6	10.0	3.6
	TOTAL	Nonrecoverable	207.0	74.1
	HARDWARE PRODUCTION COST TOTAL		279.2	100.

*Based on an HL-10 vehicle used 10 times
**Based on an HL-10 vehicle used 17 times

(147)

Table 8-9

COST TOTAL OVER A 5-YEAR OPERATIONAL PROGRAM

of		10 Launches/Yr**			20 Launches/Yr**	
st	Breakout	Cost x 10^6	Percent of Total Prod. Cost	Breakout	Cost x 10^6	Percent of Total Prod. Cost
	3 x 18.5 x 10^6	55.5	8.8	6 x 10.5 x 10^6	111.0	9.0
	3 x 0.5 x 10^6	1.5	0.2	6 x 0.5 x 10^6	3.0	0.2
	47 x 1.9 x 10^6	89.3	14.0	94 x 1.9 x 10^6	178.6	14.6
		146.3	23.0		292.6	23.8
	50 x 8.46 x 10^6	423.0	66.8	100 x 8.01 x 10^6	801.0	65.6
	50 x 0.8 x 10^6	40.0	6.2	100 x 0.8 x 10^6	80.0	6.6
	50 x 0.5 x 10^6	25.0	4.0	100 x 0.5 x 10^6	50.0	4.0
		488.0	77.0		931.0	76.2
		634.3	100.0		1,223.6	100.0

the spacecraft. In other words, it has been assumed that the $19 x 10^6 cost of spacecraft and engines is independent of the number of uses the vehicle is designed for. Only the recovery-refurbishment cost has been allowed for in this connection. Just how production cost varies with built-in vehicle use life is not known and requires further study. Such a study is beyond the scope of this report.

Considering 4 launches, 10 launches, and 20 launches per year, respectively, to be the launch requirements to support a manned space station for 5 years, the logistics operations costs can be summarized as shown in Table 8-10.

The numbers for total hardware production cost are the same as those given in Table 8-9, but are rounded off to three significant figures. The launch support cost numbers are those given in Section 8.3.2.

Table 8-10

LOGISTICS OPERATIONS COST TO SUPPORT A MANNED
SPACE STATION FOR 5 YEARS

Total Launches Over a 5-Year Period	Total Hardware Production and Recov.-Refurb. Cost $\times 10^6$	Launch Support Costs $\times 10^6$	Total Cost $\times 10^6$	Cost Per Launch $\times 10^6$
20	$ 279	$120	$ 399	$20.0
50	634	120	754	15.1
100	1,220	120	1340	13.4

Using the above information, it is of interest to examine the relationship between the cost per pound of cargo (unpackaged) and flight frequency. Cargo consisting of 19,000 lb. of unpackaged consumables and experimental equipment (not including the 2 crewmen + 6 passengers) can be supplied to a space station each flight. The costs per pound of cargo are summarized in Table 8-11.

The above data are represented graphically in Figure 8-2 for costs based both on the total program and for operations only. In both cases, the greatest

Table 8-11

COSTS PER POUND OF CARGO

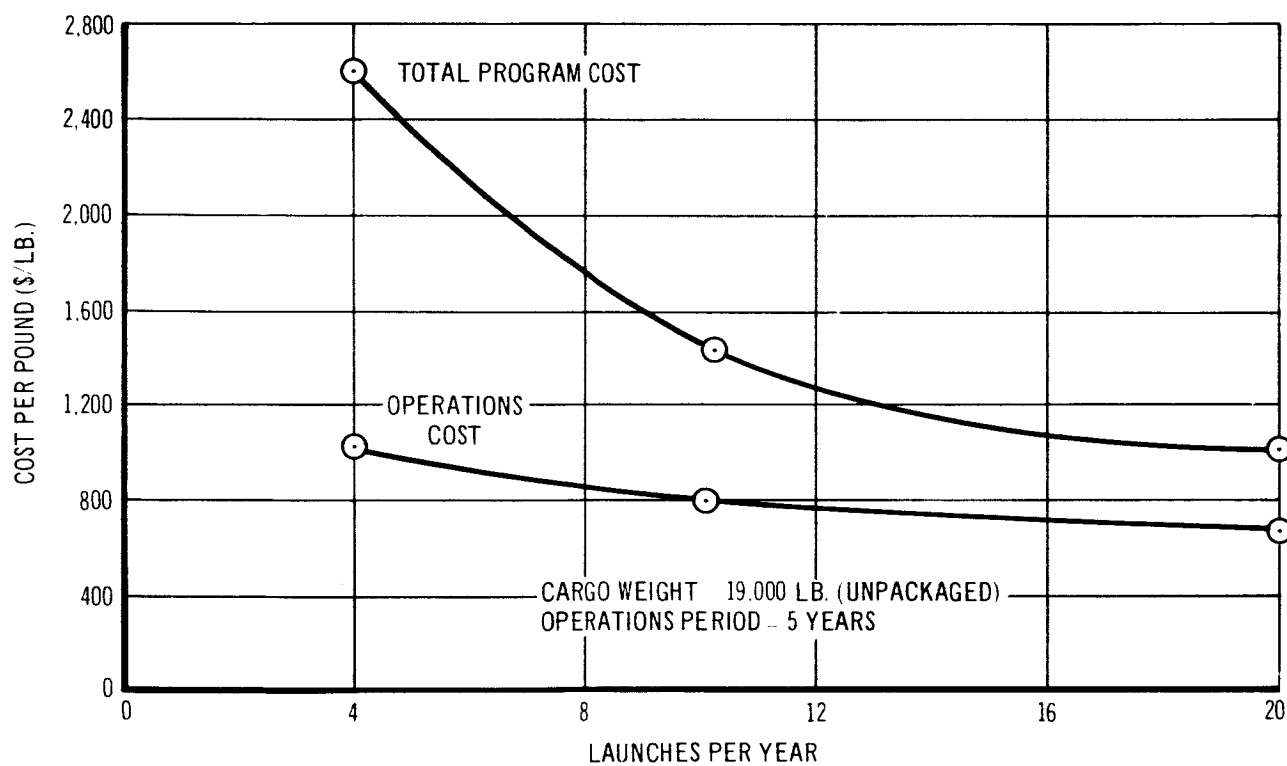| Launches Per Year	Total Operations Cost Over a 5-Year Period	Total RDT&E Training, Etc. Costs From Development Phase	Total Unpackaged Cargo Orbited In a 5-Year Period (Lb.)	Operations Cost/Lb. of Unpackaged Cargo	Total Program Cost/Lb. of Unpackaged Cargo
4	$399 x 10^6	$597 x 10^6	$ 380 x 10^3	$1,050	$2,620
10	754 x 10^6	597 x 10^6	950 x 10^3	793	1420
20	1,340 x 10^6	597 x 10^6	1,900 x 10^3	705	1020

Figure 8-2 Cost Per Pound of Cargo Delivered into Orbit vs. Launches Per Year

savings occur at the lower end of the launch frequency scale. Thus, operations cost/lb. of cargo are reduced by almost 25% in going from 4 to 10 launches per year while total program cost/lb. of cargo decreases by about 46%.

Only an 11% savings in operations cost/lb. of cargo results when launch frequency is increased 100% from 10 to 20 launches per year. On the other hand, when total program costs are considered, 28% in cost/lb. of cargo delivered is saved by doubling the yearly launch rate from 10 to 20.

8.4 TOTAL PROGRAM COST SENSITIVITY

8.4.1 Sensitivity of Program Total Costs to Program Component Costs

The total program cost presented in Section 8.1 is the sum of the estimated component parts. It is obviously of interest to see how a change in the assessment of a component cost will affect final assessment of total program cost. This highlights critical cost areas and an evaluation may be made as to which component costs are the most important in the total program cost assessment.

Total program cost can be broken down as shown in Figure 8-3.

Figure 8-4 shows how a variation in nonrecurring cost and operating cost changes the total program cost. This is done for 4 , 10 , and 20 launches/ year. Total program costs become less sensitive to nonrecurring cost as the number of logistics launches increases.

A 40% variation in nonrecurring cost will change the total program cost to support 4 launches/year by almost 25%, whereas if 10 launches/year are made, the program cost is changed by less than 18% (a 40% variation in non-recurring cost). Finally, if 20 launches/year are made, a 40% variation in nonrecurring cost will influence total program cost by only 12%. Variations in operations cost affect total cost in just the reverse manner. As logistics launch frequency increases, operations cost goes up, and hence, becomes a larger part of total program cost. Thus for 4 launches/year a 40% change in operations cost affects program costs about 16% while for 20 launches/year,
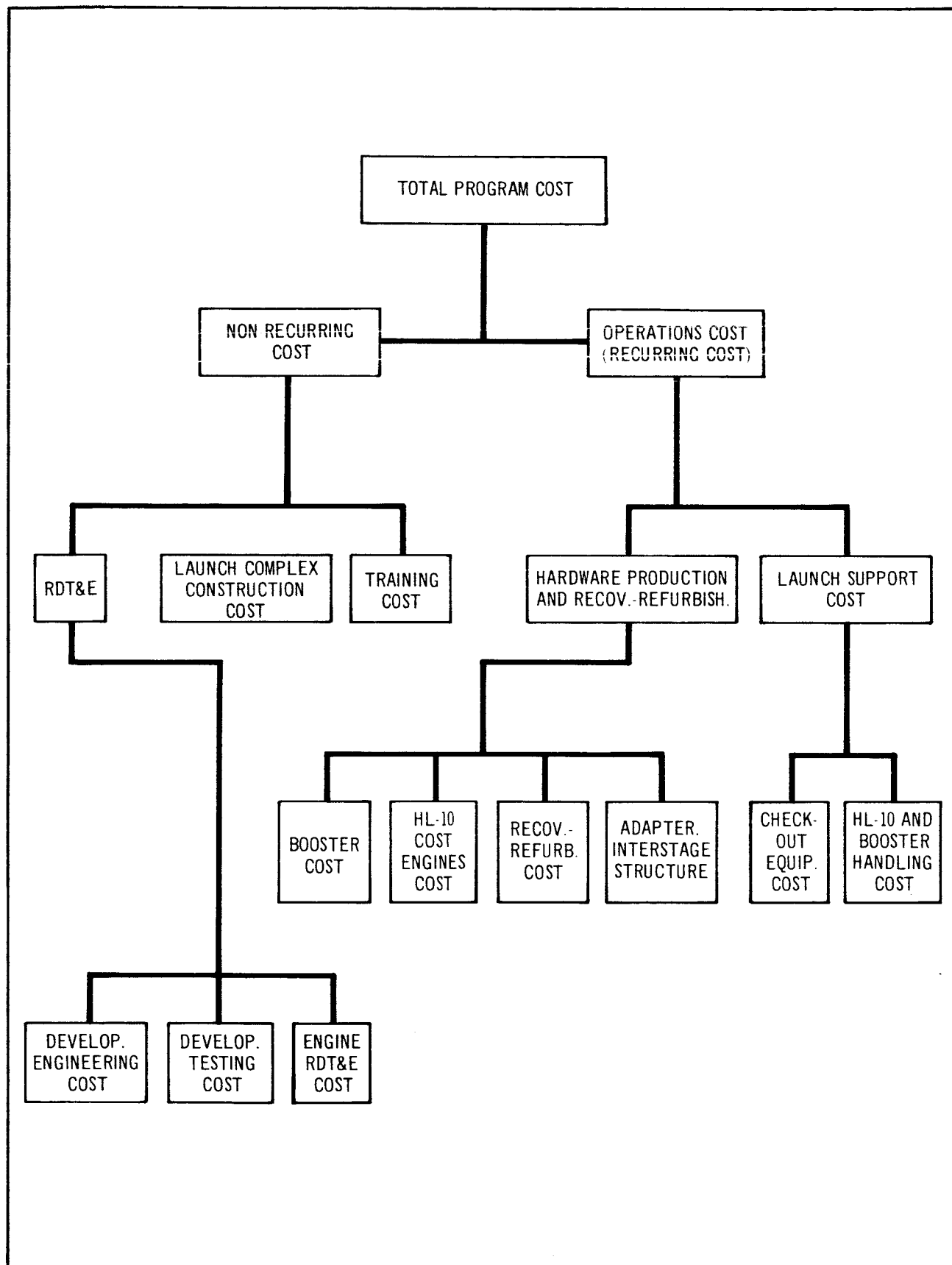
Figure 8-3 Total Program Cost Block Diagram
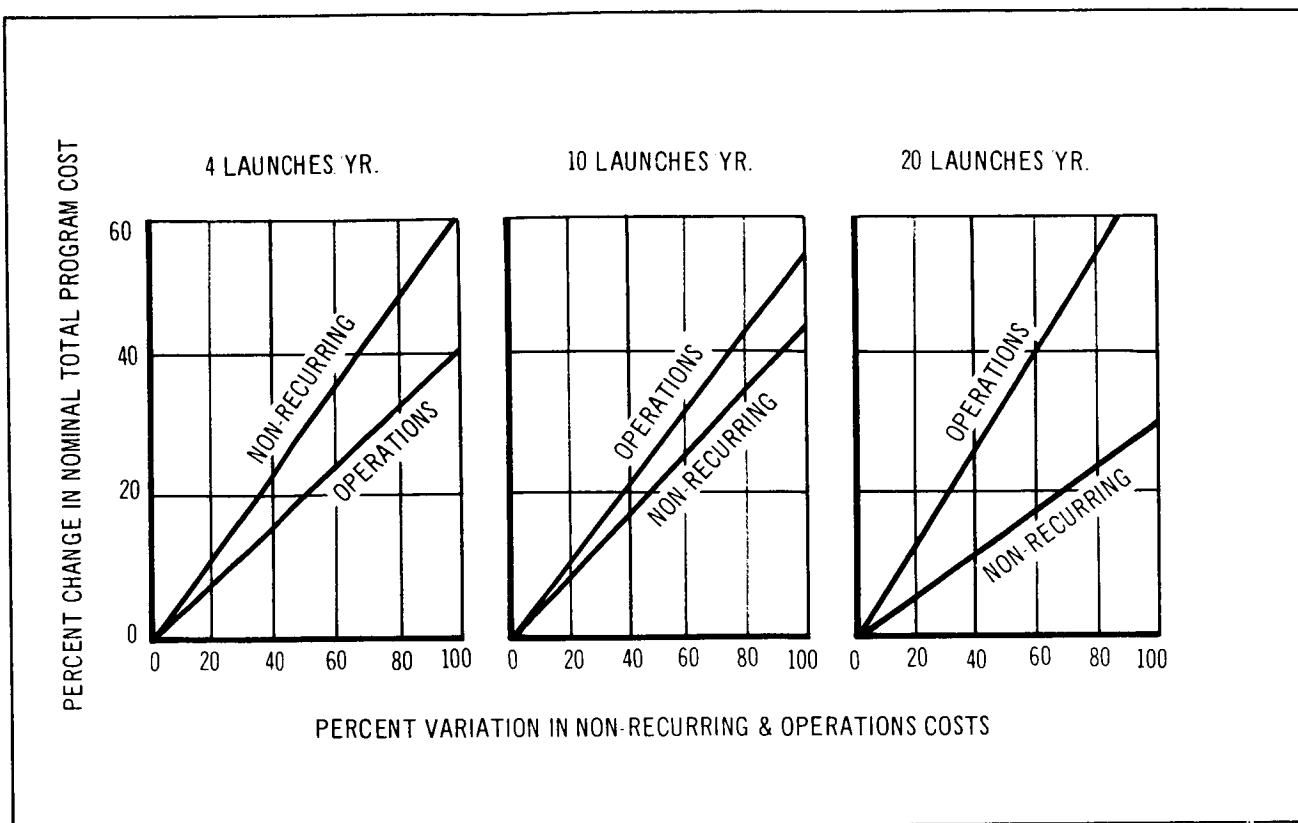
Figure 8-4 Effect of Non-Recurring & Operations Cost Variation on Total
Program Cost for a 5 Year Operation

a 40% variation in operations cost will now change program costs by nearly
28%.

Nonrecurring cost is broken down into its components. Figure 8-5 shows
how cost variation in these components individually affects total nonrecurring
cost. It should be noted that since training cost and launch construction cost
have been estimated to be of the same order of magnitude (see Section 8.2.2),
the same cost sensitive curve can be used for either of these items. Nonre-
curring cost is more sensitive to changes in development testing cost than
any other item. Therefore, if development testing cost were doubled, the
nonrecurring cost would increase about 45%, whereas if either launch complex
construction cost or training cost were doubled, nonrecurring cost would only
go up 15%. It is of interest to note that doubling steering engine RDT&E cost
will only change nonrecurring cost by about 6.4%.
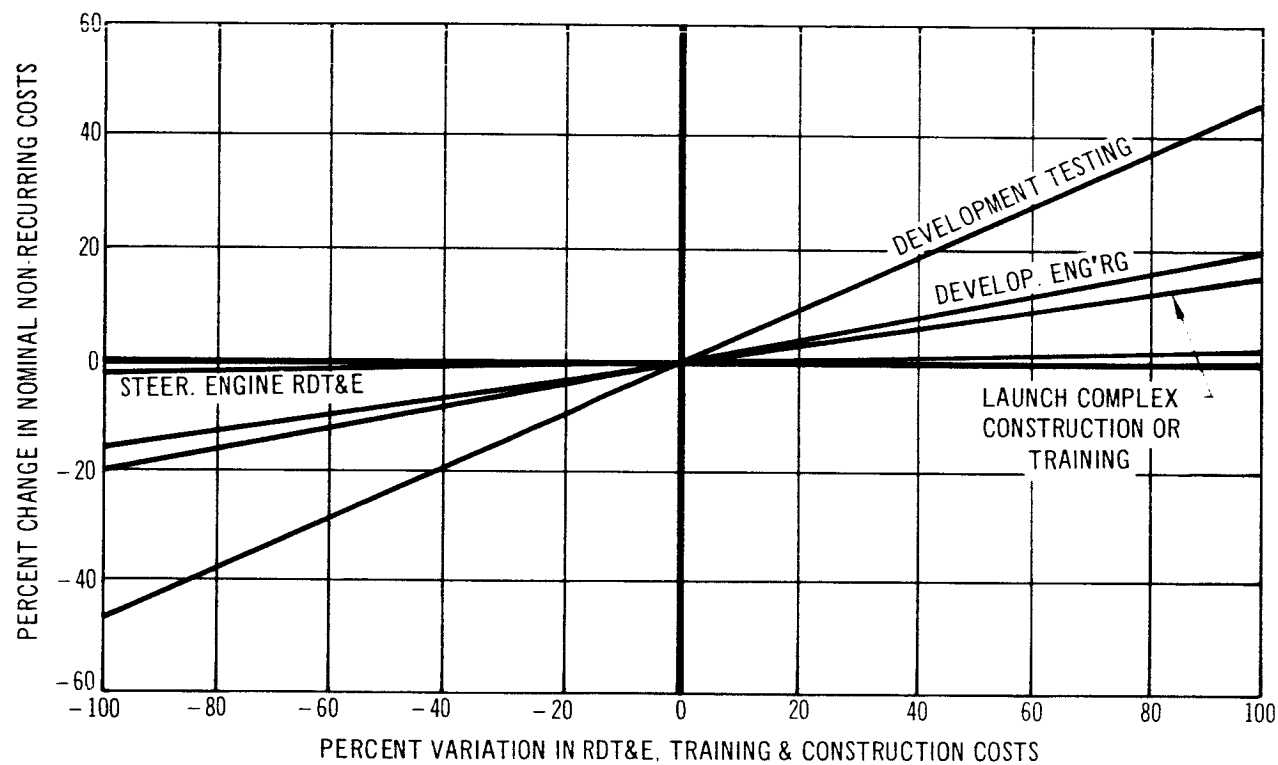
Figure 8-5 Effect of RDT&E, Training & Construction Cost Variations
on Non-Recurring Costs

In Figure 8-6, operations cost is broken down into components of hardware production cost and launch support cost. These costs are based on launch schedules of 4, 10, and 20 launches per year. Since launch support cost has been defined to be independent of launch frequency (see Section 8.3.2), it becomes a smaller part of operations cost when the number of launches increases, and therefore, operations cost is less sensitive to launch support cost as the number of yearly launches increases.

Hardware production cost is broken down into cost components in Figure 8-7. Four major hardware cost sensitivities are shown. They are:

1. Booster production
2. HL-10 spacecraft and steering engine
3. Other hardware, including adapter and interstage structure
4. HL-10 and steering engine recovery-refurbishment.

It is clear that hardware production cost is more sensitive to booster cost variation, by far, than to any other cost component. Thus, if HL-10 and
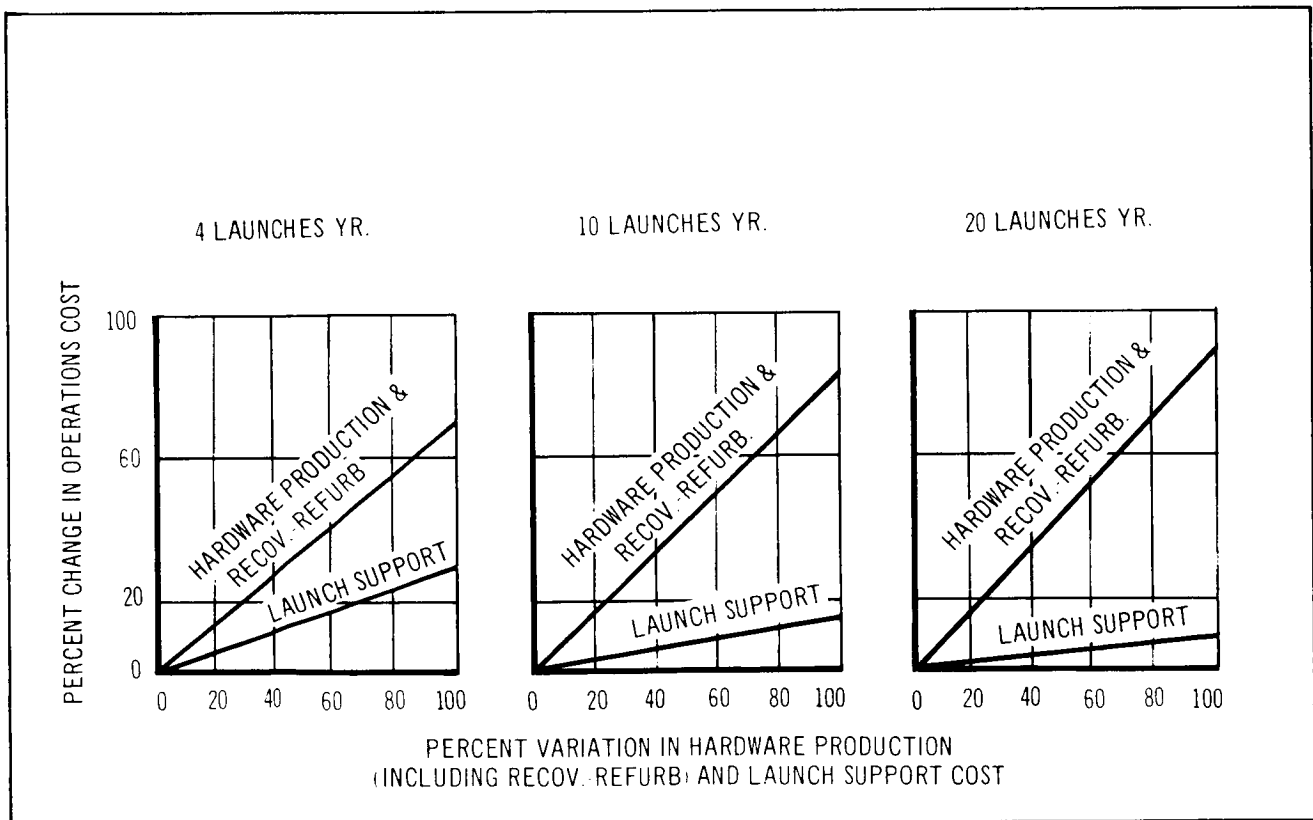
Figure 8-6 Effect of Hardware Production (Including Recov.-Refurb.) and Launch Support Cost Variation on Operations Cost

1 BOOSTER   3 HL-10. ENGINE RECOVERY-REFURBISHMENT
2 HL-10 & ENGINES   4 ADAPTER & INTERSTAGE STRUCTURE
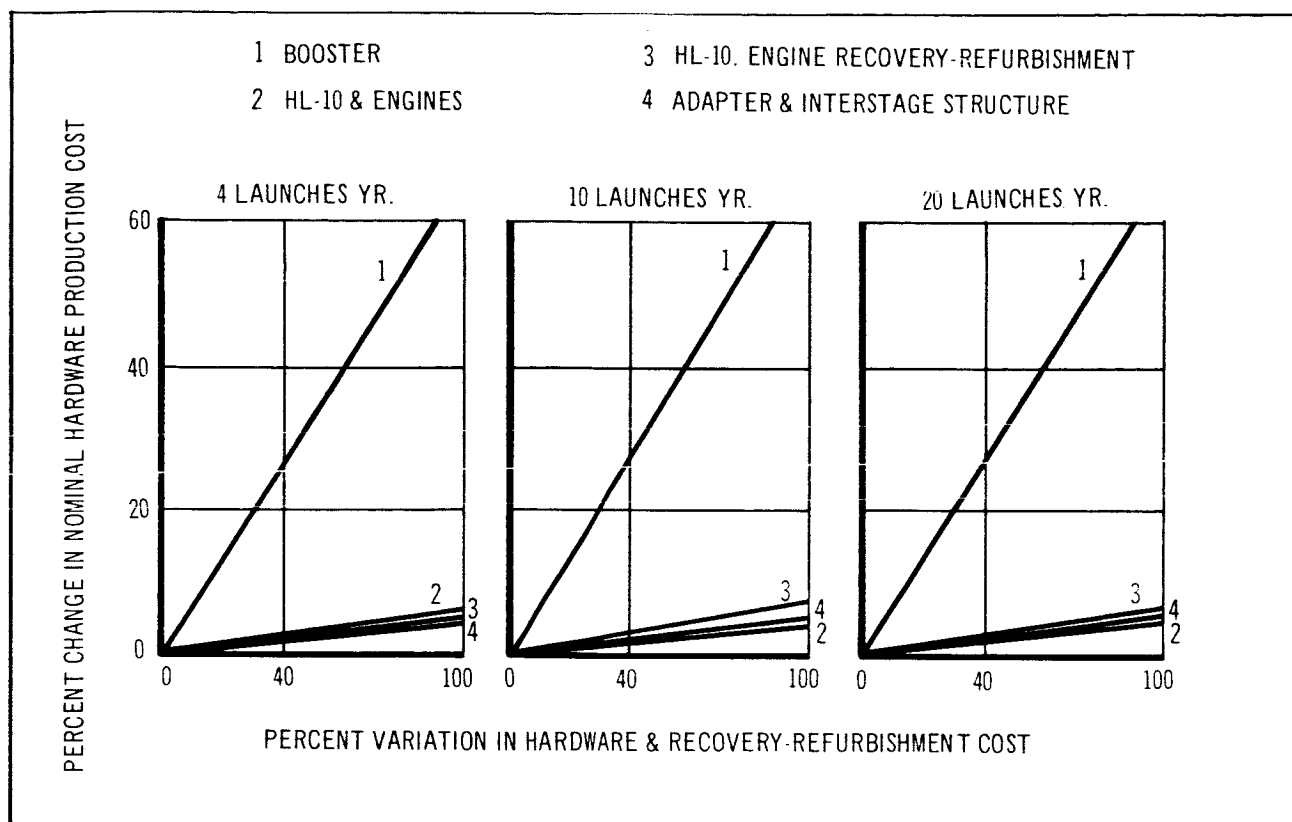
Figure 8-7 Effect of Hardware and Recovery-Refurbishment Cost Variation
on Total Hardware Production Cost

steering engine cost were doubled, total hardware production cost would only increase by about 10%, whereas production cost would go up over 65% if booster cost were doubled.

At this point, to take a specific example, it is of interest to see how total program cost is affected by changing the third stage booster cost to $3.00/lb. Although booster cost/lb. is a function of the number of launches, the greatest third stage change occurs for 108 launches (see Table 8-3). Therefore, as-sessment of booster cost sensitivity will be confined to 108 launches; the worst possible case in Table 8-3.

If $3.00/lb. is substituted in place of $2.27/lb. for the third stage cost in Table 8-3, the total three-stage unit booster cost for under 108 launches will jump from $8.01 million to $8.46 million which is a 5.6% increase. The ef-fect on total program cost can be found by utilizing Figures 8-4, 8-6, and 8-7; it is summarized as follows:

155

Change in 3rd stage booster cost   34%

Change in total 3-stage unit
booster cost   5.6%

Change in hardware production cost   3.7%

Change in operations cost   3.4%

Change in total program cost   2.3%

Therfore, if third stage booster cost is increased to $3.00/lb. the maximum change in total program costs will not exceed 2.3%.

8.4.2 Sensitivity of Program Total Costs to Certain Nominal Case Variations

The total program cost presented in Section 8.1 is based on a 4, 10, or 20 launch/year logistics requirement over a 5-year period. These costs have been assessed for a nominal case of:

1. Recoverable HL-10 vehicle and steering engines.
2. Vehicle cycle time on the order of 110 days.
3. Recovery-refurbishment cost is 15% of HL-10 production cost (based on an HL-10 and steering engine cost of $19.0 million).
4. Reliability of launch and recovery is perfect.
5. Pad tie-up time is not a constraint on cost (except as it might affect vehicle cycle time) so that launch complex construction cost does not include allowance for extra pads to more efficiently meet a launch schedule.

The effect on total hardware production cost,if the recovery-refurbishment cost is varied,is given in Figure 8-7. Thus, if HL-10 recovery-refurbishment cost is doubled from 10% to 20% of vehicle unit cost (based on a $19 million space vehicle) Figure 8-7 shows that total hardware production cost increases by less than 15%.

Figure 8-8 shows how operations cost could be affected by reliability of launch and recovery if cost and reliability were related by the simple equation:

$$C_t = C_{to}/R$$
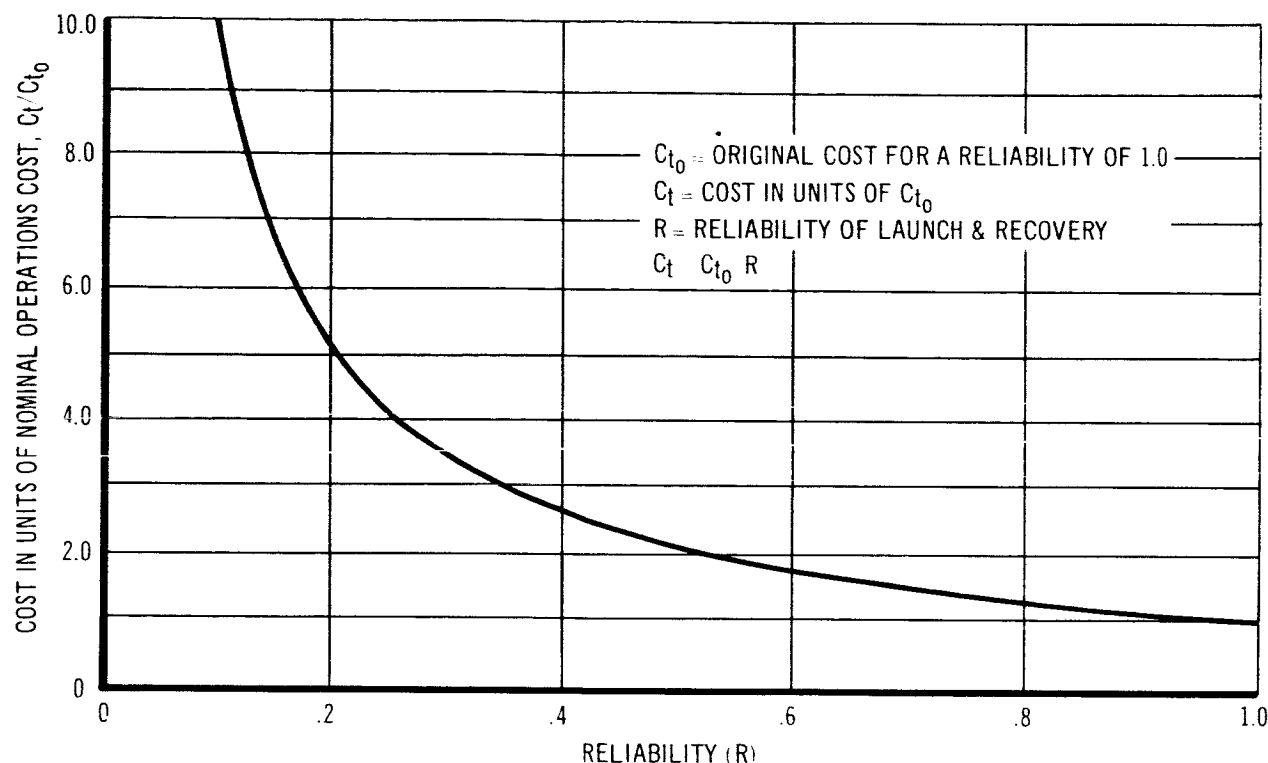
Figure 8-8 Cost Vs. Reliability

where

$$C_{to} = \text{nominal operations cost}$$

$$C_t = \text{operations cost in units of } C_{to}$$

$$R = \text{reliability of launch and recovery.}$$

Thus, if it were assumed that the HL-10 were launched and recovered with a 0.9 total reliability, this would increase the operations cost by about 10%.

Figure 8-9 shows how the number of pads required is affected by launches/ year, vehicle cycle time and pad tie-up time. In our nominal case of a 110-day vehicle cycle time, which is 30% of a year, the vehicle is on the pad 20 days or 18% of its cycle time. Only one pad is needed to sustain up to 20 launches/year. It should be noted that these numbers do not allow for pad refurbishment time after each launch. Hence, an extra pad should be built for backup purposes.
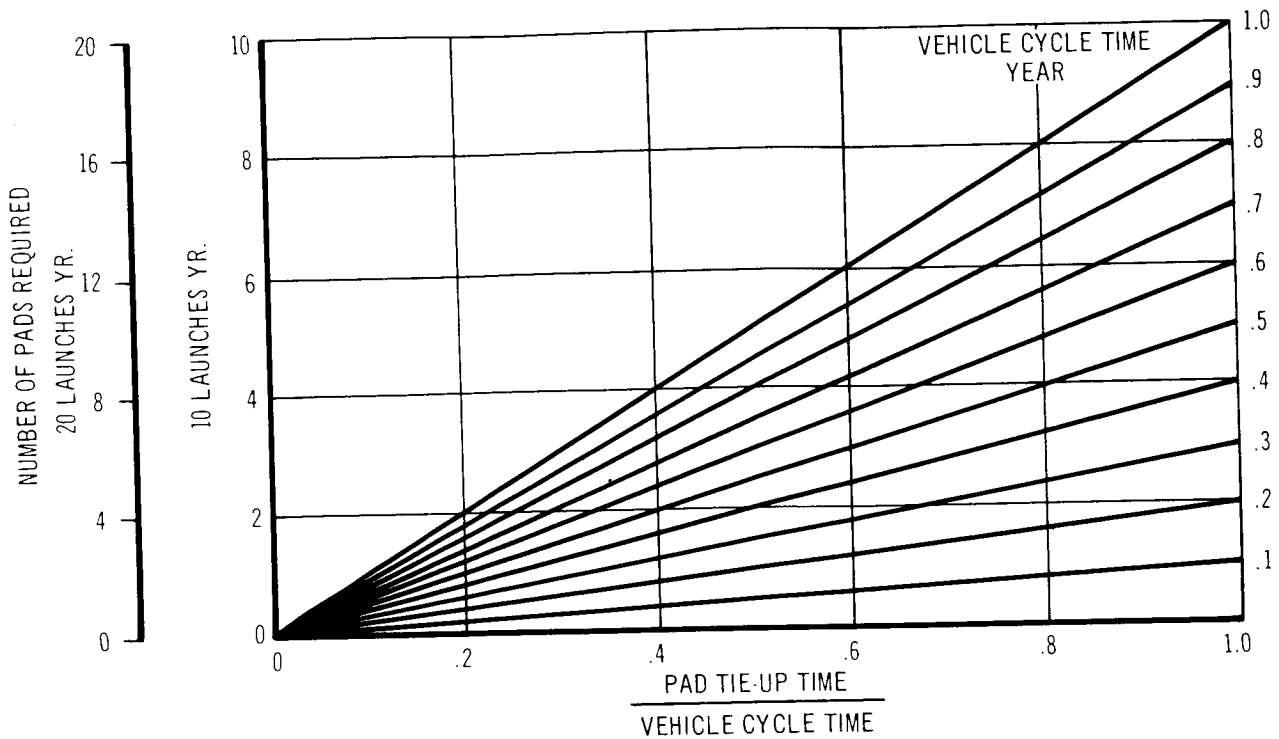
Figure 8-9 Number of Launch Pads Required vs. Pad Tie-Up Time and Vehicle Cycle Time

8.5 LOGISTICS AND DEVELOPMENT COSTS FROM OTHER SOURCES

The cost analysis results of other manned space vehicle systems are presented in Table 8-12 with the corresponding costs of the HES-2G head-end steering vehicle system. The spacecraft shown in Table 8-12 vary in size from the Gemini two-man ballistic vehicle to the HES-2G vehicle of this study. The HES-2G can carry up to 13 personnel; however, eight men is the normal complement. All of the data for the vehicles other than the HES-2G were taken from Section 8.7, Reference 5.

Since the missions and design constraints of the spacecraft are different from those used in this study, no comparison with the HES-2G vehicle is valid if the intent is to establish dollar differentials. However, gross observations noting basic differences and similarities indicate significant cost savings for the HES-2G study vehicle.

Spacecraft	Devel. Cost RDTE ($ million)	No. of Personnel	Spacecraft Avg. Unit Production Cost ($ million)
Gemini	150	2	10. 8
3-man Apollo	260	3	11. 1
6-man Apollo	323	6	12. 4
12-man Ballistic	575	12	14. 7
12-man Lifting	700	12	17. 6
HES-2G (1. 2-0. 4-0)	632	8	19. 0

NOTE: 1. Includes all nonrecurring costs: test articles, (see Section 8. 3. 1 for details).

2. Does not include development cost.

3. Based on 108 units.

4. Packaged weight.

Table 8-12

Y OF LOGISTICS SPACECRAFT COST

Booster Unit Production Cost ($ million)	Launch Support Cost ($ million)	Spacecraft Life (No. of Missions)	Recovery and Refurbish Cost ($ million)	Cargo lb. [4]	Cost/ Launch[2] ($ million)	Cost/lb.[2] Cargo
21.0 (liquid)	2.0	1		16,700	33.8	2,020
21.0 (liquid)	2.5	1		13,400	34.6	2,580
21.0 (liquid)	2.5	1		12,000	35.9	2,990
21.0 (liquid)	2.6	4	4.5	10,900	32.9	3,140
21.0 (liquid)	3.0	7	2.0	8,850	30.8	3,480
9.00[3] (solid)	2.2	17	1.9	23,750	15.1	793

support facilities, test equipment, launch support, etc.

2# 159

The launch vehicle used in the cost analysis in Reference 5 is the Saturn IB which accounts for the $21 million booster production cost for the first 5 systems shown in Table 8-12. The lower cost of the HES-2G solid booster is clearly evident; it amounts to almost 50% less than the Saturn IB.

The unit production cost of the HES-2G is higher than the 12-man lifting body vehicle of Reference 5 (also an HL-10 configuration),because of the steering engine installation and the larger size of the HES-2G. Recovery and refurbishment costs are about the same as for the 12-man lifting body.

The lower cost/launch of the HES-2G vehicle reflects lower booster production costs and the reuse of the spacecraft. The larger cargo capacity and the lower cost/launch reflect directly in the significantly lower cost/lb. of cargo delivered by the HES-2G vehicle.

Since the data for the HES-2G space system represents a first-order analysis, the significant potential for lower launch costs and for increased cost effectiveness shown in Table 8-12 indicate urgent need for additional technical definition and in-depth cost analysis not permitted in the time allotted for this study.

8.6 CONCLUSIONS ON ECONOMIC FEASIBILITY

In the gross cost analyses presented in this section, it was determined that the total program cost including research, development, test, evaluation, training, launch complex construction,and operations for 5 years at the rate of 10 flights/year would be approximately $1.4 billion.

Considering operations costs alone, the cost/launch is estimated to be $15.1 million and the cost/lb. of unpackaged cargo is in the order of $793/lb. when eight personnel are carried.

The largest single effect on operations cost is the cost of the booster motors. Though the use of large solid motors represents a cost savings of over $10 million/launch over liquid boosters, the large solid motor costs account for 46% of operations costs.

Major savings in the cost/lb. parameter are not apparent as flight frequency increases above 20 flights/year because of the expendability of the boosters. Further reductions in this parameter might be expected if recoverable boosters were incorporated in the concept.

When compared to current man-rated systems the preceding costs appear attractive and certainly exhibit no abnormally high or unusual cost requirements. An evaluation of steering engine development and production costs show that although the steering system represents a major technical consideration in the study, it produced little significant effect on total program cost or on operation costs.

8.7 REFERENCES

1. Report on the Optimization of the Manned Orbital Research Laboratory (MORL) Systems Concept. Volume XXVII - Cost Plan. Douglas Report SM-46100, September 1964.

2. Estimated Production Cost Data for 260-Inch Diameter Solid Rocket Motors. Aerojet General Corporation, 1964.

3. 260-Inch Diameter Motor Cost. Thiokol Chemical Corp., Brunswick, Georgia, January 1964.

4. Solid Motor Logistic Study. Vol. III. Martin Marietta Corp., January 1964.

5. Operations and Logistics Study of a Manned Orbiting Space Station. Lockheed California Report LR 17366. (NASA Contract NAS 1-4149).

Section 9
CONSIDERATION OF ALTERNATE VEHICLES

9.1 SPACECRAFT ARRANGEMENTS

9.1.1 Effect of Spacecraft Arrangements

A number of spacecraft arrangements were extensively investigated with respect to their applicability to, and effect on, the head-end steering concept. These studies were guided by the study objectives, guidelines, and mission considerations described in Sections 2, 3 and 4; they culminated in the selection of the arrangement designated HES-2G described in Section 5.

It was found during the course of the study, that the feasibility and desirability of the head-end steering concept is a function of the spacecraft arrangement. Consequently, a great deal of emphasis was placed on determining the most suitable distribution of crew, cargo and propulsion system elements. This, in turn, required a detailed preliminary analysis of each arrangement investigated.

The major spacecraft system components in a given arrangement are listed below:

1. Crew and passengers
2. Cargo
3. Steering and maneuver rocket engines
4. Steering propellant
5. In-orbit maneuver propellant.

The primary arrangements considered are shown schematically in Figure 9-1, which shows the locations assigned to each of these components. Table 9-1 gives a comparative listing of the arrangements and their distinctive features. The HL-10 lifting body was used throughout the study as the manned vehicle.
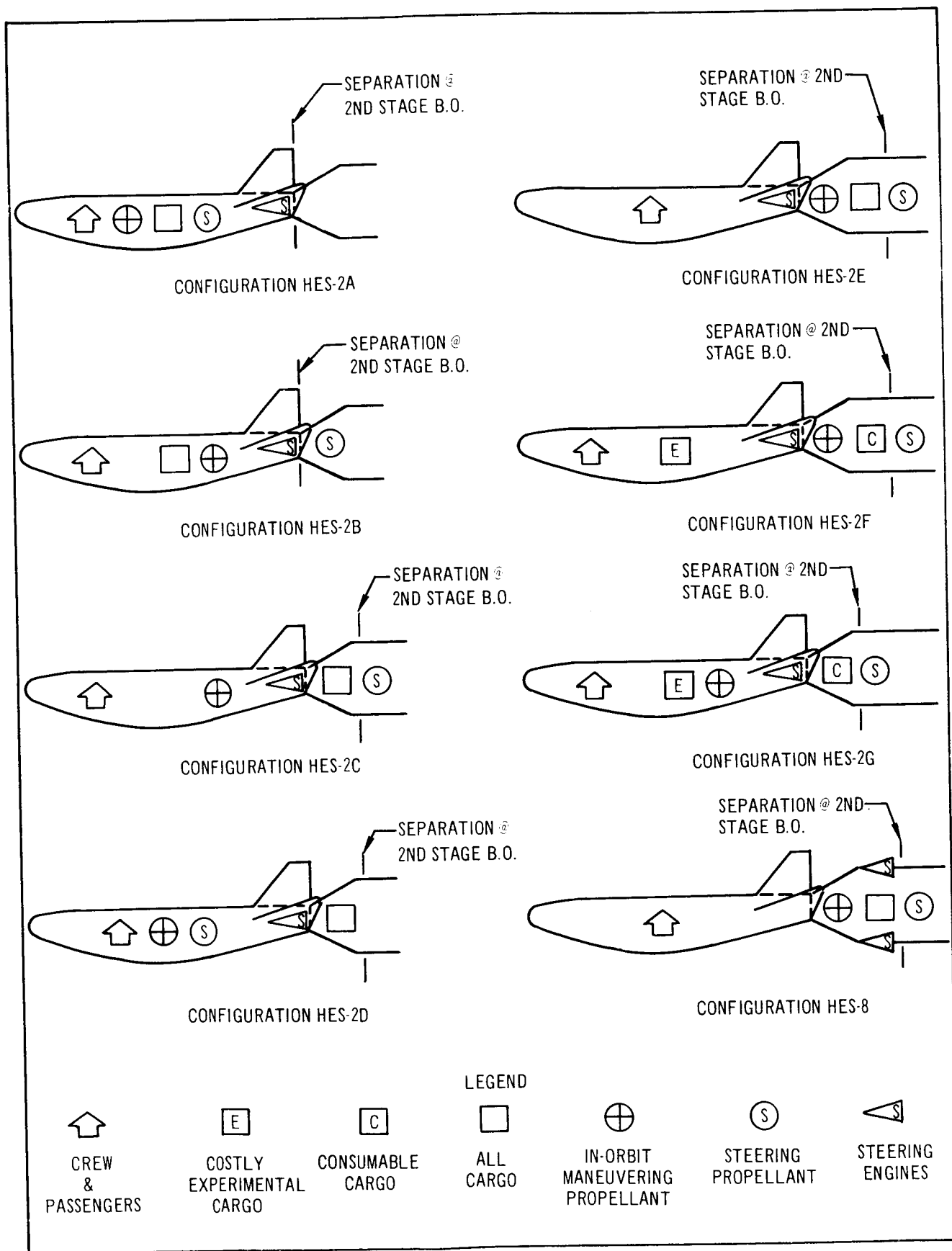
Figure 9-1 Spacecraft Arrangements

Table 9-1

SPACECRAFT ARRANGEMENT CHARACTERISTICS

| Arrangement | Location Of | | | | | | |
| | Crew and Passengers | | Cargo | | Steering Engines | Maneuver Propellant | Steering Propellant |
	Crew Area	Cargo Area	Experimental	Consumable			
HES-2A	8	3	HL-10	HL-10	HL-10 (2)	HL-10	HL-10
HES-2B	8	3	HL-10	HL-10	HL-10 (2)	HL-10	Adapter
HES-2C	11	0	Adapter	Adapter	HL-10 (2)	HL-10	Adapter
HES-2D	11	0	Adapter	Adapter	HL-10 (2)	HL-10	HL-10
HES-2E	11	0	Adapter	Adapter	HL-10 (2)	Adapter	Adapter
HES-2F	8	3	HL-10	Adapter	HL-10 (2)	Adapter	Adapter
HES-2G	8	3	HL-10	Adapter	HL-10 (2)	HL-10	Adapter
HES-8	11	0	Adapter	Adapter	Adapter (4)	Adapter	Adapter

9.1.2 Description of Sizing Techniques

Spacecraft sizing was based on the arrangement being considered and basic mission requirements such as manning, cargo capability, and performance capability. The requirement for steering propellant was determined through an iterative process; this also affected the spacecraft size.

Spacecraft size and weight, booster size, and vehicle steering requirements are all directly related. For this reason, the HL-10 portion of the spacecraft was sized based on minimum volume requirements for all vehicles with the exception of the HES-2G vehicle. This vehicle was sized on a wing loading criterion. The minimum volume sizing technique consisted of determining the best packaging arrangement possible for each of the major system components. In those arrangements with cargo on board the HL-10, the cargo compartment was volume balanced around a desired CG location at 53% of the HL-10 length. Because of a propellant-tank pressure requirement of approximately 50 psia, propellant tanks were geometrically shaped to provide lightweight, minimum distortion pressure vessels. The pressure requirement was based on overcoming the distribution system losses and the provision of acceptable turbopump inlet pressures. Crew compartments were sized to provide side-by-side seating for the two crew members with seating space available for nine passengers. It was assumed that three of these passengers would be seated in the pressurized cargo compartment when it was located on board the HL-10. Provisions were made on all the vehicles for a 30-in.-dia. crawl tube extending to the aft end of the HL-10 from the crew compartment. A 5-in. clearance to the outer skin of the HL-10 was provided in all of the vehicles.

The 44-ft. HES-2G spacecraft size was based on a maximum landing wing loading of approximately 60 lb./sq. ft. This was predicated on a landing condition corresponding to an abort situation during the launch trajectory boost phase. Because of the excess volume available on board the HL-10, it was possible to use lighter weight propellant tanks as described in Section 5.

The adapters were sized for minimum volume, length, and weight conditions for all arrangements. Cargo module volumes were based on the cargo volume

required plus crew access and docking guidance provisions. Cargo volume requirements were based on the following estimates:

1. Dry cargo

    A. Packaging weight = 25% of usable cargo weight
    B. Cargo loading efficiency of 75%
    C. Average cargo density of 20 lb. /cu. ft.

2. Liquid cargo

    A. Cargo loading efficiency of 50%
    B. Bulk density of 75 lb. /cu. ft.

The maneuver and steering propellant volumes were based on a bulk density of 74 lb. /cu. ft. and on appropriate allowances for ullage volume and residual propellants based on tank sizes and shapes. The HES-2G steering propellant requirements included an allowance of 2% of the nominal steering propellant for burn-time variation of the solid-propellant boosters.

9.1.3 Arrangement Study Results

The spacecraft arrangement investigation resulted in the selection of the HES-2G spacecraft as that being most applicable to the study objectives. A comparison of the characteristics of each spacecraft arrangement is presented in Table 9-2. These data represent the results of detailed investigations to determine spacecraft size and weight, booster size, and steering requirements.

The spacecraft arrangements selected for investigation were intended to show the effect of subsystem recoverability on vehicles using the head-end steering concept. Subsystems placed on board the HL-10 are recoverable, while those placed in the adapter are expendable. As indicated by Table 9-2, the degree of recoverability incorporated in an arrangement directly effects the size and weight of the entire vehicle. This is especially true when the steering propellant tankage is incorporated into the HL-10. It was found that in both arrangements HES-2A and HES-2D, a closed design loop evolved in the steering requirements which increased the HL-10 size. This in turn increased the booster size and the steering requirements, thereby closing the loop. The HES-2A design was never completed because it was found that the curve of HL-10 size required for a given on-board propellant weight, and the curve of

Table 9-2

SUMMARY OF HES CONFIGURATION CHAR

Configuration	HES-2A	HES-2B	HES-2C	HES-2D
HL-10 length, ft.	71.0	45.0	36.0	55.0
Number of crew	2	2	2	2
Number of passengers in crew area	6	6	9	9
Steering thrust per engine (Vacuum), lb.	130,000	58,000	38,300	56,500
Max. usable steering propellant weight, lb.	267,500	110,700	73,100	108,000
Max. usable maneuver propellant weight, lb.	111,300	46,600	31,100	61,700
Maximum cargo weight, lb.	19,000	19,000	19,000	19,000
HL-10 volumetric efficiency	0.472	0.595	0.587	0.461
HL-10 gross weight, lb.	485,300	90,900	58,900	225,700
HL-10 empty weight, lb.	93,800	38,400	27,200	52,700
HL-10 wing loading at landing (max. internal cargo) lb. sq. ft.	69.6	87.2	60.0	51.8
Forward adapter section: length[5], ft.	5.7[6]	NA	15.0	13.8
gross weight, lb.	3,800[6]	NA	10,100[4]	12,800[4]
empty weight, lb.	3,800[6]	NA	5,100	7,800
Steering propellant module: length[5], ft.	NA	19.3	17.3	NA
gross weight, lb.	NA	123,300	84,700	NA
empty weight, lb.	NA	11,500	10,900	NA
ΔV available at 19,000 lb. of cargo weight, ft./sec.	5,010	3,318	1,620	3,620
ΔV available at 4,000 lb. of cargo weight, ft./sec.	6,500	6,500	6,500	6,500
Total spacecraft length, ft.	71.0	45.0	56.1	74.3
Total length above booster, ft.	76.7	64.3	68.3	74.3
Total weight above booster at booster burnout, lb.	217,800	90,900	69,000	130,500
Booster description[7]	1	1.2-1	1.2-0	1
Total vehicle length, ft.	1	312.0	291.5	1
Total vehicle weight at liftoff, lb.	1	5,365,200	5,015,700	1
Spacecraft ΔV required to provide apogee velocity of 24,535 ft./sec. at 300 n.mi., ft./sec.	1	2,335	1,085	1

	HES-2E	HES-2F	HES-2G	HES-8
	30.8	32.5	44.0	30.8
	2	2	2	2
	9	6	6	9
	24,500	25,200	50,000	27,000
	48,200	49,500	96,300	120,000
	25,900	28,400	44,000	27,000
	19,000	19,000	19,000	19,000
	0.663	0.698	0.435[2]	0.663
	18,300	25,600	91,000[3]	15,500
	18,300	20,600	37,100	15,500
	53.5	68.0	62.3	45.6
	23,4	21.1	12.3	24.4
	38,900[4]	36,500	3,900[4]	39,900
	7,500	7,500	3,900	7,000
	14.7	15.0	16.0	17.8
	55,200	56,500	98,700	133,500
	6,100	6,000	10,300	12,300
	1,134	1,540	2,860	1,490
	6,500	6,500	6,300	6,500
	58.7	58.2	60.7	57.9
	68.8	73.5	72.3	73.0
	57,200	62,100	107,500	54,500
	1.0-0	1.0-0	1.2-.4-0	1.0-0
	261.7	266.4	356.8	266.2
	4,274,400	4,280,600	6,653,400	4,349,000
	535	835	255	985

[1] Payload exceeds large solid motor capability.

[2] HL-10 sized on basis of wing loading rather than minimum volume.

[3] Include abort rockets (3600 lb.) and more refined weight analysis.

[4] With 4,000 lb. cargo (unpackaged).

[5] Length to in-flight separation plane.

[6] Cone attached to 2nd stage booster.

[7] First and middle number refer to fraction of full-length 260-in.-dia. motor, last number refers to number of 156-in.-dia. segments; order of numbers indicates booster stage.

[8] Includes cargo module when applicable.

2#

(168)

total propellant required for a given HL-10 size were divergent. The HES-2A HL-10 size shown in the table does not allow for enough propellant to steer the vehicle and propel the spacecraft. Because the HES-2D vehicle did not have the cargo compartment on board the HL-10, the propellant requirements could be matched more closely with propellant availability. The same general trend existed for the HES-2D as that found to be true for the HES-2A arrangement. At the point that both of these arrangement studies were terminated, the required booster size exceeded the limits established as reasonable launch configurations. Both first stage boosters required far in excess of 4-million lb. of propellant.

By locating the steering propellant tankage in the adapter, as in arrangement HES-2B, the HL-10 size was appreciably decreased. It was found that the propellant requirement and availability curves converged so that entire vehicles could be sized for comparison purposes. With reference to arrangements HES-2B, -2C, -2E and -8 in Table 9-2, it is apparent that as steering propellant, cargo, in-orbit maneuver propellant, and the steering engines are transferred from the HL-10 to the adapter, both spacecraft size and launch vehicle size are decreased. This represents, however, a decrease in system recoverability and an increase in system complexity. As indicated, arrangements HES-2E and -8, which have just the crew on board the HL-10, represent the smallest size of HL-10. HES-8, which has the steering engines on the adapter, has a lower wing loading at landing but requires a larger adapter and steering propellant weight because of the necessity for four engines. Consequently, the HES-8 launch vehicle is also larger than the HES-2E. The four steering engines are required to provide roll, pitch, and yaw; whereas, with engines on-board the HL-10, only two are required to provide the same function. These two arrangements, along with HES-2F, require that the forward adapter section, which contains propellant, be carried throughout the mission flight profile in order to provide propulsion capability.

The HES-2F and -2G arrangements represent attempts to retain the recoverability benefits of the more costly subsystems, but yet retain a workable spacecraft-booster combination with respect to cost and size. An estimate of the weight of the more costly experimental portion of the cargo was placed

at 4,000 lb. of unpackaged weight. Provisions for storage of this cargo was made on board the HL-10 with the remaining 15,000 lb. of cargo (unpackaged weight) being located in an adapter module. Both of these spacecraft have their steering engines located on the HL-10. The HES-2G arrangement also has the in-orbit maneuver propellant located on the HL-10. The spacecraft characteristics shown in Table 9-2 for the HES-2G arrangement are not directly comparable to the other arrangements. The HES-2G spacecraft shown was sized on the basis of a desired wing loading of approximately 60 lb./sq.ft. to accommodate the abort landing condition. The other arrangements were sized on the basis of the minimum internal HL-10 volume required to package the required on-board subsystems. The wing loading was therefore dependent on the other sizing criteria. Figure 9-2 shows the effect of HL-10 length on wing loading for the arrangements investigated. As indicated by the curves shown, the lengths of HES-2B and -2F would have to be 61 and 38 ft. respectively to attain wing loadings of 60 lb./sq.ft.

The HES-2F arrangement, as indicated by Table 9-2, provides a smaller vehicle, but it lacks propulsion capability on board the HL-10 and requires
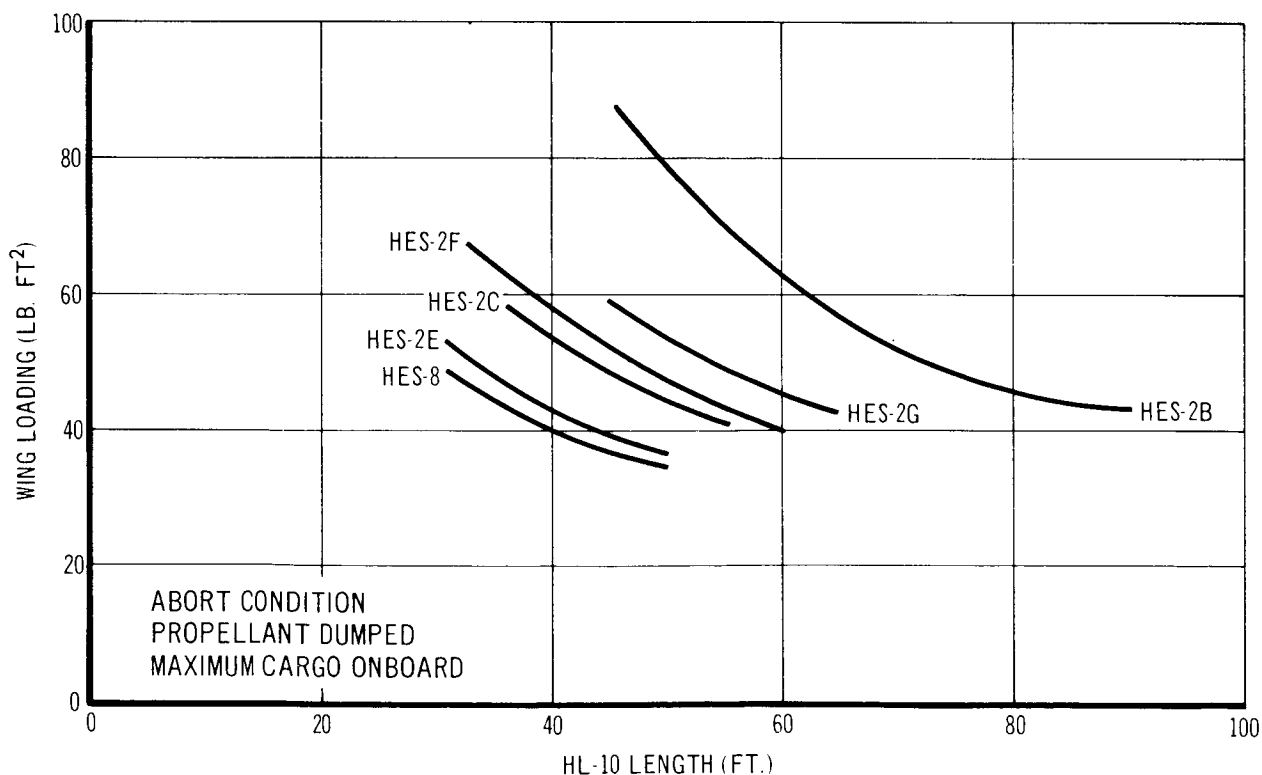

Figure 9-2 HL-10 Wing Loading as a Function of Vehicle Length

that the entire propellant tankage and pressurization system, and a major portion of the propellant distribution system, be replaced after each mission. The cost to the vehicle in terms of physical characteristics is reflected in the HES-2G arrangement.

After evaluation of steering and booster size requirements discussed in Sections 9.2 and 9.3, the HES-2G spacecraft was selected as the baseline concept because it represented the most mission flexibility, and therefore presented the broadest base on which to establish feasibility.

The final effort of the study was directed towards refining the HES-2G arrangement design, steering requirements and booster requirements. The resulting vehicle is described in Section 5 of this report.

9.2 STEERING ARRANGEMENTS

9.2.1 Recoverable Steering Engines

In keeping with the objective of maximum recoverability of steering system components, steering analysis of numerous booster-spacecraft combinations was accomplished in the final half of the study period. Installation of the steering engines on the HL-10 vehicle was common to all vehicle candidates. Section 9.1 set forth the physical characteristics of these vehicles. Table 9-3 presents the control system design requirements for each vehicle and the time during the boost trajectory which establishes the design criteria. To underscore the reasons for the selection of the HES-2G as the baseline concept, those qualities of the alternate vehicles which were deemed less desirable, or not feasible, are reviewed in the following paragraphs.

Characteristic of all vehicles under study was the peaking of the control thrust requirements at the end of the solid-propellant web burn time of each stage. This is perhaps more obbvious for upper stages where, because of the forward motion of the CG with flight time, the end of web burn time represents maximum and minimum lever arms for disturbing and control moments respectively. It is not so apparent during first stage operation where aerodynamic loads in the high dynamic pressure regimes impose significant control

| Configuration*	1st Stage Critical Parameter Values					
	Steer. Thrust Per Engine Lb. (Yaw)	Steer. Thrust Per Engine Lb. (Pitch)*	Flt. Time	l in.	b in.	δ_y(max) deg.
2A (1.2-0)						
2A (1.2-1)	69,400	33,900	B.O.	669	172	±30
2A (1.2-2)	55,700	30,000	B.O.	875	172	±30
2B (1.2-0)	58,300	29,800	B.O.	713	150	±30
2B (1.2-1)	58,000	30,700	B.O.	805	150	±30
2C (1.2-0)	38,300	20,300	B.O.	934	128	±30
2C (1.2-1)	43,200	23,600	B.O.	972	128	±30
2D (1.2-0)	52,500	26,700	B.O.	857	165	±30
2D (1.2-1)	56,500	30,100	B.O.	906	165	±30
2E (1.0-0)	24,500	13,100	B.O.	1132	106	±30
2F (1.0-0)	25,200	13,900	B.O.	1089	113	±30
2G (1.2-0.4-0)	47,300	29,200	B.O.	1763	144	±30

Notes:

*Based on δ_p(max) = ±45°

**Based on yaw steering thrust for indicated stage.

+Numbers in brackets designate booster configuration. For instance
is a 120% full-length 260-in. first stage motor and a 1 segment 156
stage motor. The HES-2G uses a .40 260-in. second stage motor a
segment 156-in. third stage motor.

REQUIREMENTS

δ_p(max) deg. **	Last Stage Critical Parameter Values						
	Steer. Thrust Lb. (Yaw)	Steer. Thrust Lb. (Pitch)*	Flt. Time	l in.	b in.	δ_y(max) deg.	δ_p(max) deg. **
	Control Reversal	Control Reversal					
±23	130,000	25,600	B.O.	97	172	±30	±10
±25	44,200	16,100	B.O.	220	172	±30	±17
±25	115,000	20,600	B.O.	76	150	±30	±10
±25	38,400	13,650	B.O.	191	150	±30	±17
±25	19,500	7,620	B.O.	193	128	±30	±19
±25	16,100	7,600	B.O.	318	128	±30	±22
±24	174,000	25,000	B.O.	64	165	±30	± 8
±25	41,900	14,200	B.O.	189	165	±30	±17
±26	5,750	3,100	B.O.	478	106	±30	±24
±25	7,650	4,050	B.O.	388	113	±30	±24
±27	33,106	18,200	B.O.	171	144	±30	±21

, (1.2-1)
-in. second
nd a zero
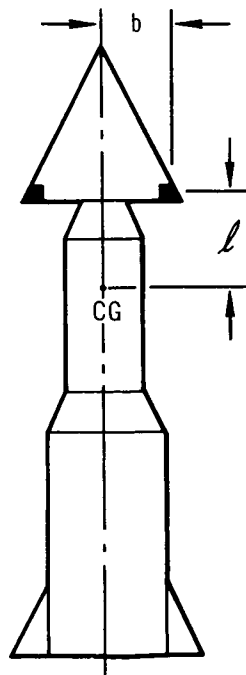
2# 172

moment requirements. However, it has been shown from work done on the baseline concept that changes in control lever arm and in the disturbing moments (associated with solid-motor thrust misalignment) between the high dynamic pressure period of flight and the end of web burn time result in nearly the same maximum demand for control thrust.

To appreciate the ramifications of the data of Table 9-3, reference is made to Figure 9-27 of Section 9.3.2.2 which illustrates the absence of any sensitivity of apogee velocity to 156-in. motor size for various payload weights. A first stage propellant loading of 4,000,000 lb. and a total payload of 100,000 lb. are representative of vehicles HES-2A through HES-2D. It is noted that essentially no performance is gained in going from a zero to a one-segment upper stage. On the contrary, this transition would result in an increase in total liftoff weight with no gain in payload. The advantages of larger 156-in. motors for these vehicles lies solely in the reduction they bring in last stage control thrust requirements which occur at the end of web burn time. Their associated burnout weights and increased lengths provide a more aft-positioned CG and, hence, a longer control lever.

HES-2A, for an optimal performance second stage (0 segment, 156-in. solid motor), develops control reversal during the second stage of boost. Since it was uncontrollable it was dropped from further consideration.

HES-2B requires an extremely high level of control thrust (115,000 lb.) at the end of web burn time of the zero-segment 156-in. motor.

HES-2C is readily controllable during all phases of flight for the optimally performing booster.

HES-2D requires an extremely high level of control thrust (174,000 lb.) at web burnout time of the zero-segment 156-in. motor.

HES-2E, which is the HES-8 (two stage) with recoverable steering engines, is easily controllable during all stages of booster flight.

The HES-2F, which is an HES-2E modified to carry 4,000 lb. of unpackaged cargo in the HL-10, is easily controllable during all stages of booster flight.

HES-2G is controllable with 50,000 lb. of thrust per engine. This is a feasible level of control thrust and requires no modification of the external lines of the HL-10.

9.2.2 Nonrecoverable Steering Engines

Before the midpoint of this study, an analysis of several vehicles employing nonrecoverable adapter-mounted steering engines was accomplished. The results of this investigation are representative of the objective of defining a minimum size HL-10. The only internal volume requirement was one of containing the crew and passengers. The result of this work was the HES-8 (two stage) vehicle shown in Figure 9-1. This configuration derived its steering control from four adapter mounted engines. Two engines were used for pitch, two for yaw, and all four for roll. All engines were gimballed ±30 degrees. The entire quantity of steering and in-orbit maneuvering propellants were carried in the adapter.

To assess the steering requirements for the HES-8, use was made of the digital simulation program described in Section 5.5.3.2. An analysis was performed to determine the influence of peak dynamic pressures on control thrust requirements. The motivation for this work stemmed from the slight increase in performance associated with shorter flight time (higher q) trajectories. Figures 9-3 and 9-4 indicate the minimum control thrust requirements per engine versus flight time for varying fin sizes (i.e., varying times of neutral aerodynamic stability). Figure 9-5 is a locus of maximum values at minimum control thrust as a function of neutral stability time for both low and high Q trajectories. It is seen that optimal fin sizing results in a per engine thrust requirement of 27,000 lb. and 44,500 lb. for trajectories having low and high dynamic pressure, respectively. Several reasons may be cited for favoring the lower dynamic pressure trajectory:

1. Higher dynamic pressures result in greater aerodynamic loads and therefore heavier vehicle structures. The resulting inert weight will tend to offset the higher performance associated with higher dynamic pressures.

2. Higher control thrust levels require that additional steering propellant and tankage weight be carried in the adapter. The effect of this weight increment is reduction in payload capability.
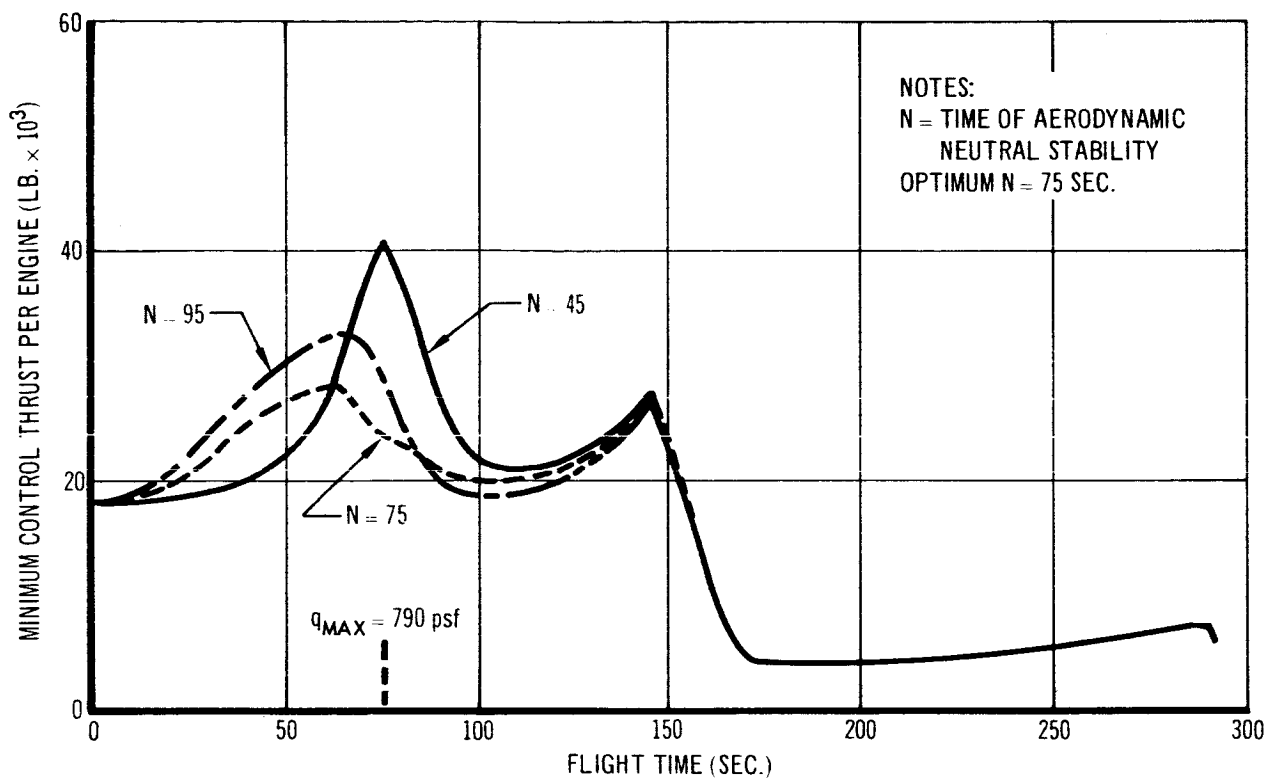
Figure 9-3 Minimum Control Thrust vs. Flight Time
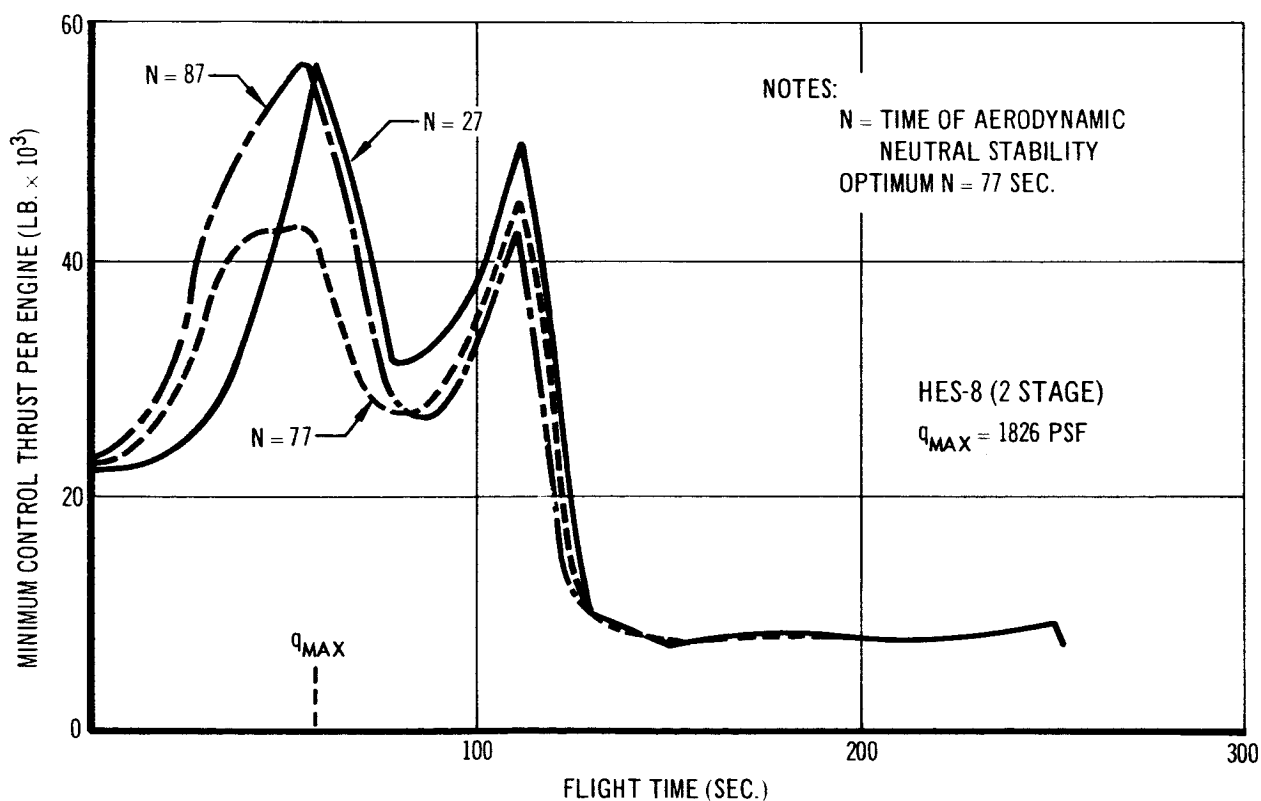HES-8 (2 STAGE) q_{MAX} = 790 PSF

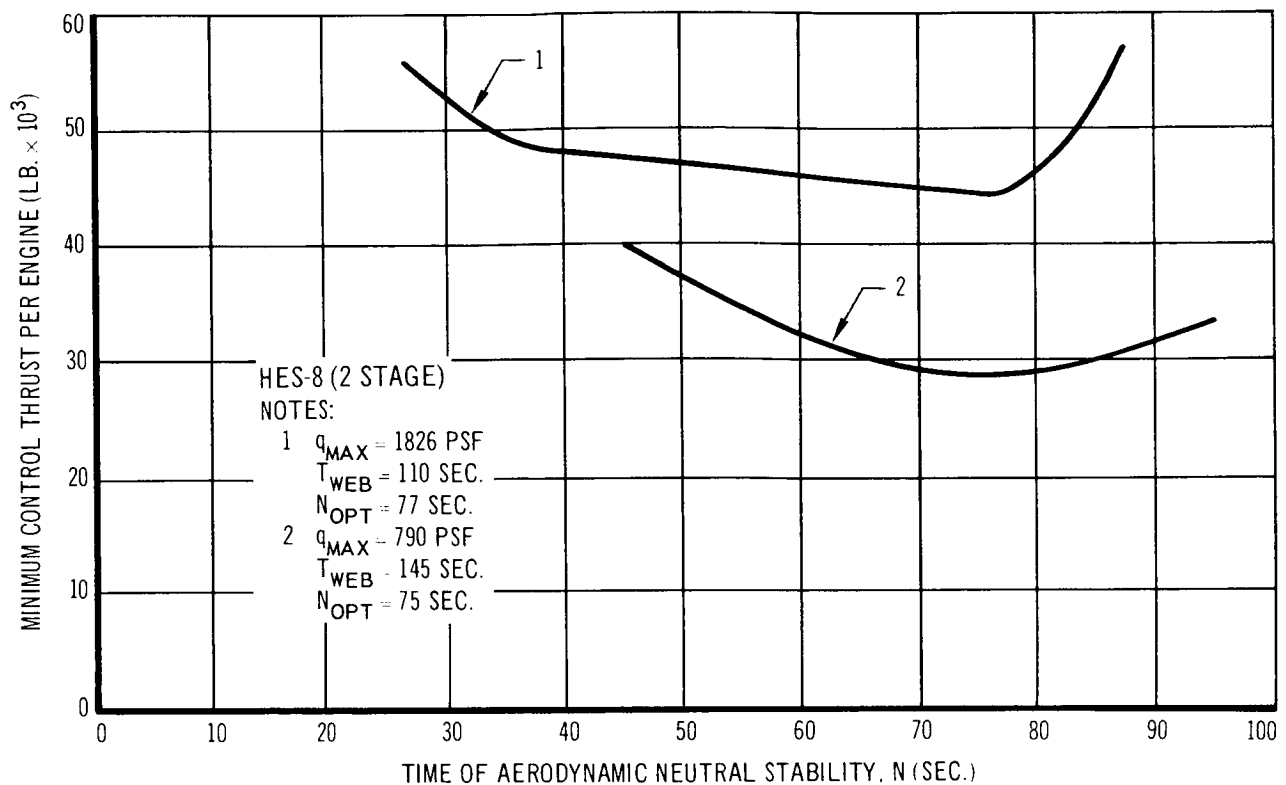**Figure 9-4 Minimum Control Thrust vs. Flight Time**

Figure 9-5 Minimum Control Thrust vs. Time of Aerodynamic Neutral Stability

3.   Higher dynamic pressures at first stage burnout impose a more severe control environment for separation.

The two stage HES-8 vehicle described above reflects a payload capability compatible with the maximum MORL mission. It was designed to carry propellants equivalent to 6,500 ft./sec. of in-orbit maneuvering velocity and 5,000 lb. of packaged cargo. Additional volume was carried in the forward adapter to permit up to 23,750 lb. total cargo capacity while maintaining a minimal impulsive velocity capability of 1,310 fps. Up to 11 passengers could be carried aboard the HL-10 for emergency evacuation.

A desire to examine the maximum impulsive velocity capability achievable within the guidelines of the study resulted in a modification of the HES-8. This modification incorporated a maximum amount of in-orbit maneuvering propellant consistent with a three stage solid-propellant motor configuration. This vehicle is capable of an impulsive velocity of 11,000 fps after achieving a 300-n.mi. circular orbit. Thrust demands versus flight time for several neutrally stable times are depicted for this vehicle in Figure 9-6. The
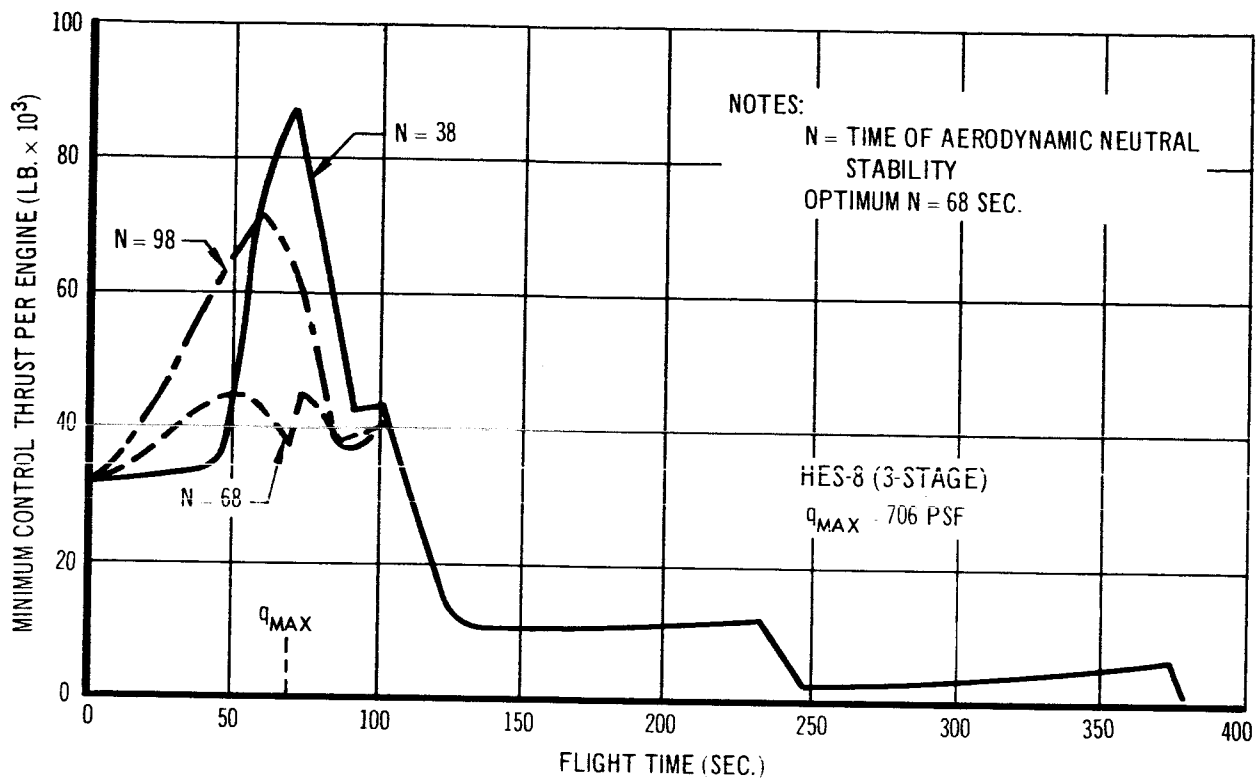
Figure 9-6 Minimum Control Thrust vs. Flight Time

corresponding locus of maximum thrust levels versus neutral stability time is seen in Figure 9-7. Optimal control thrust per engine of 46,000 lb. was the design point. Payload capability for this vehicle as well as all others analyzed in the study, reflect the influences of steering system weights.

9.2.3 Comparison of Recoverable and Nonrecoverable Steering Engines

The study has demonstrated head end steering feasibility regardless of steering engine placement (HL-10 or adapter) for a number of spacecraft arrangements. To more completely assess the many vehicles analyzed, it is desirable to group them together for an objective evaluation of their individual and relative merits. The HES-8 (adapter mounted steering engines) and HES-2A through HES-2G (HL-10 mounted steering engines) represent two design concepts based on the importance of recoverability. It can be argued that in addition to recoverability, the larger, control-engine-carrying HL-10 offers more versatility of payload and mission within a given lifting body. Retention of steering engines and maneuvering propellant within the HL-10 allows for low-altitude reconnaissance missions where atmospheric
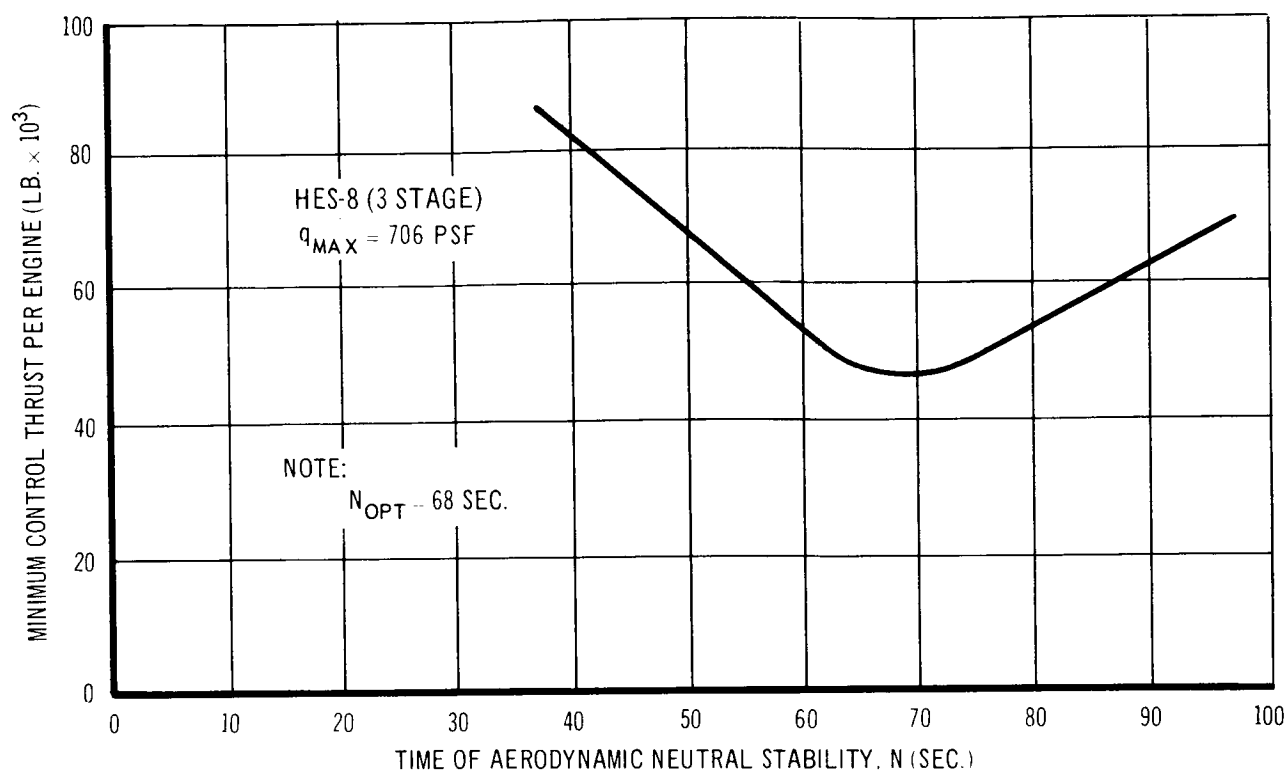
Figure 9-7 Minimum Control Thrust vs. Time of Aerodynamic Neutral Stability

maneuvering considerations would preclude the use of the aft adapters. Installation of steering engines on the HL-10 also permits their use for maneuvering during abort situations, and possibly during normal re-entry and landing phases. On the other hand, the ramifications of HL-10 structural weight penalties associated with insulation requirements and limitations on wing loading should be weighed against the HES-8 concept which houses major portions of the payload, (e.g., maneuvering propellant) more efficiently in an aft adapter.

Table 9-4 presents a summary of important characteristics relative to performance, steering, and recoverability of all booster-spacecraft candidates. To set the steering systems in proper perspective, booster arrangements given in Table 9-4 reflect last stage sizing based on desired performance rather than on steering thrust considerations.

STEERING CHARACTERISTICS

Configuration*	$q_{max.}$ (psf)	No. of Control Engines Reqd.	Min. Vac. Control Thrust Per Engine (lb.)	Critical Control Time	T (d
HES-2A(1.2-0)	810	2	Control Reversal (Uncontrollable)	B.O. of 2nd Stg.	
HES-2B(1.2-0)	810	2	115,000	B.O. of 2nd Stg.	
HES-2C(1.2-0)	810	2	38,300	B.O. of 1st Stg.	
HES-2D(1.2-0)	810	2	174,000	B.O. of 2nd Stg.	
HES-2E(1.0-0)	790	2	24,500	B.O. of 1st Stg.	
HES-2F(1.0-0)	790	2	25,200	B.O. of 1st Stg.	
HES-2G(1.2-0.4-0)	723	2	47,300	T_o + 73 sec.	
HES-8(1.0-0)	790	4	28,000	B.O. of 1st Stg.	
HES-8(1.0-0)	1826	4	44,500	B.O. of 1st Stg.	
HES-8(1.0-0.4-0)	706	4	46,000	T_o + 50 sec.	

*First and middle number refer to fractions of full-length 260-in.-dia motor in last stage; order of numbers indicates stage

**Payload exceeds large solid motor capability

, # 179

F HES CANDIDATE VEHICLES

ximum ntrol ngine ow Rate ./sec.)	ΔV Remaining to Cir. at 300 n.mi. (fps)	Pitch Stab. Fin Area Per Pair (sq./ft.)	Yaw Stab. Fin Area Per Pair (sq./ft.)	Steering System Components Recovered
.C.	**	N.C.	N.C.	Steer. engines, tank-age, and electronics
.C.	2,685	N.C.	N.C.	Steer. engines and electronics
.C.	1,435	N.C.	N.C.	Steer. engines and electronics
.C.	**	N.C.	N.C.	Steer. engines, tank-age, and electronics
.C.	885	180	147	Steer. engines and electronics
.C.	1,185	180	147	Steer. engines and electronics
2	605	197	151	Steer. engines and electronics
1	1,335	180	147	---
9	413	144	117	---
0	659	144	116	---

.C. = Not Computed

notor; last number indicates number of segments of 156-in.-dia.

2# 179

9.2.4   Alternate Steering Techniques

Several steering techniques, in addition to the chosen proportional control, were analyzed and found not to be feasible for booster control. The following sections report the work accomplished in this study on these alternate modes.

9.2.4.1   On-Off (bang-bang) Control

The use of on-off control would require control thrust levels per engine approximately equal to those of the proportional systems. This can be visualized by the fact that the mechanical advantage associated with engines mounted with their thrust lines normal to the vehicle centerline are offset by the constraint of using only one engine per axis at any given time. Furthermore, an environment of large disturbing moments will result in an unsymmetrical limit cycle, thereby pulsing one engine much more often than the other in a given vehicle axis. Associated duty cycles would be severe. A further argument against such systems in that they are nonsupportive of booster performance as opposed to proportional control. The latter, having a significant supporting component of control thrust, virtually carries the steering propellant without imposing an associated payload penalty. Further consideration of these high thrust (approximately 50,000 lb.) engines in such a bang-bang mode was not pursued.

9.2.4.2   Spin Stabilization

An investigation of the use of spin stabilization during a portion or all of the powered boost trajectory was made during the study. Its purpose was to establish whether or not a reduction in steering thrust and/or steering propellant could be realized. The analysis was divided into two sections; (1) the use of spin stabilization during first stage to reduce steering thrust and propellant and to offset the disturbing moments from solid motor thrust misalignment, thrust eccentricity, and aerodynamics, and (2) the use of spin stabilization during second stage to conserve steering propellant. The HES-8 two stage vehicle was used in this analysis.

In the examination of the spin stabilization techniques, biotechnology considerations place an upper limit to the spin rate of about 30 rpm. Figure 9-8
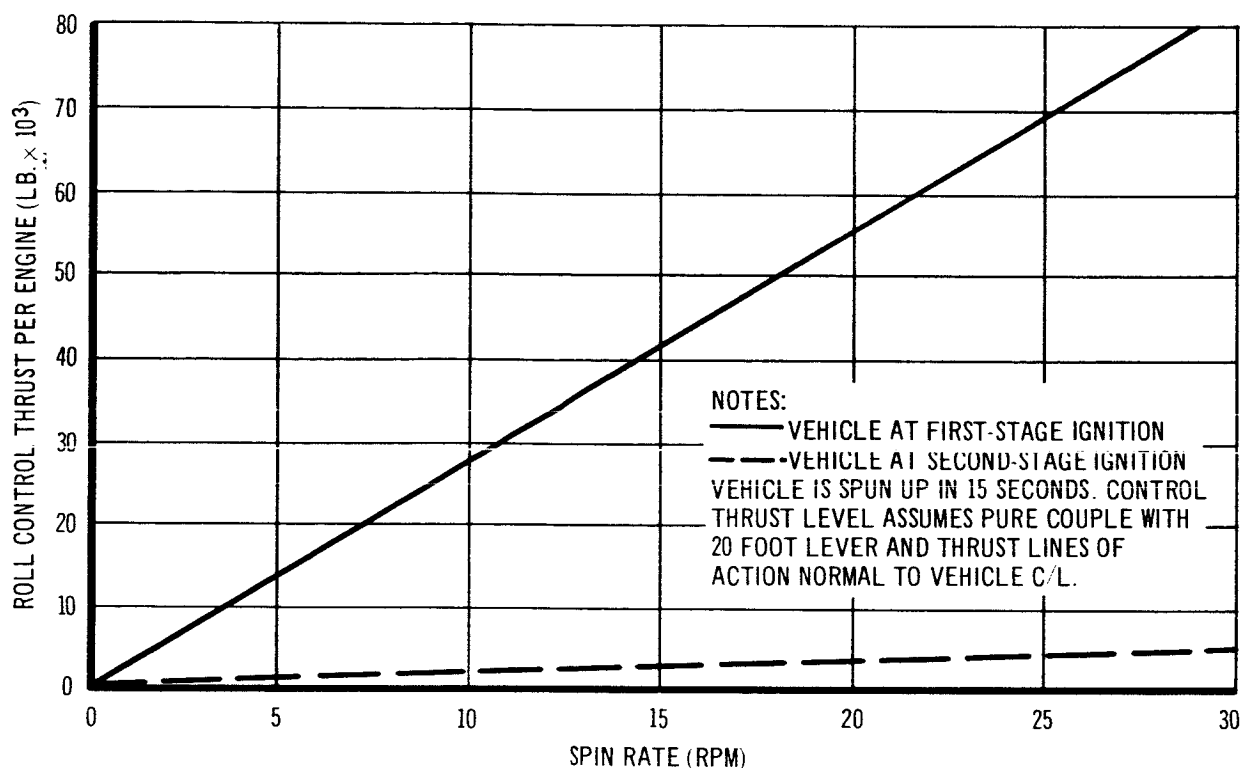
Figure 9-8 Roll Control Thrust Required to Spin Up Baseline Vehicle

presents the thrust level required per engine to spin up to rates of 30 rpm and 10 rpm in 15 sec. The requirement for the 30-rpm case is 80, 000 lb. of thrust per engine. This exceeds the thrust requirements for a proportionally guided system.

Figure 9-9 presents the vehicle coning angles resulting from the thrust misalignement and eccentricity characteristics of the first stage 260-in. solid motor. The precession angles resulting from aerodynamic disturbances caused by 95 percentile side winds are shown in Figure 9-10. These data show that both the coning and the precession angles are unacceptably large, and that spin stabilization during the first stage is impractical.

Figure 9-11 illustrates the coning angles resulting from a spun-up second stage. Since it was not obvious that 30-rpm dispersions could not be tolerated, they were superimposed on a second stage nominal trajectory so that trajectory performance could be evaluated. Results of a tradeoff analysis of the impulsive velocity required to cancel out the dispersions and of the impulsive
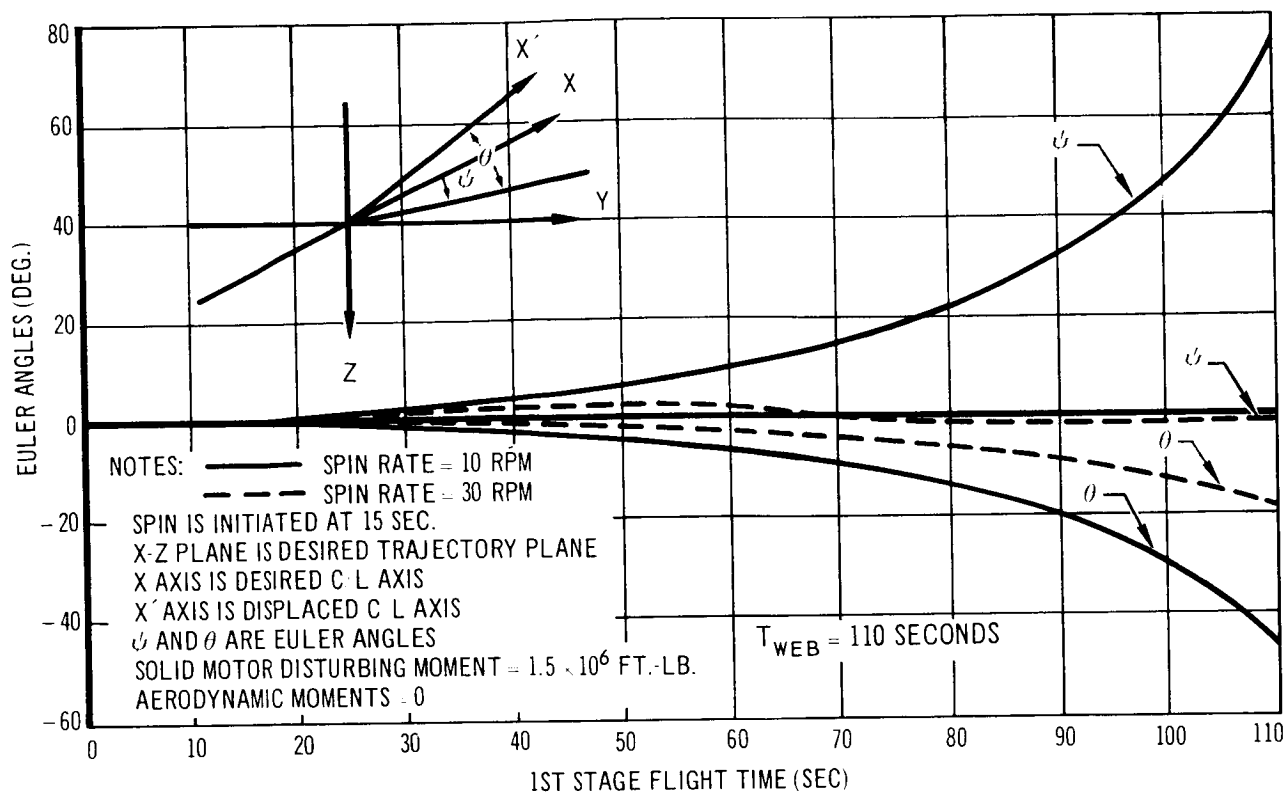
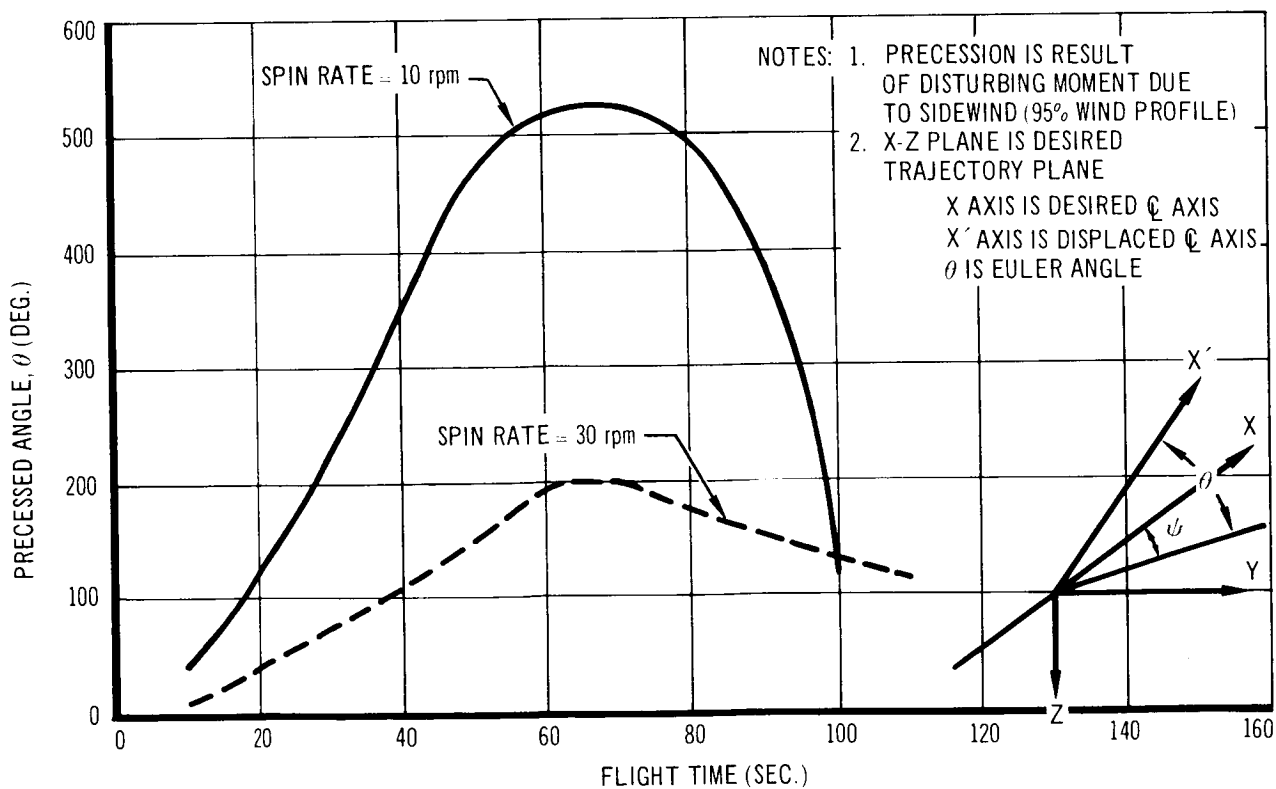Figure 9-9 Two-Stage HES-8 Vehicle Coning Angle vs. Flight Time (First-Stage)

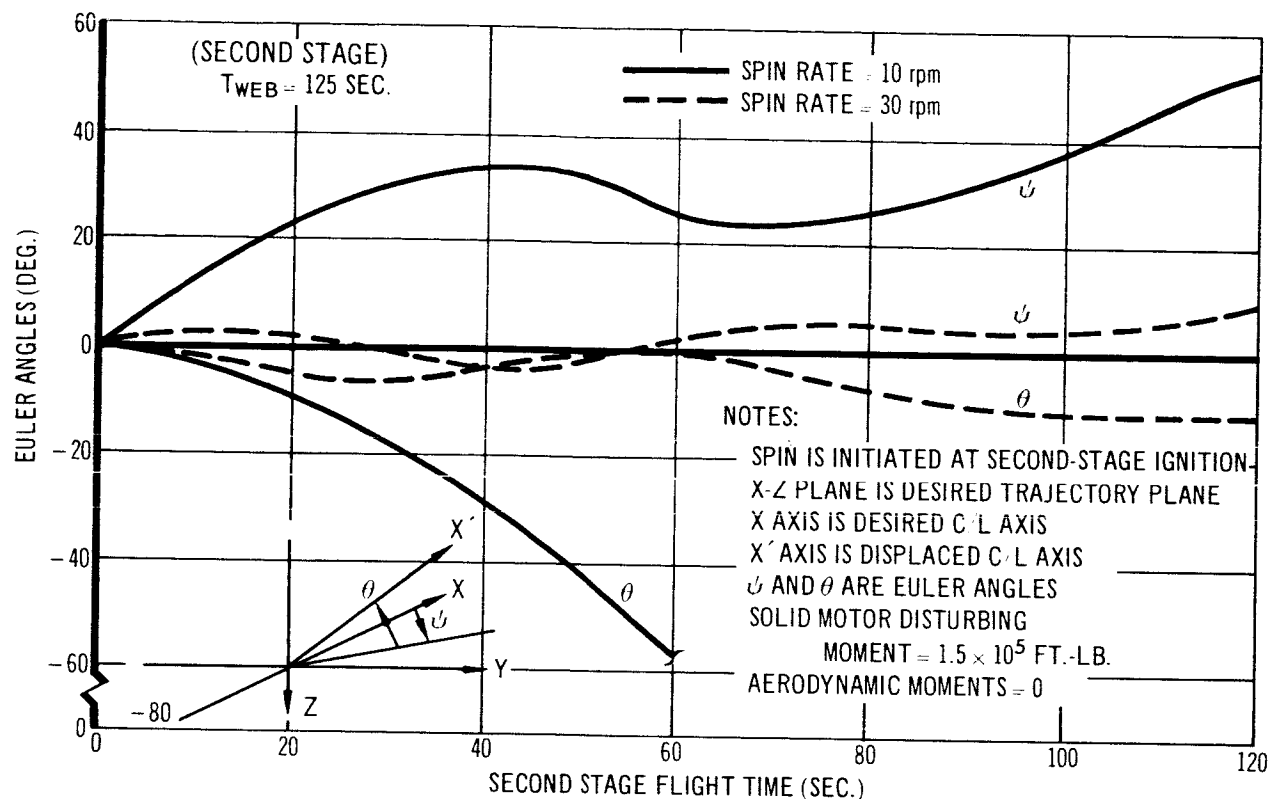Figure 9-10 Precessed Angle vs. Flight Time

$T_{WEB} = 110$

182

Figure 9-11 Coning Angle vs. Flight Time

velocity benefit gained by reduced steering propellant tankage weight show that there is no appreciable advantage in using spin stabilization over proportional control. Because of the inherent complication caused by spinning, this technique was dropped from further consideration.

9.2.4.3 Weathercocking

The objective of this analysis was to determine if a significant savings in steering propellant could be realized by shutting down the steering engines and assuming a weathercock mode of flight during the first stage of boost. Again, the HES-8 vehicle was chosen for investigation.

The highest possible thrust-to-weight ratio at liftoff was used (T/W = 2.0) and a weathercock mode was initiated at 20 sec. Peak thrust-to-weight was limited by the minimum web burn time capability of the 260-in. full length motor. The purpose in flying this high thrust trajectory was to shorten the time over which weathercocking was used, and to reduce the excursions in vehicle attitude necessary to follow the relative wind vector. Both factors

tend to constrain trajectory deviations. Table 9-5 illustrates the trajectory parameters for both weathercock and nonweathercock modes. It is noted that at first stage burnout (85 sec.) a severe dynamic pressure level exists which will render the correcting of trajectory dispersions impossible. It would be necessary to continue flying the weathercock mode throughout second stage boost. The results of this inability to maneuver away from a weathercock mode during second stage operation are noted in Table 9-5. At second stage burnout (218 sec.), the vehicle flight path angle is -65.8° with a dynamic pressure of 7,637 lb./sq.ft., a condition which could not be tolerated. It was concluded that the use of a weathercock flight mode for the stated objective, at least, was not practical. But this does not prevent the use of weathercock modes for other than the stated objective. An additional use, not investigated in this study, would be for aerodynamic load relief in the high dynamic pressure regions of flight. In this case, a reduction in vehicle structural weight might be realized. Follow-on work in this area is needed to develop the full potentialities of weathercocking.

Table 9-5

WEATHERCOCK TRAJECTORY DATA

Flight Time (sec.)	Without Weathercock Conditions				With Weathercock Conditions			
	q (psf)	γ (deg.)	V (fps)	Alt. (ft.)	q (psf)	γ (deg.)	V (fps)	Alt. (ft.)
20	681	52.5	834	6,601	769	52.5	834	6,601
25	1,116	46.5	1,131	10,318	1,269	44.7	1,125	10,251
30	1,589	41.4	1,449	14,772	1,846	38.2	1,442	14,472
35	2,068	37.0	1,799	19,882	2,468	32.8	1,792	19,141
40	2,507	33.3	2,188	25,598	3,092	28.2	2,180	24,156
45	2,863	30.1	2,621	31,891	3,678	24.4	2,609	29,437
50	3,017	27.4	3,105	38,748	4,150	21.1	3,081	34,911
55	2,923	25.0	3,651	46,173	4,298	18.3	3,603	40,527
60	2,722	22.9	4,268	54,190	4,328	16.0	4,186	46,250
70	2,119	19.7	5,794	72,229	4,138	12.3	5,605	57,991
80	1,372	17.4	7,912	93,702	4,004	9.7	7,526	70,309
85	819	16.3	8,661	108,197	3,177	8.5	8,104	77,804
218	0	11.5	21,837	444,000	7,637	65.8	4,157	30,400

Notes:

1. T_{web} (first stage) = 85 sec.
2. Vehicle is weathercocked from 20 sec. to 85 sec.
3. Power boost flight time is 218 sec.
4. T/W (L.O.) = 2.0
5. q = Dynamic pressure
6. γ = Flight path angle
7. V = Velocity

*Reflects relative wind effects

9.3 LAUNCH VEHICLE CONFIGURATIONS

9.3.1 Booster Motor Characteristics

Parametric information was generated for both 260-in. and 156-in. solid-propellant motors. The same assumptions used in determining the performance of the selected booster, Section 5.3, were used to generate these curves. They are shown in Figures 9-12 to 9-19. These curves show motor length, average web vacuum thrust, and motor mass fraction versus propellant weight for various nozzle expansion ratios and web burn times.

The 260-in.-dia. motor data are shown for expansion ratios of 10 and 20 and for a web burn time range between 90 and 120 sec. The slight discontinuities which are noted in the curves occur when the nozzle exit diameter reached 260 in. For propellant weights beyond the point of discontinuity, the nozzle exit diameter is restricted to 260 in., which results in a corresponding reduction in expansion ratio. It is noted that the mass fraction curves reach a maximum for the 260-in. motor. To the left of the point of maximum mass fraction, the dome structure weight has a predominate effect over the more efficient cylindrical section. To the right of the maximum point, the dome effects are no longer predominant. The cross-sectional loading, however, because of the large port areas required for the longer motors, reduces the propellant loading and consequently reduces the mass fraction.

The curves for the 156-in.-dia. motor are shown for an expansion ratio of 25, and for the appropriate range of propellant weight. No discontinuity occurs in these curves because the nozzle exit diameters do not reach the maximum allowable of 260 in., and consequently the expansion ratio is never restricted. The curves do not show a variation of length with expansion ratio. The nozzle, which has a truncated bell exit cone, is assumed to have a constant length-to-throat radius ratio, and consequently the nozzle length or motor length does not vary with expansion ratio.

The design points for the motors selected for the HES-2G vehicle are shown on the appropriate curves.
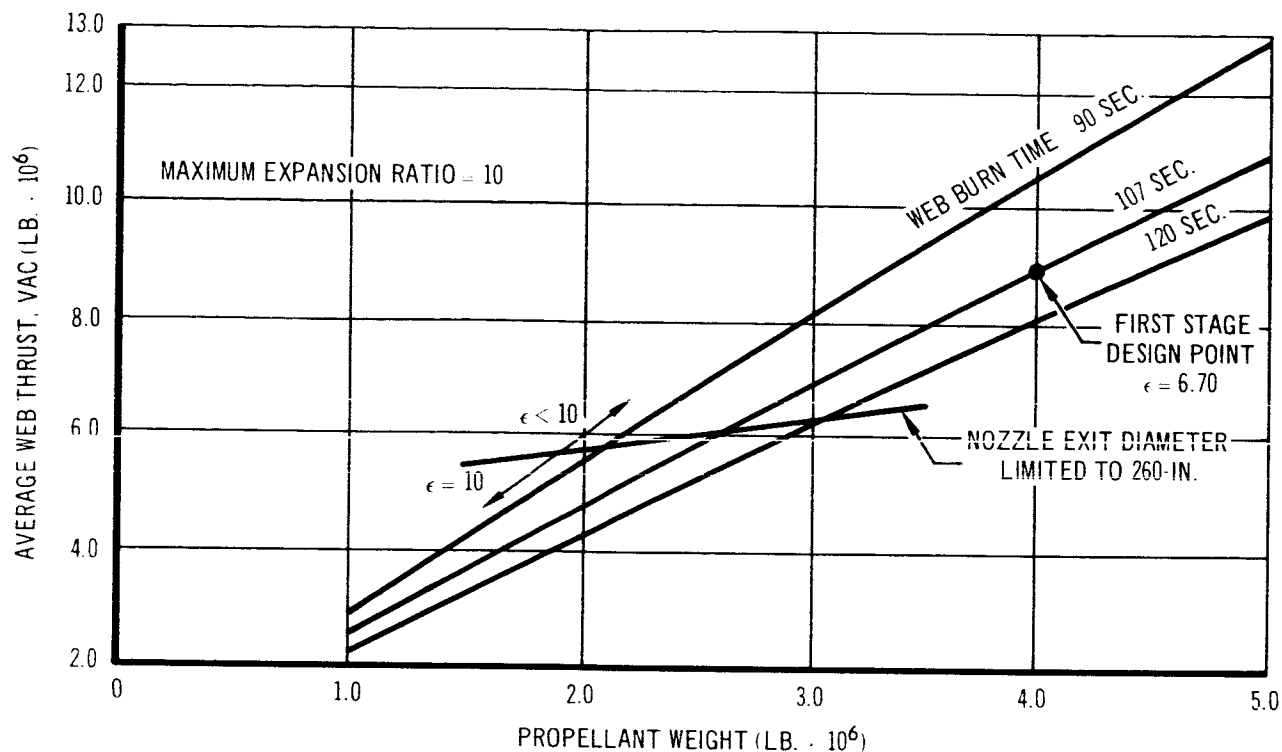
Figure 9-12 Average Web Thrust at Vacuum vs. Propellant Weight
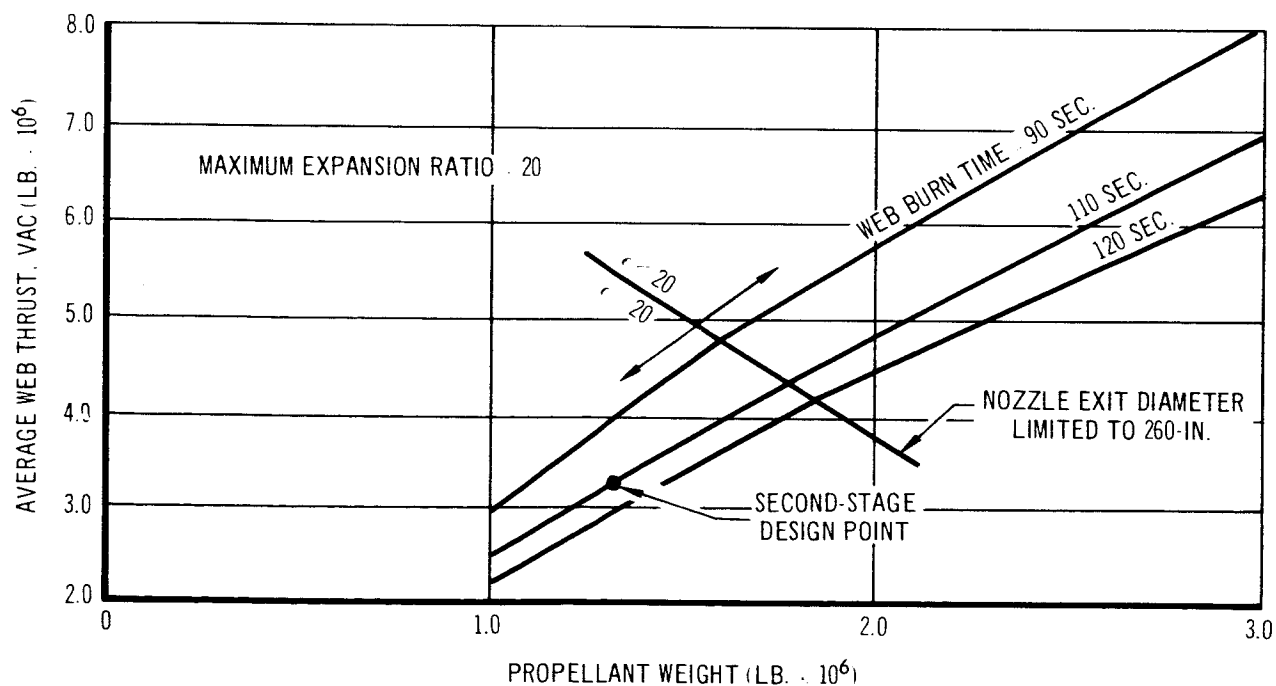260-IN. SOLID PROPELLANT MOTOR

Figure 9-13 Average Web Thrust at Vacuum vs. Propellant Weight
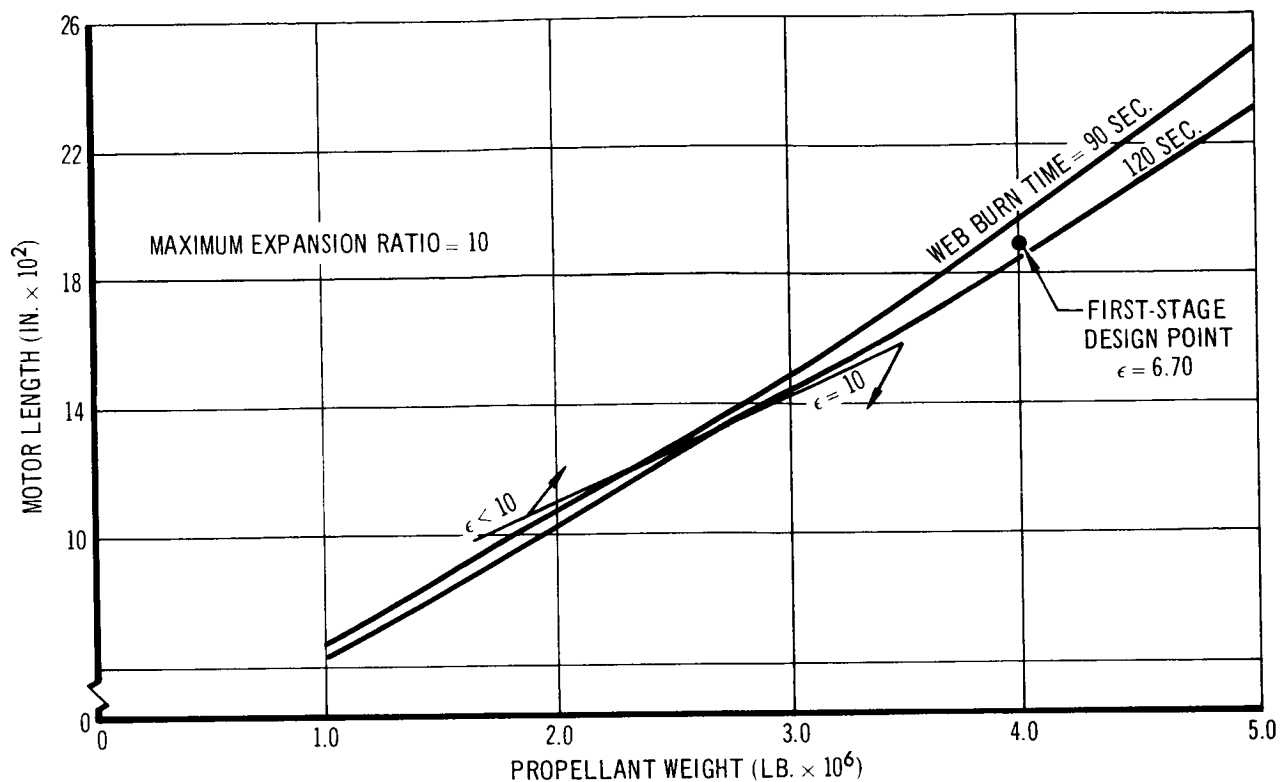260-IN. SOLID PROPELLANT MOTOR

Figure 9-14 Motor Length vs. Propellant Weight
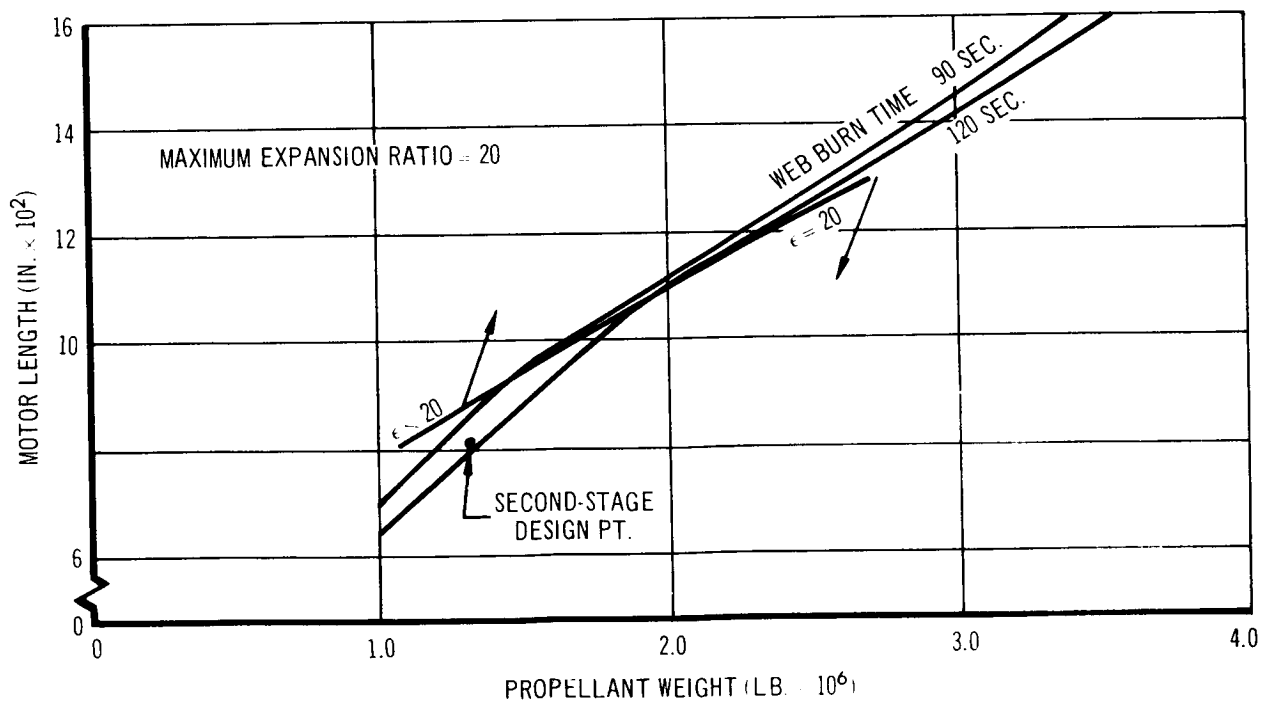260-IN. SOLID PROPELLANT MOTOR

Figure 9-15 Motor Length vs. Propellant Weight
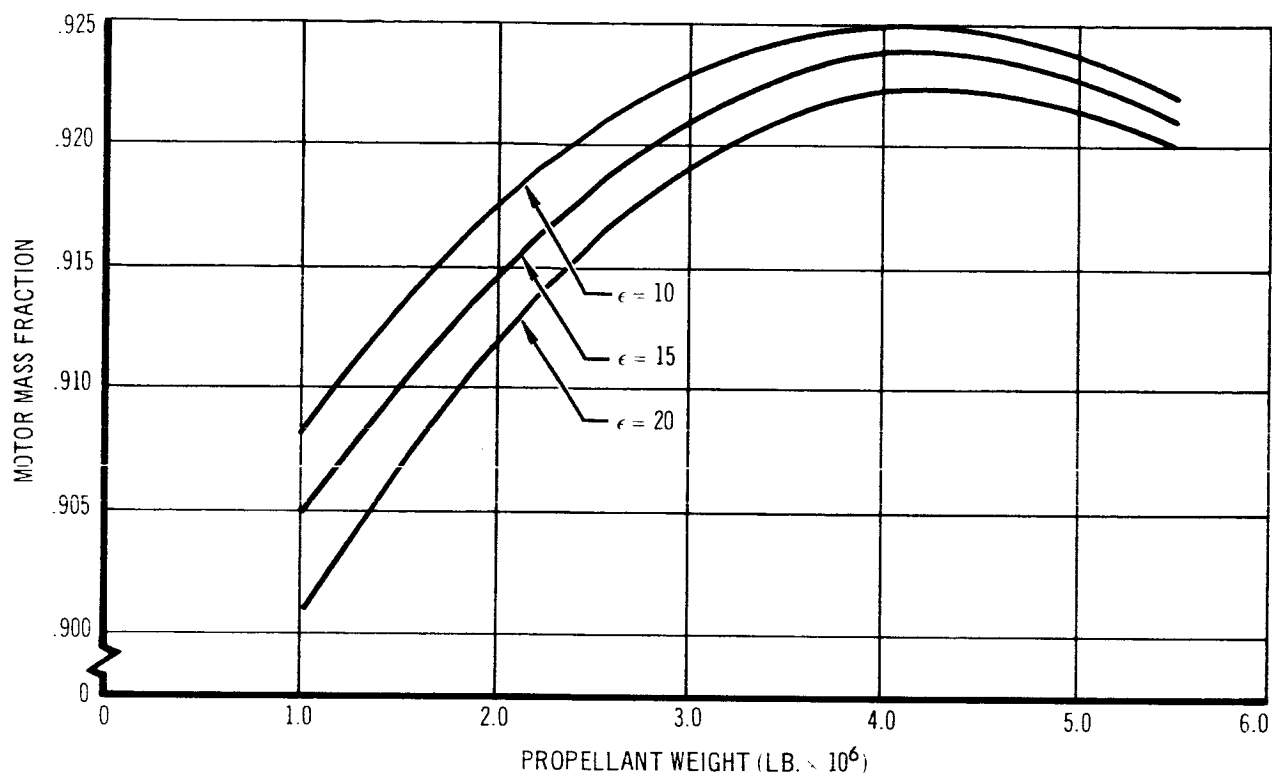260 IN. SOLID PROPELLANT MOTOR

Figure 9-16 Motor Mass Fraction vs. Propellant Weight
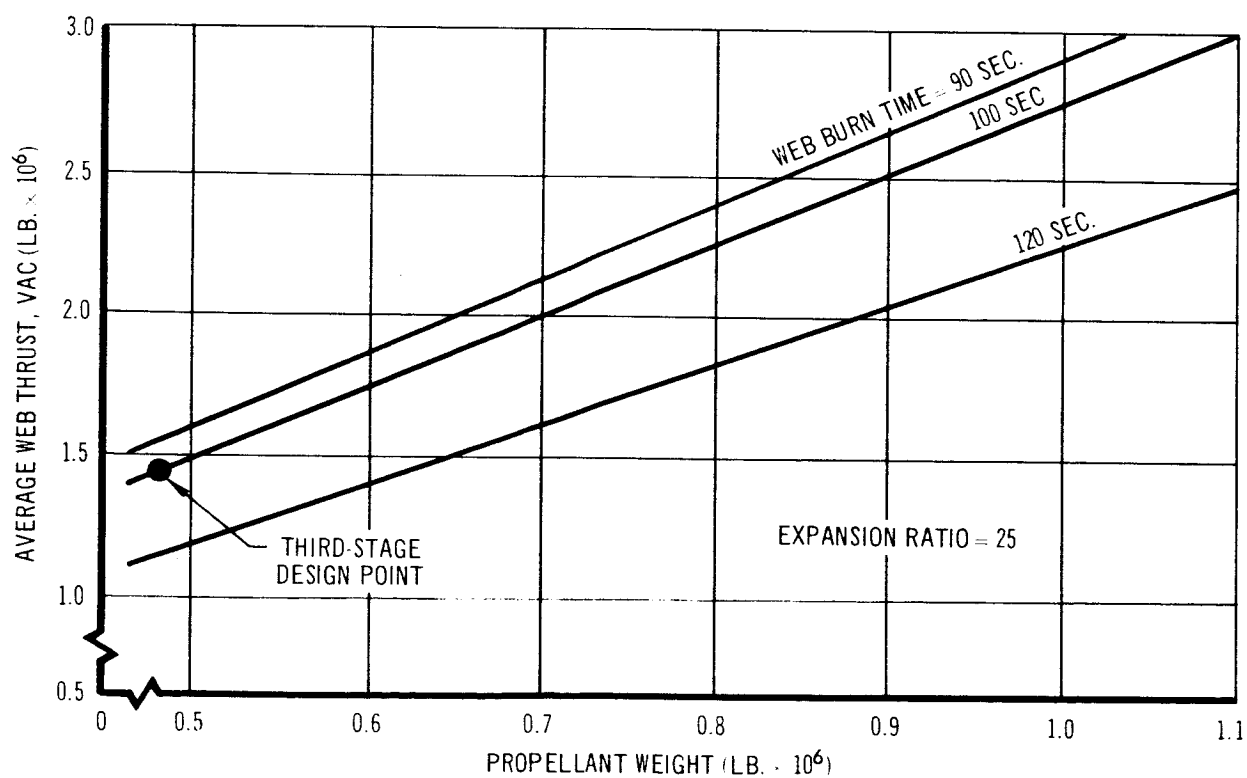260-IN. SOLID PROPELLANT MOTOR

Figure 9-17 Average Web Thrust at Vacuum vs. Propellant Weight
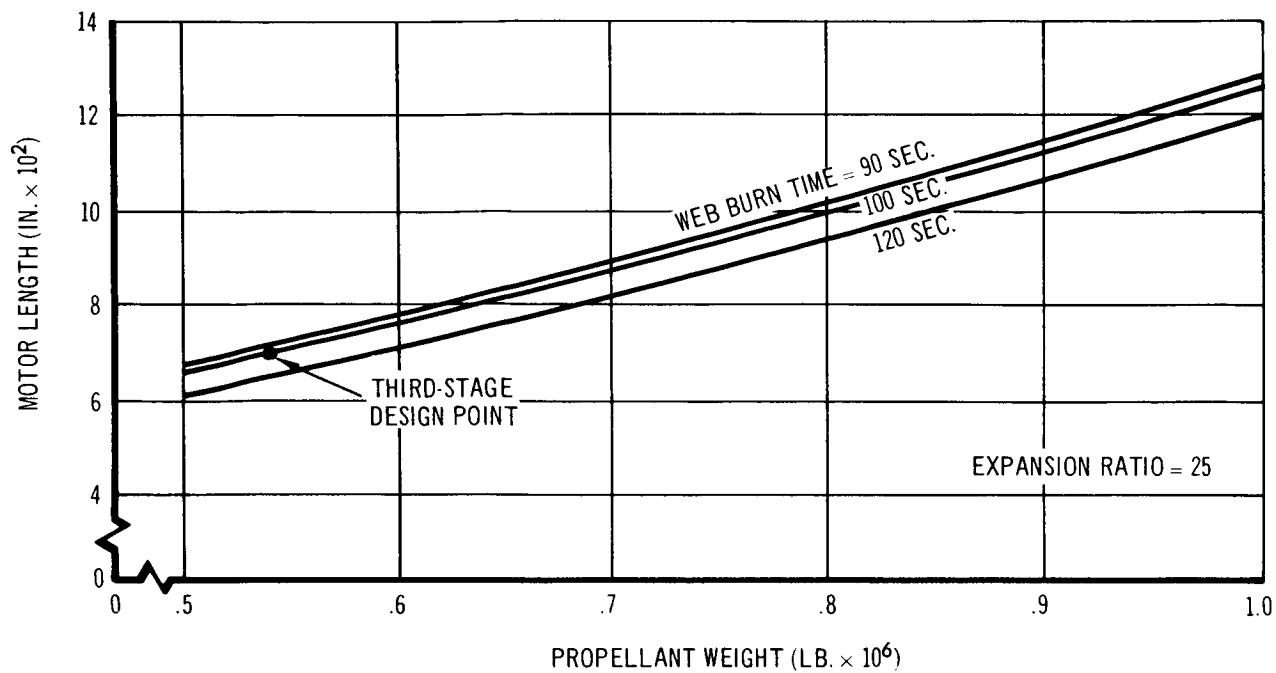156-IN. MONOLITHIC SOLID PROPELLANT MOTOR

Figure 9-18 Motor Length vs. Propellant Weight
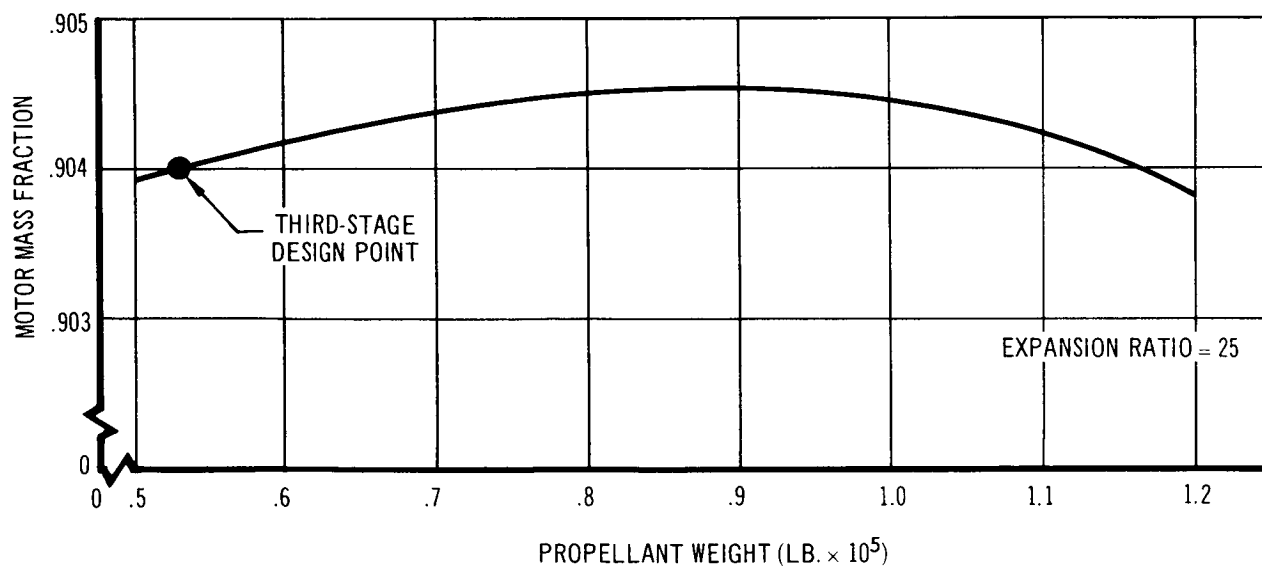156-IN. MONOLITHIC SOLID PROPELLANT MOTOR

Figure 9-19 Motor Mass Fraction vs. Propellant Weight
156-IN. MONOLITHIC SOLID PROPELLANT MOTOR

9.3.2 Launch Vehicle Sizing

9.3.2.1 General Considerations

The trajectory work leading to the selection of the final launch vehicle for the HES-2G arrangement was performed on an IBM 7094 high-speed digital computer. The program used to generate these trajectories solves the three dimensional equations of motion. It includes aero-dynamic forces in the trajectory calculations, and simulates the Earth with a rotating oblate spheriod. The program uses the 1959 Arnold Research and Development Command (ARDC) atmosphere. All the trajectories are flown from Cape Kennedy on a launch azimuth of 90° and shortly after liftoff begin a gravity turn (zero angle-of-attack) pitch program which lasts to final stage burnout. There is then a coast period to an apogee altitude of 300 n. mi. above the Earth's surface.

Since the launch vehicles are flying at zero angle-of-attack, the only aero-dynamic force considered was drag. The drag coefficient versus Mach number curve shown in Figure 9-20 was used on all the trajectories for this study. This curve was obtained for the subsonic range by adding the drag coefficient of the HL-10 to the skin friction drag coefficient of the launch vehicle. In the supersonic range, wind tunnel drag data based on the Saturn booster plus the HL-10, was corrected for the difference in skin friction and wave drag contribution of the subject study vehicle.

The thrust-to-weight ratio at liftoff, which determines the acceleration history of a particular vehicle, has a strong influence on the maximum dynamic pressure. The dynamic pressure in turn has an appreciable effect on the head-end steering requirements through the aerodynamic moments. In order to keep the maximum dynamic pressure within limits that could be handled by a feasible steering system, the thrust-to-weight ratio at liftoff was limited to 1.25.

The possible burn times of the solid-propellant steps used in the various launch vehicles varied over a broad range. Except for the first stage, the selection of the burn times were generally influenced by three factors:
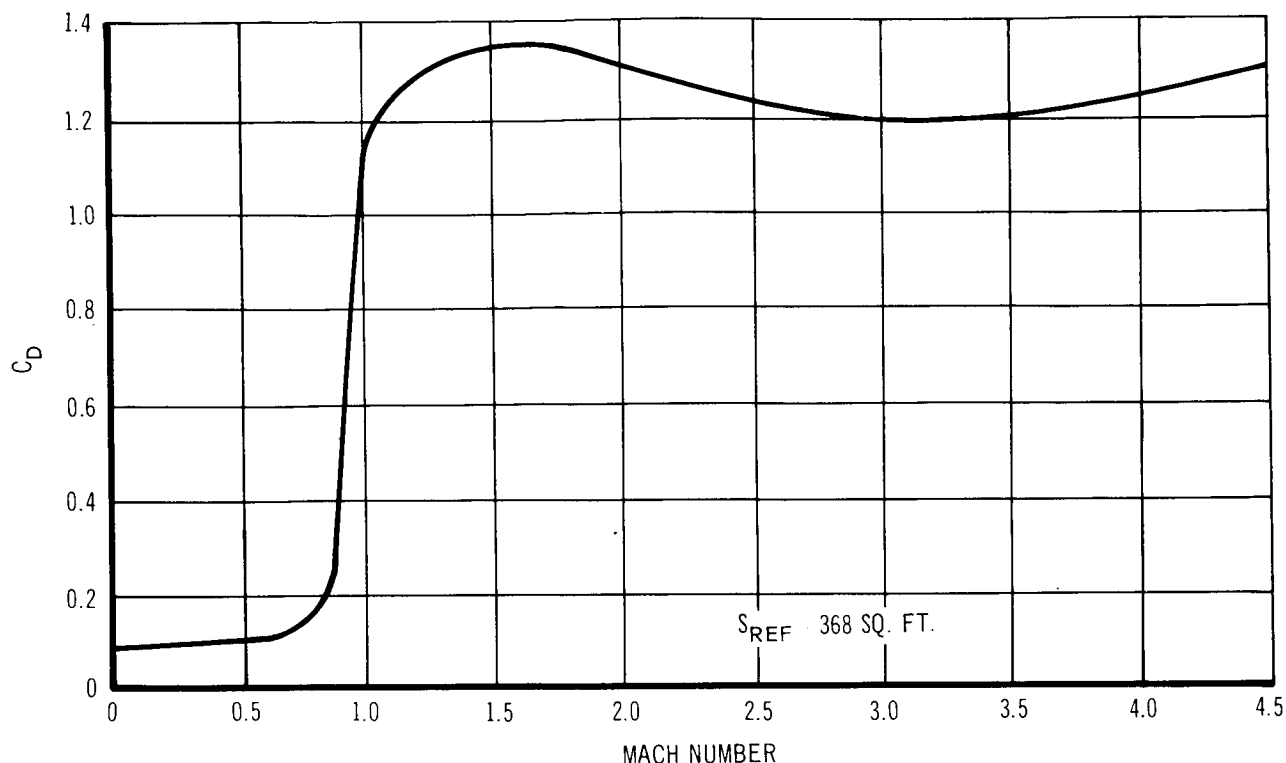
Figure 9-20 Total Vehicle Drag vs. Mach Number

1. Minimization of steering propellant by employing short burn times.
2. Reduction of burnout acceleration by long burn times and low thrust.
3. Use of burn times that were within the propellant capability.

The first stage burn time was always selected to give a thrust-to-weight ratio at liftoff, of 1.25.

9.3.2.2 Effect of Number of Launch Vehicle Stages

The selection of a three stage configuration for the launch vehicle for the HES-2G arrangement was based on work done on both three stage and two stage vehicles. The selection was based on the requirement to carry a 100,000 lb. payload to an apogee altitude of 300 n.mi. with an apogee velocity of 24,500 ft./sec.

The three stage vehicles used in the initial selection were composed of a full length 260-in. first stage, a variable length 260-in. second stage, and a zero-segment 156-in. third stage. The payload capabilities of these boosters to a 300-n.mi. apogee altitude were determined and are presented in Figures 9-21
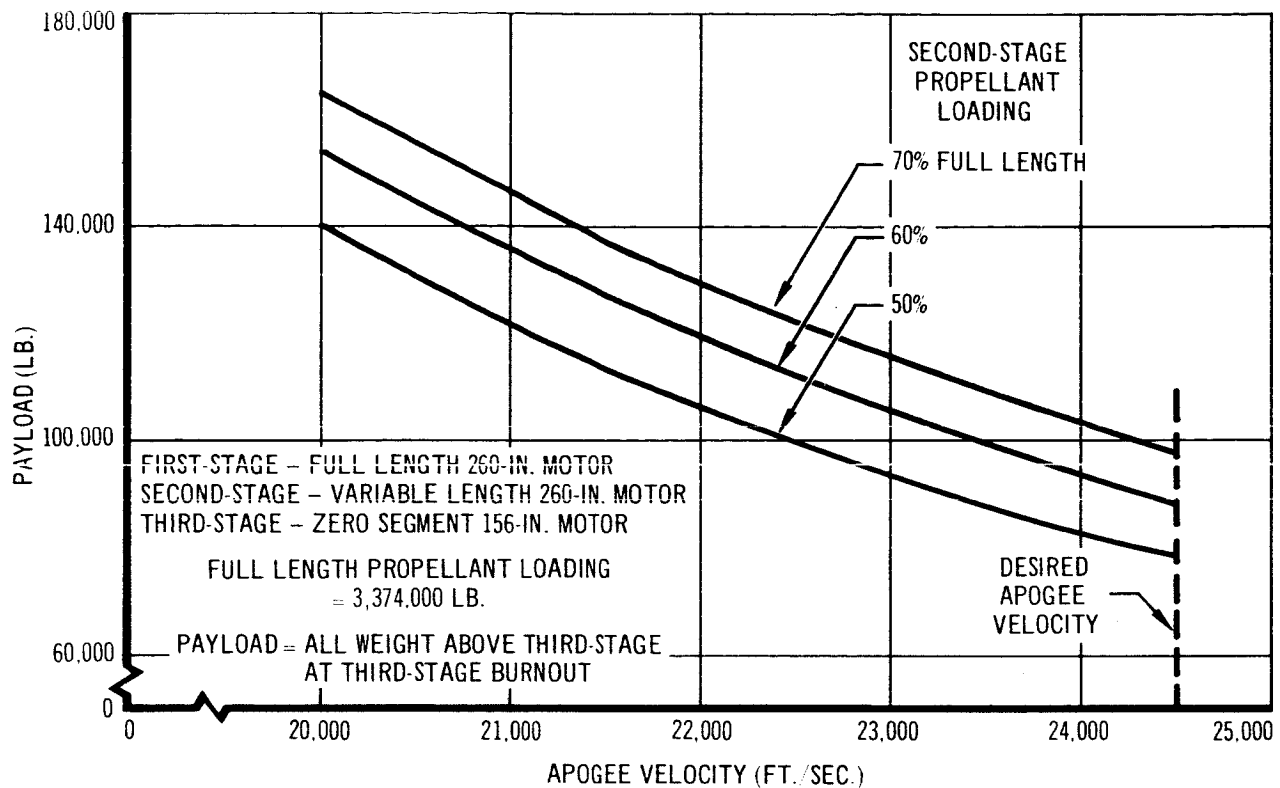
Figure 9-21 Payload vs. Apogee Velocity at 300 n. mi. – Three-Stage Vehicle

and 9-22. The trajectories for these vehicles were based on preliminary
estimates for steering system characteristics and for fin and interstage
weights. The primary purpose of these trajectories was to get a reasonable
approximation of the apogee velocity and booster size requirements as a
function of payload weight. In order to simplify the comparison of the three
stage vehicle with the two stage vehicle, only the second stage propellant
loading of the three stage vehicle was varied. It is interesting to note (see
Figure 9-22) that the maximum payload capability for this booster occurs
when the second stage consists of a 260-in. motor with about 1,350,000 lb.
of propellant (40% of full length).

The two stage launch vehicles consisted of a variable length 260-in.-dia.
first stage with 0-, 1-, and 2-segment 156-in.-dia. second stages. The pay-
load capabilities for the two stage vehicles are presented in Figures 9-23
through 9-25. Cross-plots of these data for first stage propellant loadings
of 3,000,000 lb., 4,000,000 lb., and 5,000,000 lb. are shown in Figures
9-26, 9-27, and 9-28. A comparison of the data in Figures 9-26 through
9-28 reveals that little payload benefits accrue from the use of larger
propellant loadings in the second stage when first stage propellant loadings
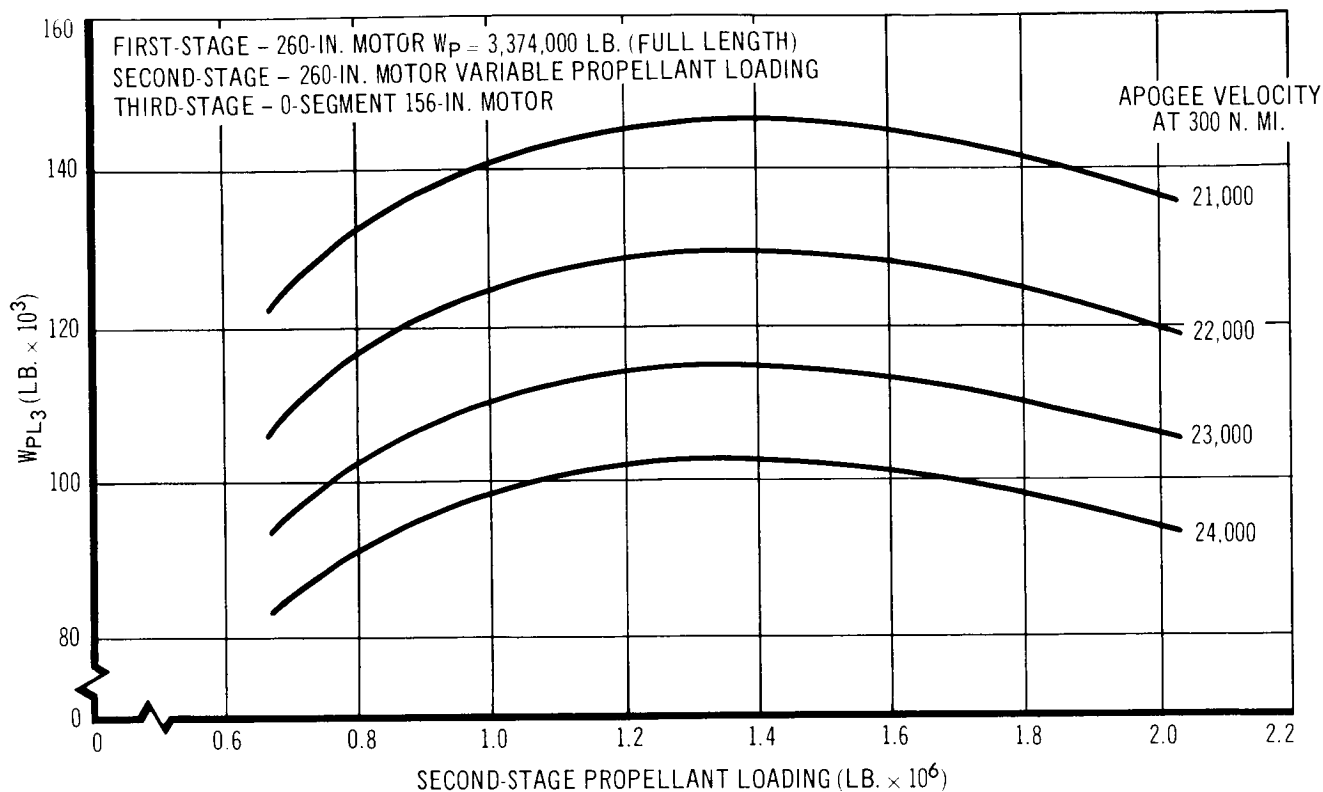
Figure 9-22 Payload vs. Second-Stage Propellant Loading – Three-Stage Vehicle

Figure 9-23 Payload vs. Apogee Velocity at 300 n. mi.– Two-Stage Vehicle
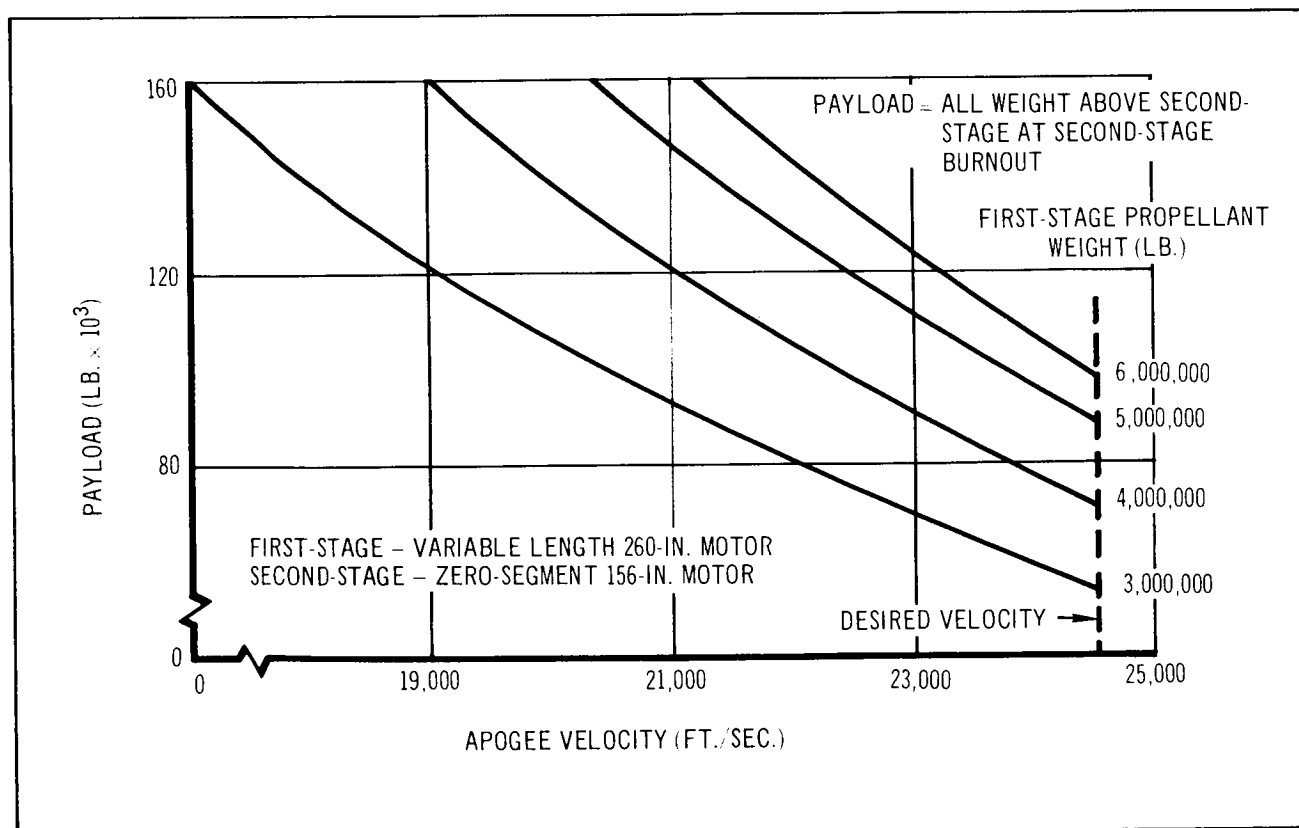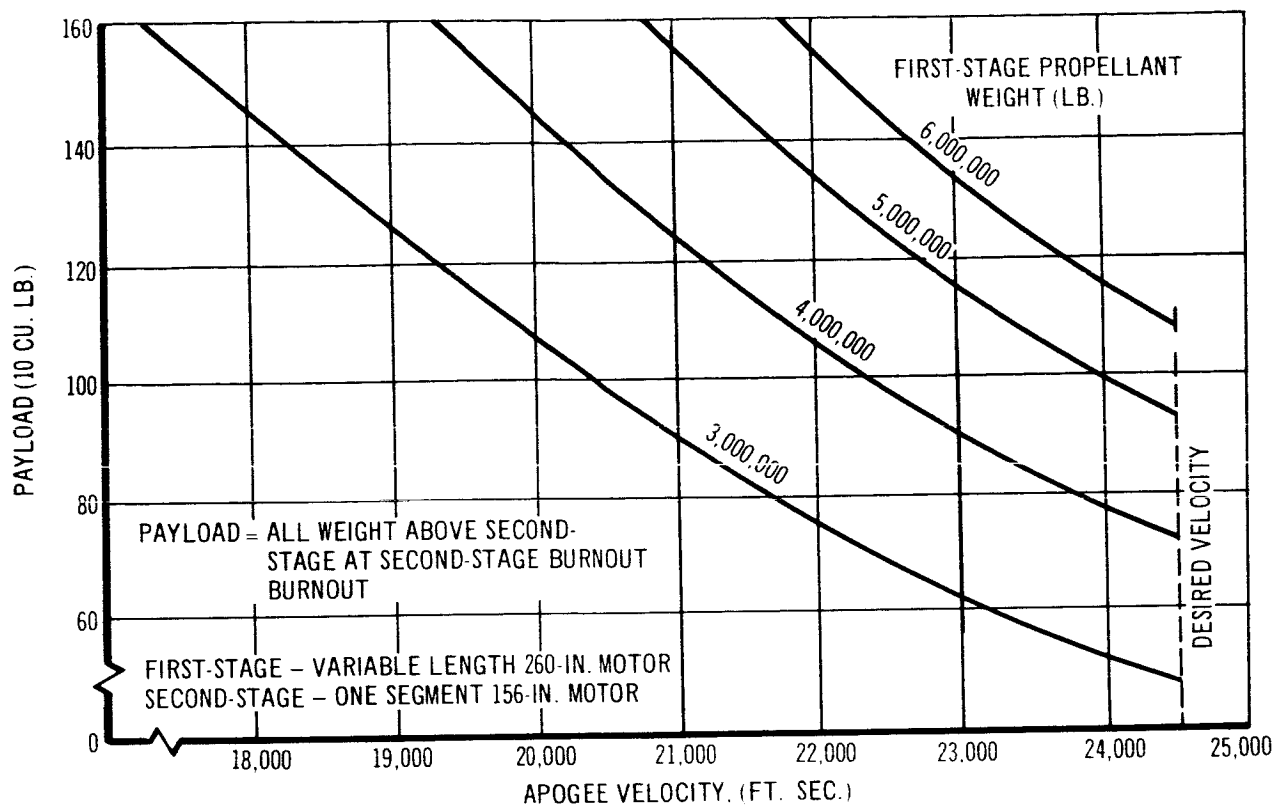
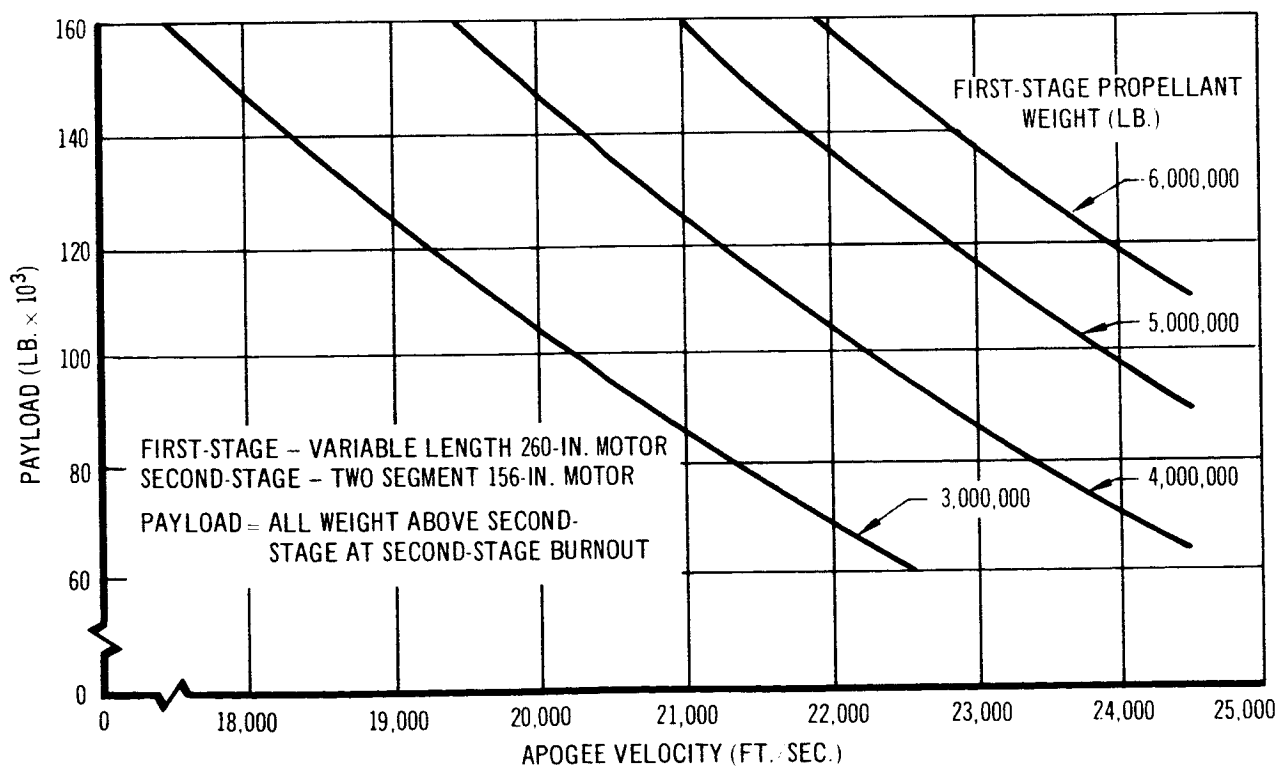Figure 9-24 Payload vs. Apogee Velocity at 300 n. mi. Two Stage Vehicle

Figure 9-25 Payload vs. Apogee Velocity at 300 n. mi. – Three-Stage Vehicle
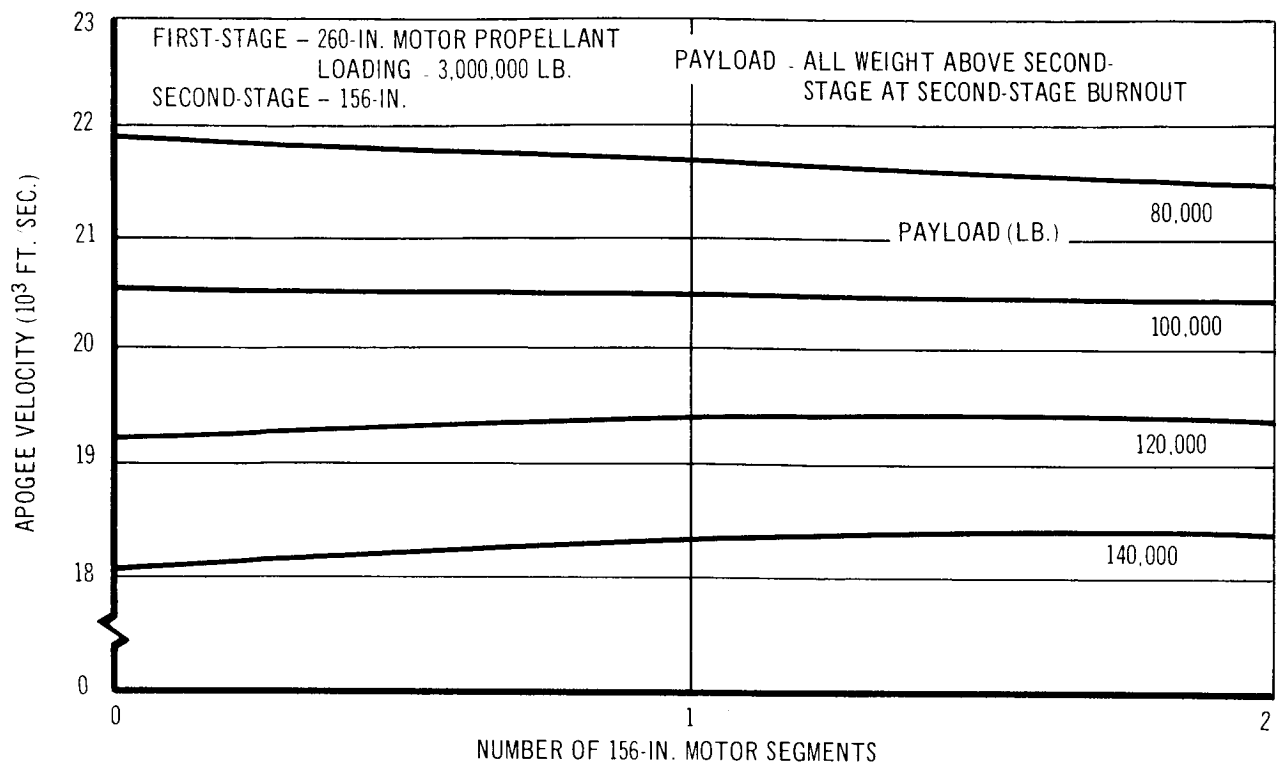
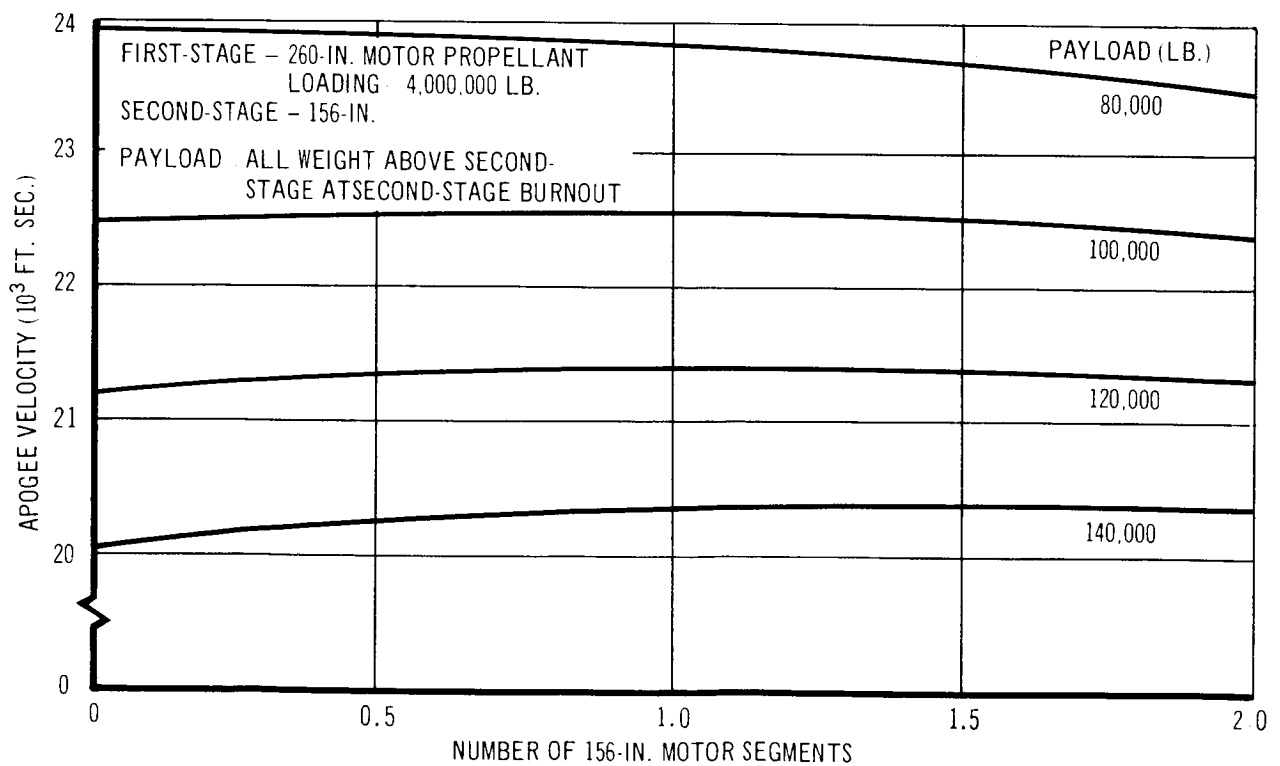Figure 9-26 Apogee Velocity at 300 n. mi. vs. Second-Stage Motor Size

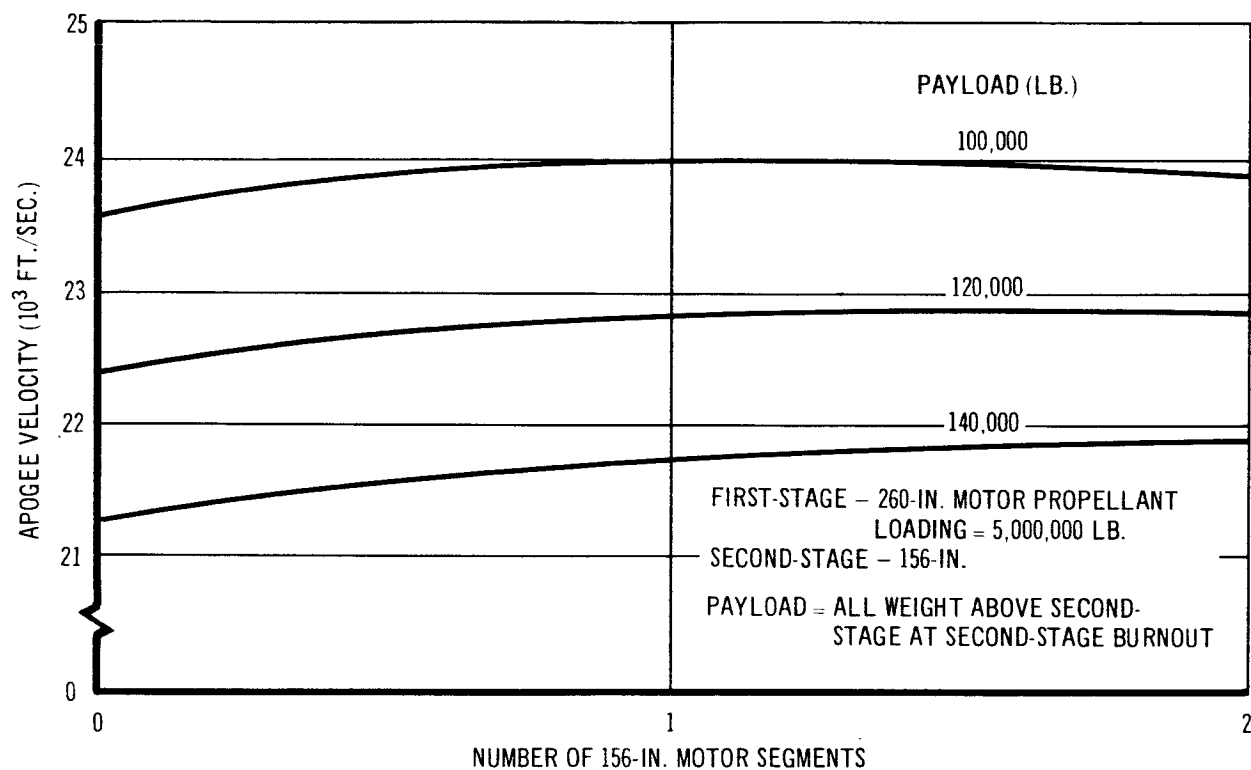Figure 9-27 Apogee Velocity at 300 n. mi. vs. Second-Stage Motor Size

Figure 9-28 Apogee Velocity at 300 n. mi. vs. Second-Stage Motor Size

are less than 6,000,000 lb. The booster with a 6,000,000 lb., 260-in. first stage and a 0-segment 156-in. second stage was selected as a representative two stage vehicle for carrying a 100,000 lb. payload. The trajectory for this vehicle was used in a comparison with a three stage booster.

Table 9-6 shows the characteristics of the two and three stage vehicle chosen for comparison. Both have comparable performance to an apogee altitude of 300 n. mi. The two stage booster, however, has a pad weight approximately 1,400,000 lb. greater than the three stage vehicle. The two stage vehicle has a lower total impulsive velocity because it is flying a lower trajectory with higher velocity. The gravity losses are less because of shorter burn time and a lower average flight path angle.

In order to reduce the velocity requirements of the spacecraft, it is desirable for the launch vehicle to fly a direct ascent into orbit. Both the two and three stage boosters, however, burn out before reaching apogee altitude. To maximize the apogee velocity it is necessary to fly a Hohmann transfer to 300 n. mi. from the maximum burnout altitude. The higher the burnout velocity, the closer the apogee velocity will be to circular satellite velocity using a Hohmann transfer ellipse. Since the three stage launch vehicles generally have a higher burnout altitude than the two stage vehicles when flying to a 300-n. mi. apogee, it should be possible to get closer to circular satellite velocity using a three stage booster by proper trajectory shaping.

Figure 9-29 shows the required inertial burnout velocity and injection velocity to achieve a circular orbit at 300 n. mi. as a function of booster burnout altitude. Figure 9-29 assumes that a Hohmann transfer ellipse is used between booster burnout and orbital injection.

Table 9-6

COMPARISON BETWEEN TWO STAGE AND
THREE STAGE VEHICLES (page 1 of 2)

*Variable	Two Stage	Three Stage
W_{P_1}	6,000,000	3,374,000
W_{P_2}	450,000	1,349,000
W_{P_3}	---	450,000
W_{PL}	100,000	100,000
T_{LD}	9,077,630	7,191,058
W_{LD}	7,241,594	5,834,670
$(T/W)_{LD}$	1.253	1.232
$\lambda'_{1_{EFF}}$	0.918	0.922
$\lambda'_{2_{EFF}}$	0.895	0.912
$\lambda'_{3_{EFF}}$	---	0.895
$I_{SP_1 VAC}$	271.5	271.5
$I_{SP_2 VAC}$	294	271.5
$I_{SP_3 VAC}$	---	294
h_a	300	300
V_a	24,391	24,227
q_{max}	1,005	706

*For definitions of symbols, see Section 9.3.2.4

Table 9-6 (page 2 of 2)

*Variable	Two Stage	Three Stage
ΔV_{TOT}	29,039	29,966
ΔV_1	15,807	7,544
ΔV_2	13,232	8,993
ΔV_3	---	13,429
GF_{TOT}	72.42	58.35
$a\,BO_f$	35.24	106.34
$\gamma\,BO_f$	-0.9083	2.9898
V_{BO_f}	26,266	25,582

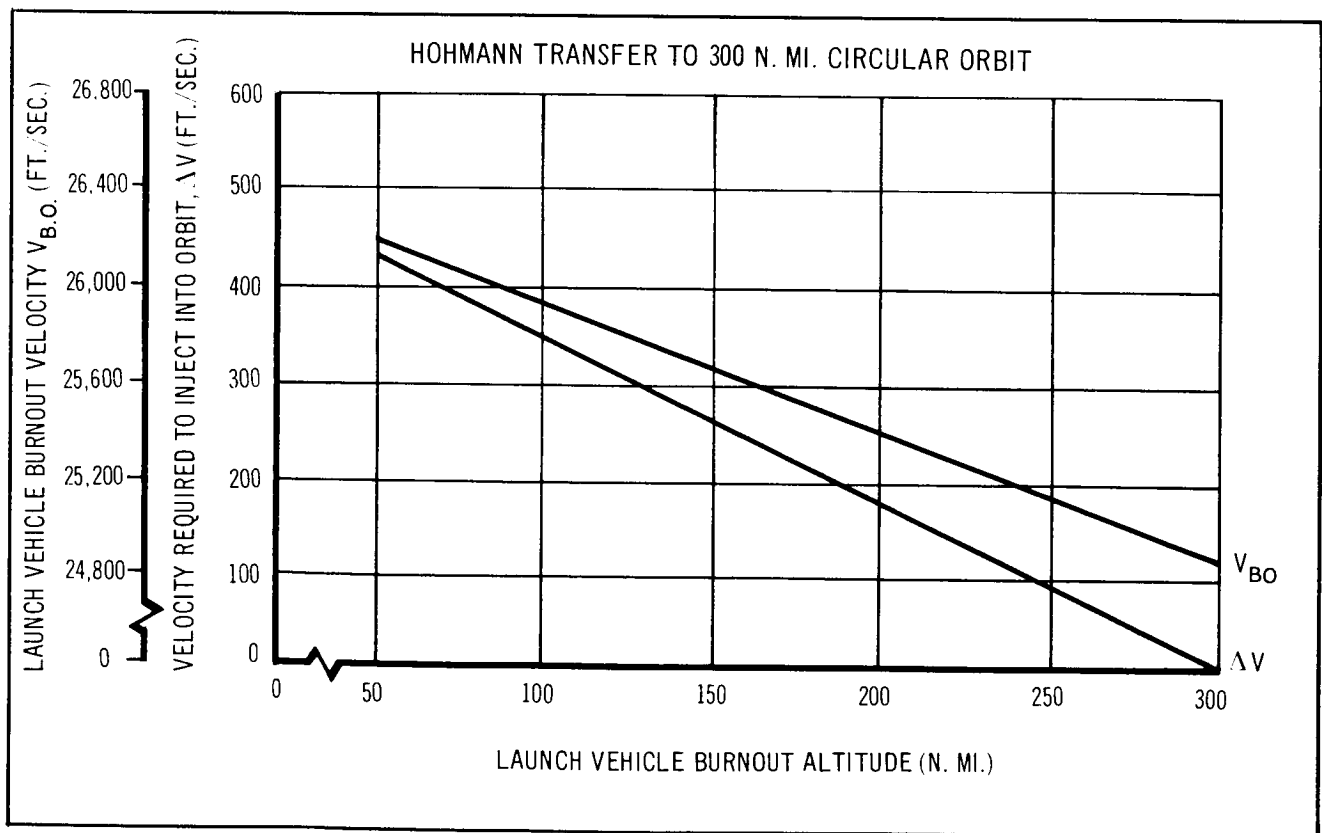*For definitions of symbols, see Section 9.3.2.4

Figure 9-29 Burnout and Injection Velocities vs. Burnout Altitude

A three stage launch vehicle was selected for the HES-2G arrangement on the basis of the above considerations. These considerations may be summarized as follows:

1. Lower total pad weight for the three stage vehicle.
2. Lower total thrust level at liftoff and resulting smaller first stage motor for the three stage vehicle.
3. Lower impulsive velocity requirements for transfer to 300-n.mi. circular orbit for the three stage vehicle.
4. Lower maximum dynamic pressures for the three stage vehicle.

9.3.2.3 Selection of Baseline Configuration

From the results of the preliminary three stage vehicle analysis discussed previously, the vehicle consisting of a 260-in. motor with 3,374,000 lb. of propellant (full length) first stage; a 260-in. motor with 1,349,600 lb. of propellant (40% full length) second stage; and a monolithic 156-in. third stage with a propellant loading of 526,100 lb. was selected for further evaluation. For the trajectory, a three-step throttling program was used on the steering system thrust to reduce the amount of steering propellant required. The throttling consisted of 100,000 lb. of steering thrust during first stage flight, 75,000 lb. during second stage flight, and 50,000 lb. during third stage flight. The information concerning fin weight, interstage weights, HES-2G weight, and motor performance of the various stages was revised and a new trajectory established. The revised trajectory showed a considerable loss in apogee velocity as shown in Table 9-7.
To determine the necessary size of the baseline vehicle, the three stage vehicle was then sized on the basis of impulse to determine the optimum velocity distribution between stages. The sizing was done using the latest information on the motor characteristics for a total impulsive velocity of 29,920 ft./sec. Figures 9-30 and 9-31 show the total vehicle growth factor as a function of velocity distribution between the stages. Figure 9-30 presents data corresponding to second stage impulsive velocities less than first stage. Figure 9-31 shows those cases where second stage impulsive velocities are greater than first stage. Increasing the size of the third stage would be off optimum, as shown in Figures 9-30 and 9-31. Decreasing the size of the third stage, though making the vehicle nearer optimum, was unacceptable because of

Table 9-7

THREE STAGE VEHICLE COMPARISON (page 1 of 2)

*Variable	Preliminary Three Stage with Full-Length 260-In. First Stage Motor	Revised Three Stage with Full-Length 260-In. First Stage Motor
W_{P_1}	3,374,000	3,374,000
W_{P_2}	1,349,600	1,350,000
W_{P_3}	450,000	526,100
W_{P_L}	100,000	103,300
T_{LD}	7,191,058	7,472,242
W_{LD}	5,834,670	5,978,007
$(T/W)_{LD}$	1.232	1.250
$\lambda'_{1_{Eff}}$	0.922	0.915
$\lambda'_{2_{Eff}}$	0.912	0.895
$\lambda'_{3_{Eff}}$	0.895	0.899
$I_{SP_{1\,VAC}}$	271.5	260
$I_{SP_{2\,VAC}}$	271.5	284
$I_{SP_{3\,VAC}}$	294	291.8
h_a	300	300

*For definitions of symbols, see Section 9.3.2.4

Table 9-7 (page 2 of 2)

*Variable	Preliminary Three Stage with Full-Length 260-In. First Stage Motor	Revised Three Stage with Full-Length 260-In. First Stage Motor
V_a	24,227	23,534
q_{max}	706	708
ΔV_{TOT}	29,966	29,519
ΔV_1	7,544	7,168
ΔV_2	8,993	8,661
ΔV_3	13,429	13,690
GF_{TOT}	58.35	57.87
$W_{A_1} + W_{Fins}$	7,000	35,500
W_{A_2}	2,000	16,500
W_{A_3}	0	5,000
aBO_3	106.34	112.58
V_{BO_3}	2.9898	5.3356
γ_{BO_3}	25,582	24,886

*For definitions of symbols, see Section 9.3.2.4
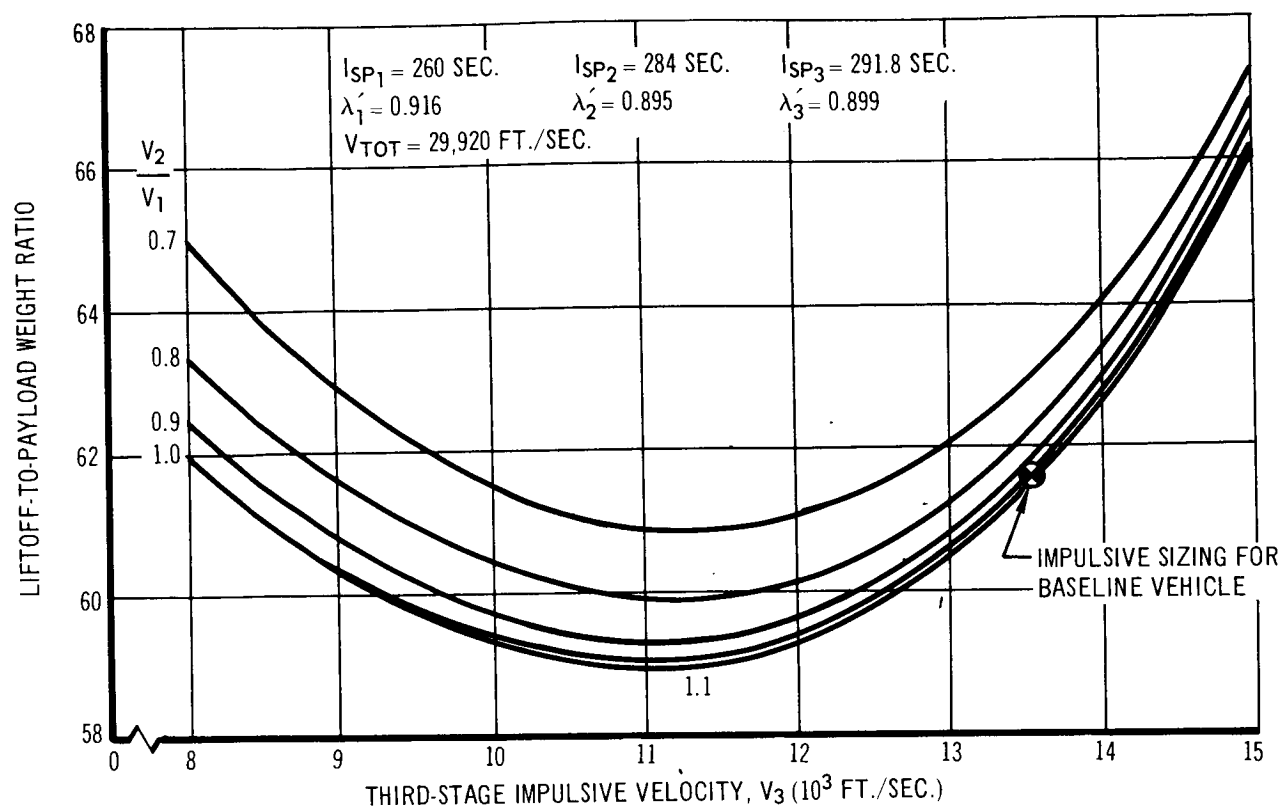
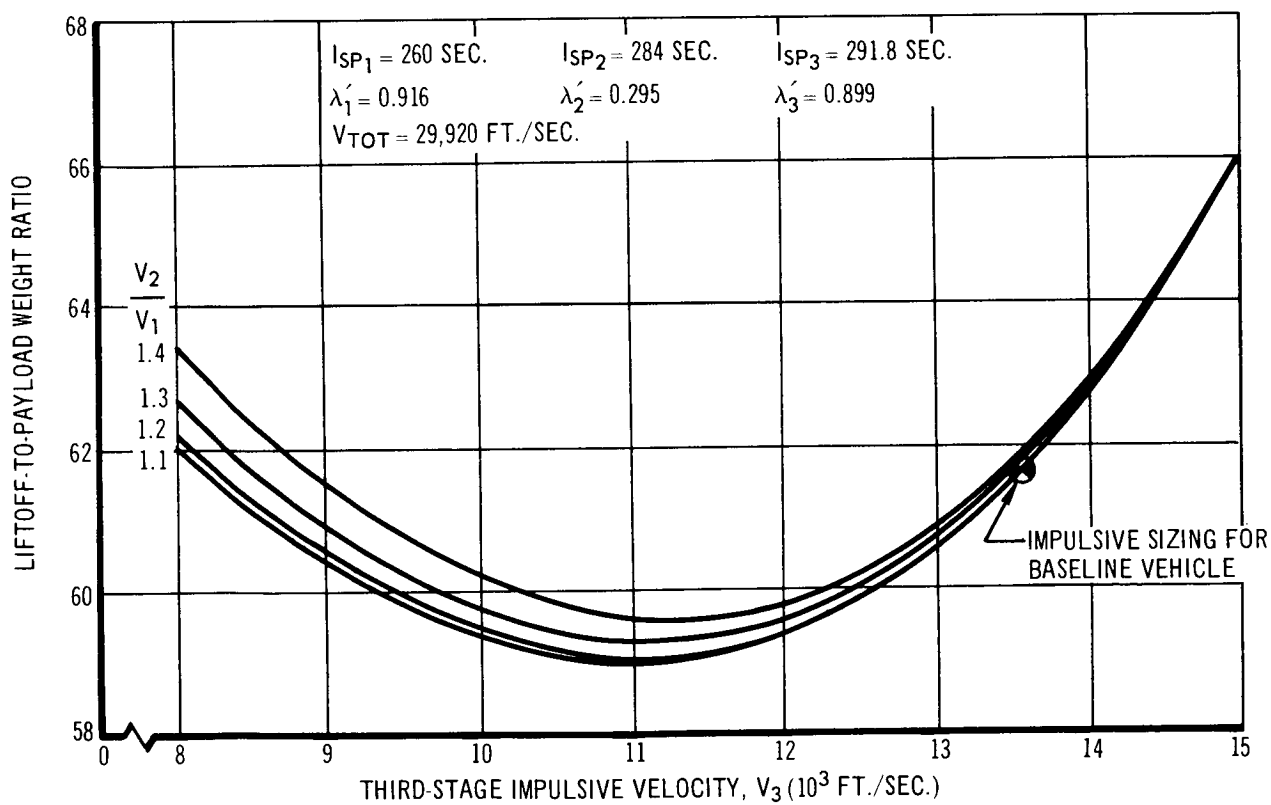Figure 9-30 Liftoff-To-Payload Weight Ratio vs. Stage Velocity Distribution

Figure 9-31 Liftoff-To-Payload Weight Ratio vs. Stage Velocity Distribution

steering system difficulties (see Figure 5-24). The third stage was therefore left unchanged.

With the incorporation of a fixed third stage motor size, a minimum vehicle growth factor occurs for a velocity ratio of 1.1 between the second and first stages. Sizing a vehicle with a third stage impulsive velocity of 13,500 ft./sec. a payload of 106,000 lb. and velocity ratio between the second and first stage of 1.1 gives a first stage propellant loading of 3,951,329 lb. and a second stage propellant loading of 1,338,063 lb. In subsequent analyses, the baseline vehicle was therefore defined as having a first stage propellant loading of 4,000,000 lb. and a second stage propellant loading of 1,350,000 lb. Both stages were 260-in.-diameter motors.

After the selection of the three stage configuration, a recheck was made of the two-stage vehicle characteristics. A two-stage vehicle was sized on the basis of impulse to determine its growth factor as a function of velocity distribution. Since a two stage booster needs less impulsive velocity than a 3-stage vehicle (because of lower gravity losses) to perform the same mission, the sizing was performed for a total impulsive velocity of 29,000 ft./sec.

The total vehicle growth factor as a function of first stage impulsive velocity is shown in Figure 9-32. It can be seen that a minimum growth factor of 72 occurs for a stage mass fraction of 0.91 compared to a growth factor of 61.4 for the selected three-stage vehicle.

A trajectory was simulated for the final baseline vehicle with (1) the HES-2G payload and (2) a revised three step throttling program of 100,000 lb. thrust during first stage flight, 32,000 lb. during second stage and 70,000 lb. during third stage flight. Table 9-8 lists the pertinent characteristics of the vehicle and the trajectory. The variation in trajectory parameters is presented in curve form in Section 6.3.

The final baseline vehicle has an overall length of 355 ft. including the spacecraft and steering propellant tanks. The two stage vehicle with a first stage propellant loading of 6,000,000 lb. and a 0-segment, 156-in. second stage has an overall length of 366 ft. This two stage vehicle is actually too small, since

Table 9-8
HES-2G BASELINE LAUNCH VEHICLE (page 1 of 2)

Variable	First Stage	Second Stage	Third Stage
	LAUNCH VEHICLE		
W_G	6,653,141	2,243,626	721,011
W_P	4,000,000	1,350,000	526,100
W_S	329,004	141,713	55,744
W_A	35,500 (including fins)	16,500	5,000
W_{PL}	2,243,626	721,011	106,000
λ'	0.924	0.905	0.904
λ'_{Eff}	0.916	0.895	0.897
	SOLID MOTOR		
T_{SL}	8,263,000	---	---
T_{VAC}	9,022,000	3,240,000	1,429,000
$I_{SP_{SL}}$	238	213	---
$I_{SP_{VAC}}$	260	284	291.8
T_{WEB}	107	110	100
T_{ACT}	123.1075	126.5591	114.7347
	STEERING SYSTEM		
T_S	100,000	32,000	70,000
W_{SP}	43,211	14,402	28,167
$I_{SP_{VAC}}$	284.5	281.2	284.5

Table 9-8 (page 2 of 2)

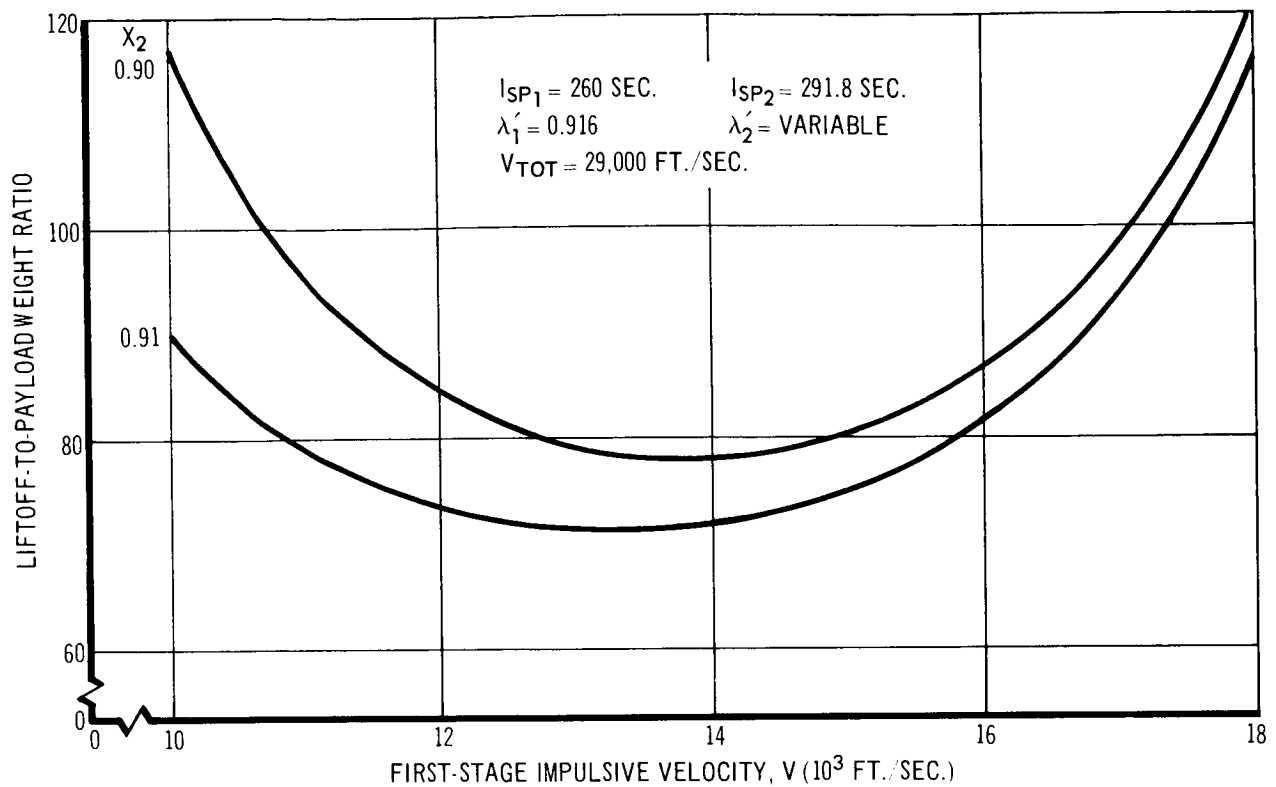| Variable	First Stage	Second Stage	Third Stage
	TRAJECTORY		
T_{BO}	123.1075	249.6666	364.4013
α_{BO}	23.53	70.96	96.22
γ_{BO}	29.15	8.66	2.71
V_{BO}	5,129	12,442	25,707
q_{BO}	38	0	0
a_{BO}	0	0	0
ΔV	7,799	8,534	13,550
q_{MAX}	721	0	0
MAX	3.12	3.35	7.181
$T/_{W}$ LD	1.250	1.455	2.056

Figure 9-32 Liftoff-To-Payload Weight Ratio vs. First-Stage Impulsive Velocity

the latest payload, fin and interstage weights, and motor characteristics are not included in the vehicle. Therefore, if a two stage vehicle were used it would be necessary to increase the size of either the first or second stage.

9.3.2.4 Symbol Definitions

W_G Gross weight at stage ignition, (lb.)

W_P Step solid propellant weight, (lb.)

W_S Step motor case and nozzle weight, (lb.)

W_A Step interstage weight, (lb.)

W_{PL} Weight above step, (lb.)

λ' Step propellant mass fraction not including interstage weight

λ'_{eff} — Step propellant mass fraction including interstage weight.

T_{SL} — Sea level thrust of solid motor, (lb.)

T_{VAC} — Vacuum thrust of solid motor, (lb.)

$I_{SP_{SL}}$ — Sea level specific impulse of solid motor, (sec.)

$I_{SP_{VAC}}$ — Vacuum specific impulse of solid motor, (sec.)

T_{WEB} — Web burn time of solid motor, (sec.)

T_{ACT} — Action burn time of solid motor, (sec.)

T_S — Thrust of steering rockets, (lb.)

W_{SP} — Steering propellant weight, (lb.)

$I_{SP_{VAC}}$ — Vacuum specific impulse of steering system, (sec.)

T_{BO} — Burnout time, (sec.)

L_{BO} — Burnout altitude, (n. mi.)

γ_{BO} — Burnout inertial elevation flight path angle, (deg.)

V_{BO} — Burnout inertial velocity, (ft./sec.)

q_{BO} — Burnout dynamic pressure, (lb./sq.ft.)

a_{BO} — Burnout acceleration, (g's.)

ΔV — Impulsive delivered during stage burning, (ft./sec.)

q_{MAX} — Maximum dynamic pressure during stage burning, (lb./sq.ft.)

a_{MAX} — Maximum acceleration during stage burning, (g's.)

T/W_{LD} — Thrust-to-weight ratio at stage ignition.

h_a Apogee altitude, (n. mi.)

V_a Velocity at apogee, (ft. /sec.)

T_{LO} Total thrust at first stage ignition, (lb.)

W_{LO} Total weight at first stage ignition, (lb.)

ΔV_{TOT} Total impulsive velocity, (ft. /sec.)

GF_{TOT} Total vehicle growth factor, ratio between liftoff weight at first stage ignition to payload weight at end of burning.

Section 10

CONCLUSIONS

This study has resulted in a first-order definition of a manned space vehicle
system whose principal mission is the logistics supply of men and materials
to an earth-orbiting space station at an altitude of 300 n. mi. The spacecraft
configuration selected for final evaluation is composed of an HL-10 spacecraft
with the capability of transporting up to eleven passengers and two crew; a
booster steering and spacecraft maneuvering propulsion system (located on
the HL-10); cargo provisions for up to 5,000 lb. (in the HL-10), and up to
18,750 lb. of cargo in a cargo-module adapter; and, an all solid-propellant
booster propulsion system. The booster consists of three stages: (1) a
260-in. dia. solid propellant first stage motor with a propellant loading of
4,000,000 lb.; (2) a 260-in. dia. second stage motor with a propellant loading
of 1,350,000 lb.; and (3) a 156-in. dia. third stage motor with a propellant
loading of 526,100 lb.

While results of the study have not demonstrated that the head-end steering
concept is a preferred approach, a first-order cost analysis indicates there
would probably be significant cost benefits in this approach. This results
not only from the use of large solid boosters, but from the concentration of
the steering function at the head-end. The use of the head-end steering
concept may also show cost advantages when used with liquid propellant
upper stage boosters.

A brief summary of the study results are:

1. Steering the vehicle during boost with two engines located on the
   HL-10 spacecraft is feasible with a thrust-level of 50,000 lb./
   engine, a gimbaling range of $\pm 30^\circ$, and using a storable liquid
   propellant.

2. The steering thrust requirement is more sensitive to changes in booster thrust misalignment than to any other design parameter considered. An increase in misalignment of 50% from 0.1° to 0.15° results in a 30% increase in steering thrust.

3. The incorporation of steering propellant in the HL-10 was not found to be feasible. However, the HL-10 lifting body vehicle was shown to be an extremely flexible configuration for transporting personnel, cargo, for in-orbit maneuvering propellants, and for the installation of rocket engine components.

4. Because the study has shown the technical feasibility of concentrating the steering function in the HL-10 spacecraft, the booster stage interfaces need to accommodate only range safety, ignition, and thrust termination functions.

5. The total vehicle shows performance sensitivities to design parameter variations typical of three-stage vehicles designed for a near optimum ratio of gross weight to payload weight.

6. Recovery of all major vehicle components except the fixed-nozzle solid motor boosters and the steering propellant tankage has been shown to be feasible.

7. A first-order evaluation of the prelaunch preparation time for the head-end steering solid motor vehicle resulted in a requirement of only 38 days of which 20 days are required for pad occupancy. This compares to 56 days for the Saturn I of which 47 days are used for pad occupancy.

8. A first-order cost evaluation of the vehicle concept shows a launch cost of $15.1 million based on cost of operations only; total program cost of $1.4 billion, and a cost/lb. of delivered cargo of $793/lb. based on the cost of operations only. These costs are based on a 5-year span of operation with ten flights/year.

Section 11

RECOMMENDATIONS FOR FUTURE WORK

This contract study of a simplified manned space vehicle using head-end steering had as an objective the study of feasibility of the vehicle design concept including the definition of steering requirements and first-order sizing of a solid-motor booster and spacecraft systems.

Several areas were identified during the course of the study which require additional analysis before total technical feasibility can be substantiated. However, study time and budget constraints did not permit additional investigation of these areas.

It is recommended that the objectives of the next segment of study activity should be to define the system concept in sufficient technical depth to permit trade-off analysis with other logistic supply concepts. This will require a determination and documentation of a preliminary design, selected and optimized for cost effectiveness and a determination of when all technological building blocks should be in hand to permit initiation of development.

11.1 SECOND-ORDER TECHNICAL EVALUATION OF THE VEHICLE CONCEPT

A second-order technical analysis should be made (1) to identify all research and development items which might impose a significant risk on the program and (2) to permit a valid cost effectiveness evaluation. Analysis tasks are identified as follows:

1. Booster cost and performance optimization
2. Structural and thermo-protection system definition of the HL-10
3. Steering subsystem sizing
4. Technical comparison of steering techniques
5. System performance sensitivity analysis

6. Systems analysis and parametric comparison with other booster-propellant types such as mixed solids and liquids

7. Identification of technical building blocks for booster and spacecraft

8. An operational analysis including:

    A. Identification of operational sequence of events throughout the mission profile

    B. Identification of launch, orbit, and recovery operational requirements as a function of mission, weather, landing aids, guidance data, etc.

    C. Preliminary development of a test plan including identification of tests, test schedules, hardware requirements, and facility requirements.

11.2 TECHNICAL PROBLEM AREAS IDENTIFIED IN THIS STUDY

A study should be initiated to evaluate and resolve technical problems identified in this study. This effort should cover three basic areas:

1. Evaluation and analysis of jet impingement heating and jet-wake aerodynamic interference on the spacecraft and booster.

2. Steering engine gimbaling techniques associated with angular throws to 45°. Primary emphasis would be, on the selection of flexlines or propellant passage through the gimbal points.

3. Spacecraft and booster compatibility with respect to launch and range safety requirements.